



Universiteit  
Leiden  
The Netherlands

## Rubin observatory LSST transients and variable stars roadmap

Hambleton, K.M.; Bianco, F.B.; Street, R.; Bell, K.; Buckley, D.; Graham, M.; ... ; Vink, J.S.

### Citation

Hambleton, K. M., Bianco, F. B., Street, R., Bell, K., Buckley, D., Graham, M., ... Vink, J. S. (2023). Rubin observatory LSST transients and variable stars roadmap. *Publications Of The Asp*, 135(1052), 105002. doi:10.1088/1538-3873/acdb9a

Version: Publisher's Version  
License: [Creative Commons CC BY 4.0 license](#)  
Downloaded from: <https://hdl.handle.net/1887/3719250>

**Note:** To cite this publication please use the final published version (if applicable).



# Rubin Observatory LSST Transients and Variable Stars Roadmap

Kelly M. Hambleton<sup>1</sup>, Federica B. Bianco<sup>2,3,4,5</sup>, Rachel Street<sup>6</sup>, Keaton Bell<sup>7</sup>, David Buckley<sup>8,9,10</sup>, Melissa Graham<sup>7</sup>,  
 Nina Hernitschek<sup>11</sup>, Michael B. Lund<sup>12</sup>, Elena Mason<sup>13</sup>, Joshua Pepper<sup>14</sup>, Andrej Prša<sup>1</sup>, Markus Rabus<sup>15</sup>,  
 Claudia M. Raiteri<sup>16</sup>, Róbert Szabó<sup>17,18,19,20</sup>, Paula Szkody<sup>7</sup>, Igor Andreoni<sup>21,22,23</sup>, Simone Antonucci<sup>24</sup>,  
 Barbara Balmaverde<sup>16</sup>, Eric Bellm<sup>7</sup>, Rosaria Bonito<sup>25</sup>, Giuseppe Bono<sup>26</sup>, Maria Teresa Botticella<sup>27</sup>, Enzo Brocato<sup>24,28</sup>,  
 Katja Bučar Bricman<sup>29</sup>, Enrico Cappellaro<sup>30</sup>, Maria Isabel Carnerero<sup>16</sup>, Ryan Chornock<sup>31</sup>, Riley Clarke<sup>2</sup>,  
 Phil Cowperthwaite<sup>32</sup>, Antonino Cucchiara<sup>33,34</sup>, Filippo D'Ammando<sup>35</sup>, Kristen C. Dage<sup>36</sup>, Massimo Dall'Ora<sup>37</sup>,  
 James R. A. Davenport<sup>7</sup>, Domitilla de Martino<sup>27</sup>, Giulia de Somma<sup>27</sup>, Marcella Di Criscienzo<sup>24</sup>, Rosanne Di Stefano<sup>38</sup>,  
 Maria Drout<sup>39</sup>, Michele Fabrizio<sup>24</sup>, Giuliana Fiorentino<sup>24</sup>, Poshak Gandhi<sup>40</sup>, Alessia Garofalo<sup>41</sup>, Teresa Giannini<sup>24</sup>,  
 Andreja Gomboc<sup>29</sup>, Laura Greggio<sup>30</sup>, Patrick Hartigan<sup>42</sup>, Markus Hundertmark<sup>43</sup>, Elizabeth Johnson<sup>44</sup>,  
 Michael Johnson<sup>45,46</sup>, Tomislav Jurkic<sup>47</sup>, Somayeh Khakpash<sup>2,4</sup>, Silvio Leccia<sup>27</sup>, Xiaolong Li<sup>2,4</sup>, Davide Magurno<sup>48</sup>,  
 Konstantin Malanchev<sup>49,50</sup>, Marcella Marconi<sup>27</sup>, Raffaella Margutti<sup>31</sup>, Silvia Marini<sup>51</sup>, Nicolas Mauron<sup>52</sup>,  
 Roberto Molinaro<sup>27</sup>, Anais Möller<sup>53</sup>, Marc Moniez<sup>54</sup>, Tatiana Muraveva<sup>41</sup>, Ilaria Musella<sup>27</sup>, Chow-Choong Ngeow<sup>55</sup>,  
 Andrea Pastorello<sup>30</sup>, Vincenzo Petrecca<sup>27</sup>, Silvia Piranomonte<sup>24</sup>, Fabio Ragosta<sup>24</sup>, Andrea Reguitti<sup>30,56,57</sup>, Chiara Righi<sup>51</sup>,  
 Vincenzo Ripepi<sup>27</sup>, Liliana Rivera Sandoval<sup>58</sup>, Keivan G. Stassun<sup>11</sup>, Michael Stroh<sup>59</sup>, Giacomo Terreran<sup>6</sup>,  
 Virginia Trimble<sup>60</sup>, Yiannis Tsapras<sup>43</sup>, Sjoert van Velzen<sup>61</sup>, Laura Venuti<sup>62</sup>, and Jorick S. Vink<sup>63</sup>

<sup>1</sup> Department of Astrophysics and Planetary Science, Villanova University, 800 Lancaster Ave, Villanova, PA 19085, USA

<sup>2</sup> Department of Physics and Astronomy, University of Delaware, Newark, DE 19716, USA

<sup>3</sup> Joseph R. Biden, Jr. School of Public Policy and Administration, University of Delaware, Newark, DE 19716, USA

<sup>4</sup> Data Science Institute, University of Delaware, Newark, DE 19716, USA

<sup>5</sup> Vera C. Rubin Observatory Construction Project, Chile

<sup>6</sup> Las Cumbres Observatory (LCOGT), 6740 Cortona Drive, Suite 102, Goleta, CA 93117-5575, USA

<sup>7</sup> Astronomy Department, University of Washington, Box 351580, Seattle, WA 98195, USA

<sup>8</sup> South African Astronomical Observatory, PO Box 9, Observatory Rd, Observatory 7935, South Africa

<sup>9</sup> Department of Astronomy, University of Cape Town, Private Bag X3, Rondebosch 7701, South Africa

<sup>10</sup> Department of Physics, University of the Free State, PO Box 339, Bloemfontein 9300, South Africa

<sup>11</sup> Department of Physics and Astronomy, Vanderbilt University, Nashville, TN 37235, USA

<sup>12</sup> NASA Exoplanet Science Institute—Caltech/IPAC, 1200 E. California Blvd, Pasadena, CA 91125, USA

<sup>13</sup> INAF Osservatorio Astronomico di Trieste (INAF-OATS), Via G.B. Tiepolo 11, 34143 Trieste (TS), Italy

<sup>14</sup> Lehigh University, Department of Physics Deming Lewis Lab 16 Memorial Drive East, Italy

<sup>15</sup> Departamento de Matemática y Física Aplicadas, Facultad de Ingeniería, Universidad Católica de la Santísima Concepción, Alonso de Rivera 2850, Concepción, Chile

<sup>16</sup> INAF-Osservatorio Astrofisico di Torino, via Osservatorio 20, I-10025 Pino Torinese, Italy

<sup>17</sup> Konkoly Observatory, Research Centre for Astronomy and Earth Sciences, ELKH, Budapest, Konkoly-Thege Miklós út 15-17., H-1121, Hungary

<sup>18</sup> CSFK, MTA Centre of Excellence, Budapest, Konkoly Thege Miklós út 15-17., H-1121, Hungary

<sup>19</sup> MTA CSFK Lendület Near-Field Cosmology Research Group, Konkoly Observatory, Budapest, Hungary

<sup>20</sup> ELTE Eötvös Loránd University, Institute of Physics, Pázmány Péter stny. 1a, 1117, Budapest, Hungary

<sup>21</sup> Joint Space-Science Institute, University of Maryland, College Park, MD 20742, USA

<sup>22</sup> Department of Astronomy, University of Maryland, College Park, MD 20742, USA

<sup>23</sup> Astrophysics Science Division, NASA Goddard Space Flight Center, Mail Code 661, Greenbelt, MD 20771, USA

<sup>24</sup> INAF-Osservatorio Astronomico di Roma, via Frascati 33, I-00078 Monte Porzio Catone (RM), Italy

<sup>25</sup> INAF-Osservatorio Astronomico di Palermo, Piazza del Parlamento, 1 I-90134, Palermo, Italy

<sup>26</sup> Università di Roma Tor Vergata, Dipartimento di Fisica, Via della Ricerca Scientifica 1, I-00133 Roma, Italy

<sup>27</sup> INAF-Osservatorio Astronomico di Capodimonte (INAF-OANA), Salita Moiarriello 16, I-80131, Napoli (NA), Italy

<sup>28</sup> INAF-Osservatorio Astronomico d'Abruzzo, Via Mentore Maggini, s.n.c., I-64100 Teramo, Italy

<sup>29</sup> Center for Astrophysics and Cosmology, University of Nova Gorica, Vipavska 13, 5000 Nova Gorica, Slovenia

<sup>30</sup> INAF-Osservatorio Astronomico di Padova, Vicolo dell'Osservatorio 5, 35122 Padova, Italy

<sup>31</sup> Department of Astronomy, University of California, Berkeley, CA 94720, USA

<sup>32</sup> Carnegie Observatories: Pasadena, CA, USA

<sup>33</sup> NASA Headquarter, 300 Hidden Figures Way SW, Washington, DC 20546, USA

<sup>34</sup> College of Marin, 120 Kent Ave., Kentfield, CA 94904, USA

<sup>35</sup> INAF-IRA Bologna, Via P. Gobetti 101, I-40129 Bologna, Italy

<sup>36</sup> Department of Physics, McGill University, 3600 University Street, Montreal, QC H3A 2T8, Canada

<sup>37</sup> INAF-Osservatorio Astronomico di Capodimonte (INAF-OACN), Salita Moiarriello 16, I-80131, Napoli (NA), Italy

<sup>38</sup> Center for Astrophysics, Harvard, Observatory Building E, 60 Garden St, Cambridge, MA 02138, USA

<sup>39</sup> Dunlap Institute for Astronomy & Astrophysics, University of Toronto, 50 St. George Street Toronto, Ontario M5S 3H4, Canada

<sup>40</sup> School of Physics & Astronomy, University of Southampton, SO17 1BJ, UK

<sup>41</sup> INAF—Osservatorio di Astrofisica e Scienza dello Spazio di Bologna, Via Gobetti 93/3, 40129 Bologna, Italy

<sup>42</sup> Physics and Astronomy, Rice University: Houston, Texas, USA

<sup>43</sup> Zentrum für Astronomie der Universität Heidelberg, Astronomisches Rechen-Institut, Mönchhofstr. 12-14, D-69120 Heidelberg, Germany

- <sup>44</sup> Johns Hopkins Department of Physics & Astronomy, 3400 N Charles St Baltimore, MD 21218, USA  
<sup>45</sup> Fundamental Physics in Radio Astronomy, Max Planck Institute for Radio Astronomy, D-53121 Bonn, Germany  
<sup>46</sup> DLR-Institute of Data Science, D-07745 Jena, Germany  
<sup>47</sup> Faculty of Physics, University of Rijeka, R. MATEJČIĆ 2, 51000 Rijeka, Croatia  
<sup>48</sup> Department of Physics and Astronomy, University of Bologna, Via Zamboni, 33, I-40126 Bologna BO, Italy  
<sup>49</sup> Department of Astronomy, University of Illinois at Urbana-Champaign, 1002 W Green Street, Urbana, IL 61801, USA  
<sup>50</sup> Sternberg Astronomical Institute, Lomonosov Moscow State University, Moscow 119620, Russia  
<sup>51</sup> INAF-Brera Astronomical Observatory INAF-OA, Via Brera, 28, I-20121 Milano (MI), Italy  
<sup>52</sup> Université de Montpellier, Laboratoire LUPM, CNRS-IN2P3, Place Bataillon, F-34095 Montpellier, France  
<sup>53</sup> Centre for Astrophysics and Supercomputing, Swinburne University of Technology, Mail Number H29, PO Box 218, 3122 Hawthorn, VIC, Australia  
<sup>54</sup> Université Paris-Saclay, 339 Rue du Doyen André Guinier, F-91440 Bures-sur-Yvette, France  
<sup>55</sup> National Central University Graduate Institute of Astronomy No. 300, Zhongda Rd, Jhongli City, Taiwan  
<sup>56</sup> Departamento de Ciencias Físicas, Universidad Andrés Bello, Fernández Concha 700, Santiago, Chile  
<sup>57</sup> Millennium Institute of Astrophysics (MAS), Nuncio Monsenor Sòtero Sanz 100, Santiago, Chile  
<sup>58</sup> Department of Physics and Astronomy, University of Texas Rio Grande Valley, Brownsville, TX 78520, USA  
<sup>59</sup> Center for Interdisciplinary Exploration and Research in Astrophysics (CIERA) and Department of Physics and Astronomy, Northwestern University, Evanston, IL 60201, USA  
<sup>60</sup> University of California Irvine, Irvine, CA 92697, USA  
<sup>61</sup> Leiden Observatory, Niels Bohrweg 2, 2333 CA Leiden, Netherlands  
<sup>62</sup> SETI Institute, 339 Bernardo Ave, Suite 200, Mountain View, CA 94043, USA  
<sup>63</sup> Armagh Observatory and Planetarium, College Hill, BT61 9DG Armagh, UK  
 Received 2022 October 31; accepted 2023 June 5; published 2023 November 3

## Abstract

The Vera C. Rubin Legacy Survey of Space and Time (LSST) holds the potential to revolutionize time domain astrophysics, reaching completely unexplored areas of the Universe and mapping variability time scales from minutes to a decade. To prepare to maximize the potential of the Rubin LSST data for the exploration of the transient and variable Universe, one of the four pillars of Rubin LSST science, the Transient and Variable Stars Science Collaboration, one of the eight Rubin LSST Science Collaborations, has identified research areas of interest and requirements, and paths to enable them. While our roadmap is ever-evolving, this document represents a snapshot of our plans and preparatory work in the final years and months leading up to the survey's first light.

*Unified Astronomy Thesaurus concepts:* [Telescopes \(1689\)](#); [Microlensing event rate \(2146\)](#); [Binary stars \(154\)](#); [Exoplanets \(498\)](#); [Young stellar objects \(1834\)](#); [Supernovae \(1668\)](#); [Blazars \(164\)](#); [Tidal disruption \(1696\)](#); [Pulsating variable stars \(1307\)](#); [Brown dwarfs \(185\)](#)

## 1. Introduction

### 1.1. How To Navigate This Document

The Legacy Survey of Space and Time (LSST) at the National Science Foundation's Vera Rubin Observatory, due to begin science operations in 2023, will be a landmark project in astrophysics (Ivezić et al. 2019). It will survey the entire southern sky every  $\sim 3$  days in 6 filters, with a spatial resolution of  $0''.2 \text{ pix}^{-1}$  and to fainter limiting magnitudes ( $g < 25.0 \text{ mag}$  in 30 s) than previously possible. Crucially, Rubin LSST will continue for 10 yr, delivering an unprecedented catalog of long-baseline light curves.

Recent improvements in data processing technology make it possible to not only reduce the survey data in real-time but also to disseminate alerts of new discoveries within seconds. This raises the possibility of detecting and characterizing previously

unexplored categories of astronomical variability for the first time, particularly transient phenomena which simply occurs too quickly to be studied by previous surveys.

Fully exploiting this ground-breaking data presents some challenges, however. The volume of data and its rate of delivery:  $\sim 20 \text{ TB}$  of data *per night*, producing  $\sim 10$  million alerts *per night* - far exceed the scale of any previous survey. Furthermore, some scientific goals will require the coordination of follow-up observations with real-time response to LSST alerts. Substantial preparation will be required in order to maximize the scientific return.

The Transients and Variable Stars Science Collaboration (TVS SC) exists to bring together scientists interested in studying these classes of object from Rubin LSST data, with the goals of preparing for and facilitating their science. The purpose of this document is to outline the *areas of scientific study of interest to TVS SC members* in sufficient detail to allow for the necessary preparations required to achieve those aims. This document does not intend to present a complete outline of all possible science cases, rather those that our members plan to research once the data



Original content from this work may be used under the terms of the [Creative Commons Attribution 3.0 licence](#). Any further distribution of this work must maintain attribution to the author(s) and the title of the work, journal citation and DOI.

become available. Further, this document is the first version of the TVS SC Roadmap, which we anticipate to grow with the growing TVS Science Collaboration.

The Roadmap is organized into four main sections, as follows:

1. Time-critical science cases: these are science cases that require prompt identifications that trigger (often automated) follow-up observations. They focus on the Rubin Alert Stream, which is discussed in Section 2.2, which will be channeled through community-led brokers (see Section 6.1.2).
2. Non-time-critical science cases: these are science cases that can be developed on the Annual Data Releases (see Section 3.2). Some of these science cases may assume that the sample is pure, i.e., that prompt identification or characterization has been achieved.
3. Deep Drilling Fields: these are small spatial regions, typically consisting of one to a few Rubin pointings, centered on areas of special scientific interest. In these regions the cadence is higher to either achieve a fainter limiting magnitude and/or a higher temporal cadence than the main survey.
4. Mini- and Micro-Surveys: these are science motivated survey strategies that are based on community-led proposals. They cover small spatial regions (typically larger than the Deep Drilling Fields) with cadence and filter selection specific to the science case.

We elected to separate the time-critical and non-time-critical science cases based on their distinct need for alerts in the Rubin LSST ecosystem. Time-critical science cases that require alerts are focused on the Rubin LSST Alert Stream, which can be accessed through multiple community-led brokers (see Section 6.1.2), and will primarily utilize the Prompt Data Products, including processed images and updated object catalogs which are delivered within 24 hr. Non-time-critical science cases, which do not require the Rubin LSST Alert Stream, for example pulsating stars, will primarily coordinate their efforts and science based on the thoroughly-processed Annual Data Releases. As these two sections form the main body of the Roadmap, at the beginning of these sections, we have included an Executive Summary that outlines the section that follows and, where available, includes the detection efficiencies for specific object types.

The next two sections are devoted to the Deep Drilling Fields (DDFs) and Mini-/Micro-surveys, where DDFs are small regions of sky that will receive a significantly larger number of observations, selected to coincide with other missions (see Section 4.1), and Mini-/Micro-surveys are user-defined small surveys with specific science goals (see Section 5.1). We additionally include a section on Methodology and Infrastructure (Section 6) to discuss the infrastructure required for time-critical science (including an extensive list of brokers) and the classification variable stars/objects. Finally, as

it is central to the workings of the TVS, we dedicate a section to equity and inclusion, which can be found in Section 7.1. This section includes the TVS *Call for Action* and the steps the TVS are taking to be a diverse, inclusive and equitable platform, focused on the exploitation of Rubin LSST data.

The four main sections describing the various science cases are further subdivided into:

1. Extrinsic transients and variability: including geometric transients such as microlensing, eclipsing binaries, and transiting planets or debris disks.
2. Intrinsic galactic and Local Universe Transients and Variables: including stellar eruptions, explosions, pulsations.
3. Extragalactic transients: including supernovae (SNe), gamma-ray bursts (GRBs), blazars.

Each of these subsections includes multiple science fields. Each science field includes science cases listed under:

1. Low hanging fruit, which are science cases that are expected to be easily obtainable with the Rubin LSST proposed survey cadence and currently available follow-up facilities and theory and
2. Pie in the sky, which are science goals that are desirable, however, additional developments in facilities and theory may be required and/or it is unknown whether Rubin LSST data will suffice.

For each science field, the requirements for achieving the outlined science cases are described. These include:

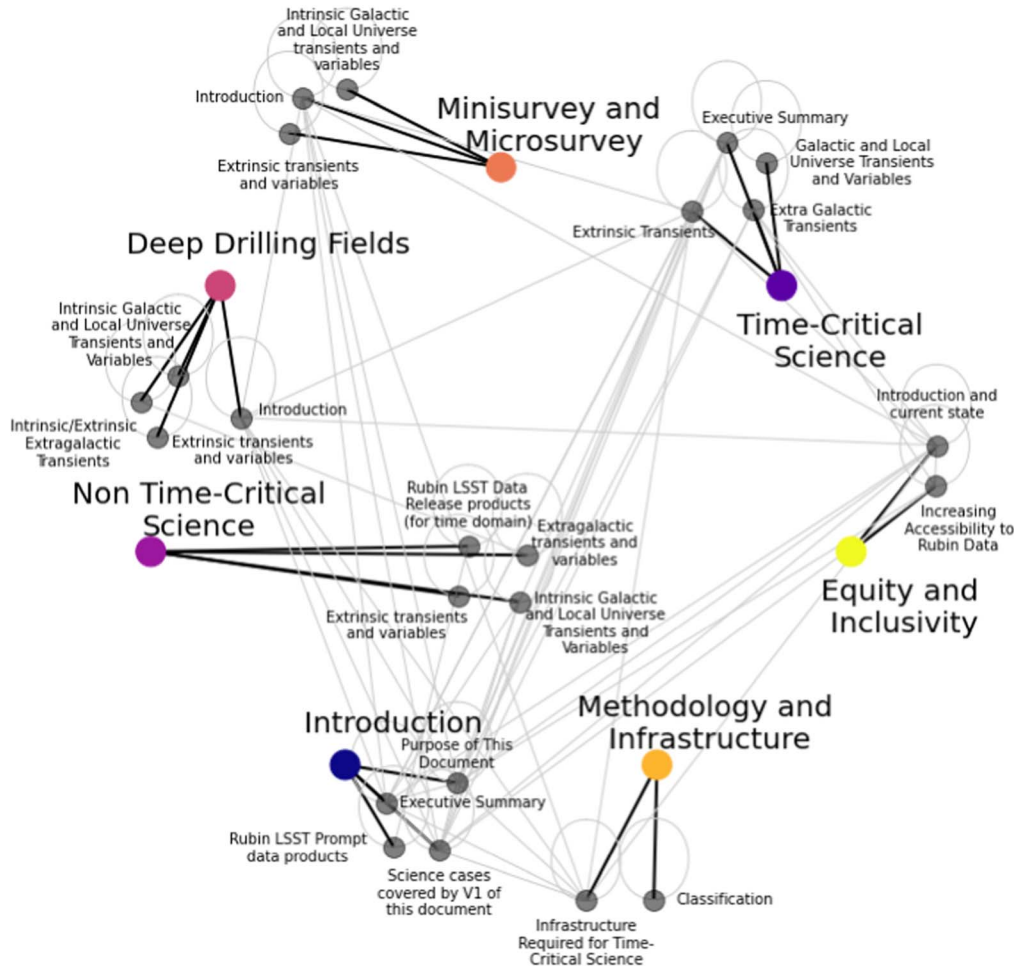
1. Observations needed ahead of Rubin LSST to narrow the space of relevant variables
2. Theory development including models, the theory required to generate predictions for Rubin LSST observables and the data integration activities required to incorporate multi-wavelength/context/other timescale data
3. Computational advancements and infrastructure required to handle Rubin LSST data volume
4. The (type of) facilities that will be used/required, and any upgrades and development needed to support follow-up.
5. Where applicable, the filters that are required for the Alert Stream.

Figure 1 provides a graphical representation of the Roadmap sections and subsections, with author connections depicted by the gray lines. Table 1 provides a table of contents so that the interested reader may swiftly access their science cases of interest.

## 1.2. Rubin LSST Data Products and Their Access—an Overview

### 1.2.1. Rubin LSST Data Products and Their Access

The Rubin Observatory Legacy Survey of Space and Time (LSST) is an astronomical project designed to generate



**Figure 1.** A spider diagram representing the various Sections (colored dots) and Subsections (gray dots) of the Roadmap. The light gray lines denote the author connections between the science cases.

significant advances in four science areas: cosmology (dark matter and dark energy); the solar system (with a focus on potentially hazardous asteroids); the Milky Way; and transient phenomena. To do this, the Rubin LSST will deliver a deep survey that covers  $\sim 18,000$  square degrees in the southern sky and will detect  $\sim 40$  billion stars and galaxies (Ivezic et al. 2008). A total of  $\sim 825$  visits to each part of the sky within this area will be made in six filters, *ugrizy*, over 10 yr. About 10% of the observing time will be devoted to community-proposed special programs that extend the areal coverage, depth, and/or sampling cadence (e.g., Mini-surveys, Deep Drilling Fields). Rubin LSST currently estimates that full operations will begin in late 2024.

Rubin LSST will: acquire  $\sim 20$  terabytes of raw data each night and process it in real-time; distribute alerts on objects that vary in brightness or position within 60 s; deliver processed images and updated object catalogs within 24 hr; and release a yearly reprocessed data set including deep image stacks

(Jurić et al. 2018). To enable science with this massive data set, the Rubin LSST Data Management System includes the Science Platform: a web-based service for data access, analysis, and processing that includes software tools and computational resources (Jurić et al. 2017). We discuss the Prompt and Data Release data products in further detail in Sections 2.2 and 3.2, respectively.

### 1.2.2. Remotely Accessible Computing Platforms for LSST Science

The size of the LSST data products, particularly the image data, is expected to break the traditional paradigm of astronomers downloading a dataset to their local machine for analysis. For many large scale analyses, it will be unfeasible or prohibitively expensive in cost and time for many users to download sufficient data for their purposes. Instead, Rubin science users are transitioning to a “next-to-the-data” paradigm, where vast data products are hosted at large, central Data

**Table 1**  
Table of Contents for Navigating This Roadmap

<i>Section</i>	<i>Section Heading</i>	<i>Page</i>
<b>1</b>	<b>Introduction</b>	<b>2</b>
1.1	How To Navigate This Document	2
1.2	Rubin LSST Data Products and their access—An Overview	3
1.2.1	Rubin LSST Data Products and their access	3
1.2.2	Remotely—Accessible Computing Platforms for LSST Science	4
1.3	Purpose of This Document	6
<b>2</b>	<b>Time Critical science</b>	<b>6</b>
2.1	Executive Summary	6
2.2	Rubin LSST Prompt Data Products	7
2.2.1	Quantities of Particular Importance to Time-Domain Studies	7
2.3	Extrinsic Transients	7
2.3.1	Microlensing	7
2.3.2	Eclipsing Binary Stars	10
2.3.3	The Search for Extraterrestrial Intelligence	11
2.4	Galactic and Local Universe Transients and Variables	12
2.4.1	Young Eruptive Protostars	12
2.4.2	Compact Binaries: Cataclysmic Variables	15
2.4.3	Compact Binaries: Neutron Star Binaries	16
2.4.4	Compact Binaries: Black Hole X-ray Binaries	17
2.5	Extra Galactic Transients	19
2.5.1	Supernovae	19
2.5.2	Intermediate-Luminosity Optical Transients	21
2.5.3	Gamma-ray Bursts	24
2.5.4	Blazars	26
2.5.5	Tidal Disruption Events	29
2.5.6	Electromagnetic Counterparts of Gravitational Wave Events	31
<b>3</b>	<b>Non Time-Critical Science</b>	<b>35</b>
3.1	Executive Summary	35
3.2	Rubin LSST Data Release products (for Time Domain Science)	36
3.3	Extrinsic Transients and Variables	37
3.3.1	Transiting Exoplanets	37
3.3.2	Eclipsing Binary Stars	38
3.3.3	Microlensing	42
3.4	Intrinsic Galactic and Local Universe Transients and Variables	43
3.4.1	Pulsating stars: General	43
3.4.2	Pulsating Stars: Cepheid and RR Lyrae Stars	45
3.4.3	Pulsating Stars: Long-period Variables	47
3.4.4	Galactic Globular Clusters	50
3.4.5	Brown Dwarfs	51
3.4.6	Young Eruptive Variables	54
3.4.7	Compact Binaries: Cataclysmic Variables	56
3.4.8	Compact Binaries: Neutron Star Binaries	58
3.4.9	Compact Binaries: Black Hole X-ray Binaries	59
3.4.10	Luminous Blue Variables	61
3.4.11	Light Echoes of Eruptions and Explosions	62
3.5	Extragalactic Transients and Variables	64
3.5.1	Blazars	64
3.5.2	Supernovae	65
<b>4</b>	<b>Deep Drilling Fields Science Cases</b>	<b>68</b>
4.1	Introduction	68

**Table 1**  
(Continued)

<i>Section</i>	<i>Section Heading</i>	<i>Page</i>
4.2	Extrinsic Transients and Variables	69
4.2.1	Transiting Exoplanets	69
4.2.2	Eclipsing Binary Stars	69
4.3	Intrinsic Galactic and Local Universe Transients and Variables	70
4.3.1	Pulsating Stars	70
4.3.2	Brown Dwarfs	72
4.3.3	Compact Binaries: AM CVn and Ultracompact Binaries	73
4.3.4	Compact Binaries: Neutron Star Binaries	73
4.3.5	Intermediate Luminosity Optical Transients	74
4.4	Intrinsic/Extrinsic Extragalactic Transients	74
4.4.1	Blazars	74
<b>5</b>	<b>Minisurvey and Microsurvey Science Cases</b>	<b>75</b>
5.1	Introduction	75
5.2	Extrinsic Transients and Variables	76
5.2.1	Microlensing	76
5.2.2	Eclipsing Binary Stars	77
5.2.3	Interstella Scintillation Toward the Magellanic Clouds	77
5.3	Intrinsic Galactic and Local Universe Transients and Variables	79
5.3.1	RR Lyrae Stars	79
5.3.2	Brown Dwarfs	80
5.3.3	Variables Stars	80
5.3.4	Compact Binaries: Neutron Star Binaries	81
5.3.5	Intermediate Luminosity Optical Transients	81
5.3.6	Young Stellar Objects	82
<b>6</b>	<b>Methodology and Infrastructure</b>	<b>84</b>
6.1	Infrastructure Required for Time-Critical Science	84
6.1.1	Rubin LSST Prompt Data Products and Alert Stream	84
6.1.2	Rubin LSST Alert Brokers	84
6.1.3	Managing Follow-up Programs	87
6.2	Classification	88
6.2.1	The Classification of Periodic Variables	88
6.2.2	Transient and Anomalies Classification Algorithm	89
<b>7</b>	<b>Equity and Inclusivity in the Transient and Variable Stars Science Collaboration</b>	<b>90</b>
7.1	Introduction and Current State	90
7.1.1	TVS Call for Action: Current Progress and Future Commitments	91
7.2	Increasing Accessibility to Rubin Data	93
7.2.1	Sonification	93
7.2.2	3D Rendering of Rubin Data	94
<b>8</b>	<b>Summary and next steps</b>	<b>96</b>
<b>9</b>	<b>Acknowledgements</b>	<b>96</b>

Access Centers, and made accessible through online platforms that users can interact with through their browser. At the time of writing, the Rubin LSST Science Platform is the most developed of these platforms, and the community are encouraged to gain experience with analysis using its tools through the Rubin Data Previews. We note that other platforms

**Table 2**  
Summary of Data Access Functionality Required by Different TVS Science Topics

Tool	Pulsating Stars	EXor/FUor	Blazars	Microlensing	Brown Dwarfs	Eclipsing Binaries
Image inspection	Yes	...	Yes	Yes	...	Yes
Interactive plotting	Yes	...	Yes	Yes	Yes	Yes
Database search	Yes	Yes	Yes	Yes	...	Yes
Python notebooks	Yes	...	Yes	Yes	Yes	Yes
APIs	Yes	Yes	...	Yes	...	Yes

are in the process of development and offer complementary and overlapping functionality, such as the LINCC Computing facilities<sup>64</sup> offered by the DIRAC Institute and the University of Washington.

The Rubin Science Platform offers three main aspects: an interactive web portal by which the database contents can be searched and visualized, a Jupyter notebook aspect providing an interactive coding environment and Application Programmable Interfaces (APIs), to enable queries of the Data Access Centers by remote services. In the expectation that different science use-cases might have different requirements for these aspects, we summarize the conclusions of the previous sections in Table 2.

### 1.3. Purpose of This Document

The goals of this document are many-fold, including to:

1. Stimulate research and preparations for Rubin LSST
2. Outline areas of necessary work (theoretical and practical)
3. Identify weaknesses and strengths of different Rubin LSST observing strategies for time domain science
4. Identify areas of research and infrastructure that are currently under prepared.
5. Facilitate the communication of ideas between TVS subgroups and with the other Science Collaborations, and reduce redundancy in our efforts.
6. Build a document that can be referenced in future grant applications.

We note that Rubin LSST has eight Science Collaborations, of which 5 (including TVS) have roadmaps describing their proposed science contributions, many of which overlap with those described here. At the time of writing, alongside the TVS, Science Collaborations with roadmaps include: the Dark Energy Science Collaboration (LSST Dark Energy Science Collaboration 2012), the Galaxies Science Collaboration (Robertson et al. 2017), the Solar System Science Collaboration (Schwamb et al. 2018) and the Active Galactic Nuclei Science Collaboration.<sup>65</sup> These roadmaps provide profound

insight into the expansive science coverage that Rubin LSST will provide. We invite the interested reader to peruse these roadmaps to learn about all the exciting science that we are planning for the years ahead in the era of Rubin LSST.

## 2. Time Critical Science

### 2.1. Executive Summary

The nature and rapid delivery of Rubin LSST Prompt Data Products, combined with the groundbreaking survey volume, will open new areas of time critical science. Here we summarize the primary science goals that are discussed in this chapter.

**Microlensing:** Rubin LSST will detect statistically significant rates of microlensing events across the Galactic Plane and Magellanic Clouds. The baseline survey duration and cadence make the data ideal to search for lensing by isolated black holes, while stellar and planetary events are likely to need follow-up observations in order to characterize the events with sufficient cadence. With Rubin LSST, we can expect an average rate of 15 microlensing events  $\text{deg}^{-2}\text{yr}^{-1}$  in the disk and 400 events  $\text{deg}^{-2}\text{yr}^{-1}$  in the Bulge Sajadian & Poleski (2019).

**Eclipsing Binaries:** During the main survey, Rubin LSST will observe  $\sim 1$  million contact binary stars (Prša et al. 2011). Of these, it is possible that, for the first time, a contact binary undergoing coalescence will be observed. The anticipated signature is the swift reduction of the orbital period.

**Rare anomalies and The Search for Extra Terrestrial Intelligence:** The consistency and duration of Rubin LSST also grants us the opportunity to search for deviations from understood physical behavior. Anomalies often reveal new physics. They can also be considered from the perspective of searching for optical signatures of extra-terrestrial civilizations.

**Eruptions and Accretion Processes:** Rubin LSST will deliver statistically significant population samples of a wide range of intrinsically rare classes of objects. These data will provide insight into astrophysical accretion processes and outbursts occurring in different contexts. These phenomena can be observed in many objects, from pre-main sequence stars to white dwarfs, neutron stars and black hole binaries. In all cases, the Rubin LSST data will highlight the impact of accretion on the evolution of these objects. Uniquely, Rubin LSST will

<sup>64</sup> <https://lsst.dirac.dev/>

<sup>65</sup> Active Galactic Nuclei.

provide both the long-baseline time-series data necessary for quantifying outburst cycles and object occurrence rates as well as the rapid alerts necessary for identifying outburst phases in progress, thus triggering more detailed follow-up studies.

**Explosive Transients:** Rubin LSST will discover extensive samples of each class of novae: intermediate-luminosity optical transients, SNe, kilonovae, and GRBs. These observations will reveal the mechanisms at work during and after the explosion or during mergers. The best estimate currently available for the nova rate in the Galaxy is  $\sim 50$  nova/yr, although with large uncertainty (e.g. Shafter 2017).

**Active Galaxies:** Rubin LSST alerts will enable the swift multi-wavelength follow-up of blazar flux-variations, including flairs. The community should expect a constant rate of 100 gamma-ray bursts/year, with at least one third of them being observable by Rubin LSST. The optical counterparts of known blazars will also be observed and will reveal the nature of double black hole binaries and the nature of neutron production in blazar jets.

**Tidal Disruption Events:** Due to the depth and temporal sampling of Rubin LSST, the number of observed tidal disruptive events (TDEs) is expected to increase by two orders of magnitude from  $\sim 10$  to  $\sim 1000$  yr<sup>-1</sup> (van Velzen et al. 2011; Bricman & Gomboc 2020). This will enable studies of supermassive black holes, host galaxies, the black hole occupation fraction and the central black hole occurrence as a function of redshift. Additionally, Rubin LSST will allow for the probing of the optical emission, the cause of which is currently under dispute.

**Gravitational Waves:** Rubin LSST's target of opportunity program will be used to perform swift electromagnetic follow-up of the gravitational waves produced by neutron star mergers, black hole mergers and black hole-neutron star mergers. The early follow-up observations of kilonovae will be triggered by Rubin LSST's rapid alerts. With Rubin LSST, we anticipate that we will detect higher rates of merger events involving neutron stars ( $\sim 10$  per year) out to distances of several hundred Mpc.

## 2.2. Rubin LSST Prompt Data Products

Every standard visit image ( $\sim 30$  s integration) acquired by the Rubin LSST will be immediately reduced, calibrated, and processed with Difference Image Analysis (DIA), wherein a template image (a deep stack of previously obtained images) is subtracted to generate a difference image. All sources detected in the difference image represent the time-variable components of transient phenomena (e.g., SNe), variable stars (e.g., RR Lyrae), and moving objects (e.g., asteroids). For all difference-image sources detected with a signal-to-noise ratio (S/N) of at least 5, an alert packet containing information about the source (location, fluxes, derived parameters, and  $\sim 6'' \times 6''$  cutouts) will be generated and released within 60 s of the end of image

readout. Alerts are world public and can be shared with anyone, anywhere. Alerts on moving objects will be integrated into the Minor Planet Center. Due to the high bandwidth of the Rubin LSST Alert Stream it will only be delivered in full, in real-time, to 7 Alert Brokers<sup>66</sup> (Bellm et al. 2018), who will share them with their communities (some brokers plan to provide public access, e.g., Narayan et al. 2018). All other prompt data products (e.g., visit, template, difference images, and catalogs of difference-image objects) will be made available to Rubin LSST members via the Science Platform within 24 hr, but will be subject to a two yr proprietary period, after which they can be shared with anyone, anywhere, worldwide.

### 2.2.1. Quantities of Particular Importance to Time-Domain Studies

There are four Prompt data types and quantities that we want to highlight that will be specifically useful for time-domain astronomy. First, all detected difference-image sources, for which there has been no variable source previously detected, will have forced photometry performed at their location using the last  $\sim 30$  days of difference images in order to, for example, look for faint precursor events. This is commonly referred to as Precovery Photometry and will be available within 24 hr (as with all Prompt Data Products). Second, all objects that were detected in difference images within the past  $\sim 12$  months will have forced photometry performed at their location in the new difference image in order to, e.g., continue to monitor known objects as they fade. This forced photometry will be available within 24 hr. Third, the catalog of difference-image sources will contain some light curve characterization parameters for, e.g., periodic and non-periodic features. The exact nature of these parameters is to be determined, but they will be updated to include new observations within 24 hr. Fourth, all difference-image sources will be associated with the nearest static-sky objects from the Data Release data products (see Section 3.2), so that the potential host galaxy and/or longer-term information about the variable star can be easily obtained. These associations will be included in the alerts and in the difference-image source catalogs. See also Jurić et al. (2018) for a full description of the Rubin LSST data products.

## 2.3. Extrinsic Transients

### 2.3.1. Microlensing

Microlensing occurs when a foreground object, lens  $L$ , passes directly between the observer,  $O$ , and a luminous background source,  $S$  (Paczynski 1986) as in Figure 2.

A review of the microlensing formalism can be found in Rahvar (2015). The gravity of the lens deflects light from the source with a characteristic radius,  $R_E$ , causing the source to

<sup>66</sup> Find the list of brokers at <https://lsst.org/scientists/alert-brokers>.



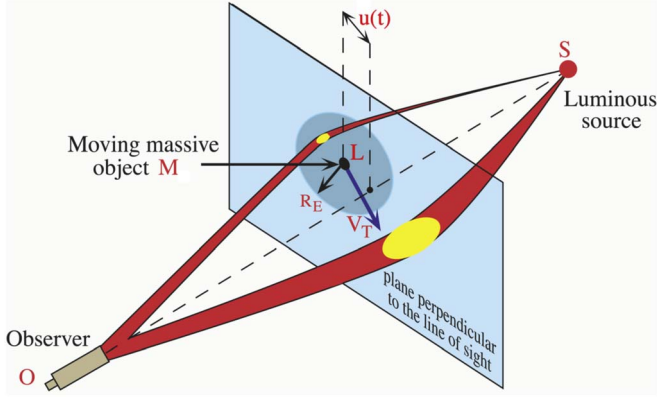


**Figure 2.** Microlensing occurs when a massive foreground object (lens,  $M$ ) crosses between the line of sight of an observer ( $O$ ) and a background star (source,  $S$ ). The figure shows how the gravity of the lens deflects light from the source toward the observer.  $R_E$  corresponds to the Einstein ring radius of the lens,  $v_T$  is the relative lens-source proper motion, and  $u(t)$  the instantaneous impact parameter. Reproduced from Moniez, 2010, with permission from Springer Nature.

brighten and fade as it moves into and out of alignment with a timescale  $t_E$  that scales with the square root of the lens mass (years for black holes, days to weeks for planets and stars). Assuming that a single point-like lens of mass  $M$  located at distance  $D_L$  is deflecting the light from a single point-like source located at distance  $D_S$ , the characteristic radius (Einstein radius)  $R_E$  is given by:

$$R_E = \sqrt{\frac{4GM}{c^2} D_S x(1-x)} \approx 4.54 \text{ au} \left[ \frac{M}{M_\odot} \right]^{\frac{1}{2}} \left[ \frac{D_S}{10 \text{ kpc}} \right]^{\frac{1}{2}} \frac{[x(1-x)]^{\frac{1}{2}}}{0.5}, \quad (1)$$

where  $G$  is the Newtonian gravitational constant, and  $x = D_L/D_S$ . If the lens is moving at a constant relative transverse velocity  $v_T$ , the characteristic lensing timescale is given by:

$$t_E \sim 79 \text{ days} \times \left[ \frac{v_T}{100 \text{ km s}^{-1}} \right]^{-1} \times \left[ \frac{M}{M_\odot} \right]^{\frac{1}{2}} \left[ \frac{D_S}{10 \text{ kpc}} \right]^{\frac{1}{2}} \frac{[x(1-x)]^{\frac{1}{2}}}{0.5}. \quad (2)$$

The so-called simple microlensing effect (point-like source and lens with rectilinear motions) has several characteristic features. Given the low probability of the alignment, the event should:

1. Be singular in the history of the source (as well as of the deflector)
2. Have magnification due to lensing, independent of the color, that is a simple function of time with a symmetrical shape

3. Have a uniform prior distribution for the events' impact parameter  $u_0$  (minimum distance,  $u(t)$ , see Figure 2) owed to the fact that the source and the deflector are independent
4. Have the same lensing probability as all stars at the same given distance and toward a given direction.

Consequently, the sample of lensed stars should be representative of the monitored population at that distance, particularly with respect to the observed color and magnitude distributions.

Since this phenomenon does not require light to be detected from the lens itself, microlensing enables the exploration of populations that are otherwise hidden from view due to their distance and/or intrinsic luminosity.

Rubin LSST offers two complementary opportunities for microlensing discoveries: by extending the Wide-Fast-Deep survey to cover the Galactic Plane and by conducting coordinated observations of a single Rubin pointing located on the Roman Space Telescope Bulge survey region. Here we describe the science cases from both observing strategies and discuss their promising scientific yield.

#### 1. Low hanging fruit

##### (a) Galactic Plane Survey: Galactic population of single and binary black holes.

Stellar evolution models imply that there should be millions of black holes residing in our galaxy (Gould 2000). The past and present microlensing surveys all suffered from a drastic decline in the detection efficiency for events with durations ( $t_E$ ) larger than a few years, which are expected from massive lenses ( $M > 20 M_\odot$ ). This is why the published limits on the contribution of compact objects to the Galactic dark matter were not very constraining beyond this mass. Recently, and following Mirhosseini & Moniez (2018), new limits have been published on the contribution of halo objects in the mass range  $10 M_\odot < M < 1000 M_\odot$  by combining EROS-2 and MACHO data (Blaineau et al. 2022), that contain 14.1 million objects in common, consequently monitored for 10.6 yr. This result illustrates the potential of 10 yr of continuous observation. The light curves measured by Rubin LSST, eventually completed by the aforementioned surveys, will reach the precision either to detect heavy black holes up to a few thousands of  $M_\odot$  and measure their Galactic density or to exclude the possibility that they form a significant fraction of the Galactic hidden matter.

The main condition for succeeding in this task is to ensure that the time-sampling of the Galactic fields and of the LMC/SMC spans the entire Rubin LSST survey duration and avoids very long gaps within the light-curves (apart from the inevitable inter-seasonal

gaps). Upon completion of the 10 yr survey, for the long timescale events, the final efficiency will not be impacted by the finer details of the cadence, so long as long gaps are avoided. In this search, the past and present survey databases will add precious information to confirm or not microlensing candidates found with Rubin LSST alone.

Rubin LSST will complement the results from the gravitational wave observatories, since it is capable of directly measuring the statistical abundances of intermediate mass black holes (single or multiple), through their lensing effect on background sources. Rubin LSST will reach fainter magnitudes than OGLE ( $< 25$   $i$ -band mag versus  $< 21$   $i$ -band mag), so we expect that by monitoring a few billion stars in the Galactic Plane, we will detect hundreds of microlensing events due to black holes.

(b) **Observing Self-lensing in the Magellanic Clouds**

By including the Magellanic Clouds in the Wide-Fast-Deep survey, Rubin LSST will be able to detect microlensing events where both the lens and the source both lie in the Clouds. Hence Rubin LSST will explore stellar and stellar remnant populations in another galaxy. By conducting a long duration, self-consistent survey that includes the Milky Way Bulge, Galactic Disk and both Magellanic Clouds (LMC, SMC) Rubin LSST will compare the populations in different local environments with different star formation histories. Since microlensing events are transients, new events reveal more of the underlying population each year.

(c) **Understanding the Galactic and Extra-galactic population of planets and low-mass stars**

Despite outstanding discoveries from Kepler (Borucki et al. 2010) and other surveys, the vast majority of known exoplanets lie within 1 kpc of the Sun.<sup>67</sup> Microlensing can probe to much greater distances ( $\leq 8.5$  kpc) and is sensitive to planetary systems with planets of all masses in orbits between  $\sim 1$ – $10$  au (Bond et al. 2001, 2004). The microlensing rate for surveys outside the Bulge has been measured in a few fields by Moniez et al. (2017) and estimated for Rubin LSST by Sajadian & Poleski (2019) based on the Reference Simulated Survey, *minion\_1016 OpSim*<sup>68</sup> with minimal coverage of Plane fields. They found an average rate of 15 events  $\text{deg}^{-2} \text{yr}^{-1}$  in the disk and 400 events  $\text{deg}^{-2} \text{yr}^{-1}$  in the Bulge. This detection rate can be doubled if the cadence is increased from 6 to 2 days. The “edge-on” orientation

of the SMC results in a higher probability of self-lensing (where both source and lens lie within the same galaxy), raising the possibility of detecting stellar and perhaps even planetary companions in a galaxy other than the Milky Way (Stefano 2000). Rubin LSST is predicted to detect 20–30 events per year in the SMC (Mróz & Poleski 2018), provided the SMC is monitored at least once every few days.

2. Pie in the sky

(a) **Galactic Plane Survey: mesolensing**

The rate of microlensing events scales as  $\sim D_L^{-3/2}$ , so nearby objects traveling at relatively high angular velocities are more likely to lens background stars than similar more distant objects (Stefano 2000, 2008). Rubin LSST will investigate the mass distribution of faint objects in the local neighborhood, such as low mass dwarfs, stellar remnants, and free-floating planets.

(b) **Galactic Plane Survey: predicted lensing**

Measurements of stellar proper motions with Rubin LSST will be valuable for predicting future microlensing events, as has been done from Gaia and Pan-STARRS 1 data (to shallower limiting magnitudes than Rubin LSST, Neilsen 2018).

*Preparations for Microlensing Science.* Microlensing events are transient in the sense that they are non-repeating, so almost all observations must be obtained during the course of a given event. Until now, searches for microlensing effects by 1–2m class telescopes have mainly detected events with strong amplification, corresponding to an impact parameter  $u_0 < 1$ . Looking forward, we will strongly benefit from the large diameter of Rubin LSST as thus will significantly improve the detection rate of weakly amplified events that have an impact parameter  $u_0 > 1$ .

The scientific goals described above necessitate the following capacities:

1. **Identifying events from alerts**

The first step in achieving the aforementioned science goals detailed as “Low hanging fruit” and “Pie in the sky” is thus to accurately identify microlensing events from Rubin LSST data, at the earliest stage possible. Heavy use of the Rubin LSST Prompt Data Products via one or more broker service is therefore anticipated, where the task of a broker is to identify targets of interest. Recent work by Godines et al. (2019) includes the application of machine learning techniques to identify microlensing events using alerts from the ZTF survey as a precursor; this is complemented by the development of metrics by Khakpash et al. (2021). Work is underway to apply Godines’ software LIA<sup>69</sup> as a filter

<sup>67</sup> <https://exoplanetarchive.ipac.caltech.edu/>

<sup>68</sup> <https://docushare.lsst.org/docushare/dsweb/Get/Rendition-39253/unknown>

<sup>69</sup> <https://github.com/rachel3834/LIA>

within the ANTARES<sup>70</sup> and the FINK<sup>71</sup> brokers, thereby supplying a detection stream to the community. We note that at the time of this writing, a number of ANTARES and FINK filters include microlensing as one of their alert products. However, more work is required to test and improve the performance of these filters in Rubin LSST-like data sampling with a realistic range of events, and to understand the selection biases. It is worth mentioning that the Photometric Rubin LSST Astronomical Time-Series Classification Challenge (PLAsTiCC, Kessler et al. 2019) has provided a large sample of simulated Rubin LSST-like light curves including a microlensing event that has initiated the development of machine learning algorithms to classify Rubin LSST light curves. In order for the classifiers to perform well, microlensing blending, second order effects like parallax, and finite source effects should be simulated more accurately.

## 2. Follow-up observations

Long timescale (several years) Rubin LSST light curves for black hole candidates are likely to be of sufficiently high cadence to mitigate the need for additional timeseries photometry. However, this is not true for stellar lensing candidates, which can exhibit anomalous variations on timescales, sometimes hours or days. Timeseries imaging of selected targets will therefore need to be obtained in rapid (<1 day) response to alerts and will sometimes need to continue for  $\sim$ weeks, with the cadence dynamically scaled to match the evolving features of the targets.

Spectroscopic follow-up of all selected candidates will be highly desirable for helping characterize the source star and for deriving an independent estimate of its angular size and distance. This information is essential for resolving degeneracies in the microlensing model.

High spatial resolution imaging, both during and several years after the event, can also be used to constrain the properties and motion of the lens.

Although microlensing events can brighten by several magnitudes, a high fraction of Rubin LSST candidates are expected to be fainter than  $i > 17.0$  mag. Photometric follow-up will require narrow-field optical (and ideally NIR) imagers on 2–4 m class telescopes, while spectroscopy will require high throughput spectrographs of  $R \sim$  few 1000 on 4–10 m facilities. AO imaging will be restricted to the brighter targets and will require 10 m class facilities.

## 3. Facilities/software requirements

Depending on the survey strategy, Rubin LSST is likely to produce a few hundred microlensing alerts outside the Galactic Bulge per year and thousands of

events within it, with a false alarm rate which has yet to be determined. Since timeseries follow-up as well as rapid-response observations will be required, a Target and Observation Manager (TOM) system will offer great advantages for managing the overall program and coordinating observing efforts.

### 2.3.2. Eclipsing Binary Stars

Binary systems are objects containing two or more stellar components that orbit around a common center of mass. When binary systems are oriented along a preferential line of sight, such that the stars pass in front of each other during their orbit, the binary system is classified as eclipsing. Eclipsing binary stars are typically considered non-transient: although extrinsically variable, most systems exhibit strictly periodic observables. Deviations from strict periodicity are, however, due to transient phenomena: spots, pulsations, gravitational and magnetic interactions between components, third body interactions, stellar evolution effects, etc. Thus, we consider these time-critical transient phenomena *extraneous* to binarity: the time-sensitive triggers should be driven by the respective transient science rather than binarity. The benefit of finding transients in binaries, of course, is access to fundamental stellar parameters; we defer the discussion of this aspect to Section 3.3.2.

One exception to the above statement is coalescence. The merging of two compact objects (white dwarfs, neutron stars or black holes) has garnered significant attention recently thanks to the recent successes in gravitational wave physics (Abbott et al. 2016). Yet, coalescence of contact binary systems (two main sequence stars sharing a common envelope) is interesting in its own right. The wealth of physics that accompanies such a dramatic event spans plasma physics, equations of state, radiative properties, energy flows with mass transfer, all the way to outbursts and rapid rotation effects. Given that contact binaries are very common (about 15% of all eclipsing binary systems), Rubin LSST is well positioned to catch such coalescence events over its nominal 10 yr survey.

#### 1. Pie in the sky

##### (a) Detecting a contact binary coalescence event

We have yet to observe such an event. The Rubin LSST survey certainly offers the prospect of capturing such an event for the first time. The 10 yr baseline for observing the expected  $\sim$ 1 million contact binaries (Prša et al. 2011) will likely catch many candidates that exhibit a decreasing orbital period; of those, the prime candidates will feature a rapid, accelerated period decrease. There should be immediate follow up on these events with point-and-stare instruments.

*Preparations for Eclipsing Binary Science.* As stated above, the vast majority of the eclipsing binary deliverables from

<sup>70</sup> <https://antares.noirlab.edu/>

<sup>71</sup> <https://fink-broker.org/>

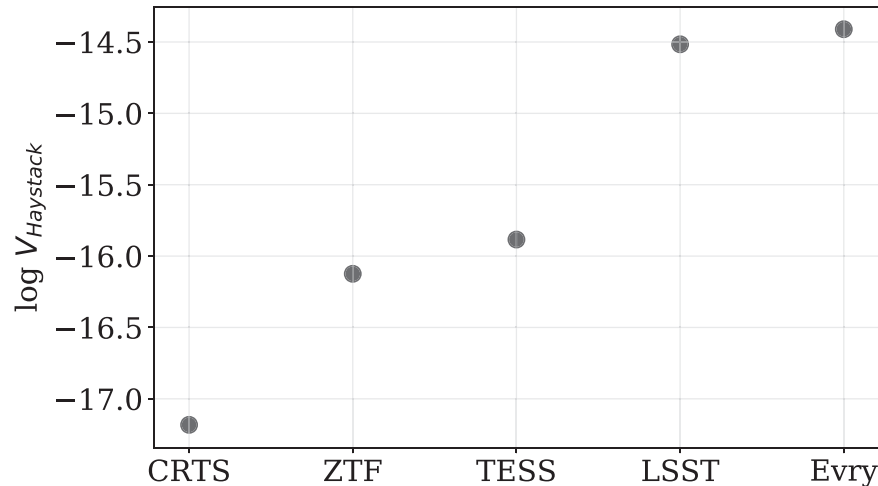


**Figure 3.** Comparison of the 8D “Cosmic Haystack” SETI search volume fraction, defined by Wright et al. (2018), computed using five optical surveys with varying designs. The Haystack fraction covered by these optical surveys is 1–2 dex larger than typical SETI programs conducted in the radio. Evryscope (Law et al. 2015) is the best survey considered here for SETI work, narrowly beating Rubin LSST due to its wide field of view and very dense light curves. Reproduced with permission from Davenport (2019).

Rubin LSST are non-time-critical. Coalescence is the exception. A coalescence event (the merging of two non-compact stars) will inevitably be a dramatic event: as the stars spiral inwards, the light curve periodicity will deteriorate and bursts of highly variable light are expected. We can bank on that variability to trigger follow-up observations of possible coalescence events.

#### 1. Identifying events from alerts

A binary light curve that corresponds to a possible coalescence precursor will exhibit a significant period shortening, followed by a number of highly variable light events. These are likely to trigger an alert. This alert should be straight-forward enough to identify and pass from the event brokers to follow-up facilities.

#### 2. Follow-up observations

Once identified, a coalescence event should be followed up photometrically and spectroscopically as quickly and as completely as possible. The process of two stars coalescing into a single rapidly rotating star has yet to be observed, but the presence of blue stragglers and yellow giants clearly indicate that these events *do* happen. While the timescales for coalescence are uncertain, and thus far only theorized, an immediate follow-up campaign is crucial for catching and characterizing a coalescence event as it is happening.

#### 3. Facilities/software requirements

Brokers are needed to properly flag a short-period (0.1–0.3 day) light curve with a shortening orbital period that starts to exhibit high amplitude light variations as these might be telltale signs of a coalescing binary system. Such events should trigger alerts for manual

vetting and, if confirmed, immediate follow-up. Depending on the magnitude of the observed object, we need some of the largest observatories pointing to it as quickly as possible, and following up for as long as possible.

#### 2.3.3. The Search for Extraterrestrial Intelligence

Traditional Searches for Extraterrestrial Intelligence (SETI) and searches for “technosignatures” (signatures in the data unexplainable by natural phenomena) currently focus on dedicated observations of single stars or regions in the sky with the aim to detect excess or transient emission from intelligent sources. The latest generation of synoptic time domain surveys, for which Rubin LSST is the flagship, enable an entirely new approach: spatio-temporal SETI, where technosignatures may be discovered from spatially resolved sources or multiple stars over time (Figure 3).

Optical searches for SETI rely on four families of technosignatures:

1. Unnatural orbit alterations of objects in the solar system (Loeb 2016).
2. Unnatural flux patterns of otherwise normal astrophysical variability (e.g., flares, pulsations, transits, etc), such as broadcasting a prime or Fibonacci sequence using transits (Arnold 2005; Guillochon & Loeb 2015; Benford & Benford 2016; Wright 2016).
3. Spatial correlations of events or phenomena: e.g., coordination of transiting systems, or rebroadcasting events such as novae along the “SETI ellipse” (the ellipsoid for receiving synchronized signals from multiple transmitters;

Makovetskii 1977; Lemarchand 1994; Tarter 2001; Shostak & Villard 2004).

4. Spatial over-densities or unusual distributions: e.g., an over-density within the “Earth Transit Zone” band of stars that would see Earth as a transiting exoplanet (Heller & Pudritz 2016), or in spatial clusters (Davenport 2019).
5. Unusual variability profiles or statistical distributions of fluxes. These can occur either on short timescales such as Boyajian’s Star (Marengo et al. 2015) or long timescales such as disappearing stars (Villarroel et al. 2019). Occasionally, missing transits can also be detected (Kipping & Teachey 2016).

All of these signals are expected to be exceedingly rare, making the search for SETI a truly difficult problem of anomaly detection, a proverbial needle in the haystack. Specific anomaly detection algorithms for the technosignatures we listed above need to be designed to tap into the enormous discovery potential that Rubin LSST’s data rate and complexity uniquely enable.

#### 1. Low hanging fruit

##### (a) Establishing a baseline for signals

Spatiotemporal monitoring of the Rubin LSST sources, in conjunction with multiwavelength observatories, will enable the establishment of a baseline for signals at the relevant frequencies. The short timescale variations can be explored with a novel observation methodology in which the Rubin LSST telescope tracking is turned off during exposures in order to produce star trail images (Thomas & Kahn 2018). These trailed images enable photometric time series to be measured for bright sources with a time resolution of 14 ms. The 9.62 square-degree Rubin LSST field-of-view dramatically extends the reach of this technique and will enable the first large scale search of this kind. The combination of these high frequency observations with standard Rubin LSST observations and those of complimentary multiwavelength observatories, will enable the creation of a framework for the detection of anomalies.

#### 2. Pie in the sky

##### (a) Detection of anomalous signals

The detection of anomalous signals or unknown-unknowns would have a profound impact on our understanding of life. A credible technosignature detected by Rubin LSST would be an invaluable discovery. While contact is not something that could be attempted with Rubin, any credible detection of anomalies that remain unexplained by any physical process would be transformational with profound implications for our self-perception and our society. As such a discovery has not yet been made, the

timeline for such a discovery would encompass the complete 10 yr survey.

#### *Preparations for SETI.*

##### 1. Identifying events from alerts

As the unnatural nature of a SETI signal is expected to be recognized through the identification of unphysical patterns, it is unlikely that a single nightly alert will generate a SETI trigger (with the exception of interstellar objects transiting in our solar system, a purview of the Solar System Science Collaboration). However, a collection of nightly alerts may be identified as a potential technosignature, and in that case immediate follow up would be desired as, due to the possible deliberate nature of the signal, it could be turned off at any time.

##### 2. Follow-up observations

All anomalous detections of this nature would require follow-up: intense, rapid follow-up in multiple wavelengths and at different time scales to ascertain the anomalous nature of the phenomenon.

##### 3. Facilities/software requirements

To fulfill the revolutionary discovery potential of the Rubin LSST project, new SETI algorithms and tools in the data-driven spatiotemporal domain are under development Davenport (2019), including a SETI framework for ingesting these alerts and searching for technosignatures in real time. Davenport (2019) provides a roadmap for the development of most of this software. A cumulative database can be re-analyzed, providing reproducibility and transparency that will increase the credibility of detections (Wright et al. 2018) Software for detection of anomalous sources in the solar system would be a purview of the Solar System Science Collaboration (Schwamb et al. 2019).

## 2.4. Galactic and Local Universe Transients and Variables

### 2.4.1. Young Eruptive Protostars

Intense accretion activity is a defining feature of the large majority of pre-main sequence stars. While small and irregular photometric variations (typically 0.2–1 mag) caused by disk accretion variability are commonly seen in the light curves of many classical T Tauri stars, some young sources display powerful UV-optical outbursts of much larger intensity (up to 4–6 mag, see Figure 4). So far, only ~20 objects have been recognized as “genuine” eruptive protostars (Audard et al. 2014) and even fewer have been monitored long-term.

Depending on their different properties (burst duration, recurrence time between subsequent bursts, accretion rate, presence of absorption or emission lines), young eruptive protostars are classified either as FUors (Hartmann &

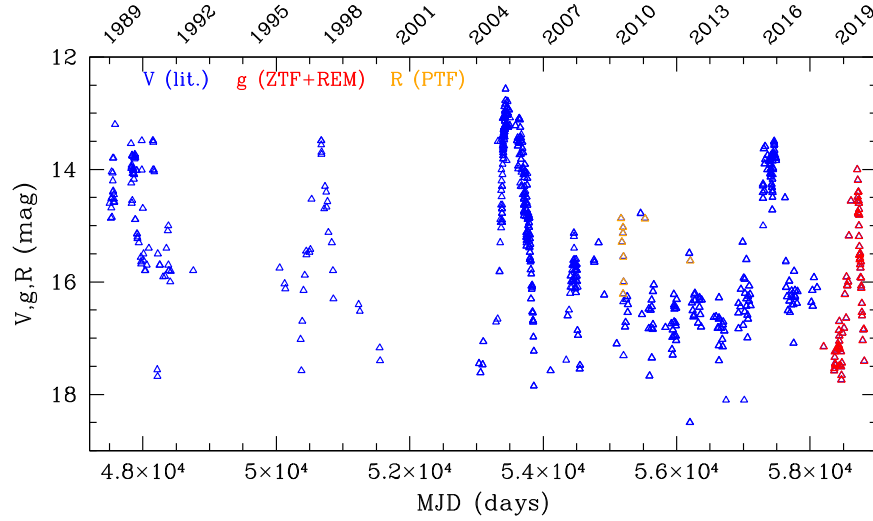


**Figure 4.** A 30 yr optical light curve of the EXor V1118 Ori. The data are taken from literature ( $V$ -band), from the Zwicky Transient Facility and robotic telescope Rapid Eye Mount ( $g$ -band) and from Palomar Transient Factory ( $R$ -band). Reproduced with permission from Giannini et al., 2020. © The European Southern Observatory (ESO).

Kenyon 1985) or EXors (Herbig 1989). Observationally, FUors and EXors are very different objects. FUors are characterized by bursts of long duration (tens of years) with accretion rates of the order of  $10^{-4}$ – $10^{-5} M_{\odot} \text{yr}^{-1}$  and spectra dominated by absorption lines. EXors undergo shorter outbursts (on the order of months to a one year) with a recurrence time of months to years and accretion rates of the order of  $10^{-6}$ – $10^{-7} M_{\odot} \text{yr}^{-1}$ ; they are characterized by emission line spectra.

For both classes of objects, it is believed that bursts are due to accretion of material that piles up at the inner edge of the disk (D’Angelo & Spruit 2010). However, the mechanism responsible for triggering the burst is not known: proposed scenarios involve gravitational or thermal instabilities inside the disk (Audard et al. 2014) or perturbation by an external body (orbiting planets or close encounters with nearby stars). At the moment, however, *none of the proposed models are able to provide a realistic view of the observed burst phenomenology*. The primary cause of this is the scarcity of observations, which prevents us from establishing tight constraints for the physical parameters involved.

The unprecedented sensitivity, spatial coverage, and, even more importantly, observing cadence of Rubin LSST will enable the first ever *statistical* approach to discovering and monitoring eruptive protostars. In particular, both the telescope’s lifetime and the sky coverage cadence will permit optimal monitoring of EXor-type variables.

#### 1. Low hanging fruit

##### (a) **Significantly increase the number of new EXor candidates identified in the Galaxy**

Approximately 20 EXors are known so far, mostly found serendipitously during observational campaigns dedicated to different scientific aims. With

Rubin LSST, we will have an unprecedented opportunity to significantly improve this number. Considering an  $r$ -band limiting magnitude of 24.7 for a single visit, we will observe all the stars with an  $r$ -band  $\sim 15$ , even in obscured regions (with  $A_V \leq 10$  mag). Our selection criteria will be based on the following criteria: the object’s location in a star formation region; the shape of the spectral energy distribution (SED), both in and out of the high brightness phase; a light-curve assessment (rise/decline timescale with a typical duration of months, a speed of about 0.05 mag/day and a burst amplitude between 2 and 4–5 mag in  $g$ -band); the burst duration (months/few years with recurrence expected at months/years); and Rubin LSST color–color analysis (during the burst phase, a significant excess emission in the UV is expected, e.g., Venuti et al. 2015). The Rubin LSST [ $g - r$ ] versus [ $u - g$ ] a color–color diagram represents a powerful diagnostic tool for selecting EXor candidates. Given the optimal sky coverage and cadence of Rubin LSST, we expect to increase the number of EXor candidates by about an order of magnitude during the first year of observations.

##### (b) **Monitor known objects to identify and characterize both their low- and high-brightness states**

The Rubin LSST main survey cadence of a couple of visits per month is ideal for properly sampling the light curves of known objects since it allows the monitoring of the rise/decline phases as well as the probing of the short amplitude variability characteristics in the quiescent phase. Our goals are to

construct a library of the light curves of known objects to be used as a reference for the identification of other members of the EXor class and to measure the physical parameters and the mass accretion rates during different phases of the source activity by means of optical/near-infrared spectroscopic follow-up. Since bursts occur typically every five to ten years, we expect to be able to observe at least one burst in a temporal range of 3–10 yr.

## 2. Pie in the sky

### (a) Discover new FUors and follow their rising phase

With a survey lifetime of about a decade, it is reasonable to expect detections of new FUors. FUor candidates will be selected from the shape of the light curve (monotonic raising with a duration of years with brightness variations up to 5–7 magnitudes) and from the location of the source in a star formation region. Prompt optical, near-IR spectroscopic, and X-ray observations are needed to characterize the physical parameters and the mass accretion rate during the rising and peak phases. FUor outbursts occur typically on time-scales of 100 yr. Therefore, it is likely that the entire telescope lifetime will be needed to discover FUor events.

### (b) Investigate the occurrence of EXor/FUor-like phenomena in evolutionary phases earlier than pre-main sequence

The large majority of EXors/FUors are pre-main sequence stars with an age of about  $10^7$  yr. In principle, however, nothing prevents the existence of eruptive variables younger than pre-main sequence stars (the so-called Class I sources, with ages of about  $10^{5-6}$  yr). However, the detection of very young eruptive variables is challenging. Being still immersed in their natal environment, they are heavily extinguished in the UV and optical bands, i.e., in the photometric bands where the accretion burst is most intense. According to the model by Whitney et al. (2003), a  $1 L_{\odot}$  Class I source at a distance of 140 pc (Taurus, the closest star formation region) has  $g$ -band  $\sim 16$  mag. Considering the  $g$ -band limiting magnitude of 25 per single visit, we will be able to detect a burst of 6–7 mag of such sources provided that the local visual extinction does not exceed 15 mag. Assuming that Class I sources undergo EXor events on timescales similar to pre-main sequence EXors, we expect to observe significant bursts in the first 1–3 yr of the telescope’s lifetime.

*Preparations for Young Eruptive Protostar Science.* Intense accretion activity is a common trait of young, eruptive protostars. The investigation of public surveys (ASAS-SN, Gaia, iPTF, ZTF), as well as the photometric monitoring (e.g., VST/OmegaCAM) of selected star-forming regions, is needed

before Rubin LSST begins in order to refine the above diagnostic tools. To further identify more of these interesting objects, we rely on broker alerts to identify eruptive events, and further follow-up observations and facilities as detailed below:

### 1. Identifying events from alerts

Candidate EXors/FUors can be identified on the basis of:

- (a) Their location within a star-forming region;
- (b) A quasi-monotonic increase of brightness in all bands, with a typical rising time of some hundredths of a magnitude per day. A prompt alert is envisaged because this could trigger a spectroscopic follow-up essential for characterizing the onset of the outburst;
- (c) Colors that become more and more blue with the increase in brightness.

At the time of this writing, none of the available brokers perform color–color analysis and computation of the rising time. Work is needed to ensure young eruptive protostars are identified in the data.

### 2. Follow-up observations

Optical/near-infrared spectroscopic follow-up is needed to confirm the presence of emission lines in the spectrum and to measure the mass accretion rate. Depending on the source brightness and visibility, we will activate ToO observations at the ESO facilities (SoXS, X-Shooter), LBT (MODS, LUCI), and TNG (GIARPS, Dolores, NICS). If a Class I outburst is detected, prompt follow-up with near-infrared imaging/spectroscopy will be activated. Such a discovery would also be worthy of observations with JWST, in order to study the accretion variability in the mid-infrared. Prompt follow-up in X-ray is also envisaged. In this respect, we remark that we will have access to GTO time for SoXS. Also, we have an ongoing program for observations with e-Rosita (Stelzer, Giannini, Bonito; 2018) to study the X-ray emission and its variability in accretion bursts. The eROSITA All-Sky Survey (in safe mode at the time of this writing) started in 2020 and will operate for 4 yrs. This time frame will allow for simultaneous observations with Rubin LSST. Multi-epoch observations, when available, will also be used to explore the variability of these sources in X-rays, thus allowing us to perform a multi-band study of variability.

### 3. Facilities/software requirements

EXor/FUor bursts occur on timescales of months. When an alert is received, we need to investigate the history of the source to reconstruct the light curve in the preceding quiescence phase. We therefore need access to all the Rubin LSST photometric data, that must be stored in a dedicated repository. To store the light curves of all the known eruptive protostars for comparison purposes

and to store all the light curves of perspective protostars, adequate computing storage is required.

#### 2.4.2. Compact Binaries: Cataclysmic Variables

Accretion onto compact objects allows for a powerful probe of binary evolution and accretion physics, particularly for those systems in tight orbits with late-type donor stars (Pala et al. 2022). Several types of systems comprise compact binaries. Cataclysmic variables have accretion onto a white dwarf (WD) and include novae with 10–15 magnitude outbursts caused by thermonuclear runaways on the white dwarf; dwarf novae with 2–9 magnitude outbursts caused by disk instabilities; and nova-like, which have high and low states of accretion (Warner 1995). The AM CVn subclass of cataclysmic variables consists of two white dwarfs, where one is accreting from a mass transferring evolved Helium WD (Solheim 2010). Additional systems include: detached white dwarf binaries; pre-cataclysmic variables consisting of a white dwarf and a low-mass companion that have emerged from a common envelope but not yet begun mass transfer (e.g., Rebassa-Mansergas et al. 2016); and short period detached binaries with a sub-stellar brown-dwarf or planet companions (Dobbie et al. 2005). Low mass X-ray binaries encompass accretion onto a neutron star or a black hole (Van Paradijs & Van der Klis 2001). They experience rare outbursts due to disk instabilities, but also vary between intermediate and quiescent states. Longer-orbital-period high-mass X-ray binaries are also comprised of neutron stars or black holes that are accreting from early type companions (Reig 2011). High-mass X-ray binaries also undergo outbursts due to enhanced accretion, either due to enhanced mass loss from the companion or periastron passage in an eccentric orbit. With a record number of different accretion states among these compact binaries, it has become critical to map the accretion history of each class of objects to correctly frame their evolutionary scenario.

Accretion onto compact objects is driven by angular momentum losses. Mechanisms of angular momentum loss have been identified as magnetic braking in the donor star and gravitational radiation losses. Which mechanism drives the angular momentum loss depends on the nature of the compact binary and its evolutionary phase (Rappaport et al. 1982). It is known that milli-second pulsars, low mass X-ray binaries, and cataclysmic variables can change their accretion states by stopping mass transfer, or by switching from high to low accretion regimes and vice-versa. The timescale for large accretion state variations is usually of the order of days to months for low mass X-ray binaries and milli-second pulsars, and from hours to years for cataclysmic variables and high-mass X-ray binaries.

##### 1. Low hanging fruit

##### (a) Identify new novae

New novae can be identified through the alert system by their outburst amplitudes. Following the alert, the community should activate spectroscopic follow-up observations (especially UV and optical, but virtually across the whole electromagnetic spectrum since novae emit from gamma to radio wavelengths) to physically characterize the event (e.g., ejecta mass, filling factor, duration of the H burning phase, WD composition) and to constrain the WD mass. The best estimate currently available for the nova rate in the Galaxy is  $\sim 50$  nova/yr, although this is largely uncertain (e.g., Shafter 2017).

##### (b) Identify recurrent novae outbursts

Continuous all sky monitoring and monitoring of known novae will potentially allow for the discovery of new recurrent novae (i.e., novae which show more than one outburst on human timescales). Increasing the sample of known recurrent novae together with the ability of characterizing each of their eruptions in detail (through spectroscopic follow-up across the whole electromagnetic spectrum) will allow us to constrain their physical parameters (e.g., ejecta mass and filling factor, super soft source phase duration, WD mass) for the comparative analysis of novae and recurrent novae.

##### (c) Analyze low states of known nova-like

We will monitor the several dozen known nova-like objects that enter low accretion states to determine when they enter these unpredictable low states. When in this state, spectroscopic follow-up will enable the identification of the underlying stars. These low states usually only last for weeks and are the only time when the accretion disk disappears and the stars can be seen. This enables the star masses to be measured in these high accretion rate systems (from time-resolved spectra) to determine their radial velocity curves. With the number of known systems, 1–2 low states are expected each year. As new systems are found during the 10 yr survey, they can be added to the list.

##### (d) Find new high amplitude dwarf novae

Through Broker alerts, the identification of high amplitude dwarf novae (greater than 5 mag, known as superoutbursts) will allow for follow-up with high cadence photometry during their 2–3 week bright phases. This will allow the determination of superhump periods which will enable the determination of the mass ratio and clues to the white dwarf's evolutionary history. Some high amplitude dwarf novae have long spells between outbursts (years) and are intrinsically faint during quiescence, making them difficult to study. However, they represent an



important tip of the iceberg for the low luminosity CV population, and will provide clues to the ultimate evolution of cataclysmic variables.

## 2. Pie in the sky

### (a) **Observe new CV eruptive behavior**

While cataclysmic variables produce several different types of known outbursts, new types and forms of the outburst behavior are still possible. Since the rise times are short (less than 1–2 days) and the entire outburst might not last long, early identification through broker alerts can enable spectroscopic follow-up that ensures a correct classification.

*Preparations for Cataclysmic Variable Science.* Cataclysmic variables produce different types of outbursts with varying amplitudes and durations. To fully take advantage of the Rubin LSST data products, as discussed above, timely alerts, follow-up observations, and specific software are required, which are detailed below:

### 1. Identifying events from alerts

All of the aforementioned science cases require rapid alerts to enable swift follow-up. Finding the outbursting objects or low states in the nova-likes will require specific filters in a Community Broker. The varying shape of a dwarf nova outburst will need particular attention in this regard to facilitate correct identification. Due to the high number of alerts expected, machine learning tools to identify this class of object, including those that display unusual outburst behavior, will be essential. The correct application of machine learning will require that we obtain a good training set during the first year, so that we may separate out normal from unusual behavior.

### 2. Follow-up observations

The correct identification of a nova versus a dwarf nova or AM CVn system will require spectroscopic follow-up with a 2–10 m class telescope to identify Balmer emission (or absorption features for a dwarf nova outburst) and Helium lines for an AM CVn system. Multiwavelength observations (X-ray, UV, IR and radio) are often needed to study the outburst once an unusual object is identified.

#### 2.4.3. Compact Binaries: Neutron Star Binaries

Neutron star (NS) binaries are binary systems with neutron star components. Some neutron star binaries contain milli-second pulsars and can either be in the accretion state (mostly discovered during outburst) or in the rotational powered state (typically discovered in radio surveys and more recently also in the  $\gamma$  energies by Fermi). According to the so-called *recycled scenario* (Alpar et al. 1982) milli-second pulsars are neutron stars that have been spun-up by a Gyr-long accretion phase equivalent to low mass X-ray binaries, once the mass transfer

has dropped enough to allow the activation of the (radio) milli-second pulsars powered by the rotation of the magnetic field.

Transitional milli-second pulsars are neutron star binaries that have been observed to switch from an accretion to a rotation powered state, or vice-versa, where mass can be “propelled” out of the system on a timescale of months to decades (e.g., Archibald et al. 2009; De Martino & De Siena 2010; de Martino et al. 2010, 2013; Papitto et al. 2013; Bassa et al. 2014; Patruno et al. 2014; Stappers et al. 2014). Hence, they demonstrate the connection between Low mass X-ray binaries and milli-second pulsars (confirming the recycled scenario) and they support the idea that transition may be driven by mass transfer variations. Only a few transitional systems are currently known. They have been observed in outburst (only one case) and in an intermediate sub-luminous state, where an accretion disk is present (Archibald et al. 2015; Papitto et al. 2015). These are the only low mass X-ray binaries that have been observed to be high energy Gamma-ray emitters (as revealed by the Fermi-LAT, de Martino et al. 2010). Radio and X-ray observations performed during the intermediate states reveal an anti-correlated behavior between these two bands indicative of intermittent jet emission (e.g., de Martino et al. 2010, 2015; Patruno et al. 2014, see also Papitto et al. 2014; Papitto & Torres 2015). Additionally, the observation of optical pulses during the intermediate sub-luminous state (Ambrosino et al. 2017; Papitto et al. 2019) poses an argument against accretion as it seems that the majority of the accretion disk material is expelled through this method.

### 1. Low Hanging fruit

#### (a) **Observe changes of state for any milli-second pulsar, low mass X-ray binary and transitional milli-second pulsar, known and/or newly discovered**

Any change of state reported (and alerted) by Rubin LSST will trigger dedicated follow-up observations aimed at solving the binary system parameters. In particular, a binary system entering into one or the other state will trigger time-resolved optical spectroscopy to determine the donor star and/or the disk parameters. If the period is unknown, with the help of optical photometry, it will be possible to trace the secondary and, in case of an accretion disk, the primary orbital motions. If a transition occurs between a low mass X-ray binary and a rotation-powered milli-second pulsar, Rubin LSST observations will be crucial for triggering optical spectroscopy and multi-band optical photometry follow-up. With these data, we can derive the donor star’s spectral type, the effects of pulsar irradiation and the orbital parameters. These low-states will enable triggering of radio pulsar searches (eg MeerKAT and SKA). The binary orbital parameters are crucial in the search for pulses in the Gamma-ray and X-ray regimes. Hence, it is of utmost

importance that we receive prompt alerts for any system entering into a sub-luminous state before it enters its radio state or resumes full accretion. Time resolved optical follow-up of systems in the milli-second pulsar state will be needed to establish binarity and constrain the companion star and the mass function of the binary system.

### (b) Super-orbital periodicities in X-ray binaries

Some neutron-star X-ray binaries (and at least one black hole binary) are known to exhibit super-orbital periods (i.e., periods greater than the orbital period of the system) in both the X-ray and optical regime (see Hu et al. 2019; Dage et al. 2022; Thomas et al. 2022 and references therein). This is thought to be due to a warped, precessing accretion disk (e.g., Brumback et al. 2020), with radiation-driven warping proposed as the lead scenario (Ogilvie & Dubus 2001). While this has mostly been studied in the X-ray, with optical photometry and time domain coverage, it will be possible to identify even larger numbers of systems with super-orbital periods, which will expand our knowledge of accretion disk geometries with unusual configurations.

## 2. Pie in the sky

### (a) Identification of unexpected transitions or transition frequencies

By observing known binary systems with neutron star components (and those that are newly observed with Rubin LSST), we are well placed to identify new and unexpected transitions. If such a transition is identified, this will imply revision of current evolutionary scenarios. We will search for such transitions throughout the 10 yr Rubin LSST survey mission.

## *Preparations for Neutron Star Binary Science.*

### 1. Identifying events from alerts

The prompt data alerts of Rubin LSST will enable an alert in real time about any change of state of known systems (whether milli-second pulsar, low mass X-ray binary or transitional milli-second pulsar) as well as for newly discovered systems (that we anticipate to discover by combining Rubin LSST with other next generation sky multiwavelength surveys—e.g., THESEUS, eROSITA and SKA). Obtaining notifications of new systems in real time will: Provide a census of the transitional systems among milli-second pulsars thus helping to frame the evolutionary phase of each accreting neutron star; and allow for dedicated follow-up that will enable the determination of the system parameters and/or characterization of the physical mechanisms behind the observed phenomenology.

It is imperative that the alert brokers are prepared to identify and produce alerts for Neutron Star Binaries.

This will need to include a list of all known Neutron Star Binaries so that they may be monitored for changes in their luminosity and so that follow-up observations may be swiftly undertaken.

### 2. Follow-up observations

By combining Rubin LSST with multiwavelength surveys such as THESEUS, eROSITA and SKA, we anticipate finding a significant number of new objects. If a transition occurs between a low mass X-ray binary and a rotation-powered milli-second pulsar, optical spectroscopy and multi-band optical photometry will be required. This will further trigger radio pulsar searches (eg MeerKAT and SKA). Follow-up X-ray and radio observations performed in the intermediate state can provide information about jet emission.

#### *2.4.4. Compact Binaries: Black Hole X-ray Binaries*

Black hole X-ray binaries are interacting binary systems consisting of a stellar-mass black hole and a donor star. Early spectral-type donor systems tend to be wind-fed, whereas in late spectral-type donors, the black hole will accrete matter from the donor via Roche lobe overflow and an accretion disk will form around it. As matter from this disk approaches the black hole, the black hole releases gravitational potential energy in the form of broadband radiation. The maximum energy release occurs in the innermost accretion zones, which have been observed to have a radiation peak in X-rays. Longer wavelength thermal radiation arises as one progressively moves away from the center, with additional bright transient radiation arising in particular components such as non-thermal radiation from plasma jets (e.g., Charles & Coe 2006). Finding and characterizing Galactic black hole binaries has important implications for the end stages of stellar evolutionary population synthesis, as well as the progenitors and physics of gravitational wave binaries.

Black hole binaries spend their lives predominantly in states of either quiescence or outburst. The explanation for the latter state was outlined by, (e.g., Lasota 2001) to be a trigger associated with accumulated matter on the inner radius of the accretion disk reaching a critical limit, causing the disk to undergo thermal runaway and initiating a shockwave that propagates away from the inner radius. As the fronts from this shockwave propagate outwards, the matter behind the fronts becomes hot and ionized, beginning to diffuse inwards and eventually triggering the outburst. These series of events cause the optical signature of the black hole binary to steadily rise over the course of years, while the matter is building up, and to sharply increase in the weeks building up to the outburst due to the critical limit being reached. This behavior has been observed directly within only a select few black hole binaries, e.g., GS 1354–64 by Koljonen et al. (2016) and V404 Cyg by Bernardini et al. (2016). The optical light curve for GS 1354–64 is shown in Figure 5. There is

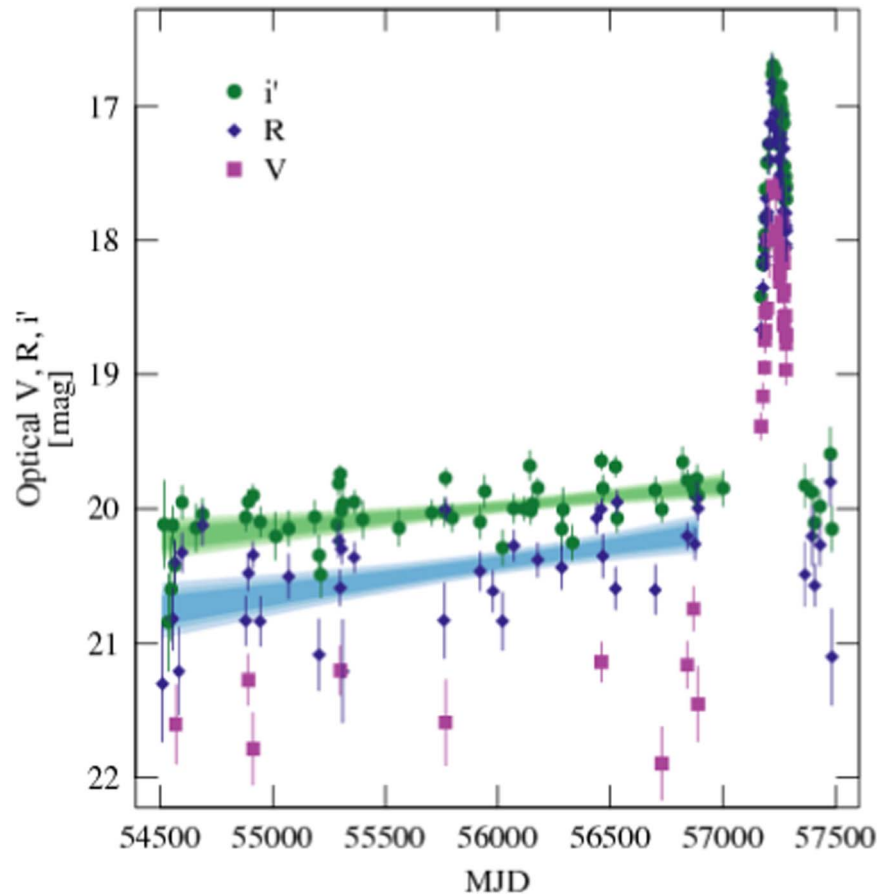


**Figure 5.** Long term optical light curve of an outburst from black hole binary GS 1354–64. The observations were made with the 2 m Faulkes Telescope South (FTS). Note the subtle but definite rise in the  $i'$  and  $R$  filters over years, before the enormous rise associated with the outburst. Reproduced with permission from Koljonen et al. (2016). Copyright © 2016 Oxford University Press.

enormous interest in being able to identify trends leading up to an outburst, not only to learn about the physical processes at play, but to make the advanced coordination of multiwavelength observations easier.

The number of black hole binaries expected to be observed by Rubin LSST was explored by Johnson et al. (2018) where they estimated the fractional Galactic low mass X-ray binary (low mass X-ray binary) population in which accurate recovery of the orbital period is likely to be possible. Furthermore, Wiktorowicz et al. (2021) calculated the number of X-ray binaries expected to be detectable with Rubin LSST via self-lensing.

#### 1. Low hanging fruit

##### (a) Observing the increase in luminosity of known black hole binaries

By observing the increase in luminosity that occurs prior to the outburst, we are able to trigger dedicated multi-wavelength follow-up in order to characterize the event. In the X-ray, black hole binaries can be identified as they tend to exhibit characteristic evolutionary paths

in X-ray flux/spectral slope (“q”) diagrams, together with strong radio emission from jets (e.g., Fender et al. 2004). They also tend to show strong stochastic correlated multiwavelength flux variability down to milli-second order timescales (e.g., Gandhi et al. 2017). Black hole binary masses can be estimated via dynamical radial velocity variations (Casares & Jonker 2014). So far, only the brightest tip of the population has been followed up in detail in the optical band (e.g., Corral-Santana et al. 2016) and only  $\sim 30\%$  of detected black hole binaries have sufficient observations to dynamically confirm the presence of a black hole. Therefore increasing these statistics is vital to improve our understanding of these outbursts. Currently, there are roughly 5–10 X-ray outbursts detected per year, only 2–3 of which are bright enough to be followed up in the optical. The deeper mag limits of Rubin LSST monitoring, as well as the possibility to access redder filters, should substantially enhance the detection of fainter and heavily extinguished optical counterparts.

## 2. Pie in the sky

### (a) Characterizing the long term trends of black hole binary outbursts

With a larger sample of better characterized black hole binaries, we will be able to better understand the long-term trends of outbursts. This could provide the key to predicting the occurrence of black hole binary outbursts, allowing us to trigger follow-up *before* the event. Additionally, the long term outburst trend is what distinguishes the optical signature of black hole binaries from other systems that also exhibit ellipsoidal modulation, such as cataclysmic variables. Characterisation of this trend may also allow for the classification of black hole binaries, without the need for X-ray follow-up. However, this characterization would require additional detailed observations and analysis of black hole binaries throughout their outburst phases.

#### *Preparations for Black Hole Binary Science.*

### 1. Identifying events from alerts

It is imperative that the alert brokers are prepared to identify and produce alerts for Black Hole Binaries. The catalog matching service from AMPEL<sup>72</sup> will be used for multiwavelength confirmation for potential black hole binaries, utilizing archival data from sources such as eROSITA, Spitzer and ZTF. For known black hole binary systems, the watchlist from Lasair<sup>73</sup> will be used to monitor for rises in the optical. As many may only be visible with the current generation of telescopes during outburst, follow-up must be triggered promptly. Further, prompt alerts will enable prompt follow-up, which is necessary for characterizing the outburst events.

### 2. Follow-up observations

The long term rise expected in the years prior to the outburst will likely be sufficiently sampled with the regular Rubin LSST cadence. A higher frequency of observations will however be required to characterize the sharp rise directly preceding the outburst. Suitable telescopes for performing these observations range from the LCOGT (0.8 m) to the New Technology Telescope (358 cm), depending on the brightness of the target.

### 3. Facilities/software requirements

Some black hole binary systems will only be observable after the brightness has begun to rise. Therefore, we require an algorithm capable of classifying the outburst from data that only cover the brightest observable section of the observable signature.

## 2.5. Extra Galactic Transients

### 2.5.1. Supernovae

SNe are powerful stellar explosions, known for their extremely bright luminosity, where the relevant star is essentially destroyed through one of two physical processes: (1) the gravitational collapse of an iron core that has reached the Chandrasekhar limit inside a more massive star or (2) the detonation of a white dwarf that has been driven over the Chandrasekhar limit by mass transfer from a companion. The latter are called SNe Ia (or thermonuclear), the former, Type Ib, Ic, and II (core-collapse). The types are based on a traditional classification scheme dependent on whether the hydrogen features appear in the spectra (Type II) or not (Type I). It is the Type Ia's that have most often been used to probe cosmic expansion and to show that this expansion of the Universe is accelerating.

In addition to being an exquisite cosmological tool (an area of specialization of the Dark Energy Science Collaboration<sup>74</sup>), SNe are important phenomena in our universe for two main reasons. The first reason lies in the chemical evolution of galaxies, because they synthesize additional heavy elements, which are distributed among the pre-explosion stars. Type Ia's provide more than half of the iron-peak elements and some intermediate mass (carbon-sulfur) material (Guo et al. 2008; Matteucci 2010; Jiménez et al. 2015; Simionescu et al. 2015). The core collapse events generate everything from helium to iron, and also elements beyond iron from slow neutron capture in the parent stars and probably from rapid neutron capture in the event itself. The second reason is that the kinetic energy of expanding SNe remnants stir the interstellar gas and provide a major source of heating, both of which prevent the dust and gas clouds collapsing down to stars quickly, allowing stars and solar systems, such as our own, to form. Thus, we are made (partly) of “star dust,” and live in a habitable solar system owing to past SNe; indeed, one that occurred just less than 5.5 Gyr ago may have triggered the formation of our own solar system (Loewenstein et al. 2006; Gatto et al. 2017).

Despite SNe having significant scientific value, their explosion mechanisms remain somewhat mysterious. They have well-specified models and progenitor theories, but the progenitors are still controversial. For example, SNe Ia have evidence for both a single-degenerate explosion scenario, where the white dwarf is accreting material from a non-degenerate companion, and a double-degenerate explosion scenario that involves two white dwarfs. Additionally, SNe classes are not completely defined. With recent surveys, more objects exhibiting behaviors of two different SNe classes have been found. It is thus important to investigate whether SN types are isolated families or a continuum, and consequently how to define them (Filippenko 2003).

<sup>72</sup> <https://ampelproject.github.io/>

<sup>73</sup> <https://lasair.roe.ac.uk/>

<sup>74</sup> <https://lsstdesc.org/>

The advances we would like to make with SN science in the era of Rubin LSST are as follows:

### 1. Low Hanging fruit

#### (a) **Create improved classification schemes**

Ultimately, observational studies of individual SN and samples of SNe rest on a robust classification system. Large numbers of Rubin LSST light curves, combined with the addition of photometric follow-up (to provide improved light-curve coverage), would improve photometric classification. Expanding the SN dataset would bring some classes of unusual, rare, difficult to observe SNe (for example fast evolving or Pair-Instability SNe, Gomez et al. 2019; Ho et al. 2021) into the statistical domain, enabling a better understanding of the boundaries (or lack thereof) between classes.

#### (b) **Refine theoretical predictions and classification methods**

An overarching goal of SNe science is the identification of SN progenitors (determining which type of star exploded, in which environment the explosion occurred, and what triggered the explosion) and the explosion mechanism. Observations of a significant number of SNe would allow for a more in-depth understanding of theory through the measurement of observables, for example: (1) the signatures of nickel distribution *versus* shock interaction in early SNe Ia light curves and (2) spectra (see Childress et al. 2015, and reference therein). While we rely heavily on spectra for the characterization and understanding of SNe, the size of the Rubin LSST sample, combined with follow-up in multiple spectral bands, would enable the spectral features of the events to be constrained photometrically.

#### (c) **Direct identification of SNe progenitors**

By employing the use of follow-up facilities (e.g., Hubble Space Telescope (HST) or JWST), the direct identification of the SN progenitor (and/or binary companion) of future, nearby SNe will be possible (see Smartt et al. 2009).

#### (d) **Understanding of the local environments of SNe**

With the large number of SNe expected to be observed with Rubin LSST, studies of event rates, environmental dependence, progenitor stellar populations, host-galaxy associations are all possible, with the potential to reveal physical insight unobtainable from direct observations (see, for example, Modjaz et al. 2020, and references therein). The high number of SNe and the detailed study of explosion mechanisms and progenitor models will help disentangle the luminosity–metallicity–distance degeneracy. This will allow a better host-galaxy association for all the

SNe detected. For this science case, however, photometric or spectroscopic redshifts are required to calibrate the photometric distance, both of which require follow-up observations.

### 2. Pie in the sky

#### (a) **Moving SN studies into the multi-messenger astronomy realm**

The prompt follow-up of SN candidates will allow for the cross correlation of events detected with multiple facilities and also through other messengers. The possibility of surveying wide areas of the sky provides an opportunity to learn about the electromagnetic signatures of fast phenomena known in other regions of the energy-frequency spectrum whose electromagnetic counterparts have been missed until now.

#### (b) **Discovering new, unknown kinds of stellar explosions**

As we open up new regions of the parameter space with synoptic observations of an unprecedented volume of space, we stand a chance to discover new phenomena, as recently happened with SNe Icn objects (Fraser et al. 2021; Gal-Yam et al. 2022; Pellegrino et al. 2022; Perley et al. 2022).

### *Preparations for SNe Science.*

#### 1. **Identifying events from alerts**

It is imperative that the brokers Section 6.1.2 are prepared to produce swift alerts for SNe. To ensure this, the community needs to continue working toward classification schemes and effective queries that will enable the brokers to identify SNe (and more generally, time-domain objects) of interest and trigger follow-up observations. This process must be largely, if not entirely, automated due to the large data volume delivered by Rubin LSST. Early classification models for SNe that are capable of identifying a transient with only a few observations are still rare (see, for example, Muthukrishna et al. 2019; Qu & Sako 2021), especially when the desired classification goes beyond “SN Ia or not” and into classification of SNe subtypes (see Facilities/software requirements).

#### 2. **Follow-up observations/archival data**

To classify and study new SNe detected by Rubin LSST (especially early on in the LSST survey, while our photometric classification schemes are preparing to take advantage of the large data volume), we will need to leverage dens(er) coverage of the light curves and spectral observations from ancillary data from other facilities. These observations will include observations in bands and wavelength regimes complementary to Rubin’s. To do this, it is essential to have a reliable network of observatories which can follow-up an object

once an alert is distributed. Ideally, the network will be an intelligent network system connecting follow-up facilities, monitoring and deploying observations in an attempt avoid the duplication of observations and to collect the most relevant data.

Moreover, synergies, such as Rubin-Roman, or Rubin-Euclid, or Rubin-4MOST, can enable ancillary data collection, which would greatly enhance our understanding of Rubin discoveries. A collection of spectra, even for a relatively small subset of the detected SNe, will enable spectro-photometric analyses. This additional information would improve our understanding of the composition of the source and the interstellar medium around it, as well as the physics mechanisms the source underwent to produce the detected event. Through the analysis of multiple concurrent data sets, we will improve our knowledge of the types of SNe and how to characterize detected transients. With the high pressure that Rubin LSST will put on follow-up facilities, selecting the most promising SNe for spectroscopic follow-up will be critical for improving our insight into stellar explosions.

### 3. Facilities/software requirements

When considering facilities and software, it is useful to separate SN science into subsets: SN precursors, SN discovery and SN modeling. Each is detailed below:

#### (a) Precursor data sets

Algorithms for the photometric classification of SN precursors are crucial both (1) for early light-curve classification from spectroscopic follow-up, and (2) for complete light-curve classification. For this, we need to obtain a more diverse, less biased sample of SNe to constrain all relevant astrophysical processes and their observational manifestations. Efforts are underway, with recent algorithms providing the fast and accurate classification of SNe in both the early and late stages of formation (Möller & de Boissière 2019; Muthukrishna et al. 2019). The current Extended LSST Astronomical Time-Series Classification Challenge (ELAsTiCC)<sup>75</sup> provides an ideal venue for the development of further models.

#### (b) Automation of the discovery and study chain

After the detection and selection of interesting SNe, enabled by expert models interfacing with alert brokers, the triggering of follow-up resources should be enabled by software packages, like AEON (Street et al. 2020), so that we may act promptly to classify young SNe. Our ability to make discoveries in the current and future era of time-domain astrophysics is limited by two aspects: (1) it will be necessary to

identify specific targets of interest amidst millions of alerts each night and (2) we will need notable alerts to be identified swiftly, ideally within hours of the initial detection, to enable prompt follow-up observations (spectroscopy and/or observations across the spectrum). Toolkits such as Target and Observation Manager systems (TOM Street et al. 2018a) allow the exploration and (importantly) the prioritization of targets in an observing run. This will help when scheduling the follow-up and will allow the science community to have a fast first look at the phenomena. Luckily, tremendous advances have been made in the automation of the discovery chain in recent years, with major facilities (e.g., the Gemini telescopes) fully endorsing and embracing software like AEON to enable the follow up of Rubin SNe. Many other facilities, especially those connected to Rubin through international in-kind data right agreements,<sup>76</sup> are working toward the integration of TOM, AEON, and similar software packages. Furthermore, the use of TOMs will be pivotal to our success with handling large data sets. For example, when deciding which object parameters to pre-calculate, store, and make available to queries versus which to compute on demand.

#### (c) Model development

To effectively deal with the 6-band sparse data (2–3 images per week with an intranight gap  $\sim 3$  days), we need a methodological development process and further, software tools that can deal with multi-filter light curves, e.g., parametric models and methods for correctly treating sparsely sampled data.

Algorithms to associate SNe with host galaxies are further needed. Efforts to organize galaxy catalogs and to create SNe matching software are underway (Gupta et al. 2016). Algorithms to select follow-up targets would also be highly beneficial. These algorithms would maximize the use of our spectroscopic resources. Concurrently, these algorithms would fine-tune our training sets for photometric classification—one of our main limitations. Efforts have started that employ Active Learning algorithms (Ishida et al. 2019). It will also be necessary to compare our different photometric classification algorithms, for which we will require a sample of benchmark systems.

#### 2.5.2. Intermediate-luminosity Optical Transients

Intermediate-luminosity optical transients (ILOTS; e.g., Berger et al. 2009) form a class of astrophysical objects identified through their relatively faint intrinsic luminosity.

<sup>75</sup> <https://project.lsst.org/meetings/rubin2022/agenda/extended-lsst-astronomical-time-series-classification-challenge-elasticc>, an upgrade of the past PLAsTiCC challenge <https://plasticc.org/>.

<sup>76</sup> <https://project.lsst.org/groups/cec/node/5>

They have intermediate absolute magnitudes, between those of core-collapse SNe and classical novae ( $-10 > M_V > -15$ ). For this reason they are frequently named ‘‘Gap Transients’’ (e.g., Kasliwal 2012; Pastorello & Fraser 2019). Only in recent years have they been studied in depth and only a limited number of ILOTs have high-quality well-sampled data sets. Thus our knowledge of their nature is still incomplete. While the early-time spectra and the luminosity of different species of ILOTs are similar, they can be produced by a wide variety of physical mechanisms and progenitor stars. Although a fraction of SNe are in the same magnitude range as ILOTs (including low-luminosity stripped-envelope SNe, such as faint SNe Iax, Ca-rich transients, Ia candidates, or other faint SNe I (Kasliwal 2013; Valenti et al. 2009), and low-luminosity Type II-P events (Pastorello et al. 2004; Spiro et al. 2014)) our team is mostly interested in non-terminal stellar transients. These include:

### 1. The giant eruptions of massive stars, in particular luminous blue variables

Luminous blue variables are very bright sources, and among the most massive stars detectable in galaxies. Famous examples in our Galaxy are AG Car and HR Car. During canonical S Dor-like outbursts, luminous blue variables experience erratic brightness variability over timescales on the order of months to a few years, with magnitude changes on the order of a couple of magnitudes (but without significant changes in their bolometric luminosities) (Humphreys & Davidson 1994; Smith et al. 2011; Humphreys et al. 2017). In this phase, luminous blue variables move to the right of the Hertzsprung–Russell diagram, becoming redder and cooler, coming back to the left side in quiescence. The situation dramatically changes during a giant eruption, when they become the most luminous stars in their host galaxies.  $\eta$  Car, in the Milky Way (MW), experienced a giant eruption in the mid-19th Century. During the giant eruption,  $\eta$  Car reached an apparent magnitude of  $-0.7$  (absolute magnitude  $M_V$  of  $-14$ , Smith & Frew 2011), while in a second obscured little eruption it reached the apparent magnitude of  $6.2$ . With the single-band magnitude limit of  $24\text{--}25$  for Rubin LSST, not only would a little eruption be visible in the Local Group (distance modulus up to  $27$ ), but a giant eruption would be visible well beyond it. Current models propose that brightness changes in  $\eta$  Car are due to an unstable multiple system, where the giant eruption was possibly triggered by a dynamically induced merger. However, other mechanisms may explain giant eruptive mass-loss events without invoking close stellar interactions in binary systems (e.g., instabilities triggered by explosive shell burnings, or pulsational pair-instability; see Smith 2014, and references therein).

During a giant eruption (which lasts years to decades), luminous blue variables experience multiple outbursts whose individual peaks reach  $M_V \approx -14$  mag (Wagner et al. 2004; Pastorello et al. 2010, 2013; Smith et al. 2010; Smith 2017). However, massive hypergiants may also have a single short-duration outburst with  $M_V$  similar to that of giant eruptions; (Smith et al. 2011; Tartaglia et al. 2015, 2016). Although their massive progenitors survive the outbursts, these transients may resemble (in energetics and spectral appearance) true SNe explosions. For this reason, extragalactic luminous blue variable-like outbursts are also dubbed SN impostors (Van Dyk et al. 2000).

### 2. Red novae and non-degenerate stellar mergers

Red novae are created by the successful ejection of a common envelope in a binary system that eventually leads to the coalescence of the two stars. The nature of red novae, such as V838 Mon, V4332 Sgr and M31-RV, was debated until V1309 Sco was discovered in 2008. A combination of spectroscopic data and a well-sampled pre-outburst light curve proved it to be the stellar merger of a common envelope binary (Mason et al. 2010; Tylenda et al. 2011). Recent discoveries of extra-galactic counterparts, the so-called Luminous red novae (Goranskij et al. 2016; Smith et al. 2016; Blagorodnova et al. 2017), have extended the red nova zoo to much higher luminosities and masses (Blagorodnova et al. 2017; Cai et al. 2019; Pastorello et al. 2019, 2021a; Blagorodnova et al. 2021; Cai et al. 2022), and are expected to dominate the Rubin LSST sample (e.g., Howitt et al. 2020). Red novae/luminous red novae show multi-peaked light curves, and spectra that progressively transition from intermediate-type stars to K- and then M-type stars.

### 3. Intermediate-luminosity red transients

Intermediate-luminosity red transients show spectra that are initially quite blue, but that become redder with time (Cai et al. 2021). They show prominent H and Ca II lines, including the typical [Ca II] 7291, 7323 Å doublet in emission. In Intermediate-luminosity red transients, the doublet is detected at all phases. Their light curves are reminiscent of those of sub-luminous Type II-L SNe (e.g., SNe 2008S and NGC300-2008OT1; Prieto et al. 2008; Bond et al. 2009; Botticella et al. 2009; Berger et al. 2009; Smith et al. 2009; Humphreys et al. 2011) or even Type II-P SNe (e.g., M85-2006OT1 and PTF10fq; Kulkarni et al. 2007; Pastorello et al. 2007; Kasliwal et al. 2011). When observed, the late-time decline rate is roughly consistent with the  $^{56}\text{Co}$  decay. In quiescence, the progenitors of Intermediate-luminosity red transients usually remain undetected in the optical and near-infrared bands, while they are fairly luminous in the mid-infrared domain. The progenitors of Intermediate-luminosity red

transients are moderately massive stars (8-15  $M_{\odot}$ ), enshrouded in dusty cocoons. Intermediate-luminosity red transients are proposed to be electron-capture SNe from super-asymptotic giant branch stars (e.g., Botticella et al. 2009; Pumo et al. 2009; Thompson et al. 2009). Although this interpretation is disputed (see, e.g., Andrews et al. 2021), recent observational arguments seem to favor the terminal SNe explosion scenario for Intermediate-luminosity red transients (Adams et al. 2016).

With the extensive deep data from Rubin LSST, we expect significant improvements in our understanding of ILOTs. Rubin LSST will facilitate the following science cases:

1. Low hanging fruit

(a) **Observations of known ordinary luminous blue variable outbursts (S Dor-like) and the detection of new luminous blue variables**

The full range of variability of a classical luminous blue variable can be comfortably monitored with single shot Rubin LSST observations up to about 30 Mpc, but with periodic stacks we can largely exceed this distance limit. For known luminous blue variables, using literature, data available in the public telescope archives, and those publicly released by surveys, we aim to obtain light curves with baselines of many decades. Multiple survey strategies may reveal different types of variability, which develop on different timescales. Well-studied luminous blue variables will become reference objects. With Rubin LSST, we expect to find new luminous blue variable candidates in outburst and determine their occurrence rates.

On the other hand, the study of the canonical variability (the S Dor phase) of known luminous blue variables in the Milky Way, Large Magellanic Cloud (LMC), Small Magellanic Cloud (SMC), and nearby Galaxies is key to understanding the role of binary interactions. The moderate-cadence of the main survey (with one observation every few days and in different filters) allows us to investigate modulations and/or periodicity features in the light curves. By combining multi-color light curves with supporting spectroscopic information, we can determine correlations among the observable features.

(b) **Observing giant eruptions/outbursts of luminous blue variables and other massive stars**

Timescales of giant stellar eruptions (the so-called SN impostors) range from a few weeks to decades (in the case of Giant luminous blue variable eruptions). As these events are mostly produced by very massive stars, they are likely rare events, however, would still benefit from long-term monitoring over several years.

We aim at monitoring SN-impostor light curves with Rubin LSST, as well as discovering evidence for pre-SNe outbursts. Understanding if pre-SNe outburst events are common in the pre-SNe stages (as claimed by Ofek et al. 2014 and observed by Strotjohann et al. 2021) is a major goal of our research. In addition, an extensive database of objects that have been extensively monitored until the very late phases is an essential tool to observationally discriminate SN impostors from faint ejecta-CSM interacting SNe. The progenitors of these SN impostors in a relatively quiescent state can be detected in earlier deep stacked Rubin LSST images.

(c) **Observing a significant number of (luminous) red novae and non-degenerate stellar mergers**

Stellar mergers are common (e.g., de Mink et al. 2014). Their rates are tightly dependent on their luminosity: Kochanek et al. (2014) estimated a Galactic rate on the order of one every ten years for V1309 Sco-like events ( $M_V \approx -4$  mag); on the order of  $0.03 \text{ yr}^{-1}$  for V838 Mon-like events ( $M_V \approx -10$  mag); and on the order of  $10^{-3} \text{ yr}^{-1}$  for NGC 4490-2011OT-like events ( $M_V \approx -14$  mag). Although low-luminosity red novae are quite frequent, only about 25 red novae/luminous red novae have been observed in the Galaxy and in the Local Universe so far. Rubin LSST is expected to find many more candidates than are currently known. A large sample of objects with high-cadence and good signal-to-noise photometric and spectroscopic observations are required for reliable comparisons with theoretical models (e.g., Matsumoto & Metzger 2022). They will be a key tool for unveiling the mechanisms triggering the RN outbursts, for discerning the fate of the binary systems (coalescence or not), and for finally allowing us to provide more robust occurrence rate estimates. This will be an ongoing project over the lifetime of the Rubin LSST survey.

(d) **Increasing the number of Intermediate-luminosity red transients**

The increasing number of intermediate-luminosity red transients discovered in nearby galaxies suggests that these transients are relatively frequent, making up about 8% of core-collapse SNe, according to Cai et al. (2021). Rubin LSST will greatly increase the number of new discoveries, providing light curves from the explosion to very late phases. All of this is essential for determining the presence of classical SNe signatures, such as the shock breakout and the light curve  $^{56}\text{Co}$  tail. In addition, stack frames collected before and years after the explosion will provide high-quality images of the Intermediate-luminosity red transient site which (in combination with deep infrared images collected with other facilities) are fundamental



to the characterization of the progenitors and their final fates.

## 2. Pie in the sky

### (a) Detection of the progenitor prior to outburst

The magnitude and color information inferred from the inspection of Rubin LSST archive images will help constrain the progenitor parameters of new ILOTs and allow us to detect variability patterns before the onset of the main transient event (e.g., Pastorello et al. 2010, 2021b; Tytenda et al. 2011). When stellar counterparts are not obviously found in single-visit images, the periodic stacks will allow us to go much deeper in magnitude, greatly increasing the probability to detect the quiescent progenitor.

### (b) Understanding the fate of intermediate-luminosity optical transients

From the observations, the interpretation of the real nature of many intermediate-luminosity optical transient species is still controversial. For Intermediate-luminosity red transients and some luminous blue variable-like eruptions, for example, it is still debated whether the star survives the eruption or not. For some luminous red novae, the fate of the binary system after the the ejection of the common envelope is still controversial (final merger versus surviving binary). The existence of an extensive image database will allow us to create deep stacked images in order to monitor the source in the optical bands up to very late phases. This is essential for following the decline to below the luminosity threshold of the quiescent progenitor, eventually observing the complete disappearance of the source. Supporting IR observations, however, is necessary for constraining the dust formation affecting the optical photometry.

### (c) Understanding the underlying distributions of ILOTs

The statistical analysis of the large distribution of well-sampled ILOTs is a key goal. This will enable (1) the identification of possible correlations between observed parameters, such as the peak absolute magnitude, the temperature evolution and the velocity of the ejected material; (2) the identification of correlations between observables and other physical parameters such as the energy released in the outburst and/or the progenitor mass; and (3) the probing of the connection between the physical parameters of ILOTs and the properties of their environments (e.g., stellar population, metallicity).

## Preparations for Intermediate-Luminosity Optical Transient Science.

### 1. Identifying events from alerts

The planned Rubin LSST cadence will allow for a collection of homogeneously sampled light curves and

colors of different Intermediate-Luminosity Optical Transient sub-types. The availability of well-sampled templates will greatly favor the identification of Intermediate-Luminosity Optical Transients for the purposes of alerts. With this in mind, our team has a dedicated observational program, and is working on the preparation of a number of reference light curve templates for the different species of Intermediate-Luminosity Optical Transients. These templates will further enable the classification of new objects, as well as the comparison and interpretation of the various transient species.

### 2. Follow-up observations

Each transient will have a well-sampled light curve with color evolution, which will allow us to discover, classify, and characterize new transients of the Intermediate-Luminosity Optical Transient type. Through multi-wavelength mid- to high-resolution spectroscopic follow-up (in the UV, optical, and NIR wavelength ranges) it will be possible to understand the ejecta kinematics, density, ionization structure, geometry and, ultimately, the dynamics of our sample. Hence, upon receiving a Rubin LSST alert, it is imperative that we proceed with dedicated spectroscopic follow-up. Only the brightest Intermediate-Luminosity Optical Transients with extended visibility will be monitored using mid- to large-sized telescopes equipped with the best multi-wavelength spectrographs (such as SoXS@NTT). Rubin LSST multi-color photometry will also enable us to detect short-duration features in the light curves (e.g., humps that are due to shell-shell collisions or reflection nebulae), and to sample the SED.

Complementary UV photometry (in the absence of UV spectroscopy) can also provide important information. Further, while it has not yet been observed, X-ray follow-up is expected to provide additional information. Photometric follow-up will also be requested in the optical and IR domains, to extend the SED sampling and to fill observational gaps due to the sparse sampling of the Rubin LSST main-survey cadence.

### 2.5.3. Gamma-Ray Bursts

GRBs were identified in the late 60's by the Vela spy satellites (Klebesadel et al. 1973). More than sixty years later, we now know that some GRBs are among the most luminous cosmic explosions in the Universe. Two classes of GRBs are currently known: the *long* GRBs (LGRBs) and *short* GRBs (SGRBs), based on the duration of the gamma-ray emission. LGRBs have a duration equal to or longer than two seconds, while SGRB emission lasts less than two seconds (Kouveliotou et al. 1993; Fishman & Meegan 1995).

LGRBs are thought to be produced by the explosion of single massive (10–30  $M_{\odot}$ ) stars (Paczynski 1986; Woosley 1993;

Fryer et al. 1999), while SGRBs are believed to be the byproduct of the merging process of two compact objects like neutron-star binaries, black hole binaries, or neutron star–white dwarf pairs (Eichler et al. 1989; Goodman 1986; Mészáros & Rees 1997).

SGRBs are also connected with the production of gravitational wave signals, as recently discovered by the LIGO-VIRGO observatories (Abbott et al. 2017a).

LGRBs are likely connected with the earliest generation of massive stars produced in the Universe. A few GRBs (GRB 090423, GRB 090429B and GRB 120923) have been either spectroscopically or photometrically confirmed at redshifts  $z \gtrsim 9.4$  (Tanvir et al. 2009, 2018; Cucchiara et al. 2011, 2013), representing the furthest stellar objects ever discovered. These events not only represent a unique laboratory for stellar evolution, but also enable us to pinpoint host high-redshift galaxies irrespective of their intrinsic mass or luminosity. Such objects become complementary to, e.g., Hubble Ultra Deep Field samples and represent unique targets for high-redshift universe explorers like JWST and the Nancy Grace Roman Telescope.

The majority of GRB emission occurs in the high-energy regimes (Gamma rays), while a low-energy multiwavelength emission, also known as the *afterglow*, can be produced in the aftermath of the GRB explosions. While early GRB studies focus only on the properties of the gamma-ray prompt emission, the launch of the Neil Gehrels Swift Observatory (formerly known as Swift) has shifted the attention to the early afterglow emission (during the first minutes to the first few hours), in particular in the X-ray to Optical wavelengths, (Racusin et al. 2008; Racusin 2009; Kann et al. 2010; Kann 2012). With this new focus on the optical region for GRBs, we are hoping to probe the following science goals with Rubin LSST:

#### 1. Low hanging fruit

##### (a) Detecting of GRB emission

LGRBs and SGRBs produce, after an initial gamma-ray radiation, a jetted emission that interacts with the surrounding inter-stellar medium (ISM). The afterglow is generated by the synchrotron emission produced by the interaction of ultra-relativistic blastwaves with the ISM (Mészáros & Rees 1997; Panaitescu & Kumar 2002). Optical/infrared rapid spectroscopy of GRB afterglows reveal the properties of the GRB host ISM as well as the presence of intervening systems. Absorption spectra have been key to investigating the cosmological metal content up to redshift  $z \approx 7$  (De Cia et al. 2012; Chornock et al. 2013; Cucchiara et al. 2015). These can also constrain the neutral hydrogen fraction and the dynamics of re-ionization.

Rapid (within minutes of the GRB discovery) spectroscopic observations with good phase coverage

have revealed the presence of varying fine-structure transitions, which hint at the interaction of the surrounding medium with the GRB emission and/or with ISM particles ionized by the surrounding stellar UV background (Vreeswijk et al. 2011). Rubin LSST’s sensitivity and survey strategy will be enable alerts that will trigger observations for newly discovered GRBs beyond what current facilities can do. Despite the degrading of space-based Gamma-ray detectors and the aging of the Neil Gehrels Swift Observatory and the Fermi satellite, the community should expect a constant rate of direct GRB observations of 100 peryear, with at least one third of them being directly observable by Rubin.

##### (b) Detection of long gamma-ray burst orphan afterglows

The Swift satellite detects 100 GRB  $y^{-1}$  on average, but the number of actual GRB events is uncertain due to the uncertainty in the jet opening angle of the initial gamma-ray emission ( $\theta_{\text{jet}}$ ). If the viewing angle (the angle between the jet axis and the observer’s line of sight) is greater than the jet opening angle,  $\theta_{\text{view}} > \theta_{\text{jet}}$ , we will not be able to detect the prompt emission. However, thanks to the deceleration of the blastwave and the subsequent decrease in the Lorentz factor,  $\Gamma$ , we will be able to detect the low-energy afterglow emission (Dermer et al. 1999). These orphan afterglows are proportional to  $(1 - \cos \theta_{\text{jet}})^{-1}$ . The peak of the detectable emission, likely occurring days post-burst, is in the MHz-GHz regime, but the Rubin LSST single visit depth ( $r \approx 24.7$ ) enables the detection of such an event. Assuming typical microphysical parameters for the GRB emission, Rubin LSST should be able to identify roughly 50 orphan afterglow GRBs per year (Cenko et al. 2015; Bhalerao et al. 2017).

##### (c) The detection of GRBs as gravitational wave electromagnetic counterparts

Short GRBs are due to the merger of two compact objects, which also produce gravitational waves. At a 200 Mpc distance, double neutron-star mergers and subsequent kilonova emission can be detected from a single visit in the *i*-band for up to 1 week. Depending on the gravitational wave trigger facilities, the observing strategy, and the intrinsic properties of the gravitational wave progenitor, we expect between 5 and 20 short gamma-ray bursts/gravitational wave events to be observable by Rubin in at least one band (Andreoni et al. 2022a).

#### Preparations for GRB Science.

##### 1. Identifying events from alerts

Swift alerts are necessary for the timely follow-up of long and short GRBs. While broker-specific capabilities

are not yet developed for GRB follow-up, we expect initially to take advantage of brokers focused on gravitational wave events, Kilonovae, and other fast transients. The capabilities offered by Swift, Fermi, and other smaller high-energy space-based observatories (e.g., BurstCube) will provide constraints on the nature of these phenomena (SGRB/LGRBs/ultra-Long GRBs) through the study of the X-ray/Gamma-ray counterparts. Finally, Rubin LSST alerts will help other multi-messenger facilities e.g., IceCube neutrino detectors, radio survey (SKA, VLA), and Cherenkov Telescope Arrays locate the possible GRB.

## 2. Follow-up observations

Absorption spectra have been key in the investigation of the cosmological metal content up to redshift  $z \approx 6$  and in further constraining the neutral hydrogen fraction and the dynamics of re-ionization. Further, spectroscopic observations have revealed the presence of varying fine-structure transitions. We plan swift follow-up observations using a plethora of facilities both on the ground and in space. These include target of opportunity observations at Gemini, Keck, the Very Large Telescope, and Telescopio Gran Canaria. Similarly, rapid response programs exist with the HST and JWST. The key role played by robotic telescopes around the World cannot be understated as they guarantee continuous observations of GRBs beyond the Rubin LSST survey.

## 3. Facilities/software requirements

We expect to access the Rubin data via the broker alert stream. At the same time, we intend to compare the candidates with existing transient catalogs, which are available through the Rubin LSST Science Platform. Due to the magnitude-limited capabilities of follow-up observatories ( $m_{AB} \approx 22$  is a reasonable limit to securely detect weak metal absorption lines with a 8 m class telescope), it is imperative that we build nightly light curves of these fast-evolving objects. A direct link to a GRB-dedicated alert system (GCN Circular Network or the newly developed GCN Kafka Broker<sup>77</sup>) will guarantee the rapid identification and dissemination of each flagged GRB's location, type, and information relating to its temporal behavior.

### 2.5.4. Blazars

Active galactic nuclei (AGNs) include a broad variety of sources that share the common property of emitting persistent huge luminosities from a very compact region ( $\sim 1$  pc). Their power is thought to come from the accretion of matter onto a supermassive black hole (with mass  $10^6$ – $10^{10} M_{\odot}$ ). Some

AGNs are very powerful radio sources, with twin jets of plasma extending up to Mpc distances from the central engine, e.g., 3C 236 and Centaurus A. When one of the jets is oriented close to the line of sight, its emission is amplified by relativistic effects and these beamed sources are called “blazars.” Therefore, blazars are the most suitable objects to investigate the physics of the inner parts of extragalactic jets.

Blazars include flat spectrum radio quasars (FSRQs) and BL Lac objects (BL Lacs). The classical separation between the two classes depends on the spectroscopic properties, where BL Lac objects show only weak emission lines, if any (Stickel et al. 1991; Stocke et al. 1991).

Blazars emit at all wavelengths, from the radio to the  $\gamma$ -ray bands, and their flux is variable on all observable time scales, from minutes to years. They also show spectral changes. The variability can be due to both geometric effects (i.e., variations of the viewing angle of the emitting regions, see e.g., Raiteri et al. 2017) and intrinsic (i.e., energetic) processes. Orientation changes can be produced by magnetohydrodynamic instabilities developing inside the jet, by orbital motion in a binary black hole system, or by a precessing jet. Energetic processes include the injection and acceleration of particles, formation of shock waves, and magnetic reconnection.

Blazar radiation is polarized. Both the polarization degree and angle are variable too. Indeed, the lower energy radiation, from radio to UV and in some cases up to X-rays, is well explained by synchrotron radiation produced by relativistic electrons in the magnetized jet, while the origin of the high-energy radiation (X rays and  $\gamma$  rays) is still debated. According to leptonic models, the high-energy radiation is produced by the inverse-Compton scattering of soft photons from the same relativistic electrons (Konigl 1981). Alternatively, hadronic models suggest that the high-energy emission is caused by synchrotron radiation produced by protons and muons and by particle cascades (Böttcher et al. 2013). Hadronic models also predict the production of neutrinos. In this respect, the recent detection by IceCube of ultra-high-energy neutrinos, which can possibly be associated with blazars, opens an exciting new observing window for these multimessenger sources (Aartsen et al. 2019).

Radio-loud AGN (and in particular blazars) are among the best sources for searching for black hole binaries, as they are hosted in giant elliptical galaxies that are thought to result from galaxy mergers. According to the binary black hole models of Lehto & Valtonen (1996) and Sundelius et al. (1997), when a secondary black hole impacts the accretion disk of the primary black hole, a periodic optical outburst signal is produced. The outburst timing gives strong constraints on the two black hole masses and a measurement of the spin of the primary black hole. This model has been successfully applied to the quasi-periodic light curve of the BL Lac object OJ 287, which shows double-peaked outbursts every  $\sim 12$  years (Valtonen et al. 2016). In contrast, Villata et al. (1998) proposed a scenario

<sup>77</sup> <https://gcn.nasa.gov/>

where the two jets, launched by the two super massive black holes of the binary system, are bent by the interaction with the ambient medium such that their axes undergo long-term precession causing the orientation of the outflow to vary quasi-periodically in time. More recently, the blazar PG 1553 +113 has been found to exhibit a two yr quasi-periodic behavior when observed in  $\gamma$  rays (Ackermann et al. 2015), which is also recognizable in optical light curves. Radio observations have revealed a processing/wobbling motion of the jet, which suggests that geometrical effects must play a major role (Caproni et al. 2017; Lico et al. 2020).

Blazars are currently the only type of AGNs that are researched by members of the TVS. For additional information on these and other types of AGNs, see the Active Galactic Nuclei Science Collaboration Roadmap.<sup>78</sup> Within the TVS, blazar research promises to include the following:

#### 1. Low hanging fruit

##### (a) **Trigger multi-wavelength observations of flares and other interesting events**

By monitoring blazar flux variations, we are able to trigger follow-up observations every time an interesting event (usually a flare) is observed. This will enable immediate observations using multi-wavelength facilities. Follow-up observations may also include optical observations in polarimetric and spectroscopic mode. Multi-frequency light curves will allow us to study cross-correlations and time delays between flux changes in the optical band and those in other bands through the application of time series analysis methods. This in turn will shed light on the emission and variability mechanisms (particle acceleration/cooling, shock waves, orientation effects), and on the location of the various emitting regions in the jet. This requires a comparison with theoretical models for blazar emission and variability.

##### (b) **Search for optical counterparts of unidentified $\gamma$ -ray sources**

Rubin LSST will observe known blazars that have previously been observed by the Fermi Gamma-ray Space Telescope satellite (and in the future by the Cherenkov Telescope Array-CTA). The Fermi Large Area Telescope Fourth Source Catalog (4FGL, The Fermi-LAT collaboration 2019) Data Release 3 (DR3) includes 6658 sources, 68% of which are identified or associated with blazars. There are 2157 sources that still lack a secure identification with counterparts at other wavelengths, most of which are expected to be blazars. The Rubin LSST discovery of optical flaring activity in sources lying in the positional uncertainty region of these  $\gamma$ -ray sources would lead to robust

identifications. Some identifications are expected during the first year of the survey.

#### 2. Pie in the sky

##### (a) **Understand the production of neutrinos by blazar jets**

By looking for active blazars in the sky locations where ultra-high-energy events have been detected by IceCube (and in the future, that will be detected by KM3NeT), we plan to verify the power of blazars as cosmic accelerators. The first robust association between a flaring blazar and a high-energy IceCube neutrino was established in 2017 (Aartsen et al. 2018). Righi et al. (2017) estimated that the future neutrino experiment, KM3Net, will be able to detect the neutrino signal of several BL Lacs in a few years. In this context, the Rubin LSST continuous mapping of the sky will be a formidable tool for establishing such connections. The comparison between the source behavior and theoretical predictions will clarify the framework in which neutrinos are produced in blazar jets.

##### (b) **Reveal the nature of periodic flux changes in binary black hole binary systems**

Geometrical scenarios versus intrinsic scenarios that describe the periodic flux changes in black hole binaries may be discerned through polarimetric measurements during the (quasi) periodic outbursts. Since Rubin LSST will monitor a large portion of the sky for  $\sim 10$  years, we expect that it will be able to either confirm or reject black hole binary candidates and detect new ones, which has important implications for gravitational wave astronomy.

#### *Preparations for Blazar Science.*

##### 1. **Identifying events from alerts**

Identifying interesting events, such as flares, in time to conduct follow-up observations will necessarily rely on the Rubin LSST Prompt Data Products delivered by a community broker. More work is required to establish suitable filters within the available broker systems and to measure their performance. Due to the nature of the phenomenon, it is particularly important that Rubin LSST alerts are cross-matched against multiwavelength information at all frequencies, from radio to  $\gamma$  rays, in real-time. Facilities that could provide these observations include: FIRST, NVSS, VLASS, WISE, 2MASS, SDSS, Gaia, ROSAT, XMM-Newton, Swift, and Fermi. Furthermore, it would be highly beneficial to cross-match alerts against catalogs of blazars and blazar candidates, such as BZCAT (Massaro et al. 2009), CRATES (Healey et al. 2007), 3HSP (Chang et al. 2019), WIBRaLS and KDEBLACS (D'Abrusco et al. 2019), BROS (Itoh et al. 2020) and ABC (Paggi et al. 2020).

<sup>78</sup> <https://agn.science.lsst.org/>

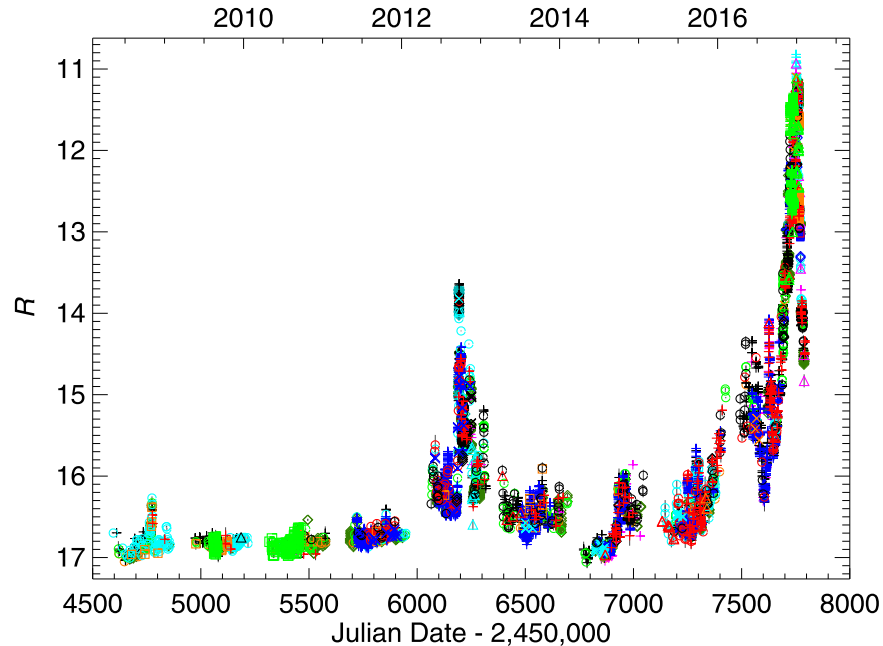


**Figure 6.** The long-term  $R$ -band light curve of the blazar CTA 102 that has been obtained by the Whole Earth Blazar Telescope Collaboration. Reproduced from Raiteri et al. 2017, with permission from Springer Nature.

## 2. Follow-up observations

The blazar science cases would highly benefit from a support telescope of the meter class equipped with a polarimeter to monitor the polarimetric behavior of selected objects, especially during active states. Polarimetric observations can distinguish between non-thermal and thermal phenomena, and are expected to give information on the jet magnetic field. Spectropolarimetry on larger telescopes would also be advantageous.

## 3. Facilities/software requirements

In addition to accessing Rubin LSST data via the brokers, it will be necessary to explore the Data Release Products, using the database search and visualization tools provided by a data access center (DAC) and hosted on the Rubin Science Platform Jurić et al. (2017). Interactive image and data plotting tools will be required, and overlaying images from surveys spanning the full wavelength range will be essential in assessing target behavior. Some very useful tools are available at the ASI Space Science Data Center,<sup>79</sup> such as the Sky Explorer, SED builder, and Multi Catalog Search tools. Implementation of tools like those in the LSST Science Platform (RSP) would improve Rubin LSST data exploitation. Moreover, the ability to cut-out images of interesting objects is important, in particular to analyze low-luminosity BL Lac objects, where the jet point-like

emission is drowned into the emission of the extended host-galaxy. Such a problem is common to other AGN studies in general.

Additionally, software tools to analyze the timeseries photometry will be required to accomplish the science goals above. As with other science cases, while some codes already exist, they are likely to require updating to handle the Rubin LSST data products and to operate within the Rubin Science Platform environment. Methods for performing time series analysis are further detailed in Section 3.5.1.

One critical point for blazar studies is the saturation limit of Rubin LSST. Blazar flaring states can involve flux changes up to six magnitudes, as shown by the  $R$ -band data obtained by the Whole Earth Blazar Telescope Collaboration<sup>80</sup> (Raiteri et al. 2017, see Figure 6). Consequently, there is an implicit danger of losing information during the most interesting phases. Therefore, methods to avoid or at least mitigate saturation are strongly needed and can involve either software or observing solutions that should be tested during the commissioning phase. Raiteri et al. (2022) performed analysis of the impact of saturation on blazar variability studies with Rubin LSST. The possibility of avoiding saturation by adopting short exposures or using star trail

<sup>79</sup> <https://www.ssd.csi.it/>

<sup>80</sup> WEBT: <https://www.oato.inaf.it/blazars/webt/>.

observing techniques (Thomas & Kahn 2018) was discussed in Raiteri et al. (2018).

### 2.5.5. Tidal Disruption Events

Tidal Disruption Events (TDEs) occur when a star passes within the Roche radius of a supermassive black hole in a center of a galaxy, where it is torn apart by strong tidal forces (Rees 1988; Evans & Kochanek 1989). After the disruption, approximately one half of the stellar debris escapes the gravitational pull of the black hole, while the other half remains bound and eventually returns to the supermassive black hole. The fallback rate of the bound material follows a  $t^{-5/3}$  decline.

The disruption can be observed as a bright flare of light originating from the center of a non-active galaxy. The observed optical emission depends on various parameters relating to the objects and dynamics involved, e.g., the black hole mass, the pericenter radius, and the stellar mass, radius, and composition (e.g., Kochanek 1994; Gomboc & Čadež 2005; Lodato et al. 2009; Guillochon & Ramirez-Ruiz 2013; Mockler et al. 2019). Thus, optical light curves of TDEs provide a unique opportunity for detecting dormant supermassive black holes and measuring their masses. TDEs enable the study of black holes with masses up to  $10^8 M_\odot$ , since at larger supermassive black hole masses the (classical) Roche radius for a solar-type star lies inside the black hole event horizon. However, if a heavier supermassive black hole is rotating rapidly, we can expect to detect tidal disruptions of solar-type stars from black holes with  $M_{\text{BH}} > 10^8 M_\odot$  (Kesden 2012), making measurements of black hole spins using TDEs a possibility.

TDEs are rare events, with the rate between  $10^{-4}$  and  $10^{-5}$  per galaxy per year (e.g., Magorrian & Tremaine 1999; van Velzen & Farrar 2014). To date the sample of optically detected TDEs consists of a couple dozen events (e.g., van Velzen et al. 2011; Gezari et al. 2012; Arcavi et al. 2014; Chornock et al. 2014; Holoien et al. 2014, 2016; Leloudas et al. 2016; Blagorodnova et al. 2017; Wyrzykowski et al. 2017; Holoien et al. 2019, 2019; van Velzen et al. 2019), mostly discovered in the last 15 years with optical surveys such as SDSS, Pan-STARRS, PTF, iPTF, ASASSN and ZTF. The majority of these events have follow-up spectroscopic observations and/or UV observations. Currently, we are detecting  $\sim 10$  TDEs per year.

The observed sample shows a variety of light curves (van Velzen et al. 2019). However, the majority of these curves exhibit a steep decay consistent with  $t^{-5/3}$  in early times with late-time accretion disk emission consistent with a near-constant power law decline. They evolve slowly, on time scales from months to years, and usually show no AGN variability in the host prior to the transient phase. The peak absolute magnitudes of TDEs are around  $-20$ , while their

spectra are blue with broad He and/or H lines. Throughout their evolution, they remain at an approximate constant temperature with  $T_{\text{BB}} \approx 2 \times 10^4$  K and show little to no color evolution. TDEs tend to show a preference toward post-starburst E+A host galaxies (Arcavi et al. 2014; French et al. 2016; Law-Smith et al. 2017; Graur et al. 2018), though they also appear in other types of galaxies.

Rubin LSST is expected to detect  $\sim 1000$  well sampled TDEs per year (van Velzen et al. 2011; Bricman & Gomboc 2020). A large sample of successfully identified objects with frequent temporal sampling is essential in order to unveil several properties of TDEs that are still not well understood. For example, our knowledge about the origin of the optical emission is incomplete. New observations are needed to determine whether the emission is due to the reprocessing of the inner disk (e.g., Loeb & Ulmer 1997; Guillochon et al. 2014) or due to shocks caused by stream-stream collisions (e.g., Piran et al. 2015; Krolik et al. 2016; Bonnerot et al. 2017). Furthermore, discovering TDEs pre-peak allows photometric and spectroscopic studies throughout the evolution of the event. These data will enable the accretion physics and environments of dormant supermassive black holes to be probed.

The availability of Rubin LSST data in real time will enable the science cases described in detail below. All science cases depend on our ability to identify TDEs from the large number of transients that Rubin LSST will discover each night. Therefore, an automated algorithm for the early-time photometric identification of TDEs, which is able to distinguish them from other transients (especially SNe), is required.

#### 1. Low hanging fruit

##### (a) Probing the origin of the optical emission

The properties of early-time, pre-peak light curves at low-redshift TDEs can be determined through the consideration of the optical emission. Thanks to the depth of Rubin LSST, we can measure the temperature (from the  $u - r$  color) and the rise of the earliest emission from low-redshift TDEs ( $z \sim 0.05$ ), which will provide new insight into the origin of their optical emission. If the emission is due to the reprocessing of the inner disk, we should expect a smooth rise to peak and a large blackbody radius, while emission due to shocks from intersecting streams should yield a smaller blackbody radius and may show larger rms variability.

##### (b) Increasing the number of well-sampled TDEs

Rubin LSST is expected to detect  $\sim 1000$  well sampled TDEs per year (van Velzen et al. 2011; Bricman & Gomboc 2020), which will allow statistical studies of supermassive black holes. TDEs discovered with Rubin LSST will increase the current observed sample by a factor of  $\sim 10$ . This will enable

correlations between the observed properties of TDEs to be analyzed, for example: galaxy mass, peak luminosity, peak time, and the color at the peak. A larger observed sample will enable measurements of the luminosity function of TDEs as a function of galaxy mass or galaxy type.

(c) **Determination of the masses of quiescent super-massive black holes**

Frequently sampled light curves of TDEs observed with Rubin LSST will enable numerically predicted models to be fitted to observations and consequently the determination of supermassive black hole masses. To achieve this science goal, we need accurate models that can describe the optical light curves of TDEs and can provide supermassive black hole mass estimation. An example of such models include `MOSFIT` (Guillochon et al. 2018), which does a great job describing “normal” events. See (Mockler et al. 2019). However it struggles to reproduce TDEs with “unusual” properties, e.g., ASASSN-15lh (Dong et al. 2016; Leloudas et al. 2016) or AT2018fyk (Wevers et al. 2019).

(d) **The late-time observations of accretion disks**

The depth and frequent temporal sampling of Rubin LSST will enable late-time ( $>1$  yr post peak) observations of the brightest events. The detection of these plateaus will enable black hole mass measurements (van Velzen et al. 2019).

(e) **Assessing the relationship between color and TDE host galaxies**

With a sample of  $\sim 1000$  TDEs and information on their host galaxies, we will be able to investigate whether the color of the host galaxy is correlated with the probability of a TDE going off in the galaxy. Since TDEs seem to favor post-starburst hosts, with a clear preference toward E+A galaxies (Arcavi et al. 2014), information on the type of galaxies in Rubin LSST’s field of view will be useful for faster classification of the events (French & Zabludoff 2018). An example of this is that a nuclear transient in E+A/post-starburst galaxy is more likely to be a TDE than a SNe.

2. Pie in the sky

(a) **Redshift evolution of the TDE rate**

After a year of the Rubin LSST operations we should have a sample of  $\sim 1000$  photometric TDE candidates with photometric redshift from their host galaxies. After turning this into a volume-limited sample, the number in different redshift bins is directly proportional to the disruption rate at each redshift. If the TDE rate is proportional to the galaxy merger rate, we can expect a strong increase of the disruption rate from  $z = 0.1$  to  $z = 1$ . On the other hand, the decreasing density of  $M \sim 10^6 M_{\odot}$  black

holes with redshift may lead to a decrease of rate (e.g., Kochanek 2016).

(b) **Black hole occupation fraction**

After a few years of Rubin operations (with a sample that exceeds 1000 photometric TDEs), we can measure the rate as a function of galaxy mass (and galaxy type). Comparing this to the predicted rate as a function of mass, we obtain the fraction of galaxies that host black holes, i.e., the black hole occupation fraction.

(c) **Off-nuclear TDEs observed indirectly through recoiling black holes or stripped satellite galaxies**

After we have established the photometric properties of nuclear TDEs as seen by Rubin LSST, we can relax our requirement for the location of the transient in the host galaxy and search for these more rare events. A measurement of the fraction of non-nuclear massive black holes provides constraints on their seed formation mechanism in the early universe (Greene et al. 2020).

*Preparations for TDE Science.*

1. **Identifying events from alerts**

The targets from Rubin LSST will be selected in real time, via filters in brokers. The main challenges involved in identifying TDEs are:

- (a) How to reliably identify TDEs based solely on Rubin LSST’s photometric data, which may not have ideal time and multi-band coverage (in particular in the  $u$ -band filter)
- (b) How to measure the purity of the filtered TDEs using realistic light curves of the most frequent contaminants (e.g., SNe and AGNs)
- (c) How to identify a TDE before the peak in the light curve, which may be on the order of days to weeks, depending on the time of the first detection

A filter to select TDE candidates based on light curve properties is being developed for the Ampel (Nordin et al. 2019b) Broker. For the purpose of detecting TDEs, a filter should incorporate the following steps:

- (a) Extract nuclear flares (from the centers of galaxies)
- (b) Extract the photometric features (e.g., rise-time, color, color-evolution, fade timescale)
- (c) Photometric typing, including machine learning.

Required data would be the information included in the Rubin LSST Alerts: the history of an object, full photometric light curve, astrometric data (galaxy cross-match, off-set from the galactic center), galaxy photoz, and galaxy color/type. The TDE filter output would be a stream of nuclear flares with light curve features, including classification labels or probabilities. We expect the initial sample (including false positives) will be  $\sim 10,000$  per year and the filtered sample of accurate detections to be  $\sim 100$  per year at magnitude  $\sim 20$ .

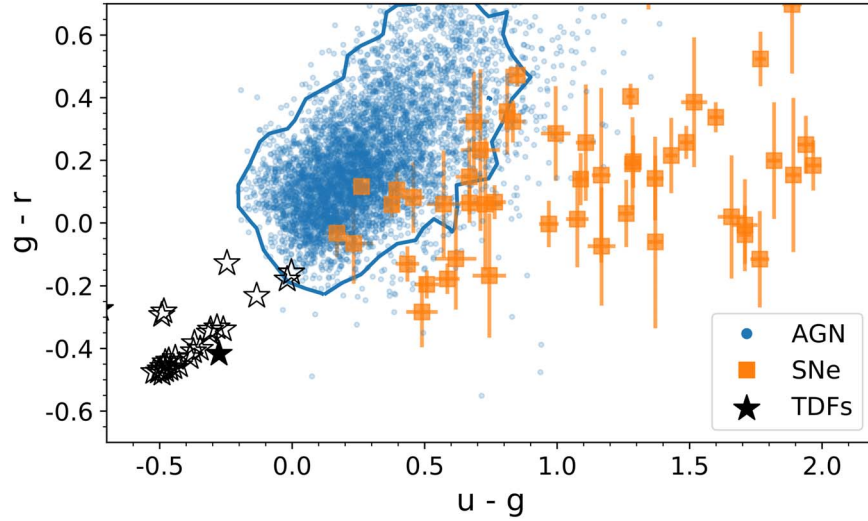


**Figure 7.** Color–color diagram of nuclear transients: mean  $u - g$  color vs. mean  $g - r$  color. TDEs lie in the lower left part of the diagram, with blue mean colors  $u - g \sim -0.5$  and  $g - r \sim -0.4$ , making them clearly recognizable from SNe and AGN. Adapted from van Velzen et al. 2011 © IOP Publishing Ltd. All rights reserved.

## 2. Follow-up observations

Simultaneous observations in UV and X-ray, together with spectroscopic observations of the brightest events, are required for constraining the emission mechanism. As Rubin LSST is a photometric survey that will achieve unprecedented depth, there will be no spectra for the majority of the candidates and we will need to rely on the photometric identification of TDEs from a large sample of transients. It is essential that TDEs are discovered pre-peak and that the observed light curves have sufficient multi-band/mult-wavelength coverage with frequent color measurements, especially in the bluer bands ( $u$ ,  $g$ ,  $r$ ). We emphasize observations in  $u$  band are crucial to discern between SNe and TDEs (van Velzen et al. 2011; Hung et al. 2018; van Velzen et al. 2019). see also Figure 7.

## 3. Facilities/software requirements

emcee or other MCMC fitting code for light curve feature extraction will be required (fitting can take  $\sim 10$  seconds per light curve). This will be important in the determination of colors from observations that are taken in different filters on different nights.

For TDE identification, photometric and spectroscopic follow-up in UV, X-ray and optical bands are possible for the brightest events. Additional data about the galaxy types in the Rubin LSST field of view will also be required. Population studies can be done with Rubin LSST data only. For follow-up observations, Swift-like observations in UV/X-ray bands are required for events at  $z < 0.2$ . Optical spectra from 2–8 meter class telescopes are also important. Additionally, archival data

products from eROSITA, Gaia, WISE (final co-adds), and BlackGEM will be essential.

### 2.5.6. Electromagnetic Counterparts of Gravitational Wave Events

The discovery of the electromagnetic counterparts to the binary neutron star merger GW170817 at 40 Mpc has opened the era of gravitational wave+electromagnetic multi-messenger astronomy (Abbott et al. 2017b). The true power of gravitational wave detections becomes apparent when they are paired with electromagnetic data. The identification of an electromagnetic counterpart provides numerous benefits including: improved localization leading to host-galaxy identification; determination of the source’s distance and energy scales; characterization of the progenitor’s local environment; the ability to break the modeling degeneracies between distance and inclination; insights into the hydrodynamics of the merger and the physics of the jet launching mechanism; and information about the quantities of heavy elements synthesized in such events. Furthermore, the identification of the electromagnetic counterpart facilitates other fields of study such as determining the primary sites of heavy r-process element production, placing limits on the neutron star equation of state, and making independent measurements of the local Hubble constant (see e.g., Margutti & Chornock 2021, for a recent review).

Gravitational waves have now been detected from many black hole–black hole mergers (Abbott et al. 2016), from binary neutron star mergers (Abbott et al. 2017, 2020) and most



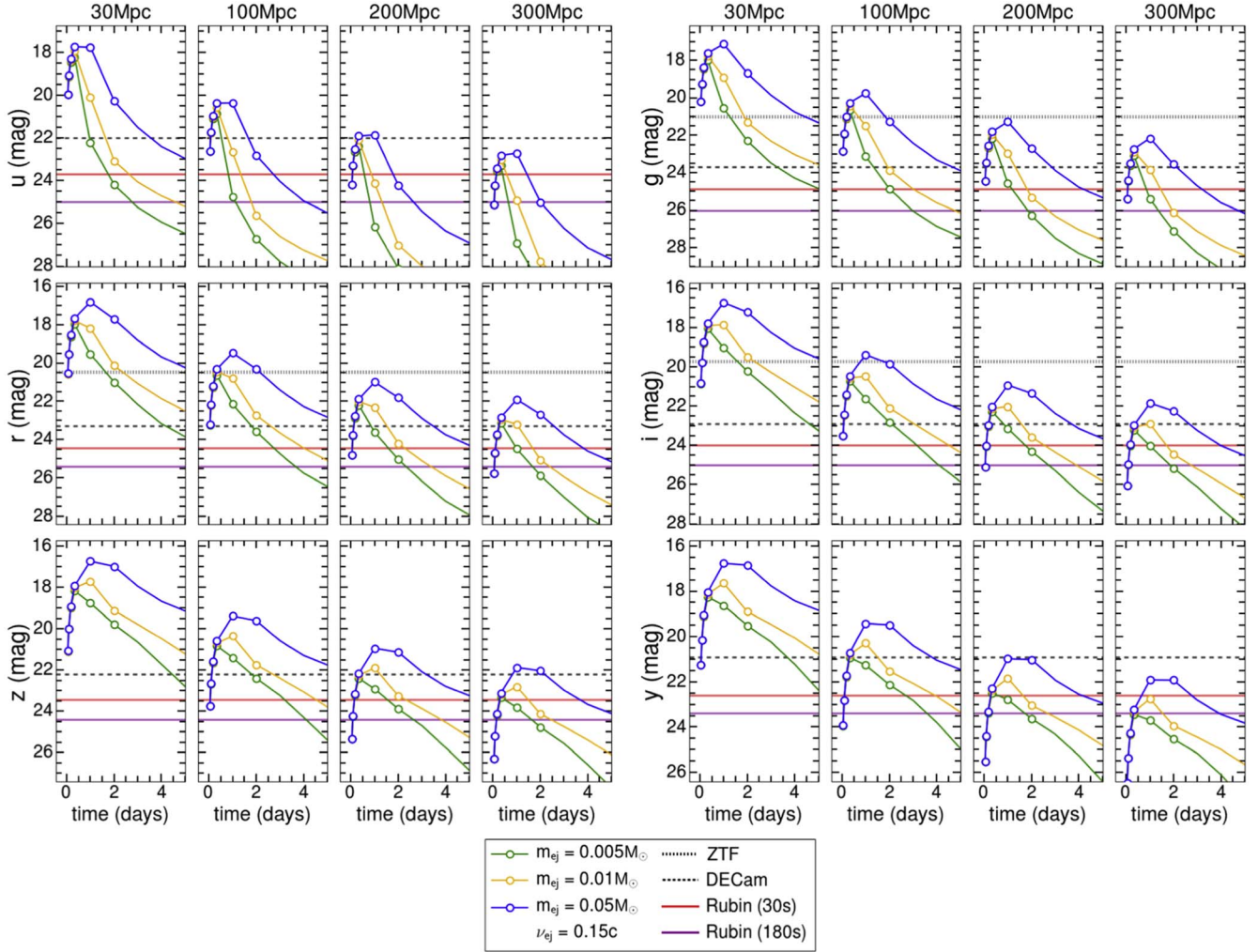


**Figure 8.** Simulated kilonova light-curves in the six Rubin LSST filters for different properties of the ejecta (mass and velocity) at four representative distances (30, 100, 200, and 300 Mpc). Dotted and dashed horizontal lines mark the typical  $5\sigma$  detection thresholds of the ZTF and DECam observations, respectively, assuming 30 s exposure times. Red and purple solid lines: Rubin LSST  $5\sigma$  detection thresholds for exposure times of 30 s and 180 s under ideal observing conditions. The superior sensitivity of the Rubin Observatory is essential to detect the multi-color emission from kilonovae. Reproduced from Andreoni et al. (2022a). CC BY 4.0.

recently from the merger of a black hole with a neutron star (Abbott et al. 2020).

In this rapidly evolving field, the frontier is now to characterize the diversity of the electromagnetic counterparts to compact-object mergers. Additionally, new sources of detectable gravitational wave emissions might soon be revealed, e.g., in the form of a gravitational wave-burst from a highly asymmetric stellar explosion or more exotic event.

Rubin LSST can play a critical role in this nascent field of multi-messenger astronomy in the 2020s, when the gravitational wave detector network is expected to detect higher rates of merger events involving neutron stars ( $\sim 10$  per year) out to distances of several hundred Mpc. Rubin LSST, equipped with target-of-opportunity (ToO) capabilities and the optimal strategies for the follow-up of gravitational-wave sources, will

be the premiere machine for the discovery and early characterization for neutron star mergers and other gravitational-wave sources. Specifically, Rubin LSST ToOs of optical counterparts of gravitational wave sources, which can be both thermal kilonovae (KNe) and gamma-ray burst afterglows, will uniquely enable the following science, if equipped with the ToO observing strategy as in Figure 9:

1. Low hanging fruit
  - (a) **Population studies of electromagnetic counterparts of neutron star mergers**

The primary science goal for studies of electromagnetic transients from gravitational wave sources in the 2020s will be growing the sample size of known events, with a strong focus on finding the faintest

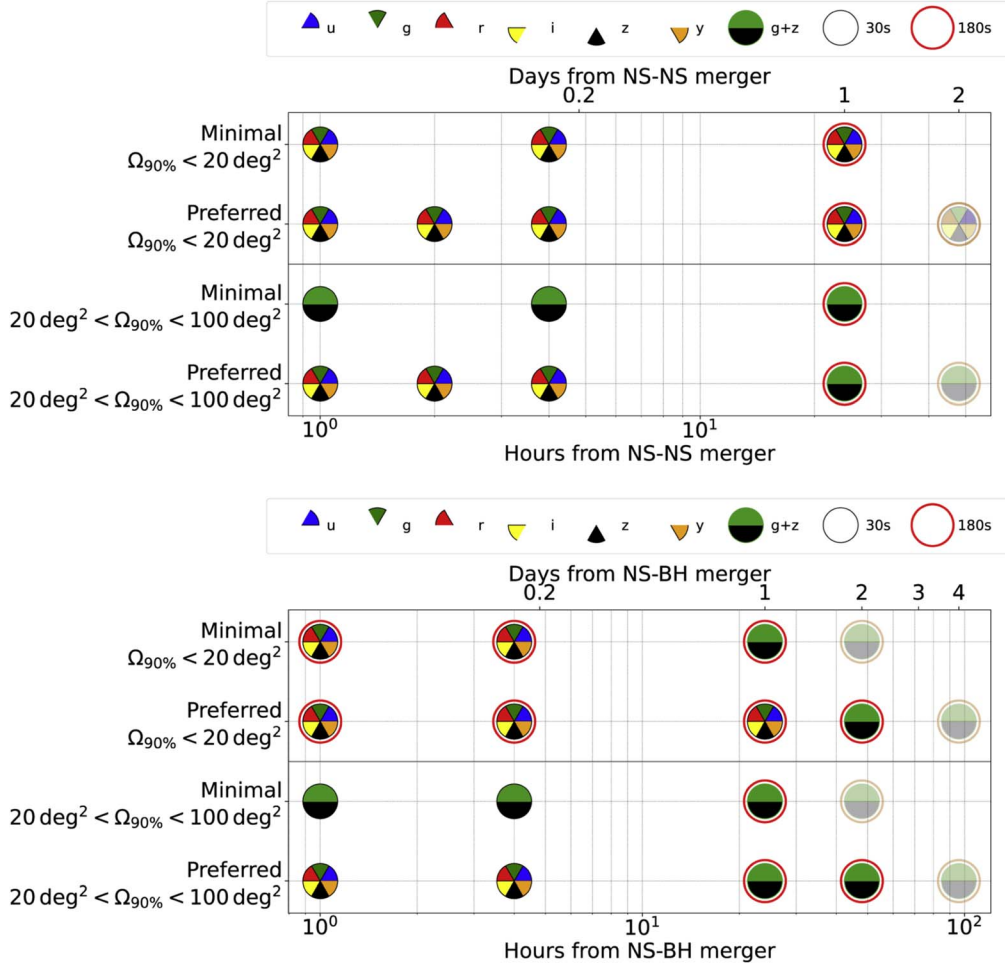


**Figure 9.** Rubin LSST observational follow-up strategy for neutron star-neutron star (top) and neutron star-black hole (bottom) mergers for different gravitational wave localization regions  $\Omega$ . Solid markers indicate planned observations over the entire localization area, while semitransparent markers indicate possible extra observations to be carried out if the optical counterpart has not yet been identified. Additional details can be found in Andreoni et al. (2022a). Reproduced from Andreoni et al. (2022a). CC BY 4.0.

events at the edge of the detection horizon of gravitational wave detectors. Targeted follow-up (see Figures 8 and 9, and Table 3) will be much more efficient at achieving this goal compared to waiting for serendipitous discoveries from the Rubin LSST Wide-Fast-Deep (WFD) survey (e.g., Cowperthwaite et al. 2019; Setzer et al. 2019; Andreoni et al. 2022b) and a combined multi-messenger analysis will be of much higher scientific value (e.g., Dietrich et al. 2020). Using Rubin LSST for targeted follow-up will build a large sample of electromagnetic counterparts, which are essential for conducting statistically rigorous systematic studies. These data will allow us to understand the diversity of electromagnetic behaviors for gravitational waves, the host environments of the mergers, the nature of merger remnants, and the

contribution of the event to the chemical enrichment of the Universe through cosmic  $r$ -process production, which shapes the light-curves and colors of kilonovae associated with gravitational wave events (e.g., Metzger et al. 2015).

(b) **Very early observations of kilonovae (e.g.,  $\lesssim 10$  hr post-merger)**

Despite the fact that the optical counterpart of GW170817 was discovered less than 11 hr post-merger (e.g., Andreoni et al. 2017; Arcavi et al. 2017; Coulter et al. 2017; Cowperthwaite et al. 2017; Drout et al. 2017; Kasliwal et al. 2017; Lipunov et al. 2017; Smartt et al. 2017; Soares-Santos et al. 2017; Tanvir et al. 2017; Valenti et al. 2017; Villar et al. 2017), these observations were still unable to definitively determine the nature of the early time emission.

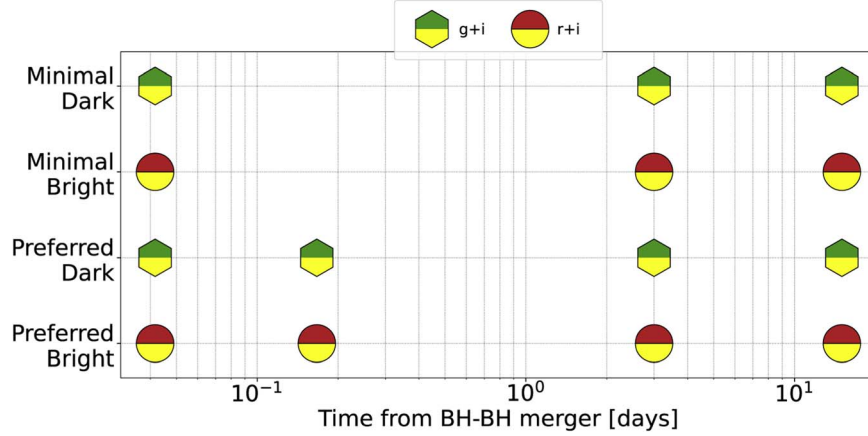


**Figure 10.** Rubin LSST observational follow-up strategy for black hole–black hole mergers for different gravitational wave localization regions  $\Omega$ . Additional details in Andreoni et al. (2022a). Reproduced from Andreoni et al. (2022a). CC BY 4.0.

**Table 3**

Predicted Number of Neutron Star–Neutron Star (NS–NS), Neutron Star–Black Hole (NS–BH) and Black Hole–Black Hole (BH–BH) Merger Gravitational Wave Detections during the Fifth LIGO, Virgo, and KAGRA (LVK) Observing Run (O5), with Which Rubin LSST Science Operations will Likely Overlap, Assuming a Duration of One Calendar Year for the Run

	O5		
	Total	$20 < \Omega_{90\%} \leq 100$ (Rubin)	$\Omega_{90\%} \leq 20$ (Rubin)
NS–NS	$190_{-130}^{+410}$	$22_{-15}^{+49} (12_{-3}^{+8})$	$13_{-9.1}^{+29} (7_{-5}^{+15})$
NS–BH	$360_{-180}^{+360}$	$45_{-23}^{+45} (24_{-12}^{+24})$	$23_{-12}^{+23} (12_{-6}^{+12})$
BH–BH	$480_{-180}^{+280}$	$104_{-39}^{+61}$	$70_{-26}^{+41}$

**Note.** Numbers within brackets indicate the events that will be accessible to Rubin LSST. Reproduced from Andreoni et al. (2022a). CC BY 4.0. Based on results by Petrov et al. (2022).

Understanding this early-time emission is crucial for identifying emission mechanisms beyond the KNe, e.g., neutron precursor, shock-cooling (Piro & Kollmeier 2018). In particular, mapping the rapid broad-band SED evolution will allow us to separate these components, and also to distinguish KNe from most other astrophysical transients. Rubin LSST’s prompt data alerts will enable the rapid follow-up of KNe for the purpose of identifying their emission mechanisms (see Figures 8–9 and Table 3 for follow-up and detection details).

(c) **Discovery of the electromagnetic counterparts of neutron star–black hole mergers**

Neutron star–black hole mergers can produce KNe under some physical conditions. However, depending on the mass ratio of the binary and the neutron star equation of state, there may be less or more material ejected (e.g., Foucart et al. 2018), and

hence a brighter or fainter electromagnetic counterpart. It is also unclear if neutron star–black hole mergers will be able to produce the bright early-time blue emission seen in GW170817 (Metzger et al. 2015). Furthermore, these systems will be gravitationally louder and thus gravitational wave detections will, on average, be at greater distances. This combination of increased distances and potentially fainter counterparts means that Rubin LSST will be an essential tool for discovering these electromagnetic counterparts (see Figures 8 and 9 and Table 3 for follow-up and detection details).

2. Pie in the sky

(a) **Discovery of electromagnetic counterparts of binary black hole mergers**

There are numerous speculative mechanisms for the production of an optical counterpart to a black hole–black hole merger (e.g., Perna et al. 2016; Loeb 2016; de Mink & King 2017; Stone et al. 2017; McKernan et al. 2018). Yet, none have been unambiguously observed. Rubin LSST will be able to place the deepest limits on the optical emission from black hole–black hole mergers, with a high statistical confidence in the case of non-detections, and may be able to discover the first electromagnetic counterpart to a black hole–black hole merger. In general, Rubin LSST has the best capabilities (with its co-added limiting magnitude of 27.5 in the  $r$ -band) for exploring the currently uncharted territory of electromagnetic counterparts of unidentified gravitational wave sources. See Figure 10 for a diagram describing the follow-up procedures and Table 3 for the probability of detection with Rubin LSST.

*Preparations for Electromagnetic Counterpart Science.***1. Identifying events from GRB triggers**

While, for the most part, Rubin LSST will be used for the purpose of follow-up in the context of gravitational wave science, triggers from gamma-ray space observatories will be used to identify and to prompt expeditious follow-up observations of gamma-ray bursts and kilonovae. We plan to work with current and future X-ray/radio/UV facilities that interface with brokers: to reduce the sky localization areas to search, to filter out “undesired transients,” and to ensure that the relevant information is shared. This will allow us to make important decisions about which sources to observe with Rubin LSST.

**2. Follow-up observations**

Once the gravitational wave counterpart is identified, a deep pointed multi-band follow-up is required to extract as much information as possible about the physics governing the thermal and non-thermal emissions associated with the gravitational wave sources. Given the current estimates of kilonovae rates, Rubin LSST will be able to detect  $\sim 10^2$ – $10^3$  events within  $z = 0.25$ , but their classification might be challenging. Using several simulated cadence strategies for Rubin LSST, Andreoni et al. (2022b) found that currently available cadences will be able to identify more than 300 KNe out to  $\sim 1400$  Mpc over a 10 yr survey. Among those, we expect about 3–32 KNe that are recognizable as fast-evolving transients, similar to the GW170817. The samples of candidate counterparts coming from the Rubin LSST search will be photometrically and spectroscopically followed up by larger telescopes to determine their nature, removing the numerous expected contaminants. Once the most promising counterpart candidates are selected among the yet unclassified sources, deep photometry and spectroscopy are required for studying all the properties of the emission. While the selection of the most promising candidates can be done using 1–3 m telescopes (such as the Palomar 200 inch Hale telescope, the Liverpool Telescope, the Telescopio Nazionale Galileo, and the Nordic Optical Telescope), to capture detailed features of the KN spectrum and its evolution, larger telescopes of 4- to 10-meter class are required. Some examples of the required instruments are the X-shooter spectrograph on the ESO Very Large Telescope, the EFOSC2 instrument in spectroscopic mode at the ESO New Technology Telescope, the Goodman Spectrograph on the 4 m SOAR telescope, and the FLAMINGOS2 near-infrared spectrograph at Gemini-South. The HST and JWST are additional key instruments that avoid challenging atmospheric absorption lines that plague infrared spectroscopy.

**3. Facilities/software requirements**

Considering that only through real-time follow-up we can learn about the nature of these fast transients, once we have access to the Rubin LSST data via the broker alert streams, we will need fast transient discovery algorithms (e.g., Andreoni et al. 2022b) and software able to classify the light curves of these fast-evolving candidates every night. This requirement is mandatory and will help us confirm the discovery of a gravitational wave counterpart so that we are able to obtain swift multi-wavelength follow-up with other observing facilities.

**3. Non Time-critical Science***3.1. Executive Summary*

The wide-fast-deep 10 yr long survey will provide a plethora of data spanning the entire southern sky. This unparalleled volume of data will provide extensive new insights into non-time critical transient and variable star science. Here we summarize the sections of this chapter along with the primary science objectives for each science field.

**Transiting Exoplanets:** It is anticipated that hot jupiters around Sun-like stars within distances of approximately 0.1 AU from their host stars will be prime targets for Rubin LSST. Other missions, such as TESS, will be used to calibrate Rubin LSST’s planet detection methods.

**Eclipsing Binary Stars:** A full census of short-period and contact binary stars will be obtained with Rubin LSST, which can further be used as a population probe of the Galaxy. Color information will provide temperature estimates for all known eclipsing binaries in the Southern sky. Binary stars will further provide calibration for trigonometric parallaxes. Rubin LSST will provide a deeper understanding of contact binaries and is expected to identify  $\sim 1$  million contact binaries (Prša et al. 2011) during the 10 yr survey.

**Microlensing:** With Rubin LSST, we can expect an average rate of 15 microlensing events  $\text{deg}^{-2} \text{yr}^{-1}$  in the disk and 400 events  $\text{deg}^{-2} \text{yr}^{-1}$  in the Bulge Sajadian & Poleski (2019). With the Annual Release Data, the microlensing optical depth, event rate and event duration distributions will be analyzed, which will provide information about the mass density distribution and the kinematics of compact objects. Through injection of simulated events into the data from the Annual Data Releases, the selection bias for microlensing events will be analyzed.

**Pulsating Stars (General):** Classification of pulsating stars and the subsequent creation of a pulsational H-R diagram form the primary goals for general pulsating star science with Rubin LSST. Due to the relatively large gaps between data points, the initial focus will be on long period pulsating stars, with lower amplitude short-period pulsators and multi-periodic pulsators

becoming more accessible, at least from a statistical perspective, later on in the survey.

**Pulsating Stars (Cepheid and RR Lyrae Stars):** Cepheids and RR Lyrae stars are widely revered as exceptional standard candles. The depth and breadth of Rubin LSST observations will enable the 3D structure of many systems, including the Local Group galaxies, to be studied in detail using these bright pulsating stars. Rubin LSST will further enable the period–luminosity and period–luminosity–color relations to be calibrated (including the metallicity term). These improvements will, in turn, improve estimates of  $H_0$ , especially with additional observations of Ultra Long Period (bright) Cepheids.

**Pulsating Stars (Long-period Variables):** The primary goal for long-period variables is to further understand them in the context of standard candles. In the infrared bands, long-period variables have been shown to have scatter in their period–luminosity relation similar to that of Cepheid variables. By collecting data in the reddest bands with Rubin LSST, long-period variables could provide new additional evidence toward the Hubble tension.

**Galactic Globular Clusters** The stellar populations within globular clusters will be probed using Rubin LSST, including cataclysmic variables, exotic binary star systems (i.e., systems containing neutron stars and black holes) and pulsating stars. The distribution of globular clusters in the galaxy will also be analyzed to understand the effects of tides.

**Brown Dwarfs:** The known sample of brown dwarfs has previously been hampered by their low luminosities. As such, obtaining extensive light-curve coverage has proved difficult. Rubin LSST will generate a large census of brown dwarf light curves to significantly greater distances than before. The yield of brown dwarfs over the 10 yr survey are expected to be as many as 10,000 for the hotter, L0 and L1 brown dwarfs, and as few as  $\sim 10$  for the coolest, T4 brown dwarfs. This will further enable the study of brown dwarf variability, which is currently attributed to weather in the atmospheres of the brown dwarfs.

**Young Eruptive Variables:** Rubin LSST will enable the statistical study of accreting pre-main sequence objects that undergo outbursts (EXor), which are currently only thought to make up 2% of pre-main sequence objects. Further, the mechanism that triggers the observed outburst events will be assessed through the analysis of a statistically significant sample of light curves, e.g., through the identification of periodicities, asymmetries and other morphological changes. With Rubin LSST, we expect to increase the number of EXor candidates ( $\sim 20$ ) by about an order of magnitude during the first year of observations.

**Compact Binaries (Cataclysmic Variables):** All the known Cataclysmic Variables will be continuously monitored and new cataclysmic variables will be discovered and classified. Additionally, cataclysmic variables in eclipsing binaries and polars will be observed, which will enable a deeper look at the mass distribution of cataclysmic variables and the ultimate

evolution of high magnetic field systems after the common envelope phase.

**Compact Binaries (Neutron Star Binaries):** A census of transitional milli-second pulsars, milli-second pulsars and low mass X-ray binaries will be obtained with Rubin LSST. The various types will be analyzed to answer important questions about neutron star state changes.

**Compact Binaries (Black Hole Binaries):** With Rubin LSST, long term observations of a large number of black hole binaries in quiescence will be undertaken for the first time. This will enable a deeper understanding of the companions in these systems and further will enable period determination. In optimal cases, constraints can be placed on the binary component masses.

**Luminous Blue Variables:** Extended observations of luminous blue variables with Rubin LSST will enable: a significant number to be observed during outburst; the association of the identified luminous blue variable (in its eruptive state) with its non-eruptive counterpart; and the identification of luminous blue variables that are SN precursors.

**Light Echoes of eruptions and explosions:** Light echoes can be studied to understand the dust distribution in the region that is local to stellar explosions and to understand the explosion itself. Using Rubin LSST, known light echoes will be studied to eventually form a training set to identify new light echoes. Light echoes can set constraints on galactic explosion history and lead to the discovery of unknown SNe.

**Blazars:** Long term observations of blazars will enable the statistical study of their behavior including periodicities and chromatic flairs. Using Rubin LSST data, the environment of the blazar host galaxies can be better understood and the blazar population as a function of redshift can be explored. The community should expect a constant rate of 100 gamma-ray bursts/year, with at least one third of them being observable by Rubin LSST.

**Supernove:** The long-term monitoring of SNe will enable a deeper understanding of their rates and progenitors. A comparison of SN rates with models will be undertaken and the intrinsic properties of SNe as a function of redshift will also be measured. Light curves of all types of SNe will be obtained, which will enable a more complete understanding of star formation history.

The follow-up and archival data, alongside any software and hardware necessary to complete the outlined objectives are detailed in the relevant sections.

### 3.2. Rubin LSST Data Release products (for Time Domain Science)

After the first half yr of operations, and on an annual basis thereafter, Rubin LSST will process and release all of its data via the Science Platform. This will include all of the data products associated with difference imaging analysis (DIA;

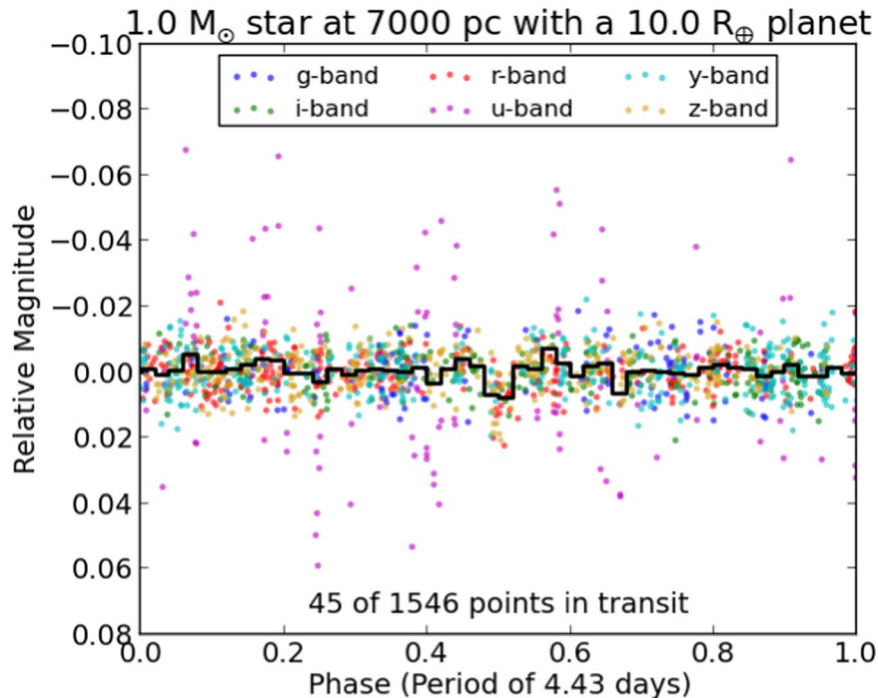


**Figure 11.** Phase-folded simulated light curve of a transiting Hot Jupiter observed in all 6 bands of a Wide-Fast-Deep field. Reproduced from Lund et al. 2015. © IOP Publishing Ltd. All rights reserved.

very similar to the Prompt data products discussed in Section 2.2), the raw and calibration images, deeply coadded all-sky image mosaics in each filter, and object catalogs with measurements and parameters derived from both the visit and coadded images (including catalogs of moving-object orbits based on Rubin LSST data alone). Object catalogs of forced photometry in all direct images for the union set of all objects detected in any image (or image stack) will also be provided. In general, for time-domain studies the annual data release will be the most highly *characterized* set of data products, and will be best suited for e.g., population studies and event rate analyses. See also Jurić et al. (2018) for a full and complete description of the Rubin LSST data products.

### 3.3. Extrinsic Transients and Variables

#### 3.3.1. Transiting Exoplanets

It is known that nearly all stars are orbited by exoplanets, and nearly all known exoplanets with precisely measured physical properties come from transit surveys, such as Kepler/K2 (Borucki et al. 2010; Howell et al. 2014) and TESS (Ricker et al. 2015). For a transiting planet that can also be dynamically measured (such as with radial velocity measurements), one can determine the planet mass, radius, orbital period, orbital eccentricity, and bulk density. Even if the mass of the planet cannot be measured via radial velocity data, due to the small radial velocity signal or faintness of the host star, knowing the

radius and orbital period of large numbers of planets can enable demographic studies of exoplanetary populations, as with the Kepler mission (Bryson et al. 2020, and references therein).

Surveys searching for transiting planets are generally only able to probe a limited parameter space of host stars. Most searches that observe large areas of the sky are only able to search for transits of relatively nearby stars, as these surveys tend to focus on brighter stars. Some searches probe more distant stars, but only in a single region of sky, such as the Kepler field. This trade-off in survey design is a result of the two ways that planet yields can be increased, either through higher cadence observing a narrow region, or by observing more stars down to a fainter limiting magnitude with a wider field. Rubin LSST is not designed with transiting exoplanets in mind, and so provides different challenges and opportunities. The deep-drilling fields constitute a small fraction of the Rubin LSST survey, but have a comparable cadence to ground-based planet searches. The wide-fast-deep fields observe at a lower cadence, but will cover half the sky with a limiting magnitude that is much fainter than surveys that are focused on exoplanet detection (with a magnitude of  $r = 24.7$  for a single visit and  $r = 27.5$  for coadded image, stacked over 10 yr). Exoplanet transits will be detectable in these light curves, as shown in Figure 11. The result is that the detection efficiency will be lower, but the range of stars being searched will include populations not normally prioritized in transiting planet searches, such as very late type stars, white dwarfs, stars in the galactic bulge, and stars in clusters. This will enable Rubin LSST to

provide insight into the planet occurrence and formation rates around stars of different masses, metallicities, and in different stages of stellar evolution.

## 1. Low hanging fruit

### (a) **The Detection of Hot Jupiters**

We expect to observe hot jupiters, planets with the approximate mass of Jupiter found within 0.1 AU of their host star, around a range of main sequence stars (with smaller planets being detectable when orbiting smaller host stars). Standard exoplanet transit detection methods include the search for periodic transit signals in light curves with algorithms like Box Least Squares (Kovács et al. 2002), coupled with careful exclusion of likely false positives, such as various types of eclipsing binary stars (there may also be a significant benefit to newer transit detection methods that have been proposed such as Sparse Box Least Squares (Panahi & Zucker 2021), a recent effort to optimize the Box Least Squares search algorithm for sparsely-sampled light curves). These tools, when applied to Rubin LSST light curves of all colors, should provide candidate exoplanets that would not have been found using any other planet searches (Lund et al. 2015; Jacklin et al. 2015, 2017). The search for hot jupiters will be ongoing through the main survey.

### (b) **The calibration of Rubin LSST's planet detection through other missions**

Rubin LSST's detection of planets may be compared to pre-existing planet searches. The faint end of TESS host stars may overlap with the bright end of stars observed by Rubin LSST. With TESS optimized for detecting short-period planets, Rubin LSST's detection efficiency could be calibrated by trying to recover exoplanets that are found by TESS around stars in the magnitude overlap.

## 2. Pie in the sky

### (a) **The detection of planets orbiting white dwarfs**

It is possible that planets will be detected around white dwarfs. Such detections would provide insight into the formation and structure of planetary systems. The occurrence rate of planets around white dwarfs currently only has upper limits. So far, transit surveys have been unable to survey large numbers of white dwarfs due to their intrinsic faintness and roughly even distribution across the sky. Since even an Earth-sized planet transiting a white dwarf will block a significant amount of light, these events will be detectable with only a few points in transit. The ability of Rubin LSST to detect transiting planets around white dwarfs has been preliminarily explored in both Cortés & Kipping (2019) and Lund et al. (2018b).

## *Preparations for Transiting Exoplanet Science.*

### 1. **Follow-up observations/archival data**

After transit surveys identify candidate transit signals, there are a series of additional observations and analyses required to verify that the signals are indeed arising from exoplanets, and also to measure the properties of the planets. The full process typically involves multiple rounds of follow-up spectroscopy and/or photometry (e.g., Collins et al. 2018) to identify particular types of false positives (Brown 2003; Sullivan et al. 2015). Some follow-up observations will be possible for particular transit candidates identified by Rubin LSST. However, the faintness of the typical star observed by Rubin LSST ( $V < 16$ ) is much fainter than the bulk of transit host stars. Consequently, the majority of exoplanet candidates will not be bright enough for follow-up observations.

In general, such observations include: moderate-precision RV observations to rule out certain false positives caused by EBs and to better characterize the stellar properties; high-spatial-resolution imaging (via AO or Speckle) to identify nearby unseen luminous neighbors; and subsequently precision radial velocity observations to dynamically confirm the planet and measure its mass.

### 2. **Facilities/software requirements**

There are two main types of software that are required for transiting exoplanet science. We will need the ability to search for transit signals in Rubin LSST light curves using Box Least Squares or other transit search tools, and potentially also detrending software. Modern signal detection techniques, such as those based on machine learning algorithms, might be necessary given the the number of stars observed by Rubin LSST. Current software does not exist for such large scales and will likely be created as part of the Rubin Science Platform.<sup>81</sup>

### 3.3.2. *Eclipsing Binary Stars*

Eclipsing binary stars (EBs) play an important role in stellar astrophysics primarily because they allow us to determine stellar masses and radii to an unparalleled accuracy, often exceeding 1–3% (Torres et al. 2010). The run-of-the-mill process of determining these fundamental parameters involves acquiring photometric and spectroscopic data, fitting the data by a sophisticated eclipsing binary model such as WD (Wilson & Van Hamme 2014) or PHOEBE (Prša 2018), critically evaluating the solution uniqueness and, finally, deriving fundamental parameters.

<sup>81</sup> <https://data.lsst.cloud>

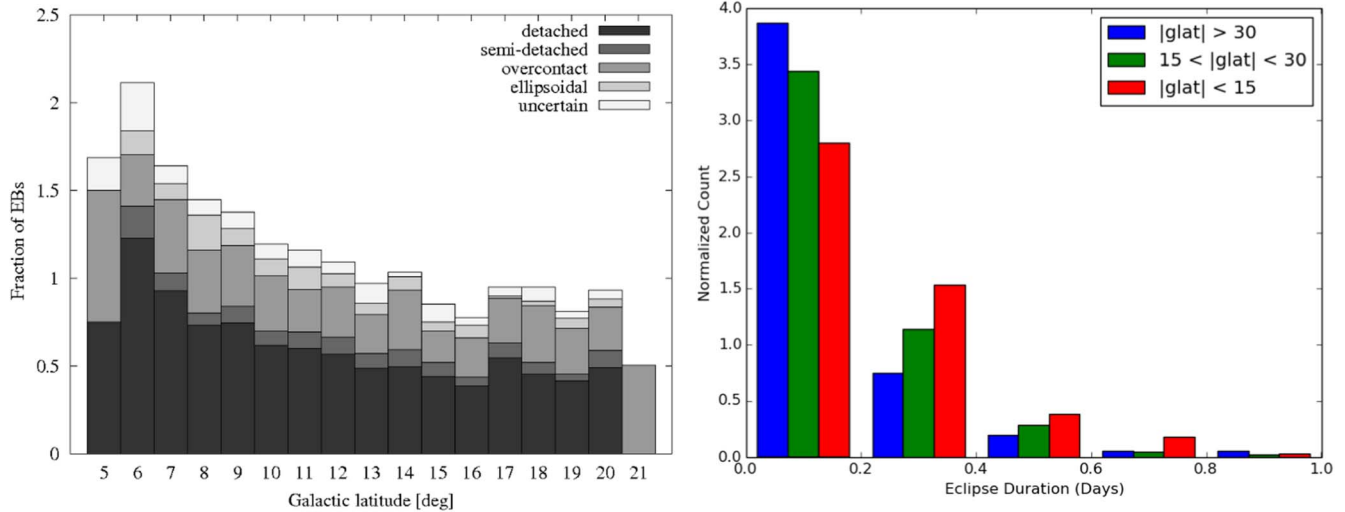


**Figure 12.** Density function of eclipsing binary stars as a function of galactic latitude, observed by the Kepler mission. The left panel depicts the area- and number-normalized count of eclipsing binaries as a function of the inferred morphology type. The right panel depicts the distribution of eclipse durations as a function of galactic latitude. Both panels provide strong evidence that the increasing occurrence rates toward the galactic plane are *not* a consequence of the increased number of stars, but of the genuine differences in the sizes of stars belonging to different stellar populations.

To derive *absolute* parameters (e.g., masses in  $M_{\odot}^N$  or radii in  $R_{\odot}^N$ ), we need to be able to convert angular dimensions to absolute dimensions, and photometry gives us only the former. Thus, without spectroscopy or another means of determining absolute dimensions, the path to absolute dimensions from eclipsing binary modeling remains elusive. This implies that, with Rubin LSST data alone, we will only be able to obtain *relative* sizes of stars; to transition to absolute sizes, we will need additional data or additional assumptions.

Even relative sizes provide us with a wealth of information about stellar populations. Figure 12 depicts a density distribution of EBs as a function of galactic latitude: the left panel provides the area- and number-normalized fraction of EBs as a function of latitude, and the right panel compares eclipse durations for three groups of EBs delineated by latitude. If the number of EBs were uniform across the galaxy, then the left panel distribution would be flat, and the three groups in the right panel would exhibit the same behavior. The observed occurrence rate dependence on galactic latitude clearly indicates that there is an intrinsically higher probability for binaries to eclipse when they are closer to the galactic disk, implying that the stellar population of stars closer to the galactic plane features comparatively larger stars. This conclusion can be drawn even though the absolute scales of these binaries are not known.

To evaluate the effectiveness of the Rubin LSST survey, we simulated Rubin LSST observations of all southern sky binaries discovered by the Transiting Exoplanet Survey Satellite (TESS; Ricker et al. 2015) during their first 26 sectors of observations. Rubin LSST timestamps were simulated by the opsim 2.1 run

(Bianco et al. 2022); they covered the Main Survey, Deep Drilling Fields, and Mini-surveys. For each survey mode we counted the number of field visits and compared them to the number of visits while binaries are in eclipse. This fraction is used as a metric to determine the detection efficiency of EBs. Figure 13 depicts the results for the main survey: top panel shows the distribution of field visits that contain TESS EBs; the middle panel shows the distribution of field visits while the EBs are in primary eclipse; and the bottom panel shows the ratio between the two. The larger the number of in-eclipse visits, the better the odds of detecting EB variability, determining the correct orbital period and classifying it as an EB.

### 1. Low hanging fruit

#### (a) Observing known EBs in the southern sky

Rubin LSST will, as part of the main survey, observe the fields in 6 passbands up to  $\sim 900$  times. The use of passbands will provide us with color information on these targets, which in turn will yield effective temperature estimates. As we know that the objects are EBs ahead of time, this science goal can be met as soon as the survey starts. Given the survey's bright magnitude limit, the obvious sources of known EBs are OGLE, Gaia and, to a lesser extent, TESS.

#### (b) Creatino of a near-complete census of short-period EBs

Thanks to the increased probability of eclipses, short-period EBs are easy targets for long baseline surveys. Additionally, because of tidal and rotational distortion, the amount of received light varies even



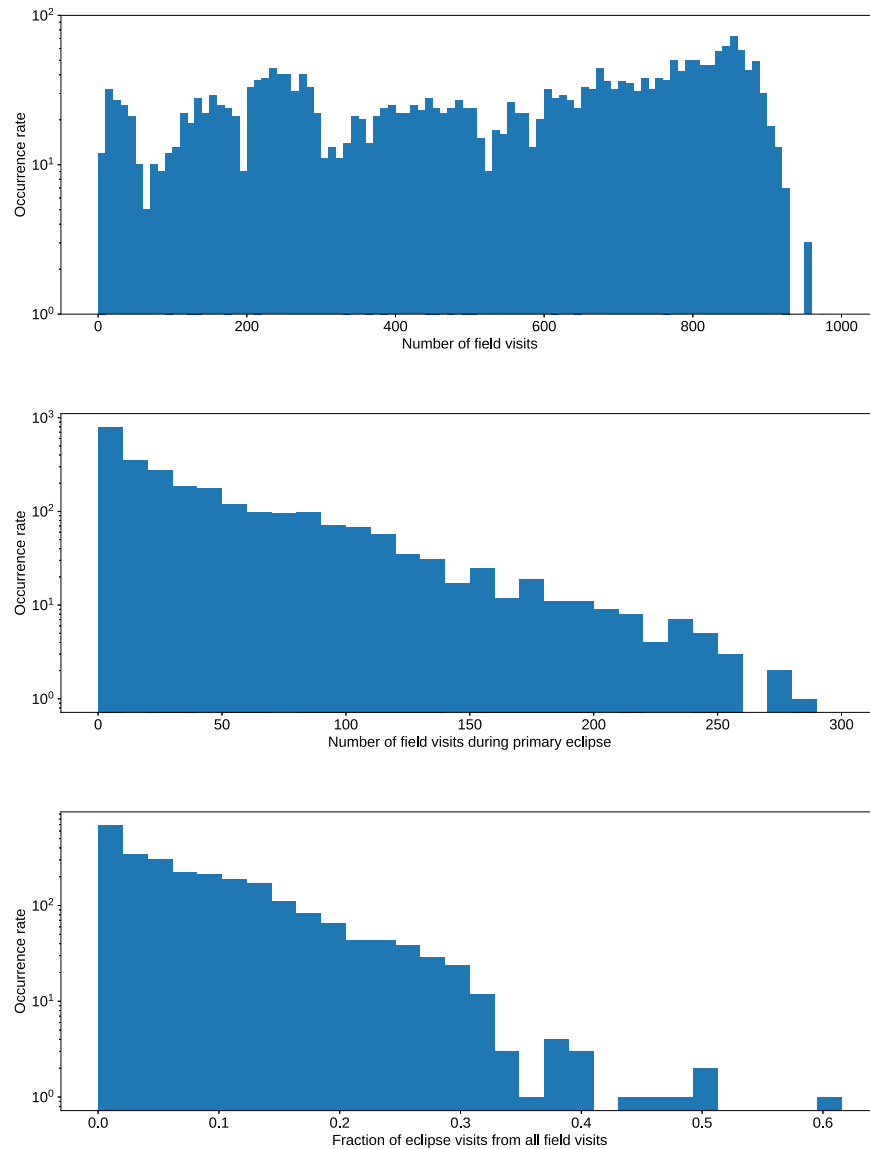


**Figure 13.** Field visit distributions for southern TESS eclipsing binary stars. Top: the overall distribution of field visits over LSST’s 10 yr span. Middle: the distribution of primary eclipse visits. Bottom: the fraction of primary eclipse visits to all field visits. This measures the likelihood that an eclipsing binary will be detected: the higher the fraction, the likelier the detection (assuming other variables, such as eclipse signal-to noise ration, are equal). Note the log-scale of occurrence rates in all three panels. The relationship between occurrence rates and primary eclipse visits, and the relationship between occurrence rates and fractions, are remarkably log-linear.

when there are no eclipses. Given the 10 yr span of the main survey and the large number of in-eclipse observations, we expect the census of eclipsing binaries with periods shorter than  $\sim 1$  day to be near-complete. Another added benefit is that, while we need to wait 10 years to maximize fidelity and ephemeris accuracy, discoveries and reliable classification can happen much sooner, likely within the first 2 years for the bulk of the sample. Typical candidates with short orbital periods include contact binaries

(W UMa-type systems), semi-detached binaries (Algol-type systems) and close detached binaries.

**(c) Detection of non-conservative mass loss in contact systems**

Contact systems share a common envelope; if that envelope becomes too large, either because of the evolutionary expansion of one of the components or because of mass transfer within the system via Roche lobe overflow, mass can be lost through Lagrangian points L2 or L3. When this happens, mass loss is

non-conservative: there is no mechanism to reclaim that mass. This stage of stellar evolution is fleeting, but can be detected through theoretically driven cross-cuts in the parameter space of the contact binary evolution, most notably, significant changes occur for the mass ratio and the period. As already stated, the main survey will provide us with an unprecedented number of contact binaries and is thus quite likely to provide us with the discovery of non-conservative mass loss candidates. Because of the sensitivity to period changes, a full 10 yr survey will likely be needed for this task.

(d) **Calibration and data integrity validation using high S/N EBs**

While not strictly astrophysical in nature, this project allows us to better qualify the survey output. EB light curves are specific in their shape and, when their S/N is high, it is difficult to confuse them with other types of variables. When there is a bright EB with a high S/N in a field, looking for “ghost” signals elsewhere in the same field will provide us with insight into potential instrumental artifacts such as blooming, electronic crosstalk and saturation artifacts.

(e) **Calibration of trigonometric parallaxes and the near-field distance scale**

Because the luminosities of EBs can be determined without the knowledge of the distance to the EB, EBs can be used as standard candles to test trigonometric parallaxes and to calibrate the distance scale (see, e.g., Stassun & Torres 2016, 2018, 2021). For example, with a sample of  $\sim 150$  benchmark-grade EBs, Stassun & Torres (2021) have demonstrated the ability to constrain global systematics in the Gaia parallaxes down to  $\sim 20 \mu\text{as}$ , for EBs as far as the Magellanic Clouds.

(f) **Application of the period–luminosity relation for (late-type) contact binaries**

The empirical  $gr$ -band period–luminosity (PL), period–Wesenheit (PW) and period–luminosity–color (PLC) relations have been derived by Ngeow et al. (2021) for late-type contact binaries, which could be used for distance measurements as an alternative to pulsating stars. Even though these  $gr$ -band PL/PW/PLC relations are in the Pan-STARRS1 system, they can be used to cross-check distance measurements derived from pulsating stars (e.g., RR Lyrae) for nearby (dwarf) galaxies in the early stage of Rubin LSST, even before these PL/PW/PLC relations have been derived in native Rubin LSST filters.

2. Pie in the sky

(a) **Understanding the binary population across the Galaxy and in neighboring galaxies**

Given the survey’s 6 passbands, we will get

effective temperature estimates for *millions* of EBs (Prša et al. 2011). That will allow us to study statistical population properties such as: the distributions of binary stars as a function of galactic latitude (perhaps even longitude); multiplicity rates as a function of spectral type; and individual stellar populations across the Galaxy and in neighboring galaxies.

(b) **Characterization of contact binary stars**

The main benefit of contact binaries in terms of modeling is that their tidal deformation depends on the mass ratio between the two components. That implies that mass ratios can be recovered photometrically (Terrell & Wilson 2005). For those stars where Gaia distances are also available, we will have the absolute scale of the systems and, thus, a full set of fundamental parameters. To further understand contact binary systems, this is imperative because, to date, we do not understand how energy and heat are transferred in common envelopes, even though we have seen it observationally for decades. Further, low mass ratio binary components in contact binaries exhibit similar surface brightnesses, which is only possible when there is a strong amount of mixing in the envelope. Through knowledge of their fundamental parameters, we will be able to probe the envelope mixing of contact binary stars.

(c) **Discover EBs in the fundamentally new regime**

With the survey’s  $r \sim 24.7$  magnitude limit, we will for the first time probe regimes that have been hitherto unexplored. This is predominantly the case for low mass components in tight binaries, e.g., M–M pairs. These systems are intrinsically too faint for current surveys to survey extensively and consequently, the binarity rates are uncertain. In addition, there is a significant discrepancy between observed radii and theoretical predictions of low-mass components (M- and K-types) in binaries: observed radii seem to be larger by as much as  $\sim 10\% - 20\%$ . Rubin LSST will provide us with the means to probe this regime in detail and address both multiplicity rates and obtain, with the help of Gaia distances, fundamental parameters that can further calibrate models of stellar structure and evolution.

*Preparations for Eclipsing Binary Science.*

1. **Follow-up observations/archival data**

There are several surveys and noteworthy catalogs of eclipsing binary stars that can be used to augment Rubin LSST’s dataset: OGLE (Udalski et al. 2015), Gaia (Gaia Collaboration et al. 2022), and TESS (Ricker et al. 2015). We do not anticipate a strong need for follow-up observations mostly because of the faint regime of Rubin LSST: most of the targets will be out of reach for

spectroscopic follow-up, and the bright end of Rubin LSST targets will overlap with Gaia parallaxes, thus providing us with their absolute scales.

## 2. Facilities/software requirements

Eclipsing binary targets may be identified using data from Prompt Processing (24 hr) or the from the Annual Releases, but more work is necessary to ensure that suitable filters are available to identify binary stars. For successful identification, cross-matching Rubin LSST detections against the Gaia and OGLE catalogs will be mandatory, while cross-matching with other catalogs, such as VMC, VVV, ZTF and POSS, is highly desirable.

The VaST tool<sup>82</sup> will be used to search for variable stars. We plan to generate a Jupyter notebook that will work as a demonstration for the whole community. Necessary analysis steps will include the application of algorithms to search for variables and for period finding. Some software exists for this purpose, but is likely to need expanding, and adapting to work within the Rubin LSST Data Access Center environment known as the Rubin Science Platform (which allows for interaction with the data at one of the Data Access Centers). For example, current software requires ASCII or FITS files containing the light curve data whereas this information may be provided via database query within the Rubin Science Platform.

To assess targets, we will require the ability to interactively assess images and light curves, in addition to database search functions that can be customized to use our selection criteria. A Jupyter notebook environment is considered to be a flexible means to achieve these analyses (making use of matplotlib for instance) within the Rubin Science Platform but interfacing with the VaST Tool will also require the use of Application Programming Interfaces (APIs).

The overall scale of user-generated data products can be estimated from ongoing work by the TVS Crowded Field Photometry Task Force. Preliminary estimates suggest that  $\sim 100$  KB of output will be produced for each confirmed variable, including text and plotted figures.

### 3.3.3. Microlensing

A detailed introduction for Microlensing can be found in Section 2.3.1. Here we discuss the science objectives for microlensing from a non-time critical perspective, which focus on the distribution of microlensing events.

The microlensing optical depth toward a given source is the instantaneous probability for that source to lie behind the Einstein ring of a lens. It only depends on the mass density

along the line of sight from the observer to distance  $D_S$  of that source:

$$\tau(D_S) = \frac{4\pi G D_S^2}{c^2} \int_0^{D_S} x(1-x)\rho(x)dx, \quad (3)$$

where  $\rho(x)$  is the mass density of deflectors at distance  $x D_S$ . When considering a sample of  $N_{obs}$  sources observed during a duration  $T_{obs}$ , the probability for any source to lie behind a lens has to be averaged over the  $D_S$  distribution to be connected with the event frequency and duration estimates through the expression:

$$\tau = \frac{1}{N_{obs} T_{obs}} \frac{\pi}{2} \sum_{events} \frac{t_E}{\epsilon(t_E)}, \quad (4)$$

where  $\epsilon(t_E)$  is the average detection efficiency of microlensing events with a timescale  $t_E$ . This number is conventionally defined as the ratio of the number of detected microlensing events with duration  $t_E$ , to the expected number of events where the source gets behind the Einstein ring of a lens during  $T_{exp}$ . The optical depth can be considered as a probe that brings information about the mass density distribution of compact objects toward a given direction.

#### 1. Low hanging fruit

##### (a) Optical depth, event rate and $t_E$ distribution

The distribution of the microlensing durations  $t_E$  allows us to probe the kinematics of the population of compact objects. The optical depth determination and the best use of the microlensing durations both require a careful estimate of the detection efficiency  $\epsilon(t_E)$ . This estimate requires the simulation of events in the domain of the parameter space that exceeds, by a large amount, the expected domain of sensitivity, and averages are computed over all the parameters other than  $t_E$  (including the impact parameter, source luminosity, color and distance, and time of maximum magnification). The estimate of this efficiency is a difficult aspect of the microlensing interpretation, since identified sources of bias (like blending and the parallax of finite source effects) are complicated to take into account. When analyzing a set of past data, these biases are untargeted, in the sense that they do not vary during the event progress, and the efficiency studies are similar for all microlensing surveys.

Since the Rubin LSST survey strategy will not vary depending on what events are discovered, the simplest approach would be to exploit the Rubin LSST data in isolation, excluding follow-up. Simulated events could be injected into real Rubin LSST time series photometry following a Data Release. Subsequently, the same detection algorithms could then be applied to the all light curves available up to that point. By detecting events after the fact from a

<sup>82</sup> <http://scan.sai.msu.ru/vast/>

largely “complete” sample of light curves, we will be able to evaluate an algorithm’s selection bias.

#### *Preparations for Microlensing Science.*

##### 1. Follow-up observations/archival data

The cross-matching of Rubin LSST DIA sources against other catalogs would be beneficial, but not essential, to accurately estimate the stellar properties and spectral types for our objects. For example, the Gaia catalog would provide distance information and spectral types for the brighter objects observed by Rubin LSST.

##### 2. Facilities/software requirements

Since this work will require access to the full light curve data for tens of hundreds to thousands of stars, at least some of the work is envisioned to be conducted through the Rubin Science Platform (which provides access to the data stored at the Data Access Centers). Selecting suitable DIA sources will require access to the variability statistics computed on the Rubin LSST timeseries photometry, and an extensive catalog search. The event simulation could also be conducted through the Rubin Science Platform, or on the downloaded timeseries.

### 3.4. Intrinsic Galactic and Local Universe Transients and Variables

#### 3.4.1. Pulsating stars: General

Rubin LSST observations will significantly improve our knowledge of pulsating stars. Stars in many stages of evolution experience global pulsations. These oscillations propagate through, and are affected by, the structure of the stellar interiors. They manifest as photometric variations in the time domain with frequencies equal to the stellar eigenfrequencies. By measuring these frequencies, we can constrain the interior stellar structure and fundamental parameters, which are otherwise not accessible in non-pulsating stars (e.g., Yu et al. 2018). This is one of the most powerful methods for probing stellar structure, which would be otherwise impossible. Global properties (e.g., luminosities, radii and masses) obtained from the analysis of pulsations also enable many types of science: they can provide distance determination through the use of pulsating stars as standard candles, can be used as tracers of stellar populations and additionally, can enable the determination of the absolute sizes/masses of exoplanets and binary companions (Beck et al. 2014).

The research of pulsating stars is multi-faceted and impacts a wide variety of science fields. Here we discuss the (general) pulsating star science that Rubin LSST data will enable:

##### 1. Low hanging fruit

###### (a) The classification of an extreme number of pulsating stars

Classification is one of the most prominent goals for pulsating stars science with Rubin LSST. While it is not expected that this will be complete, in the first years it will include mid- to long-period regular variables such as Cepheids and RR Lyraes. On longer timescales, the long timebase of observations will enable some multi-periodic and semi-periodic signals to be resolved, such as those from subdwarf B stars, gamma Doradus stars, Delta Scuti stars and Mira variables. The catalog will grow incrementally with each additional Annual Data Release.

The minisurveys and Deep Drilling Fields can also provide additional support for this goal, as the reliable classification of pulsating stars in a smaller field with a higher cadence could, in principle, provide a training set for machine learning algorithms to classify further pulsating stars in the main survey.

###### (b) The generation of a Rubin LSST pulsational H-R diagram

The different colors provided by Rubin LSST will enable the temperature determinations of all identified objects through the consideration of the average color of each object in several different bands. Further, when we combine Rubin LSST parallaxes and magnitudes, it will be possible to obtain the luminosities of all our objects. Thus Rubin LSST will provide the opportunity to generate a pulsational H-R diagram of an extreme number of pulsating stars in the Southern hemisphere (Figure 14 is an example of a current pulsational H-R diagram). Upon commissioning, the first H-R diagram will be created, which can be built upon with subsequent data releases.

###### (c) Population studies of pulsating stars

The large spatial coverage of Rubin LSST will allow for population studies where positional variations can be taken into account and considerations, for example, the association with the thin and thick disk, can be statistically analyzed. For the shorter-period variables, typical pulsation timescales can be measured from computing structure functions (records of typical magnitude differences at different time lags, as often employed in quasar analyses, see e.g., Hughes et al. 1992). Again, the likelihood of identifying short period variables will increase with time and so this project will be ongoing throughout the 10 yr survey.

##### 2. Pie in the sky

###### (a) The classification and period determination of multi-periodic variables and variables with short periods

The 3–5 day cadence of Rubin LSST is well suited to studies of long period pulsating variables, such as Cepheid variables. The study of short-period multi-periodic variables, such as white dwarfs and

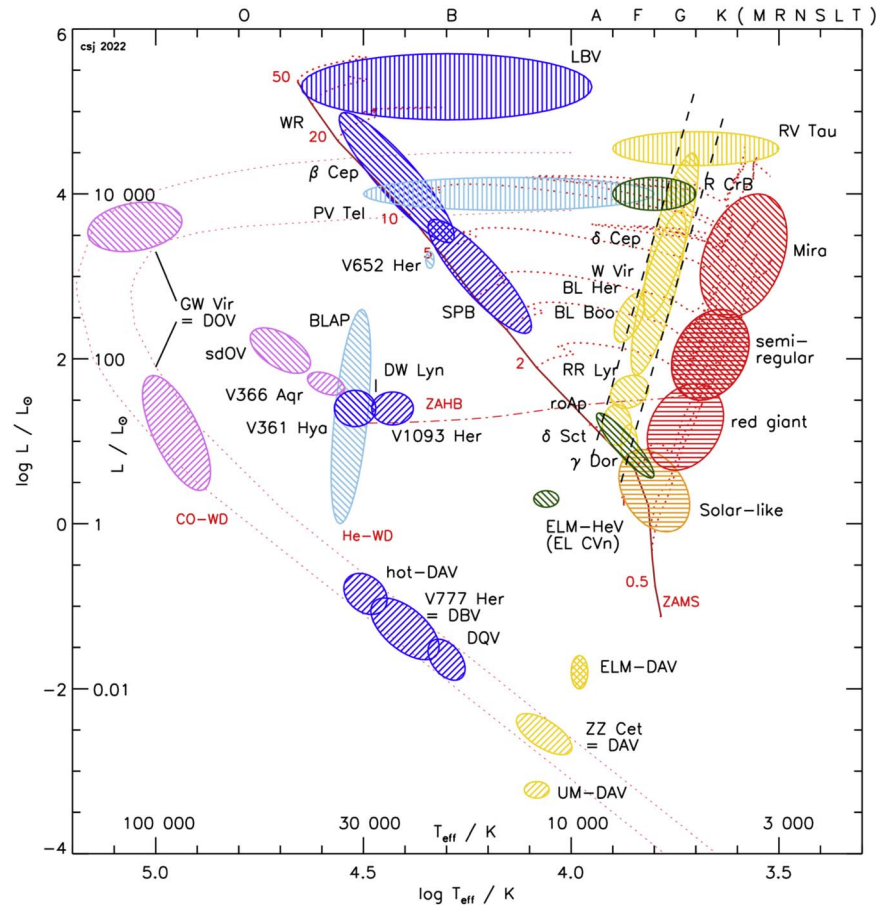


**Figure 14.** A pulsational H–R diagram that provides a schematic of the regions where various pulsating stars reside. Each known type of pulsating star is depicted. The solid red line represents the zero-age main sequence, the dotted red lines are evolutionary tracks for various masses, where the masses are the numbers along the ZAMS line (provided in solar masses). The cross-hatchings represent the primary mode types: acoustic  $p$  (pressure) modes (\\); gravity (buoyancy)  $g$  modes (//); stochastically driven pulsators ( $\equiv$ ); and strange modes (|||). This figure is courtesy of Simon Jeffery, and is based on Figure 1 of Jeffery et al. (2015). Copyright © 2015 Oxford University Press.

delta Scuti stars, for the purpose of asteroseismology will likely be more complicated and require the complete survey mission. Comparing the amplitudes of variations in specific frequency ranges in different filters can help to constrain (at least statistically) the geometries (spherical degree) or types of pulsation modes (gravity modes and pressure modes), however, this is better suited to Deep Drilling Fields.

**(b) Identifying new types of pulsating stars**

In the last 40 years, since the advent of space missions, tens of new types of pulsating stars have been found. While Rubin LSST is better suited to detect long period pulsators, the depth and coverage of observations do not exclude it from identifying new types of pulsating star. Sparse ground-based survey photometry from the Zwicky Transient Facility, for example, recently revealed a new class of blue large-amplitude pulsators (BLAPs; Kupfer et al. 2019).

*Preparations for Pulsating Star (General) Science.*

**1. Follow-up observations/archival data**

The most scientifically compelling pulsating star discoveries made from the Rubin LSST data (e.g., new variable classes, planet hosts, those with extreme pulsational characteristics or that belong to important stellar populations) can be targeted for follow-up with high-speed cameras on large telescopes to obtain data sets suitable for full asteroseismic analyses. SCORPIO on Gemini-S is one example of an instrument with high-speed capabilities that will be able to probe the Rubin LSST survey volume.

Additionally, representative samples of each class of pulsating variable star should be identified in existing survey data (e.g., stars with time domain photometry from PTF/ZTF, colors from SDSS, and distances from Gaia), to define initial classification algorithms. Different summary

statistics (rms scatter, structure function turnover time lag, etc.) from other time domain surveys (PTF, ZTF, Pan-STARRS, ASAS-SN, etc.) should be considered in order to identify the features that best discern the variable subclasses and that relate to physical properties of interest.

## 2. Facilities/software requirements

To store the catalog data, computing facilities are required with large amounts of storage ( $\sim$ Tb). Additionally, a server and the infrastructure to host an online version of the catalog would be a long term service goal.

The tools to determine the temperature and luminosity of a vast number of pulsating stars can undergo development prior to data acquisition. Furthermore, an analysis of the limitations placed by the spectral window of the main survey strategy is necessary to understand where asteroseismic results may be reliable. The development of tools that enable the separation of frequency aliases from the asteroseismic solution may revive the potential to seismically constrain stellar interiors with Rubin LSST data, at least at the population level. Since the majority of identification will be undertaken by assessing the scatter in the data (combined with color and temperature information) it is unlikely that significant headway will be made until the nominal mission is well underway due to the large number of data points needed.

Additional tools that will be required include period finding tools. Current tools, such as Period04 (Lenz & Breger 2005), are not well suited for bulk operations. Work is currently underway to generate such tools that will be applicable to the Rubin LSST extensive data set, i.e. Gatspy (Jake VanderPlas 2014) and the Pyriod<sup>83</sup> software package.

### 3.4.2. Pulsating Stars: Cepheid and RR Lyrae Stars

Cepheid and RR Lyrae stars are bright pulsating stars that expand and contract due to the Kappa mechanism, which acts like a heat engine. They pulsate in the first overtone and fundamental modes and have periods on the order of days (RR Lyrae stars) to hundreds of days (Cepheids). Pulsating stars play a fundamental role both as distance indicators and stellar population tracers. Indeed, they can be used to obtain individual and mean distances and to calibrate secondary distance indicators that allow us to reach cosmological distances ( $> 100$  Mpc). At these distances, the Hubble flow is undisturbed and it is possible to determine the Hubble constant  $H_0$ . In addition, different types of variables, depending on their masses, belong to different evolutionary phases. Consequently, they can be used to obtain information about the age and chemical composition of their host stellar populations and hence can be used to define the 3D distribution of stellar

systems. As such, pulsating stars could, in principle, trace the presence of radial trends, halos and streams, providing important clues about the star formation history of the host galaxy.

As distance probes, the most prominent classes of pulsating stars are the classical Cepheids, the RR Lyrae, the Population II Cepheids (P2C), the anomalous Cepheids (ACs) and the SX Phoenicis variables (SXPhs). Classical Cepheids, as Population I stars, and RR Lyraes, as Population II stars, represent the first rung of the cosmic distance ladder. The role of classical Cepheids and RR Lyraes as distance indicators is based on the period–luminosity (PL) and period–luminosity–color (PLC) relations for the former and on the period–luminosity–metallicity (PLM) relation in the  $B$  and  $V$  optical bands, and on a period–luminosity in the NIR bands for the latter.

In spite of the large number of observational and theoretical studies, a general consensus on the coefficients of these relations has not been reached. In particular, many uncertainties remain regarding the dependence on the host galaxy’s chemical composition for the period–luminosity relation (for both for classical Cepheids and RR Lyraes). While the Gaia mission is providing the most accurate distance determinations obtained so far for more than 1% of the Milky Way stellar content (see e.g., Gaia Collaboration et al. 2021), the largely discussed problem of the  $H_0$  tension (Verde et al. 2019; Riess et al. 2021) remains unresolved. Indeed, the Hubble constant value based on the extragalactic distance scale, which is based on classical Cepheids is  $H_0 = 73.04 \pm 1.04 \text{ km s}^{-1} \text{ Mpc}^{-1}$  (Riess et al. 2021) whereas the Planck Cosmic Microwave Background measurements, assuming a  $\Lambda$  Cold Dark Matter Model, suggest a value of  $H_0 = 67.4 \pm 0.5 \text{ km s}^{-1} \text{ Mpc}^{-1}$  (Aghanim et al. 2020).

Multi-band time series data collected by Rubin LSST, combined with its very accurate parallaxes and proper-motion measurements, will provide a fundamental benchmark, extending Gaia’s capabilities to five magnitudes fainter. This will allow observations of variable stars not only in the Milky Way, but also in the Local Group of galaxies (see e.g., Oluseyi et al. 2012).

The possibility to improve the knowledge of the ultra long period Cepheids (ULPs) is also a very exciting prospect. Currently, the number of known ULPs is small (72; Musella et al. 2021; Musella 2022) often lacking homogeneous, accurate photometry. These variables, characterized by periods longer than about 80 days, are hypothesised to be longer-period, higher-mass versions of classical Cepheids. Thanks to their luminosity, ULPs are observable up to cosmological distances (larger than 100 Mpc), which should enable the measurement of the Hubble constant without the need for secondary distance indicators. Such measurements would significantly reduce the uncertainty on the Hubble constant value obtained through standard candles. In spite of this exciting prospect, the ULPs are not completely understood from the theoretical point of view. Further, current stellar evolution and pulsation models do not predict such long

<sup>83</sup> <https://github.com/keatonb/Pyriod>

periods in the corresponding color–magnitude diagrams, in particular in the lowest metal regime. In this context, to better understand and interpret observational data, we also need a solid theoretical scenario.

During the last two decades, an extensive and detailed theoretical scenario for several classes of pulsating stars, including Cepheids and RR Lyrae stars, has been built on the basis of nonlinear convective pulsation models (see e.g., Marconi et al. 2005; Fiorentino et al. 2007; Bono et al. 2008, 2010; Marconi et al. 2010, 2011, 2013, 2015; De Somma et al. 2020). These models allow us to derive all observables, for example, the boundaries of the instability strip, light curves, periods, amplitudes and mean magnitudes. They cover a large range of masses, luminosities, metallicities and helium contents, and thus represent a robust and unique theoretical tool to interpret the observed behavior of different classes of pulsating stars and to fully exploit their crucial role as distance indicators and stellar population tracers.

### 1. Low hanging fruit

#### (a) **Determine the 3D structure of the studied systems**

Using the aforementioned period–luminosity/period–luminosity–color/period–luminosity–metallicity relations, in the first three years, we plan to obtain distance measurements and 3D distributions of variable stars in stellar systems. This will be done through the comparison of theoretical models with observed light curves. The Rubin LSST data will be combined with all the other public multiwavelength data sets including PTF/ZTF, SDSS and Gaia to achieve this objective. As additional data are received, we will continue to update our findings.

#### (b) **Constraining the coefficients of period–luminosity and period–luminosity–color relations**

Using Rubin LSST data, we will constrain the coefficients of the period–luminosity and period–luminosity–color relations of Cepheid and RR Lyrae stars to an unprecedented level of accuracy. This result will be obtained after the 10 yr survey. The calibration of these relations for classical Cepheids and RR Lyrae stars will include the debated metallicity term (see Ripepi et al. 2021).

#### (c) **Very accurate estimates for the stellar masses of RR Lyrae and Cepheid stars**

This will be obtained through the comparison of the very extensive and accurate Rubin LSST light curves with theoretical light curves. Stellar masses are crucial for the derivation of firm constraints on: the efficiency of non-canonical phenomena (such as overshooting and mass loss in stellar evolution models); pulsation–convection coupling; and on the very debated (and fundamental) parameters such as

the helium-to-metal enrichment ratio. Indeed, this ratio has a key role in several fields of stellar and galactic astrophysics and has been shown to affect the predicted metallicity dependence of Cepheid period–luminosity relations (see e.g., Marconi et al. 2005, and references therein).

#### (d) **Obtain an large sample of ULPs**

With Rubin LSST, we will observe a large, photometrically-homogeneous sample of ULPs with accurate period determinations. This is possible with Rubin LSST thanks to the long observational baseline. Such a large sample will allow us to test the reliability of ULPs as standard candles that we are able to observe out to cosmological distances without the adoption of secondary distance indicators.

### 2. Pie in the sky

#### (a) **RR Lyrae and Cepheid stars as stellar population tracers**

The pulsational characteristics of RR Lyrae and Cepheid stars depend on their physical and chemical properties. Therefore, in principle, they can be (and have been) used to identify the different stellar populations of the Milky Way and to characterize the properties of the Galactic components (e.g., the so-called Oosterhoff dichotomy that separately characterizes RR Lyrae in Galactic globular clusters and in the field of the Galactic Halo). The increasing quantity and quality of photometric data in different bands, together with the availability of the kinematic information from Gaia, provides us the opportunity to test pulsating stars as a tool to unveil the formation and accretion history of the Milky Way. As such, methods have been proposed to gain accurate distances, and to determine accurate reddening and metallicity values using optical-NIR photometry (Karczmarek et al. 2017). In particular, these methods make use of the *BVIJHK* passbands. While the use of the Johnson filters can be easily replaced with the Rubin LSST *gri* filters, *JHK* wavelengths are not covered by Rubin LSST. This opens the question of whether the reddest Rubin LSST passbands, namely *zy*, can be effectively used for this method. Moreover, the availability of a large number of homogeneous *u*-band light curves opens the possibility to use the *u*-band band in this context.

#### (b) **Firm constraints on the physical and numerical assumptions adopted in the pulsation models for RR Lyrae and Cepheid stars**

As a final and very ambitious goal, we aim to put firm constraints on the physical and numerical assumptions adopted in the stellar-pulsation

hydrodynamical models (e.g., the adopted opacity tables or the treatment of convection and overshooting). Such constraints would provide additional calibrations for the extragalactic distance scale and further improve the accuracy of variable stars as standard candles. Such work is of particular importance for the debated  $H_0$  tension.

*Preparations for Pulsating Star (Cepheids and RR Lyrae) Science.*

### 1. Follow-up observations/archival data

The aforementioned science cases can be developed in synergy with all the existing and coming variability surveys that provide extensive data sets for RR Lyraes and Cepheids. The comparison of theory with accurate and extensive observations is mandatory to test and improve our pulsation models. The main surveys we plan to incorporate are:

- (a) Gaia **DR3** for the comparison between theoretical and observational light curves and to compare individual distances obtained through theoretical tools with those inferred from Gaia parallaxes. Such comparisons are crucial to constrain the physical and numerical assumptions of pulsation models and in turn to improve our knowledge of stellar physics (see e.g., Gaia Collaboration et al. 2017; De Somma et al. 2020).
- (b) **The VISTA near-infrared  $Y J Ks$  survey of the Magellanic System (VMC)** for testing the predictive capabilities of pulsation models in the near-infrared filters. This will be achieved through the comparison of predicted pulsation properties for Cepheids and RR Lyraes with VMC@VISTA time-series data in the Magellanic Clouds (see e.g., Marconi et al. 2017; Ragosta et al. 2019).
- (c) **Optical Gravitational Lensing Experiment (OGLE)** for testing the predictive capabilities of pulsation models in the optical filters through the comparison of predicted pulsation properties with OGLE time-series data for Cepheids and RR Lyrae in the Magellanic Clouds (see e.g., Marconi et al. 2013).

### 2. Facilities/software requirements

In the next year, before Rubin LSST's commissioning phase, we will build a complete theoretical scenario for Cepheids and RR Lyrae stars in the Rubin LSST bands to compare the observed pulsation properties with our models. To do this, we plan to enlarge the already-computed extensive sets of nonlinear convective pulsation models for Cepheids and RR Lyrae stars for varying chemical compositions ( $Z$  and  $Y$ ), masses and luminosities (see e.g., Bono et al. 1999; Fiorentino et al. 2002; Marconi et al. 2003; Criscienzo et al. 2004; Marconi et al. 2005, 2010; De Somma et al. 2020, for pulsational

models in the Johnson-Cousins filters). We will then transform these pulsational models into the Rubin LSST photometric *ugrizy* bands.

The *ugrizy* light curves, mean magnitudes, colors, pulsation amplitudes and color-color loops will be derived, together with periods and analytical relations connecting pulsational to intrinsic stellar parameters (e.g., period-luminosity, period-luminosity-color and Wesenheit relations). We will also probe their possible dependence on metal content. Analogous works have already been developed to study the theoretical intrinsic properties of RR Lyrae and Cepheid stars in the SDSS bands (Marconi et al. 2006; Criscienzo et al. 2012) and for Cepheid stars in the HST/WFC3 filters, which are typically used to study these variables (F555W, F606W, F814W and F160W; Fiorentino et al. 2013). First results have also been very recently obtained for the new theoretical period-luminosity-metallicity relations for RR Lyrae in the Rubin-LSST filters (Marconi et al. 2022). Rubin LSST observations will provide a very large database of pulsating stars from a variety of environments with different chemical compositions. This will allow us to test the accuracy and reliability of our models and enable the refinement of the input physical parameters to obtain good agreement between theoretical and observational models.

To host our theoretical templates, we need to have a dedicated powerful ( $\sim 32$  core) server. For the data analysis, we require software for period finding and for the classification and characterization (amplitude, mean magnitude, Fourier parameters) of pulsating stars, as described in Section 3.4.1.

#### 3.4.3. Pulsating Stars: Long-period Variables

Long-period variables are cool giants with periods or variation timescale of 100–3000 days, and V-band peak-to-peak amplitudes of  $\sim 0.1$ –4.0 mag. Being on the asymptotic giant branch, they comprise a degenerate core composed of oxygen and carbon (or neon), a triple  $\alpha$  burning zone and a region with CNO nuclear activity. This compact core (size  $1/100 R_\odot$ ) is surrounded by the convective envelope (size 100–500  $R_\odot$ ) that has a surface temperature of  $\sim 3000$ –4000 K. The surface chemistry of these stars may be altered by Hot Bottom Burning (HBB) and the Third Dredge-Up (TDU), whose efficiency depends on initial stellar mass and metallicity. In addition to convection and chemistry, pulsation and mass-loss are critical. Intense mass ejection creates an expanding, dust-producing low-density envelope. Despite recent progress on asymptotic giant branch evolution (Höfner & Olofsson 2018), it still remains a challenge to establish a consistent link between evolution, convection, chemistry, pulsation, shocks, dust formation, and mass loss. Rubin LSST will provide multi-



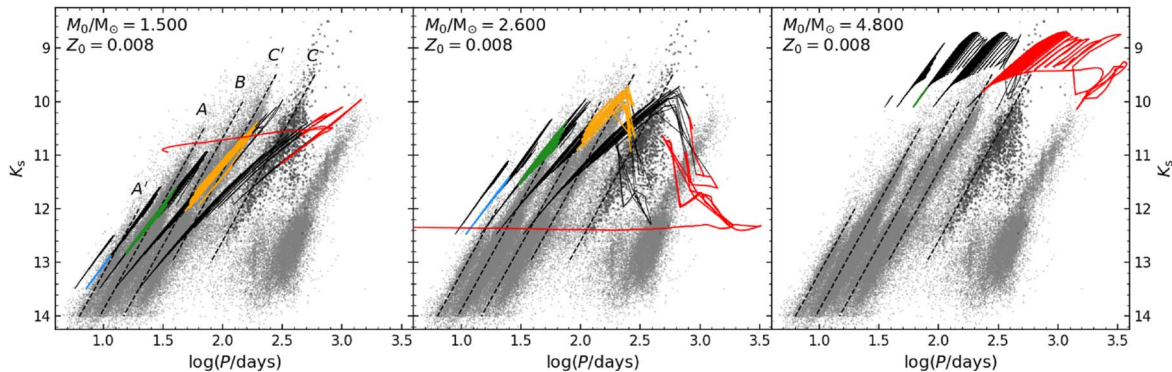


**Figure 15.** Evolutionary tracks for theoretical stars with  $M = 1.5M_{\odot}$  and (left panel),  $M = 2.6M_{\odot}$  (middle panel) and  $M = 4.8M_{\odot}$  (right panel), and with  $Z = 0.008$  (all panels) at the beginning of the asymptotic giant branch. The tracks are superimposed on to the  $K_s$ – $\log P$  diagram of observed long-period variables in the LMC, from the OGLE-3 Catalogue (Soszyński et al. 2009). Dashed lines identify the position of observed period–luminosity sequences. Observed stars that are classified as Miras are shown with darker colors on sequence C. For each evolutionary track, the periods of five modes are shown with colored, solid lines where dominant, and black lines otherwise. This figure is courtesy of Michele Trabucchi and is based on Figure 23 of Trabucchi et al. (2019). Copyright © 2019 Oxford University Press.

color light curves, which will help to constrain pulsation models.

We also note that the calibration of period–luminosity and period–Wesenheit relations of Mira stars and Semi-Regular Variables, as well as ULPs, will provide new, important standard candles with the power of reaching distances further than Classical Cepheids.

## 1. Low hanging fruit

### (a) Understanding long-period variable pulsations

Pulsations have been observationally identified but their physical understanding is in an embryonic state (despite its tremendous importance for Miras as standard candles, Huang et al. 2018). OGLE and MACHO experiments have shown that in the period–Luminosity diagram, long-period variables form six distinct parallel sequences. We know that membership in each of the sequences depends on the pulsation mode responsible for their variability (Wood 2015), but understanding which of these relationships is important for standard candles is not a simple question. However, long-period variables are multi-periodic and normally only the primary period (the higher amplitude pulsation) is used in the period–luminosity relation. Trabucchi et al. (2019) showed that, as the star evolves, specific overtone modes gradually become stable and the primary mode shifts toward lower radial orders. In particular, the star initially rises on the period–luminosity diagram while traversing these sequences from left to right (see Figure 15).

Since Rubin LSST will measure thousands of long-period variable light curves, either for Galactic disk stars or stars in external galaxies (with a range of metallicities and ages), studies comparable to those of

OGLE and MACHO will be achievable, with the advantage of extending the analysis to different Local Group environments.

Theoretical predictions of pulsation properties as a function of stellar parameter along the asymptotic giant branch need to be refined. Enough observations should be obtained during commissioning and in the first year to detect most long-period variables within a few Mpc, 5–10 yr will be necessary to firmly establish the longest periods (mostly  $\sim 2$  yr) and eventually the long secondary periods.

### (b) To learn about the dust production of long-period variables in galaxies

Long-period variables in galaxies are a dominant cause of dust enrichment (silicates and carbon dust) and the enrichment of some elements like carbon and lithium. Due to their large mass-loss rates and cool temperatures, the asymptotic giant branch winds are a favorable site for dust production, via the condensation of gas molecules into solid grains. Recent investigations by Ventura et al. (2012, 2014), Criscienzo et al. (2013), Dell’Agli et al. (2019), Nanni et al. (2014) set the theoretical framework to model dust formation in expanding asymptotic giant branch winds. Rubin LSST will measure the pulsation periods or multi-period character of asymptotic giant branch stars. It will also provide multi-color time-dependent information helping us to understand optical absorption/scattering by grains. The extensive knowledge of circumstellar dust at all metallicities is imperative for the SED fitting of long-period variables undergoing huge mass-loss because they dominate the dust production rate of the host galaxy. This is of special importance at high redshifts.

## 2. Pie in the Sky

### (a) Understanding long secondary periods

long secondary periods happen for about 25%–30% of long-period variables, as shown by the LMC/SMC surveys. The long secondary period is the reddest sequence in the period–luminosity diagram (called D sequence), and has an unknown origin. It cannot be a radial fundamental pulsation since the period is  $\sim 4$  times longer than the fundamental period. The most favored explanations are binarity and non-radial  $g$  modes, but not without significant problems. The link between long secondary periods and mass loss via dust driven winds was raised by Wood & Nicholls (2009). They showed that long secondary periods display some mid-IR excess compared to stars without long secondary periods. Long secondary periods cause mass ejection from giant stars. This mass and accompanying circumstellar dust is most likely in either a clumpy configuration or disk configuration. Ten years of Rubin LSST observations will be fundamental to understanding how the presence of long secondary periods depends on environment or binarity, and for quantifying the percentage of long-period variables that show this type of secondary variability.

### (b) Searching for symbiotic stars

Symbiotic stars are composed of a giant and an accreting white dwarf or neutron star. They can play a role as progenitors of SNe Ia. Symbiotic binaries are considered to be among the widest interacting binary stars, which allows the onset of different phenomena such as the formation of accretion disks, Roche-lobe overflow, thermonuclear runaway, slow and recurrent nova outbursts on the surface of the compact component. Rubin LSST will help detect symbiotic stars with its *ugrizy* colors (Lucy et al. 2018) and will enable us to measure their asymptotic giant branch periods and/or provide typical light curves (such as those shown by Ilkiewicz et al. 2018). By surveying part of the Galactic disk, the halo and nearby dwarf galaxies, Rubin LSST will provide complementary information on symbiotic star populations and their evolution. Note that only  $\sim 250$  Galactic and  $\sim 70$  extragalactic symbiotic stars are known so far (Merc et al. 2019). A systematic search of symbiotic-star light curves in available databases (OGLE, Catalina, ATLAS, ZTF) should be carried out to prepare for the characterization of symbiotic stars in Rubin LSST data. In order to test different theoretical models of interacting phenomena such as nova and recurrent nova outbursts, determination of mass loss rates from the cold components (Akras et al. 2019), as well as the mass transfer mechanisms, is of key importance.

Rubin LSST photometry will greatly contribute in classification of symbiotic stars, the determination of the physical characteristics of the cold component, and the dust characterization and mass loss rates of the cold component in D-type symbiotic stars, especially when combined with near- and mid-IR surveys and observations (2MASS, WISE). Comparison between light curves in different bands could lead to detection of ellipsoidal variability (Mikołajewska et al. 2002), which in turn could contribute to a better understanding symbiotic stars with Roche-lobe overflow as a mass transfer mechanism.

### (c) The refinement of pulsation and shockwave models

We will refine the pulsation and shockwave models for thousands of long-period variables using Rubin LSST multi-color (*ugrizy*) light curves. This science has already commenced with Gaia 2-filter photometry. But Rubin LSST will surpass Gaia because it will last approximately twice as long and because its data will have higher cadence with more filters. To our knowledge, there are no theoretical models to mirror Rubin LSST’s observations, although they would have the potential to identify dependencies on metallicity, luminosity, dust production, etc. To help constrain gas hydrodynamics and shocks and to complement Rubin LSST’s photometry, we will additionally need high resolution spectral monitoring of a few dozen periodic long-period variables (of diverse origin); this task has been shown to be feasible by Alvarez et al. (2001). To obtain this goal, the complete 10 yr survey is required. However, the first year of data will provide 2–3 periods for pulsators with  $P \sim 100$ –200 days.

### (d) The fine tuning of long-period variables as standard candles

This goal is fundamental to Rubin LSST as it is imperative that we determine which Miras are suitable for this science.

The Mira infrared period–luminosity relation shows scatter that is comparable with that of Cepheids, but documentation on their infrared ( $\sim 1$ – $4 \mu$ ) light curves is scarce. In addition, dust can be involved either in emission or in absorption in infrared light curves. For this reason, we require deep-learning software to search for subgroups of OGLE and Rubin LSST Miras that would decrease the period–luminosity relation scatter. A theoretical/empirical link between Rubin LSST optical light curves and  $2 \mu$  light curves must be achieved. It is only after  $\sim 5$ – $10$  yr of operation that we shall have this information, provided a significant number of  $\sim 2 \mu$  light curves are obtained with additional ground based-telescopes.

*Preparations for Pulsating Star (Long-period Variable) Science.*

### 1. Follow-up observations/archival data

Long-period variables are important for stellar evolution and stellar population studies and could be decisive in the discussion on the local  $H_0$  measurement. In fact long-period variables could hypothetically be used in place of local SNe Ia, whose sample size limits the precision of  $H-0$ .

Unfortunately, until now, these type of studies have been very limited (Huang et al. 2020) due to the lack of observations with a long (years) baseline, which are necessary to derive periods and the shape of the light curve from which accurate infrared mean magnitudes can be derived. Rubin LSST will partially fill this void but additional follow-up observations will be necessary after or during the survey. In fact, Rubin long-period variable light curves will be mainly used to derive accurate period measurements and derive the shape of the light curve but infrared follow-up observations will still be needed to produce useful period–luminosity relations (unless the period–luminosity relations in the reddest Rubin bands can be derived). Infrared surveys will also be necessary to discriminate between C/O chemistry, which is important for the study of the effect of metallicity on period–luminosity relations. This is especially important in the case of carbon stars, to correct for circumstellar reddening. Ongoing survey such as the DUSTINGS program (Boyer et al. 2014) (started with Spitzer) must be pursued to obtain (at least) some temporal information in phase with Rubin LSST.

Last but not least, Rubin will never reach the HST (or better JWST) resolution, so for distant galaxies ( $>1.5$  Mpc), there may be a problem due to crowding (angular confusion) with neighboring stars that will impede the detection of many of Miras. However, if the HST, JWST or similar can provide a list of potential Miras in distant galaxies in the next few years, perhaps Rubin LSST could monitor those pixels and provide accurate periods.

### 2. Facilities/software requirements

Periodic and pulsating variables will primarily be identified with the Rubin LSST light curves, once the baseline extends beyond a few times the main period of the object in question. For most of the variables in this section, this means that targets will be identified in the Second Annual Data Release, through the application of selection cuts in photometric color and through cross-matching with a number of external catalogs, particularly OGLE, Gaia, 2MASS, TESS and Spitzer. This can be achieved using the Rubin LSST Science Platform.

To achieve our outlined goals, good quality

photometry from the crowded star fields in the Galactic Plane are needed. Additionally, the Rubin Science Platform would need to include timeseries analysis tools, such as Period04 (Lenz & Breger 2014).

The task of identifying candidates will be considerably easier if tables of basic variability statistics (including period and amplitude) are made available and if Rubin LSST stars are cross-matched against existing catalogs in advance. For long-period variables, cross-matching with near infrared and infrared surveys, such as 2MASS, WISE, DUSTINGS, is desirable in order to search for the optical counterparts of dusty objects. Some work remains to extend existing software tools (designed for single light curve analysis) and adapt them to handle Rubin LSST’s multi-filter light curves in an optimal way.

#### 3.4.4. Galactic Globular Clusters

Galactic globular clusters are old and large groups of stars that are gravitationally bound. These systems can reach central stellar densities as high as  $10^6$  stars per cubic parsec, which makes them excellent laboratories to test theories of stellar dynamics and evolution. Due to their large concentration of stars, interactions among their members are common, giving birth to exotic systems (see Maccarone & Knigge 2007, for a review), several of which have not been found to exist in the field so far (e.g., yellow and red stragglers). Furthermore, the old age of globular clusters guarantees a sizeable sample of evolved stars and stellar remnants, which can be found either in isolation, in binaries or in triples, many of which are variable over different time scales. The variability and/or transient behavior of these exotic systems can be due to accretion, pulsations or the binary’s configuration (e.g., high inclination systems). Below, we discuss the globular-cluster research-goals that we propose to pursue with Rubin LSST.

#### 1. Low hanging fruit

##### (a) Study the stellar populations of globular clusters

Despite their predicted abundances, the known populations of variable stars in globular clusters are incomplete. Rubin LSST will help uncover the relative sizes of different stellar populations by combining light-curve variability and multicolor photometry, which we will combine with additional follow-up observations in other bands (e.g., UV, X-rays, radio). The large (temporal and spatial) coverage of Rubin LSST will open the possibility to observe, for the first time, “missing” binaries such as symbiotic stars, which are expected to reside in the outskirts of nearby low-density globular clusters. While the stars in the crowded cores of clusters will not be individually resolved by Rubin LSST alone, techniques such as

differential photometry will enable the identification of transients and variables in the inner regions of globular clusters. The comparison of observed populations with population models will provide insights into the creation and evolution of the different populations including the initial conditions (parameters).

**(b) Identification of dwarf novae**

The most abundant stellar remnants that have been identified in globular clusters are white dwarfs. Due to stellar interactions and their primordial formation, several of them are thought to be in cataclysmic variables. While many cataclysmic variables are expected to be in the cores of clusters due to mass segregation, around 50% of the predicted detectable cataclysmic variables are believed to be outside the half-light radius, particularly in those globular clusters with half-mass relaxation times longer than a few Gyr (see Belloni & Rivera Sandoval 2021, for a review on cataclysmic variables in globular clusters). The wide-field coverage and 10 yr duration of Rubin LSST will allow us to identify dwarf novae in the outskirts of globular clusters through their outbursts. Photometry in multiple filters will be helpful to corroborate variability detection and to place the identified systems in the color–magnitude diagram of the host cluster. This will be useful to further investigate the two-population problem of cataclysmic variables in globular clusters (e.g., Cohn et al. 2010; Belloni & Rivera Sandoval 2021)

**(c) Characterization of exotic binaries and pulsating stars**

Recent studies have shown the presence of several X-ray sources in the outer parts of globular clusters, which indicates binary interactions. Therefore, besides detecting accreting white dwarfs, the 10 yr duration and multicolor photometry of Rubin LSST will help to characterize binaries with neutron stars or even black holes. For example, by identifying the orbital periods of radio or X-ray sources such as binary pulsars (including spider millisecond pulsars with long periods, Pichardo Marcano et al. 2021) or low mass X-ray binaries. We can also obtain information about the period and luminosity distributions of cataclysmic variables and other exotic objects, which can then be compared to evolutionary models and to systems in the field. These comparisons will provide clues about the role and impact of stellar interactions and cluster parameters (such as the initial binary number and initial cluster mass) on the currently detectable populations. Besides this, Rubin LSST will enable us to obtain the periods of pulsating stars such as SX-Phoenicis and RR-Lyrae stars. For

example, combining the light curve analysis of RR Lyrae stars with semi-empirical relations, it will be possible to calculate parameters such as the effective temperature, luminosity, distance, metallicity ( $[Fe/H]$ ), and mass of these pulsating stars (e.g., Arellano Ferro et al. 2013). See Section 3.4.2 for further discussion on RR Lyrae variables. These studies additionally hold value because the characterization of exotic objects and pulsators provides information about the host globular clusters themselves.

**(d) Study the effects of galactic tides**

By studying the kinematics, position and structure of the outermost regions of globular clusters located at various distances from the Galactic Bulge, we can obtain information about the effects of galactic tides (e.g., Piatti & Carballo-Bello 2020). Since a significant fraction of the known globular clusters are on the Galactic plane, the monitoring of these region by Rubin LSST will be important to carry out such studies.

*Preparations for Galactic Globular Cluster Science.*

**1. Follow-up observations/archival data**

To further investigate the nature of transients and variable stars in globular clusters, multiwavelength observations in other bands such as X-rays, ultraviolet, infrared and radio waves with facilities like the Chandra Observatory, HST, JWST and the VLA are desirable. For exotic/interesting systems identified in the outer regions of globular clusters, as crowding will not be a concern, follow-up spectra taken from the ground with mid- or large-size telescopes will provide information for classification and further analysis. Additional photometry and/or spectroscopic follow-up will be likely required to determine membership to the host cluster. Archival observations from space telescopes or ground-based telescopes with adaptive optics will also enable the investigation of systems in the inner parts of clusters.

**2. Software Requirements**

Pipelines to detect transient and variable sources in very crowded environments, especially those including differential photometry techniques, will be needed. Codes to determine the variable star periods will also be required. Up to date population models based on  $N$ -body or Monte Carlo methods are needed to make a fair comparison with the obtained observations.

*3.4.5. Brown Dwarfs*

Brown dwarfs are objects with masses between the deuterium and helium burning limit. Mature-field brown dwarfs cover a surface temperature range from 2000 K down

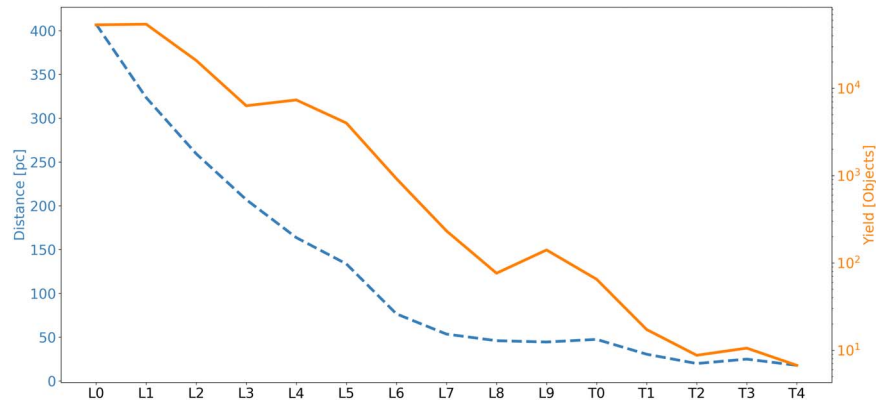


**Figure 16.** Expected distances and yields of brown dwarfs from spectral types L1 to T4 assuming the main survey covers 25,000 square degrees. Results are based on magnitudes estimates from Hawley et al. (2002) and space densities from Kirkpatrick et al. (2021).

to 400 K. Their faintness makes them hard to detect, especially in the optical range. Due to their temperatures, brown dwarfs are brighter in the near-infrared wavelength range and most studies have been done from 1 micron onwards.

A study about the spatial distribution of brown dwarfs by Kirkpatrick et al. (2021) showed that brown dwarfs are well distributed across the sky. The Rubin Observatory, with its 8.4 m mirror combined with a large etendue, will probe a large sample of brown dwarfs in the optical wavelength range. In Figure 16 we show the expected yield of brown dwarfs for the LSSTCam’s field-of-view. We will not only be able to detect brown dwarfs, but we will also get photometric time-series observations.

Photometric monitoring has shown that brown dwarfs have a rotational modulated variability. Almost all brown dwarfs show variability at a certain level (Metchev et al. 2015) and  $\sim 40\%$  of brown dwarfs at the L/T transition show amplitude variabilities larger than 2% (Radigan 2014; Eriksson et al. 2019). It is predicted that this variability is due to a global weather phenomena in the atmosphere. This prediction has initiated research about weather patterns in substellar objects outside our solar system. While cloudy atmospheres could explain the observed variability (see e.g., Marley et al. 2010), some problems can only partially be explained by a resurgence of FeH absorption. As such, additional hypotheses were proposed, i.e., the idea that the brightness fluctuations in brown dwarfs might emanate from non-uniform temperature profiles or perturbations in the atmosphere’s temperature structure (Robinson & Marley 2014). An additional alternative, proposed by Tremblin et al. (2016), claims that non-uniform surface opacities, caused by chemical abundance variations, are the origin of the observed variabilities.

In Section 4.3.2 we show how observations in the Deep Drilling Fields can contribute toward the variability study of brown dwarfs. Further, in Section 5.3.2 we discuss the opportunities presented by the commissioning tests, which

are anticipated to include high-cadence observations. Regions overlapping with other missions, e.g., NASA’s Roman Space Telescope, can provide additional information in a different wavelength range. Minisurveys and microsveys in crowded fields will probe regions neglected in the past (see Section 5.3.2). Here we discuss the science goals for the main survey.

#### 1. Low hanging fruit

##### (a) Enlarging the sample of brown dwarfs

Our current sample of brown dwarfs is limited to objects in our close Solar Neighbourhood due to the faintness of brown dwarfs, which make measurements difficult. As such, the detection of early type L-dwarfs with Gaia has only been achieved within a distance of 24 pc (Smart et al. 2017). Also, Kirkpatrick et al. (2021) presented a volume limited sample of brown dwarfs in the celestial sphere with a radius of 20 pc. The Rubin Observatory will allow the detection of fainter objects and as such can produce a volume limited sample which will be complete to larger distances.

##### (b) Detection of weather patterns in brown dwarfs

The sample of substellar objects monitored in the optical wavelength range is still too small to draw a meaningful conclusion. In addition, it is difficult to detect and monitor these objects, as shown by the example of Luhman-16 AB, which is the closest substellar object that does not belong to our solar system. Despite being very close to us, it was discovered only recently in 2013, but on the other hand, it has also become a benchmark system (see e.g., Buenzli et al. 2015; Street et al. 2015; Karalidi et al. 2016, for the study of variability in brown dwarfs). To date, only a few variability surveys have been conducted for brown dwarfs, most of them in the

near-infrared bands. Unfortunately, a lack of high-precision light curves in the near-infrared wavelength range, combined with short observation spans, has hampered any robust conclusions. So far, the longest observing span has been obtained by Street et al. (2015) and Apai et al. (2021). Street et al. (2015) observed Luhmann-16 in the optical band with the LCO 1-m telescope network for 42 days. These observations showed variability with an amplitude of 0.05–0.1 magnitudes and periodicities between 4.46 and 5.84 hr. Apai et al. (2021) analyzed a TESS light curve of Luhman-16 spanning several rotation periods and found changing periodicities, which they attributed to planetary-wave beat patterns. Long-term optical observations have also been obtained for the  $\epsilon$  Indi Ba/Bb brown-dwarf binary. The detection of long-term variations, but the lack of variation on short timescales (a few hours, corresponding to the rotation period) suggests that the system is pole-on and that the variations are caused by long-term cloud evolution. Instead of observing confirmed brown dwarfs one-by-one, we can take advantage of Rubin LSST’s extensive sky coverage. Given the faintness of these objects and the planned photometric precision of Rubin LSST, this facility will be the perfect way to photometrically monitor many brown dwarfs at once.

(c) **Distance and parallax measurements**

The long baseline of the mission, the large field-of-view and the astrometric precision of the observations will provide us important astrometric parameters, including parallaxes and proper motions. These distance measurements are required to obtain robust classifications for brown-dwarf candidates through luminosity estimates. This mitigates the immediate need for follow-up observations for classification. We also note that Gaia can only probe the bright end of the brown dwarf population, whereas the depth of Rubin observations will provide measurements of fainter brown dwarfs.

2. Pie in the sky

(a) **Detection of sub-stellar companions using astrometry**

Astrometric variability can be indicative of an unseen companion. The astrometric signal can be divided into 2–3 main components: the parallax ellipse, the object’s proper motion, and in the presence of a possible gravitationally bound companion, the orbital signature. If a companion is gravitationally bound, the latter is only part of the astrometric signal. Additionally, the companions’ orbital signature can be estimated by unraveling the proper motion and parallax effects from astrometric measurements. Rubin LSST will provide a multi-yr time-series of

high precision astrometric measurements for stars and brown dwarfs, which will allow the disentanglement of the three major astrometric components and enable us to infer possible limits on gravitationally bound companions. As differential chromatic refraction will likely be the determining systematic effect that limits the astrometric error budget, it is important that that data are carefully calibrated in each filter.

(b) **The study of extremely short scale variability in brown dwarfs**

While atmospheric variability due to rotation can be measured over a long time span, further short-term transient effects might be introduced through lightning and Aurora activity. Several works by Helling et al. (2013), Bailey et al. (2014) and Hodosán et al. (2016) among others, discuss the possibility and detection of lightning effects in brown dwarf atmospheres. While the possible detection of lightning has been discussed theoretically, Aurora activity in brown dwarfs has already been detected by Hallinan et al. (2015). The nature of these transient effects might be detected as very short brightening effects, usually only one exposure. The difficult task will be to identify these effects as anomalies in the light curves.

*Preparations for Brown Dwarf Science.*

1. **Follow-up observations/archival data**

Follow-up observations will be necessary to identify objects that might have been misidentified as brown dwarfs as well as for spectral typing the objects of interests. These follow-up observations are essential in the first year as Rubin LSST parallaxes are not available, which will lead to a high rate of misidentified brown dwarfs. Follow-up observations to better characterize these objects are most efficient in the near-infrared wavelength range because brown dwarfs are brightest in this range, and their rich molecular features are best identified via near-infrared spectroscopy. For spectral typing, one high signal-to-noise spectrum covering the near-infrared wavelength range is necessary. As we go to cooler temperatures, the atmospheric chemistry of these objects changes, L-dwarfs lose the vanadium and titanium oxide features, which are seen in M-dwarfs, but they exhibit hydroxides. Even cooler T-dwarfs show a methane rich spectrum, while the ultra-cool Y-dwarfs exhibit ammonia absorption features. Therefore, spectra in the near-infrared range are essential to classify these objects. Besides estimating the spectral types from spectroscopy, we can independently estimate the rotation period through the measurement of  $v \sin i$  from spectral lines and subsequently, this can be compared with the rotational modulated photometric observations. Ideal facilities are the ARCoIRIS spectrograph mounted at

the 4 m SOAR telescope and the Fire spectrograph at the 6.5 m Baade telescope. Brighter brown-dwarf candidates can be cross-matched with existing brown-dwarf catalogs and near-infrared catalogs as well as with Gaia DR3.

As the Rubin LSST parallaxes become available, we will be able to identify brown dwarfs better through distance measurements and luminosity estimates. The parallaxes, alongside proper motions, improve our ability to detect possible companions. Near-infrared photometry can provide further information by increasing the cadence and supplying additional color information. From these multi-color observations, we will be able to extract differences between amplitudes and phases at different wavelengths, which will help us to understand the possible mechanisms causing this variability.

Brown dwarf candidates will be identified in the Rubin LSST Annual Data Release photometric catalogs using the Rubin Science Platform (which provides access to the data at the Data Access Centers). Cross-matching Rubin LSST data against the Gaia, 2MASS and WISE catalogs will provide the colors and proper motion information necessary to accurately select candidates.

## 2. Facilities/software requirements

Existing procedures, as outlined in e.g., Kelly et al. (2014), Foreman-Mackey et al. (2017), Feigelson et al. (2018), Vos et al. (2020) and Apai et al. (2021) will be applied to Rubin LSST photometric and astrometric timeseries via the Rubin Science Platform. This will be done using interactive Jupyter notebook environments and plotting tools. Multi-core or GPU computing facilities will be necessary to process the large data sets in a reasonable amount of time using Monte-Carlo Markov chains (Foreman-Mackey et al. 2013) or a Nested Sampling Monte Carlo (Buchner et al. 2014).

### 3.4.6. Young Eruptive Variables

We have described young eruptive variables of the EXor/FUor type extensively in Section 2.4.1 and so refer the reader to this subsection for a basic overview of the objects. Here we focus on non time-critical EXor and FUor science.

#### 1. Low hanging fruit

##### (a) Define the statistical impact of eruptive versus non-eruptive mass accretion in pre-main sequence stars

It is presently unknown whether EXors and FUors are peculiar objects or rather if they represent a short and recurring phase that all pre-main sequence stars experience during their evolution. To answer this question, we need to compute the percentage of eruptive versus non-eruptive pre-main sequence stars in different star-forming regions. In particular, at least

two outburst episodes are required to classify a source as an EXor-type variable. Present observations indicate that only about 2% of pre-main sequence stars are eruptive variables, mostly identified through serendipitous observations during campaigns carried out to pursue different scientific aims. We expect, therefore, that the percentage of eruptive versus non-eruptive pre-main sequence stars is largely underestimated. A statistical study based on Spitzer/WISE data was already performed by our group (Antonucci et al. 2014a). But now, in preparation for Rubin LSST observations, we intend to exploit the present public surveys to explore the topic in the optical domain, where bursts are far more intense. With Rubin LSST, we expect to reach a statistically significant sample of eruptive protostars within 3 years.

##### (b) Discriminate between intrinsic (EXor) and extrinsic (UXor) pre-main sequence variables

This can be achieved through understanding relationships between accretion and extinction. The classification of a source as an EXor is often uncertain. Indeed, the observed properties (burst amplitude, cadence, optical/infrared colors) are often attributable to accretion as well as: eclipse events related to orbiting bodies, the evaporation/condensation of circumstellar dust, and ejected material caused by powerful outflows that moves along the line of sight (Grinin 1988). Also, many young variables show both intrinsic and extrinsic variability, whose mutual prevalence depends on the level of activity. Hence, it is becoming clear that it is crucial to infer the variation of the mass accretion rate, the time dependence of visual extinction  $A_V$  and more importantly, the possible existence of (inter-)relationships between accretion and extinction events. A secure method for the discrimination between EXor and UXor can be achieved through monitoring the flux over 1–3 yr. This is needed to separate light curves showing long periods of quiescence with superposed accretion bursts (EXors) from light curves that show quasi-periodic dimmings from a constant (high) brightness level (UXors).

##### (c) Learn about the mechanisms that trigger outbursts through light curve comparison

Through the analysis of light curves in a statistically significant sample of objects, we aim to identify observational clues about the mechanism(s) triggering outbursts. Rubin LSST observations will provide an invaluable test-bed for existing models. For example, periodicities in the light curves (see Figure 17), burst durations, or asymmetries in the rising/declining phases,

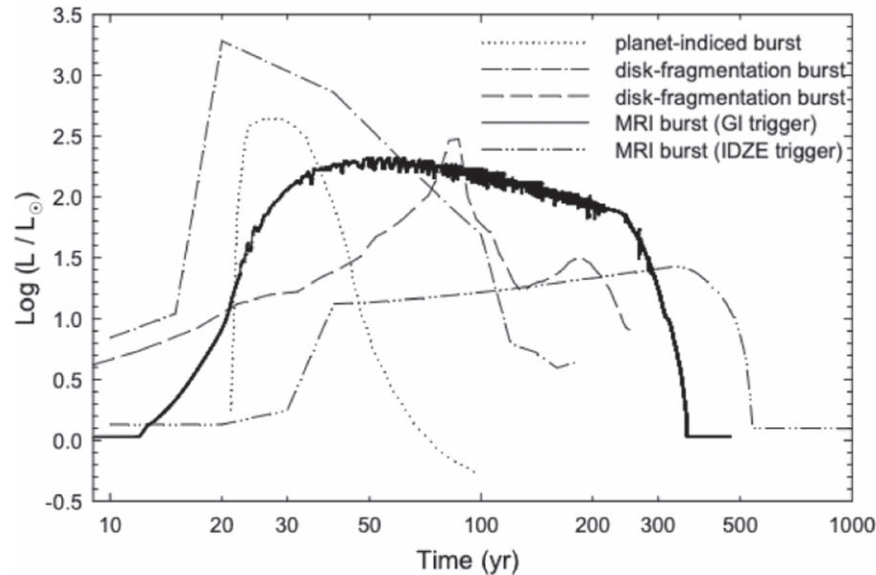


**Figure 17.** Time evolution of individual luminosity outbursts in different burst-triggering models. The zero-time is chosen arbitrarily to highlight distinct models from Audard et al. (2014). “Figure 7” from Audard et al.’s “Episodic Accretion in Young Stars” in *Protostars and Planets VI*, edited by H. Beuther, R. Klessen, C. Dullemond and T. Henning. © 2014 The Arizona Board of Regents. Reprinted by permission of the University of Arizona Press.

would represent observational constraints that we could use to discriminate thermal or gravitational instabilities inside the disk (slow rising, non-periodic light variations), from perturbations induced by external bodies (fast rising and periodic light variations). To reach this goal, we need extensive monitoring of these objects, and therefore we hope to obtain significant results within 10 years.

## 2. Pie in the sky

### (a) Understand whether and how eruptive accretion can solve the “luminosity problem”

The identification of a statistically significant sample of EXors (and possibly FUors) will allow us to understand the role of eruptive mass accretion in the more general context of star formation studies. In a classical star formation scenario for low-mass objects, about 90% of the final mass is accreted onto the star in about  $10^5$  yr, with typical mass accretion rates of  $10^{-7}$ – $10^{-5} M_{\odot} \text{ yr}^{-1}$ . Following this, the accretion progressively fades to rates of  $10^{-9}$ – $10^{-10} M_{\odot} \text{ yr}^{-1}$ .

In this quasi-stationary scenario, however, protostellar luminosities should be largely higher than observed leading to the so-called “luminosity problem” (see Figure 18). Variable (and possibly eruptive) accretion has been proposed as a way of reconciling the observed star formation time and the mean protostellar luminosity (Dunham et al. 2015). Offner & McKee (2011) also found that episodic accretion contributes toward a significant fraction of the stellar mass. Rubin LSST will provide the opportunity to

systematically cover and monitor most of the known star-forming regions. These are the ideal conditions to determine the *true* percentage of eruptive variables, at least in regions where the extinction is not prohibitive. To solve the luminosity problem, however, we would need to demonstrate not only that eruptive pre-main sequence star variables are much more common than presently expected, but also that the burst frequency and amplitude produce an increase in the accretion luminosity that is high enough to compensate for the low values observed during the (much longer) fainter stages. The complete survey lifetime is needed to reach such an ambitious goal.

### *Preparations for Young Eruptive Variable Star Science.*

#### 1. Follow-up observations/archival data

Optical/near-infrared spectroscopic follow-up is needed in order to confirm the indications retrieved from the light curves, since the shape of the continuum differs for EXors and UXors and the emission/absorption lines present in the spectrum also differ. Systematic monitoring of known objects is presently on-going at the Large Binocular Telescope (Antonucci et al. 2014b; Giannini et al. 2016a, 2016b, 2018), with the aim, among others, to construct template spectra of EXor and UXor sources. These templates will provide a reference for the spectroscopic follow-up of Rubin LSST observations. We intend to use our guaranteed telescope observations with the SoXS (Son Of X-Shooter) instrument on the New



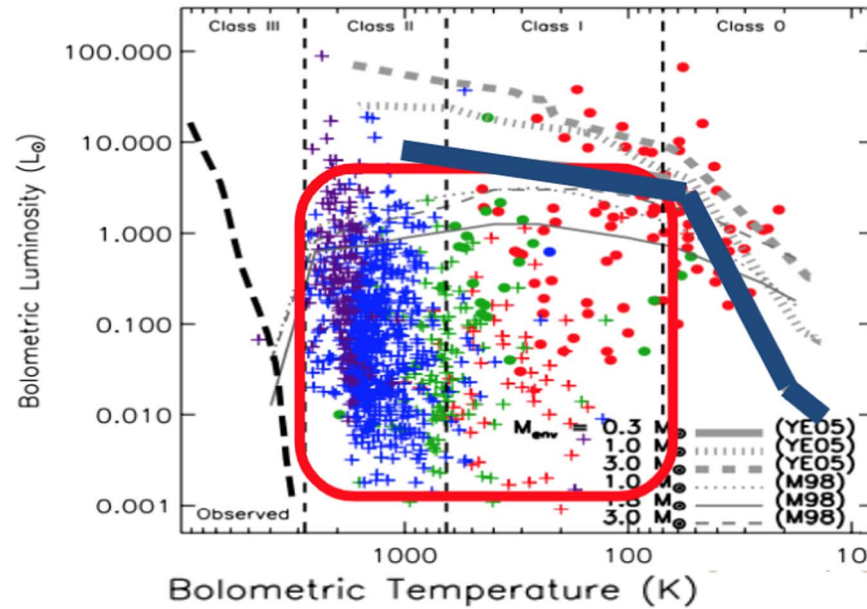


**Figure 18.** Bolometric luminosity ( $L_{\text{bol}}$ ) is plotted vs. the bolometric temperature ( $T_{\text{bol}}$ ). The bulk of the observational points (colored dots) are located *under* the model predictions (black lines) inside the red box, indicating the “luminosity problem.” Adapted from Evans et al. (2009). © IOP Publishing Ltd. All rights reserved.

Technology Telescope for the same purpose.

Due to the nature of emissions during accretion events, it is highly desirable to cross-match the Rubin LSST Annual Data Release products against catalogs with observations in other wavelengths, especially the ultraviolet and infrared products of the Vista surveys, 2MASS, Gaia, Gaia-ESO survey (GES), WISE, Spitzer, Chandra, Herschel and eROSITA (when the data are made public). A database search interface that enables the user to select candidates based on predefined criteria will be essential to target selection, and should include Application Programmable Interfaces (APIs) that allow other data services to interact with Rubin LSST data products.

## 2. Facilities/software requirements

Further work is needed to develop a suitable algorithm capable of identifying these targets and cross-matching them against other catalogs (the Gaia catalog, in particular, will be essential). Once the objects are identified, however, a dedicated software package is needed to analyze the photometry. If one is not available in the Rubin Science Platform, our group will develop a suitable tool for this kind of analysis.

### 3.4.7. Compact Binaries: Cataclysmic Variables

Figure 19 depicts an Artist’s Cataclysmic Variable consisting of a white dwarf accreting from a late-type (typically K–M) companion. The variability of cataclysmic variables involves

timescales ranging from minutes for AM CVns and other ultra-compact binaries to 30 yr for low-mass-accretion-rate dwarf novae, and amplitudes from one magnitude to 15 magnitudes. While the time-critical studies will address some science goals related to the immediate discoveries of novae and other outbursting systems (see Section 2.4.2, which describes the time-critical science cases for cataclysmic variables), there are many aspects that need the 10 yr coverage afforded by Rubin LSST. Long term studies of cataclysmic variables from the Rubin LSST archive, starting from year one and continuing to the full ten years of the survey, will involve the following science goals:

#### 1. Low hanging fruit

##### (a) Discover and classify new dwarf novae

This will be achieved using light and color curves, amplitudes and outburst recurrence timescales derived from the survey data. Their spatial distribution and distances will determine their number density in the galaxy as a function of galactic latitude. The newly identified distribution of objects will be used to compare with population models. The full 10 years of the survey will be required to generate a representative sample, as the majority of objects are expected to have long (decades) timescales between outbursts. Better population models are needed to provide a comparison of the resulting number densities with expectations from evolution models.

##### (b) Monitor the known nova-like variables

Since nova-likes are known to sometimes decrease their mass transfer and at times to totally

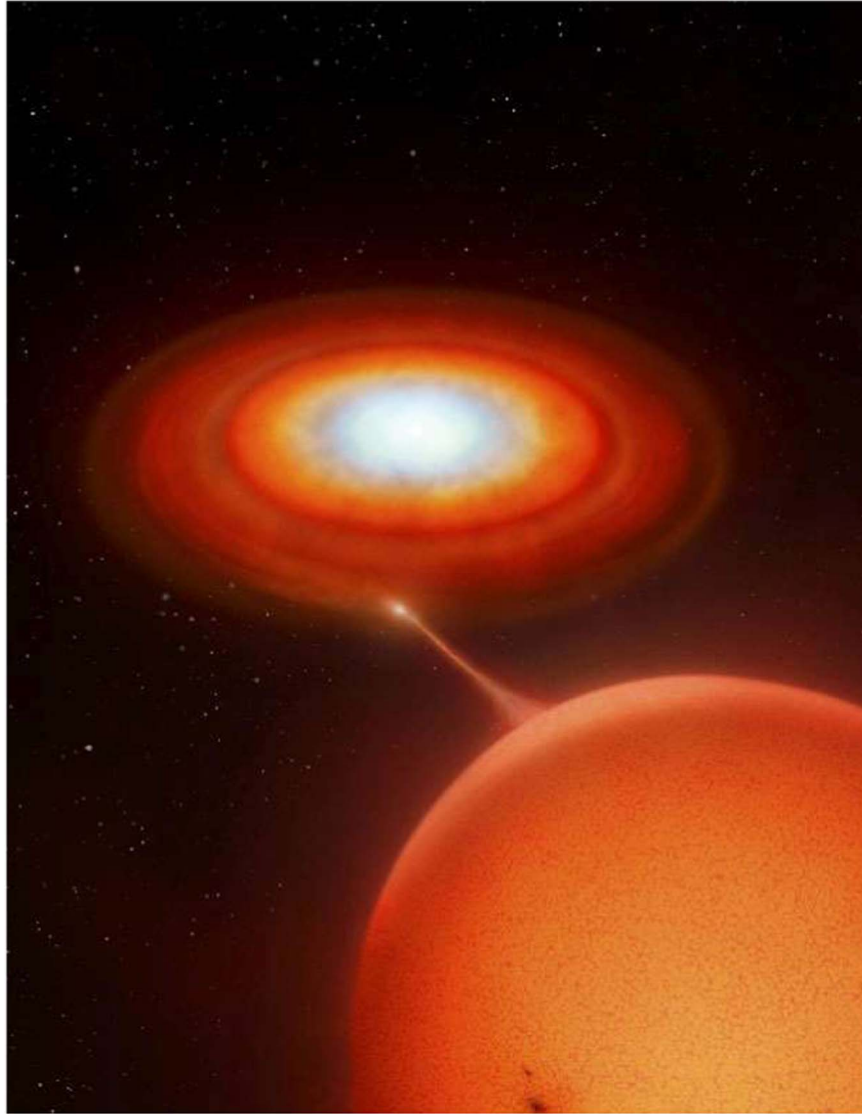


**Figure 19.** An artist's impression of a Cataclysmic Variable consisting of a white dwarf accreting from a late-type (typically K–M) companion. Most of the optical luminosity and transient outbursts typically come from the surrounding accretion disk, which is continuously fed by an accretion stream from the Roche-lobe filling companion star. Illustration created by M. Garlick, 2023 (<https://www.space-art.co.uk/>).

stop mass transfer, by observing the length of time that known nova-like variables spend in low versus high accretion states, we can begin to understand the total mass accreted and the angular momentum losses in these systems. This will require the long temporal base of 10 years.

(c) **Find candidate magnetic white dwarf systems (polars and intermediate polars)**

Using the shape of the light and color curves and the detection of relatively long-lived (weeks/months/years) bright and faint states, we are able identify new examples, which will lead to a better understanding of the ultimate state of high magnetic field systems after

common envelope evolution. To confirm their magnetic nature, circular polarimetry and/or medium resolution spectroscopy will be required. Faint, low accretion rate systems are also expected to be discovered, which are important in understanding their ultimate evolutionary fate. While results will be found on a yearly basis, the full 10 yr survey is needed to determine final numbers of magnetic versus non-magnetic systems and to understand how cataclysmic variables are distributed in the galaxy. Such data will also help characterize the duty cycles and morphology of long-term light curves in terms of high, low and intermediate accretion states.

**(d) Find candidate eclipsing systems**

Eclipsing systems enable inclinations (from light curve modeling) and stellar masses (from radial velocity studies) to be determined. This will require follow-up observations to provide high cadence light curves and we will further need time-resolved spectra to obtain radial velocity curves.

**2. Pie in the sky****(a) Determination of the orbital period distribution for candidate dwarf novae**

By obtaining follow-up photometric and spectroscopic observations, we will be able to compare our results with population models. For comparison, we will also need to determine the mass of the secondary component for the shortest period systems, so that we may identify those after the “period bounce” (when the secondary has become degenerate and the period of the system increases rather than decreases). This effort will require time-resolved spectra from large (at least 10 m) telescopes.

**(b) Determine the spin and orbital periods of candidate intermediate polars**

Despite the non-uniform temporal distribution of the survey data and the typical few day cadence, in some cases it may still be possible to detect short periods (minutes) in power spectra associated with the white dwarf spin in intermediate polars. Time-resolved (5–15 minutes) spectroscopic follow-up data for objects showing light curves resembling intermediate polars will enable the determination of their orbital periods. Using high cadence (seconds–minutes) photometric observations from follow-up data, we can determine the spin period which will confirm an intermediate polar classification. Obtaining the number of systems of this type will help us understand the magnetic binary evolution.

**(c) Accomplish follow-up polarization studies of candidate polars**

This will enable us to estimate the magnetic fields of the white dwarf components in order to confirm their classifications and further understand the evolution of white dwarfs in binaries (compared to isolated single white dwarfs).

*Preparations for Compact Binary (Cataclysmic Variables) Science.***1. Follow-up observations/archival data**

Due to the faint magnitudes of Rubin LSST, large (at least 8 m to 10 m) telescopes will be required for many of the follow-up observations. For the purpose of classification, spectroscopic follow-up is needed. To confirm the polar candidates, we require circular polarimetry and/or medium resolution spectroscopy. For intermediate polar

candidates, high cadence light curves and time-resolved spectra for radial velocities will be needed.

**2. Facilities/software requirements**

Machine learning techniques will need to be developed to recognize the various types of dwarf novae and nova-likes that need follow-up spectra. To obtain the follow-up for detailed classifications, large telescope facilities equipped with medium resolution spectrographs as well as spectropolarimeters will be needed, as well as continuous blocks of time in order to obtain the orbital periods.

*3.4.8. Compact Binaries: Neutron Star Binaries*

The study of transitional milli-second pulsars, milli-second pulsars and low-mass X-ray binaries, (i.e., accreting neutron stars) is not limited to time-critical science, which requires the Rubin LSST alerts. Additionally, it will greatly benefit from the all-sky, long-term monitoring characteristics of the complete survey. For a detailed introduction to Neutron Star Binaries see Section 2.4.3. Here we detail the science cases for non-time critical neutron star binary science.

**1. Low hanging fruit****(a) Generating a census of transitional milli-second pulsars, milli-second pulsars and low mass X-ray binaries**

The multi-band, deep Rubin LSST observations will be combined/cross-matched with data from other next-generation X-ray surveys, such as THESEUS or eROSITA, allowing for the discovery of new accreting neutron stars. Population analyses will be applied to the resulting census once the Rubin LSST data are cross matched with GAIA parallaxes and proper motions.

**(b) Long term monitoring of all known transitional milli-second pulsars, milli-second pulsars and low mass X-ray binaries**

The Rubin LSST light curves of known objects will enable us to assess the long term variability of each system. Known systems (milli-second pulsars, transitional milli-second pulsars and low mass X-ray binaries) will be part of the monitoring program starting with the commissioning observations. New systems will be added to the monitoring program once early Rubin LSST data sets are cross-correlated with candidate milli-second pulsars, transitional milli-second pulsars and low mass X-ray binaries from the coming radio and X-ray observations from the SKA and X-ray surveys. From the beginning to the end of the Rubin LSST survey mission, the database of accreting neutron stars will gradually increase in

sample size, eventually culminating in a 10 yr long multi-color light curve for each system.

(c) **Mapping of the variability patterns displayed by interacting compact binaries**

Understanding the variability patterns will be invaluable for learning about the history of the mass accretion rate of each object so that we may determine the correct evolutionary scenario for each subclass of compact binaries. This is particularly important for the transitional milli-second pulsars (de Martino et al. 2010; Papitto et al. 2013), which are milli-second pulsars that have recently been discovered to change from a radio pulsar propeller state to that of an accreting low mass X-ray binary, or vice-versa. They have also been observed to have intermediate states with subluminescent accretion disks that maybe related to the launching of jets. By properly framing the milli-second pulsar population in the context of low mass X-ray binaries, we will be able to answer the questions: (1) do all milli-second pulsars become transitional and (2) whether the transitional milli-second pulsar phase is an evolutionary phase that precedes the total exhaustion of the donor star.

(d) **Answer important questions about neutron star state changes**

While the change of state of an accreting neutron star might trigger follow-up observations (see Section 2.4.3, which describes neutron star binaries from a time-critical perspective), the long-term (multi-color) light curve of each system will allow for the determination of the timescale on which changes occur, as well as the duration of each state and the driving factor for the change of state. Unanswered questions include:

- i. Does the change of state depend solely on the change of the mass transfer rate?
- ii. Does the mass transfer rate depend on the nature of the secondary star or other system parameters?
- iii. Are transitional milli-second pulsars a specific evolutionary phase between the low mass X-ray binaries and the milli-second pulsars or can any system turn into a transitional milli-second pulsar?

These questions are now becoming more important, given that the number of known milli-second pulsars has more than tripled since 2010 (thanks to both radio surveys and blind searches in the Fermi-LAT sky scans, which have discovered a number of pulsar-like  $\gamma$ -ray sources that were eventually confirmed to be milli-second pulsars). The number of such systems is expected to further increase even more dramatically once SKA is operational (enabling much improved timing precision of the binary pulse). Furthermore, next generation X-ray missions will permit the discovery and high signal-to-noise modeling of X-ray pulsed signals.

*Preparations for Compact Binary (Neutron Star Binary) Science.*

1. **Follow-up observations/archival data**

For the new milli-second pulsars discovered via radio surveys (e.g., ngVLA, ASKAP, MeerKAT, SKA), finding the X-ray and/or optical counterpart is a crucial first step to properly characterizing the population of milli-second pulsar binaries in their various subclasses (e.g., black-widows with degenerate donors, and red-backs with non-degenerate donors). Rubin LSST will provide the optical light curve data to enable the classification of new milli-second pulsars.

3.4.9. *Compact Binaries: Black Hole Binaries*

Of the millions of stellar-mass black holes that have formed through the collapse of massive stars over the lifetime of the Milky Way, only  $\sim 20$  have masses that have been dynamically confirmed through spectroscopic measurements (e.g., Corral-Santana et al. 2016). Expanding this sample of black hole masses could aid in answering many questions central to modern astrophysics.

There is expected to be a large population of black hole binaries in quiescence with low X-ray luminosities from  $\sim 10^{30}$ – $10^{33}$  erg s $^{-1}$ . Such systems can be identified in the optical as variables that show unique, double-humped ellipsoidal variations of typical peak-to-peak amplitude  $\sim 0.2$  mag due to the tidal deformation of the secondary star, which can be a giant or main sequence star. In some cases, analysis of the light curve alone can point to a high mass ratio between the components, suggesting a black hole primary; in other cases, the accretion disk will make a large contribution to the optical light which results in intrinsic, random, and fast variations in the light curve. The contribution of the disk to the optical light can vary over time, and several years of data are required to properly subtract the accretion disk contribution and subsequently fit the ellipsoidal variations (Cantrell et al. 2010). As a result, data products generated by Rubin LSST for studying the ellipsoidal variability of black hole binaries will begin to become useful around the 3 yr mark, allowing for some probe of the variability. However the results will be much improved after the full 10 yr survey. The characteristic ellipsoidal modulation of X-ray binaries can also be observed in other classes of binary systems. Therefore, X-ray follow-up observations are required in order to classify X-ray binaries.

Black hole binaries typically spend most of their time in quiescence, where the optical emission is dominated by the companion star. However, many systems undergo periods of outburst, thought to be triggered by instabilities in the accretion disk (Lasota 2001). These outbursts are characterized by very rapid and dramatic increases in optical luminosity and during outburst the disk becomes the dominant component in the

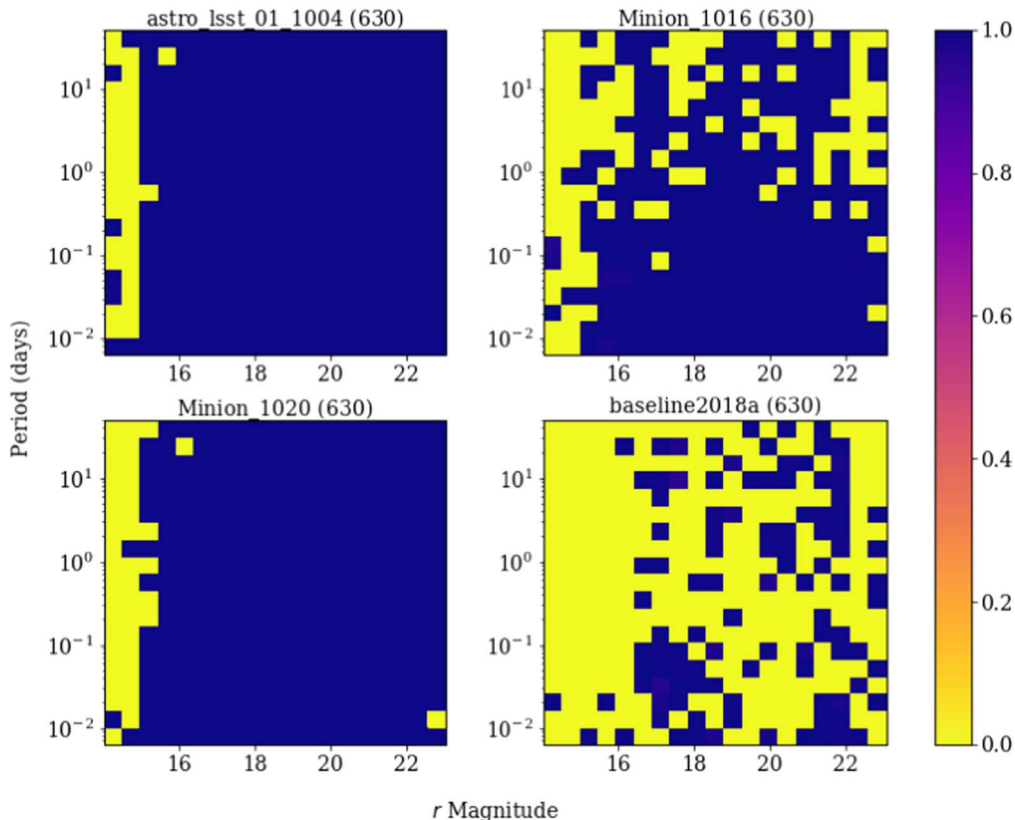


**Figure 20.** Color maps displaying the period determination of low-mass X-ray binaries that are observable with observing strategies `astro_sim_01_1004`, `Minion_1016`, `Minion_1020` and `baseline2018a`, which are Rubin LSST survey strategies that have been proposed by the Survey Cadence Optimization Committee. All observations used were of Rubin LSST field 630 which is in the Galactic Plane. The y-axis denotes the orbital period in days, the x-axis denotes the  $r$ -band magnitude before adding contributions from ellipsoidal modulations, flaring and noise. The color denotes the significance of the period detected. If the measured period differed from the actual period by more than 5%, then the significance was set to zero.

optical luminosity and the characteristic ellipsoidal modulation can no longer be observed.

Rubin LSST is expected to discover many unknown black hole binaries, therefore we expect archival pre-Rubin LSST data (i.e., prior to discovery) will be superfluous. The brighter sources will be spectroscopically observable with the current generation of 4–10 m telescopes to dynamically confirm new black holes; spectroscopy of all candidates should be possible with the forthcoming generation of large telescopes. Thus, Rubin LSST will trigger a rich variety of observational investigations into the accretion/outflow processes through studies of this large, dark population.

### 1. Low hanging fruit

#### (a) **Period determination and quiescent magnitude observations**

Many black hole binary candidates have currently only been observed during outburst as they are too faint to be observed with sufficient sensitivity in quiescence. To date, observations during quiescence have only been possible for a few of these systems. Rubin LSST should be able to observe a large fraction

of these systems in quiescence, for the first time, during the first year of its operations. As the companion star cannot always be observed during outburst, this will allow for counterpart identification for many of these systems.

#### (b) **Period determination**

We will obtain the periods of a meaningful fraction of the black hole binary population. The majority of Galactic black hole binaries will likely be too faint to be observed by Rubin LSST. However, the fraction that Rubin LSST should be able to observe through ellipsoidal variability (approximately 1/3, Johnson et al. 2018) should prove to be statistically significant with regards to population studies of black hole binaries. The current computational techniques are capable of determining the period through ellipsoidal variability. Figure 20 shows results for the period determination of black hole binaries with Rubin LSST over a broad range of parameter space when using different observing strategies from Johnson et al. (2018).

## 2. Pie in the sky

### (a) Measure the masses of the binary components

Through knowledge of the binary component masses, we are able to learn about the history and evolution of black hole binaries. Antokhina & Cherepashchuk (1997) found correlations between the parameters of black hole binary optical light curves and the physical parameters of the system, such as binary component mass or orbital inclination. Therefore, Rubin LSST could be used to place constraints on these physical parameters in black hole binaries that are observed in quiescence. Potentially, this information could then be used to answer questions such as: “Which stars produce black holes versus neutron stars?”; “Whether there is a true gap in mass between these two types of compact object?”; and “Whether SN explosions result in large black hole kicks?” Current constraints on black hole samples detected by Gaia are limited by small number statistics and non-negligible systematic uncertainties on the masses (Atri et al. 2019; Gandhi et al. 2019). However, these techniques will have to be investigated further, while using simulated Rubin LSST data, in order to determine their applicability.

*Preparations for Compact Binary (Black Hole Binary) Science.*

### 1. Follow-up observations/archival data

For classification purposes, X-ray follow-up is required. Follow-up for the majority of the discovered systems should be possible with the next generation of X-ray telescopes, e.g., at the deep sensitivity limits expected with Athena (Barret et al. 2018), though the nearby population should also be detectable with eROSITA (Merloni et al. 2012).

### 2. Facilities/software requirements

Due to the expected total population of low-mass X-ray binaries in the Milky Way ( $\sim 1300$ ; e.g., Corral-Santana et al. 2016), we require storage to host all images for each of the objects (or at least to store the regions in which they are contained). For period determination, we need computing resources to generate  $\sim 10^5$  power spectra per system.

#### 3.4.10. Luminous Blue Variables

Luminous blue variables are very bright sources, and among the most massive stars detectable in galaxies. Famous examples in our Galaxy are AG Car, HR Car, and  $\eta$  Carinae. In the nearby Universe, we should also mention: S Doradus (Leitherer et al. 1985) in the large Magellanic cloud (LMC); AE And and AF And in M31; and Var C and Romano’s Star (GR 290) in M33 (Richardson & Mehner 2018). There are additionally

several well-studied luminous blue variables in NGC 2403 (Tammann & Sandage 1968). Collectively, they are known as the Hubble-Sandage variables (Hubble & Sandage 1953). During S Dor-like outbursts, luminous blue variables experience erratic brightness variability over timescales of several months to a few years or decades, with  $\Delta M$  of a couple of magnitudes, typically  $\Delta M = 1\text{--}2$  mag. Traditionally, it had been assumed there was no significant change in the bolometric luminosity (Humphreys & Davidson 1994), but this has more recently been challenged (Clark et al. 2009; Groh et al. 2009). During outburst, S Doradus luminous blue variables move to the right of the Hertzsprung–Russell diagram, becoming redder and cooler, following which they return to the left side of the Hertzsprung–Russell diagram during quiescence. The reason for the Hertzsprung–Russell diagram excursions is as yet unknown although envelope inflation due to the proximity to the Eddington limit is the main contender (Vink 2012; Gräfener et al. 2012; Grassitelli et al. 2021).

The full range of variability of classical luminous blue variables can be comfortably monitored with Rubin LSST observations up to about 30 Mpc, but with stacked images, we can largely exceed this distance limit. Further, an  $\eta$  Carinae Great Eruption-like event (Smith & Frew 2011) could be detected at tens or even hundreds of Mpc. With Rubin LSST, we plan to observe known luminous blue variables and expect to find new luminous blue variable candidates in outburst.

### 1. Low hanging fruit

#### (a) Observations of ordinary luminous blue variable outbursts (S Dor-like)

Known S Dor variables will automatically be observed and this will greatly enhance the baseline and quality of reference objects. In addition, some luminous blue variables are known to undergo multiple giant outbursts. An example of such a restless luminous blue variable is SN 2000ch, the luminous blue variable in NGC 3432 (Wagner et al. 2004; Pastorello et al. 2010). Some luminous blue variables may be identified in the first year of Rubin LSST observations, but given that the average time-scale of S Dor variations is about a decade, the sample will only start to become complete after 10 years.

#### (b) Direct association of luminous blue variables, identified in their eruptive states, with their quiescent counterparts

The magnitude depth and resolution of Rubin LSST will allow the identification of stars in the Local Volume. With a single-image  $r$ -band magnitude of 24.7 and a corresponding coadded  $r$ -band magnitude of 27.5, the quiescent counterpart of outbursting luminous blue variables should be detectable in the 10 yr Rubin LSST image stacks. Detailed progenitor information alongside the characterization of pre-

eruption sources at the positions of the luminous blue variable will be a major contribution of Rubin LSST to luminous blue variable science.

(c) **Identifying SN precursors**

Precursor eruptions that precede the explosions of interacting SNe, often associated with luminous blue variable-like progenitors (Gal-Yam et al. 2007), have been conclusively observed (see, e.g., Fraser et al. 2013; Pastorello et al. 2013; Margutti et al. 2014; Reguitti et al. 2019; Jacobson-Galán et al. 2022). Rubin LSST promises to provide a sufficiently large sample to distinguish which of these optical transients are SN precursors, and which are not.

2. Pie in the sky

(a) **Determination of the evolutionary state of luminous blue variables**

Using the “reference frame” of known objects, new S Dor variables will be discovered with Rubin LSST in a variety of environments. Ultimately, it is the comparison of luminous blue variables with respect to ordinary blue supergiants that will enable the determination of the duration of the luminous blue variable phase and thus the evolutionary state of luminous blue variables (Kalari et al. 2018).

*Preparations for luminous blue variable Science.*

1. **Follow-up observations/archival data**

For known luminous blue variables, using literature and archive data, for example, data from AAVSO, PanStarrs and Atlas, we aim to obtain light curves with baselines of many decades. This multi-survey strategy may reveal variability that develops on different time-scales. Well-studied luminous blue variables will become reference objects.

2. **Facilities/software requirements**

Software to generate periodic stacks will be needed to detect luminous blue variables farther than 30 Mpc. Likely, this can be done using the Rubin open software pipeline in-between data releases, possibly leveraging infrastructure such as LINCC.<sup>84</sup> Software to identify the quiescent state of luminous blue variables in Rubin LSST stacks (whether Annual Data Releases or custom made stacks) by co-location will be required. Depending on the location of the star, this operation may be complicated by crowdedness and blending.

In addition to relying on observed reference objects, the theoretical development of envelope inflation and atmosphere modeling is needed to predict a range of luminous blue variable colors as a function of metal content. The need for modeling is particularly clear when considering that known transients show a rather wide

range of behavior (Smith et al. 2011), which makes the simple use of templates rather limited for identification and classification.

3.4.11. *Light Echoes of Eruptions and Explosions*

Light echoes are the reflection of stellar explosions on interstellar material. As the light from a transient propagates into space, it may be reflected toward Earth and our telescopes. If it encounters a sheet of interstellar material, it will generate a light echo. The geometry of light echoes is straightforward, a transient and the Earth are at two foci of a 3D ellipsoid; all light from the transient that is reflected off dust that intersects the same ellipsoid surface will reach Earth at the same time. As time goes by, the ellipsoidal surface expands. Due to the extra travel time, a light echo reaches the observer at a later time than the light directly detected from its source.

Light echoes provide unique insight into the transients that generate them and the dust that produces them (see Figure 21). However, they are very challenging to detect. Light echoes appear as faint, extended, time-varying features (Rest et al. 2005, 2013). The complexity of their shape is determined by the complexity of the underlying structure of the reflecting medium, while the time-changing aspect is due to the traveling of light across the dust sheet.

Light echoes help characterize stellar explosions by offering the view of an explosion from different lines of sight, a unique opportunity in astrophysics (Rest et al. 2011; Finn et al. 2016) and allow us to revisit events, even when the transient was not originally detected (Rest et al. 2011). The detection of light echoes across a large portion of the sky, which Rubin LSST can observe, could lead to the detection of an unknown galactic SN. Furthermore, it could provide an additional way of tracing the Milky Way dust structure that compliments current stellar extinction and direct detection surveys. Improved dust maps can improve our understanding of extragalactic sources by constraining extinction. A large scale census of light echoes could constrain the rate of massive star eruptions and thus inform the evolutionary history of the Galaxy and Local Volume.

With its unique combination of deep, high-resolution imaging with observations of the whole southern sky every  $\sim 3$  nights, Rubin LSST is the ideal survey to detect light echoes. However, light echoes are extremely hard to detect. As part of its federally funded operations, Rubin LSST will produce  $10^6$  nightly alerts Section 2.2, each one announcing a changing or moving source. It will detect thousands of transients and variable “point sources” in each image, but diffuse light echoes will not reach the  $5\sigma$  significance level over the size of the Rubin PSF and will be entirely missed.

To date, light echoes are still discovered chiefly by visual inspection, a method that obviously does not scale to the Rubin LSST data volume. Even crowd-sourcing cannot help this

<sup>84</sup> <https://www.lsstcorporation.org/lincc/node/1>

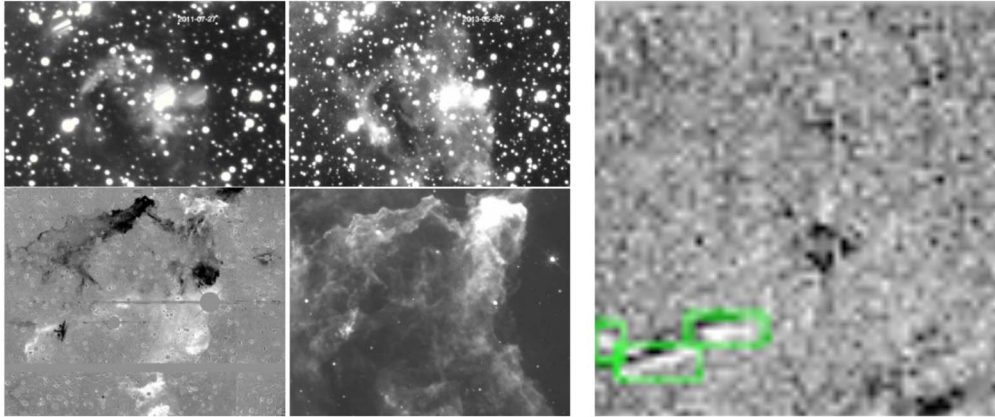


**Figure 21.** Left: The top two images show light echoes from Eta Carinae’s Great Eruption that light up the dust structure about 30 arcminutes away from the star. Adapted from Rest et al. 2012, with permission from Springer Nature. The images, taken about 2 years apart, reveal the time-evolving structure of the light echo phenomenon. On the bottom left, a light echo of Eta Carinae in difference imaging. To its right, a Spitzer infrared image of the same dust structure illuminated by the light echoes. The reflected light reveals an astounding level of detail in the dust structure. Right: a difference image of an ATLAS (Tonry et al. 2018) field with a light echo complex, labeled for ingestion by a Regional Convolutional neural network (RCNN, Ren et al. 2015). This image shows the difficulty of the labeling exercise: the light echo complex is composed of different echoes (different dust sheets) that are blending. Several artifacts are present (saturated stars, star streaks, etc.) which are not labeled in this example. In reality, because light echoes diffuse until they blend into the noise, forming a continuum in detectability space, the Regional Convolutional neural networks cannot rely on the assumption that the labels are complete (i.e., that they identify each light echo instance in the training set) and artifacts have to be labeled as negative examples as well (Li et al. 2022).

science in the Rubin LSST era: simple scaling from the Galaxy Zoo (Rest et al. 2008; Fortson et al. 2012) project indicates that the entire population of the Earth would be insufficient to study the full dataset using the same method. Feature based approaches fail to separate the rare true positives from the many false positives, which include a vast array of artifacts in sky images.

#### 1. Low hanging fruits

##### (a) Observations of known light echoes, which will form a training set for future detections

Several historical SNe and stellar eruptions have known light echoes (Rest et al. 2008, 2012) and their detection is trivial with Rubin LSST. These light echoes can serve to train and tune models to detect lower signal-to-noise, unknown light echoes. Their monitoring will trace interstellar dust filaments and provide detailed light curves of the explosions and eruptions.

#### 2. Pie in the sky

##### (a) Setting constraints on the Galaxy’s explosion history

The detection of light echoes across the southern hemisphere can be linked to stellar explosion models for the Galaxy. This will enable a more detailed understanding of the Galaxy explosion history.

##### (b) The discovery of unknown SNe

The detection of “orphan” light echoes could lead to the discovery of an unknown Galactic SN, which

could be classified based on light echo spectra collected from large telescopes.

#### Preparations for Light Echo Science.

##### 1. Follow-up observations/archival data

Once detected, light echoes require repeated images to confirm their nature and to monitor their evolution. If bright enough, spectroscopic follow-up with large telescopes (8 m class or greater) will be applied to characterize the transient. The large aperture is required because the phenomena are faint (typically ten times fainter than the original transient).

The current dataset of observed light echoes is extremely small (tens of examples, mostly from telescopes and surveys with vastly different properties than Rubin Observatory) and not enough to train automated machine learning models for the detection of new light echoes. The current dataset should be augmented with simulations, either entirely machine-learning based simulations (e.g., Generative Adversarial neural networks, Goodfellow et al. 2014) or based on the forward modeling of dust maps.

##### 2. Facilities/software requirements

A pipeline for the detection of light echoes needs to be developed that reprocesses the Rubin LSST’s difference and/or possibly the original images. This pipeline should run at a Data Access Centers to avoid transferring large image data sets and would produce large databases (however, small compared to the image



database). These databases should then be cross-referenced with explosion and eruption historical and contemporary data sets.

Neural Networks, including Deep Convolutional neural networks (Ren et al. 2015), Generative Adversarial neural networks (Goodfellow et al. 2014) and Bayesian neural networks (Charnock et al. 2020) to quantify uncertainties, and other methods in the neural networks family are promising to address this low signal-to-noise regime computer-vision challenge. The first pipeline for the automated detection of light echoes at scale will likely include one or more of the aforementioned neural networks.

### 3.5. Extragalactic Transients and Variables

#### 3.5.1. Blazars

While the detailed study of the jet emission variability in blazars is time-critical (see Section 2.5.4) because it requires simultaneous multiwavelength observations, especially during active states, important information can be determined by studying blazars in the non-time critical sense. These include the statistical analysis of properties related to a single blazar class or blazar subclass (BL Lacs and FSRQs). Of particular interest is the analysis of the cosmological properties of blazar and their relationship with radio galaxies, which represent the unbeamed parent population of blazars, according to unified models of active galactic nuclei (AGN Capetti & Raiteri 2015a). Another important topic that is also connected to the understanding of the blazar parent population is the study of the environment of the blazar host galaxies. Blazars are commonly hosted by giant elliptical galaxies, mostly located in dense environments, but the picture needs to be investigated further with a large sample of objects covering a wide range of redshifts. With Rubin LSST data we plan to undertake the following science-driven projects:

#### 1. Low hanging fruit

##### (a) **Perform a statistical study of long-term blazar variability**

Statistical studies will allow the duty cycles of the various blazar classes to be analyzed. Further, we will search for peculiar behaviors that can shed light on the underlying variability mechanisms, such as periodicities, or strongly chromatic flares, i.e., flares characterized by noticeable color changes.

##### (b) **Study the environment of blazar host galaxies**

Several radio-loud AGN are located in rich environments (Kotyla et al. 2016). The most powerful of them lie in galaxy clusters and those with the most massive hosts are found in the central cluster regions (Magliocchetti et al. 2018). If radio galaxies are the parent population of blazars, both classes

should share the same clustering properties. However, this has recently been put into question by an analysis with a relatively small sample of objects (Sandrinelli et al. 2019). The matter needs to be further investigated using the deep images of blazar and radio galaxy environments that Rubin LSST will provide.

The presence of a galaxy cluster around a blazar can be ascertained by looking for a “red sequence” of early-type galaxies in the color–magnitude diagram, where the color and slope will depend on the blazar redshift. The higher the redshift we want to consider, the deeper the observations must go. We estimated (Raiteri et al. 2018) that magnitudes of 24, 25, and 26.5 must be reached in the  $z$  band to extend the study to redshifts of 0.5, 1 and 2, respectively. Therefore, as time goes on, Rubin LSST will allow us to explore the environments of sources that are farther and farther away, starting with the Local Universe in the first year, and extending out to cosmological distances at the end of the 10 yr survey. At the same time, Rubin LSST will also sample fainter and fainter galaxies at low redshifts, increasing the environment richness.

#### 2. Pie in the sky

##### (a) **Explore the cosmological properties of a much wider blazar population**

The identification of new blazars, together with the availability of their radio fluxes, will allow us to build luminosity functions and to determine the cosmological evolution of the various blazar classes. Wolter et al. (1994) derived radio, optical and X-ray luminosity functions for two small samples of radio-selected and X-ray-selected blazars. Through the comparison between luminosity functions, they investigated the evolution of the blazar population(s). They found that the X-ray selected sources have a negative evolution, i.e., they were fewer or fainter in the past, while the radio-selected objects have a marginal positive evolution in the radio band. A number of studies can be found addressing the radio luminosity function of blazars (see, e.g., Capetti & Raiteri 2015a, 2015b, and reference therein). The 1.4 GHz radio luminosity function shows a break at  $\log L_{\text{radio}} \sim 40.6$  [erg/s], which implies an abrupt decrease of the number of sources at low radio powers. The break is likely connected to the minimum power needed to launch a relativistic jet. For this kind of study, redshift is a necessary ingredient, so supporting spectroscopic observations will be needed to enlarge the blazar sample that will subsequently contribute to luminosity function studies.

*Preparations for Blazar Science.***1. Follow-up observations/archival data**

To identify new blazars, we need multiwavelength follow-up, in particular in the radio band because blazars are radio-loud objects that are characterized by a flat radio spectrum. Finding diagnostic methods for blazar detection is a critical issue that should be tackled ahead of Rubin LSST's first light. Its solution would also allow Alert Brokers to characterize sources that are ideal for gamma-ray follow-up, since blazars are the most abundant population in the gamma-ray sky (see Section 2.5.4). To further study the blazar population, it is important to know the associated redshift, and so spectroscopic follow-up is necessary.

**2. Facilities/software requirements**

As in the time-critical case (see Section 2.5.4), methods to analyze time series will be required to identify characteristic variability time scales and possible (quasi) periodicities. Classical methods include the Structure Function (Simonetti et al. 1985), the Discrete Correlation Function (Edelson & Krolik 1988; Hufnagel & Bregman 1992) and the Lomb–Scargle Periodogram (Press et al. 1992; VanderPlas 2018). The robustness of the results will increase as the Rubin LSST monitoring continues. These methods are expected to be applied to a wide variety of science cases both in the Transiting and Variable Star Science Collaboration (TVS SC) and in other Science Collaborations.

While diagnostic methods based on variability and colors that separate quasars from variable stars do exist (e.g., Butler & Bloom 2011), we lack a similar method to identify blazars. Only the most violently variable blazars are clearly recognizable through their optical light curves without further spectroscopic or multiwavelength information.

One options may be to employ the Discrete Correlation Function, which can also check cross-correlations between flux variations in different bands and look for possible time delays. As mentioned in Section 2.5.4, this gives information on the emission processes and on the location of the emitting zones inside the jet. Therefore, although Rubin LSST data alone will allow us to investigate several blazar science cases, the availability of multiwavelength time series is of great importance for the study of other blazar topics. Figure 22 shows a comparison of light curves of BL Lacertae in different bands (Raiteri et al. 2013). It is clearly visible that the behavior in  $\gamma$ -rays is well correlated to that in the optical band (with some differences) while the trend in X-rays is more similar to that observed at millimeter wavelengths.

**3.5.2. Supernovae**

The identification of the progenitors of both SNe Ia and Core collapse supernovae (CC SNe) is of great importance in several astrophysical contexts including: constraining the evolutionary paths of close binary systems; measuring cosmological parameters; understanding the chemical evolution of galaxies and the intergalactic medium; understanding the evolution of galactic winds; and interpreting the gravitational wave emissions from merging binaries. In spite of the great efforts over the last decades on both the theoretical and observational sides, the question about the nature of SN progenitors is still far from settled.

The measurements of SN rates for different stellar populations and their correlation with the properties of their parent galaxies provides an important tool to understanding the different types of SNe and their progenitors. Due to the short lifetime of progenitor stars, the rate of CC SNe directly traces the current star formation rate of the host galaxy. Additionally, the mass range for CC SNe progenitors can be probed by comparing the birth rate of stars and the rate of CC SNe occurring in the host galaxy, assuming the distribution of the masses with which stars are born follows the initial mass function.

On the other hand, the rate of SNe Ia echoes the whole star formation history of the host galaxy due to the time elapsed from the birth of the binary system to the final explosion, referred to as delay-time. Type Ia SNe are observed to explode both in young and old stellar populations and the age distribution of their progenitors is still a considerable matter of debate e.g., Maoz et al. (2014). The cosmic evolution of the volumetric SN Ia rate and the measurements of the SN Ia rate per unit mass in the less massive and younger galaxies suggest a distribution of the delay times that are less populated at long delay times than at short delays e.g., Cappellaro et al. (2015) and Botticella et al. (2017). By comparing the observed SNe Ia rate with what is expected for the star formation history of the parent stellar population, it is possible to constrain the progenitor scenario and the fraction of the binaries exploding as SNe Ia (Greggio 2005; Greggio & Cappellaro 2009; Greggio 2010). The success of the analysis of transient population demographics with respect to the stellar parent population depends on the selection of unbiased transient and galaxy samples, and a statistically significant number of transients.

The currently available surveys do not allow us to draw strong conclusions on the SN progenitor problem, due to both insufficient statistics and systematic effects. Primarily, this is related to the difficulty in determining the star formation history for the sample galaxies (Figures 23 and 24).

The Rubin LSST survey will provide a large number of events in galaxies with a large range of ages, strongly improving both the statistical uncertainty and the systematic uncertainty associated with the intrinsic properties of the parent stellar populations. Important constraints on the progenitors of

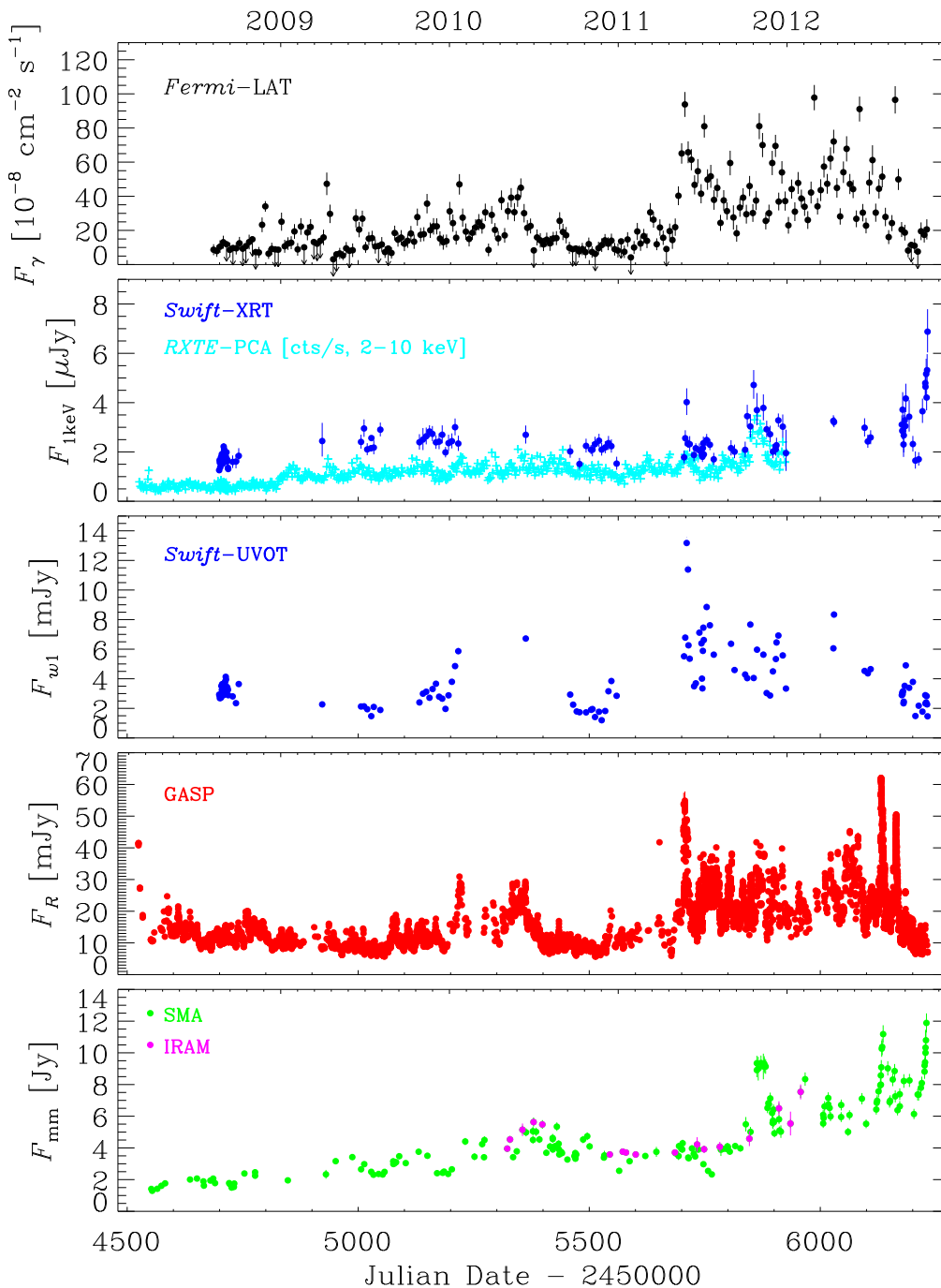


**Figure 22.** Multiwavelength light curves of BL Lacertae. From top to bottom showing data in  $\gamma$ -rays (data from the Fermi satellite), X-rays (data from the Swift and RXTE satellites), in the ultraviolet (data from the Swift satellite), in the optical (data from the GASP Project of the Whole Earth Blazar Telescope), and millimeter bands (bottom, data from the SMA and IRAM facilities). Adapted with permission from Raiteri et al. (2013). © Oxford University Press.

all SN types will be derived by studying the rates as a function of both the cosmic time and the parent galaxy properties including: mass, color, star formation rate and metallicity (see, e.g., Greggio & Cappellaro 2019).

Given the cosmic star formation rate and the star formation rate in a galaxy sample monitored for SNe using Rubin LSST, the trend of the SN Ia rate with redshift and with galaxy colors will be obtained. This will be used to derive information on the

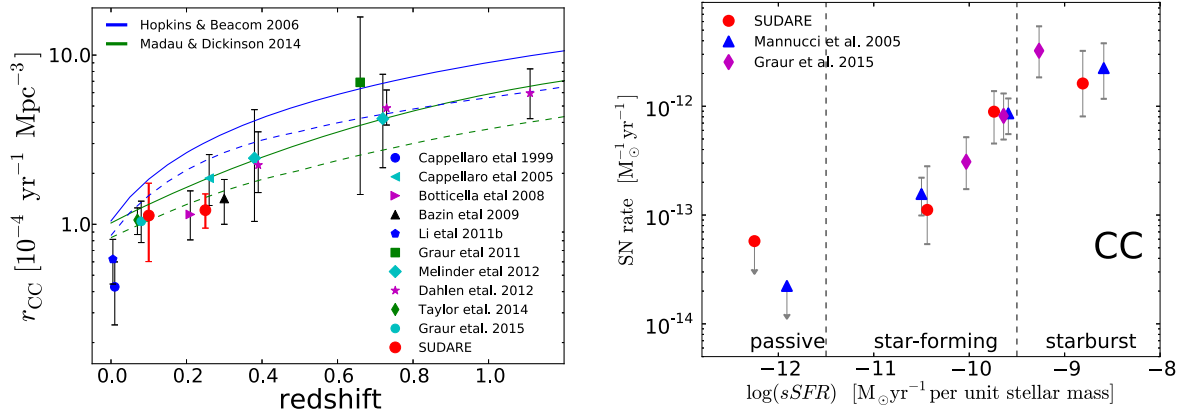


**Figure 23.** Left panel: Volumetric SN rates vs redshift for CC SNe. Reproduced with permission from Cappellaro et al. 2015 © The European Southern Observatory (ESO). The filled symbols show measurements from literature (with no correction for hidden SNe). Lines show the predicted CC SN rate from two different star formation histories (green for Madau & Dickinson 2014 and blue for Hopkins & Beacom 2006). Both adopt  $8 M_{\odot}$  and  $40 M_{\odot}$  as the lower and upper mass limits for CC SN progenitors. The dashed lines show the predicted SN rates assuming the fraction of hidden SNe given in Mattila et al. 2012. Right panel: SN rates per unit mass vs specific star formation rate (sSFR). The galaxies are grouped into three groups based on their specific star formation rate: the first group of passive galaxies with a zero mean star formation rate; the second group of galaxies with  $-12.0 < \log(sSFR) < -9.5$ ; the third group of galaxies with  $\log(sSFR) > -9.5$ . Reproduced with permission from Botticella et al. (2017). © The European Southern Observatory (ESO).

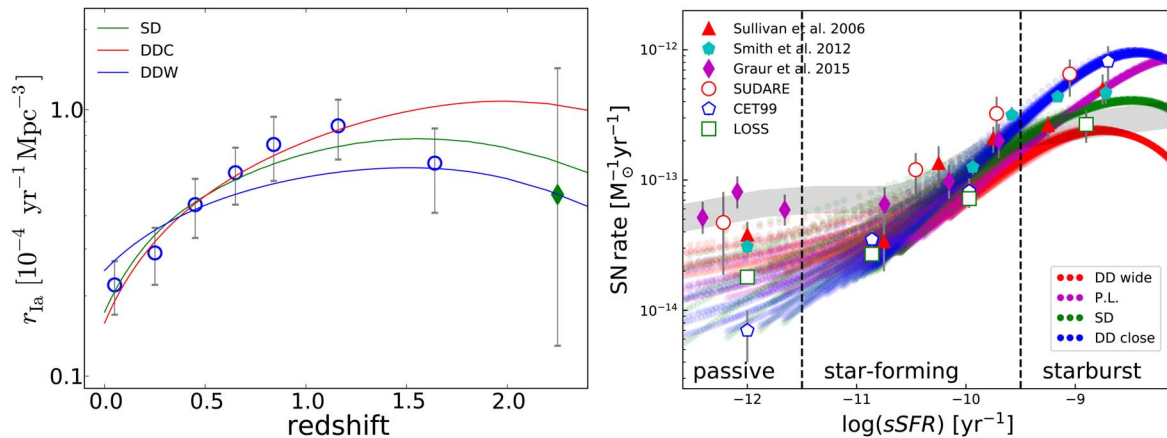


**Figure 24.** Left panel: volumetric SN rates as a function of redshift for SNe Ia from Cappellaro et al. (2015). The open circles depict the averages of all values found in the literature. The lines show the predicted rates as a function of redshift for three different Greggio models for single degenerates (SDs), double degenerates close (DDC) and double degenerates wide (DDW), assuming the Madau and Dickinson cosmic star formation history. Right panel: SN rates per unit mass vs specific star formation rate in three different groups of galaxies based on their specific star formation rates for CC SNe. Reproduced with permission from Greggio & Cappellaro (2019). © The European Southern Observatory (ESO). Filled circles show Greggio's models computed with a log-normal star formation history plotted with four different delay time distributions (colors as labeled). Open symbols show literature data (see legend in the top left corner). The gray stripe shows the result of the simulations from Graur et al. (2015).

distribution of the delay times and on the efficiency of SN Ia production from stellar populations.

The observed rate of CC SNe as a function of cosmic time and galaxy mass will allow us to check how well this rate traces the global star formation rate in the Universe, as derived from other measurements. The proportionality constant will yield information on the mass range of the CC SN progenitors (Cappellaro et al. 2015; Botticella et al. 2017). With the improved statistics from Rubin LSST, it will be possible to

constrain the mass ranges of the different CC SN subtypes, and derive the dependence on metallicity. The primary goals of our project are:

### 1. Low hanging fruit

#### (a) Understanding the evolutionary scenarios, light curve differences and progenitors for all SNe

For SN Ia's, this will involve constraining the evolutionary scenario for their progenitors and

understanding the origin of the diversity of SN Ia light curves. For CC SNe, this will involve constraining the mass range for the progenitors of the different CC SNe subtypes and searching for trends related to the properties of the parent galaxy e.g., metallicity.

The goals will be achieved by measuring the rates of the different SN types (Ia, Ib, Ic, IIP, IIL, IIn, SuperLuminous) as function of redshift for all types of galaxies and examining the dependence of these rates on the star formation history of the parent galaxy.

To measure unbiased SN rates we need: (1) to collect the light curves of all transients, (2) to identify the host galaxy for each transient (3) to obtain the photometric classification of each transient and the type for each SN, and (4) to estimate of the detection efficiency of the SN search as a function of the SN magnitude light curve morphology and as a function of the survey strategy.

We aim to exploit the data from the main Wide-Fast-Deep Survey to obtain the detailed rates for all the SN sub-types in the local Universe ( $z < 0.1$ ). The Deep Drilling Field surveys will enable the exploration of the evolution of the rate of SNe (both type Ia and CC) at high redshifts.

The project will progress incrementally. Preliminary results can be achieved after the first three years of the survey. The whole 10 yr lifetime of the survey is needed to reduce statistical errors on SN rates and to obtain a more accurate galaxy characterization.

## 2. Pie in the sky

### (a) Comparison of the SN rate measurements with theoretical predictions

Direct comparison will allow us to discriminate between different progenitor scenarios. The detailed analysis of the observed rates and of the host galaxies' properties will also help to shed light on the origin of the SN diversity.

### (b) Measure intrinsic SN properties and their evolution through time

With the increase in the number of known SNe at different redshifts, there is a new opportunity to model the intrinsic properties of SNe (e.g., decay rates and color) and their evolution through cosmic time. This will provide insights into SN progenitors and their diversity.

### (c) Obtain light curves of all SN types

A large number of light curves will become available for the various SN types, enriching the template database, especially for the rarest types. The analysis of the light curve properties for a sample of high statistical significance will enable studies aimed at understanding the origin of the SN diversity. With

this large database in hand, the accuracy of the photometric classification will improve. Especially given the opportunity to include rare events in the sample, and to produce well sampled templates for all SN types.

## Preparations for SN Science.

### 1. Follow-up observations/archival data

For the SN detection and typing we will rely entirely on Rubin LSST data. This study will be based on the accurate characterization of stellar populations in all galaxy types, which will be achieved through the detailed modeling of each galaxy's SEDs to estimate the galaxy colors, photometric redshifts and the star formation history. We aim to take full advantage of the Galaxies Science Collaboration determination of the photometric redshift and of the star formation history of the galaxies in the survey (see the Galaxies Science Collaboration Roadmap Robertson et al. 2017, for more information). Ancillary data on the latter, where available, may be used to better constrain the star formation history.

### 2. Facilities/software requirements

A pipeline needs to be developed to: deal with transient multi-band light curves; cross-match galaxy photometric redshift catalogs; and to combine different wavelength data from other surveys (e.g., Euclid). A method to associate transients with host galaxies, to classify transients and to determine the type of SNe will be required.

We will perform simulations to understand the anticipated SN occurrence rates. We will use current SN progenitor models and estimates of the galaxy mixture evolution with cosmic time to predict the number of SNe for the different survey strategies and their expected light curves. We will compute the expected SN rates up to  $z = 1$  to assess the trends of SN rates assuming different progenitor models. We will perform tests to assess the detectability of the various SN types in the galaxies populating the observed field. This will be done by inserting artificial SNe into images and light curves to evaluate both the detection efficiency and the classification efficiency. The simulation tools developed for Rubin LSST survey simulation are essential for this task.

## 4. Deep Drilling Fields Science Cases

### 4.1. Introduction

Complementing the regular cadence of the Wide-Fast-Deep wide-area survey, Rubin will pay significantly more visits to a small number of selected regions known as the Deep Drilling Fields (DDFs). These are small spatial regions, typically consisting of one to a few Rubin pointings, centered on areas of

**Table 4**  
The Deep Drilling Field Pointings Selected for Rubin LSST

	ELAIS S1	XMM-LSS	Extended Chandra Deep Field-South	COSMOS	Euclid <sup>a</sup> Deep Field-South
RA J2000.0	00 37 48	02 22 50	03 32 30	10 00 24	61 14 24
DEC J2000.0	−44 00 00	−04 45 00	−28 06 00	+02 10 55	−48 25 12
Galactic l [°]	311.30	171.20	224.07	236.83	256.060572
Galactic b [°]	−72.90	−58.77	−54.47	42.09	−47.17137
Ecliptic l [°]	346.68	31.74	40.99	151.40	36.49
Ecliptic b [°]	−43.18	−17.90	−45.47	−9.39	−66.60

**Note.**

<sup>a</sup> Proposed field, endorsed for selection in 2022. Barycentric True Ecliptic coordinates are quoted in each case, though the exact coordinates are to be finalized.

special scientific interest. The scientific goals of each DDF varies with location, but usually requires repeated imaging either to reach a fainter limiting magnitude and/or to achieve a high temporal cadence during the survey. The science motivations were presented in the 2018 Rubin survey cadence White Papers<sup>85</sup> and include: the discovery of Kuiper Belt objects; studying the origins of dark energy, galactic structure, large-scale structures and cosmology; and mapping the Magellanic system. The current set of selected DDFs is presented in Table 4. The original four selected DDFs were recently extended to include a proposed field covering the Euclid Deep Field South region (Guy et al. 2022), based on work by a joint Euclid-Rubin Working Group. In this section, we explore the benefits that these intensive observations will bring to time-domain science.

## 4.2. Extrinsic Transients and Variables

### 4.2.1. Transiting Exoplanets

An introduction to transiting exoplanets can be found in Section 3.3.1. As discussed in Section 4.1, the Deep Drilling Fields constitute a small fraction of the Rubin LSST survey. However, the Deep Drilling Fields will have a comparable cadence and number of observations to ground-based planet searches, which will enable the following science cases:

#### 1. Low hanging fruit

##### (a) Detect planets orbiting stellar populations not usually observed

Exoplanet transits will be detectable in the Deep Drilling Field light curves, as shown in Figure 25. The result is that, for these fields, the detection efficiency will be greater than for the wide-fast-deep fields. Consequently, the range of stars being searched will include populations not normally prioritized or accessible for most transiting planet searches, such as: very late type stars, white dwarfs, stars in the

galactic bulge, and cooler main sequence stars in clusters. This will enable Rubin LSST to provide insight into planet occurrence and formation rates around stars of varying masses, metallicities, and in different stages of stellar evolution.

### 4.2.2. Eclipsing Binary Stars

In Sections 2.3.2 and 3.3.2 we addressed the time-critical and the non-time-critical aspects of eclipsing binary science, respectively; here we discuss the impact of Deep Drilling Fields.

Naturally, as cadence increases, so does the sensitivity to time-variable phenomena on shorter timescales. Figure 26 depicts 4 TESS light curves sampled in Rubin LSST's Deep Drilling Field cadence, depending on their location. Fluxes are normalized and offset for better visibility; no actual color effects have been taken into account, only cadence sampling. While it is clear that the increased cadence helps a lot (cf., top panel), it can still fall short of full phase coverage for longer period systems (cf., third panel). The 20k plus visits are a significant improvement on the ~800 visits of the main survey, but spread over 10 years still implies fewer than 6 observations per night (on average), distributed across the 6 passbands.

#### 1. Low hanging fruit

##### (a) Extending the completeness to longer orbital periods

While the diurnal cycle certainly prevents us from reaching true completeness for short period systems, an increased number of visits over the same baseline will significantly improve the detection of longer-period systems. A ~20× increase in the number of visits will increase the phase coverage (barring the diurnal cycle) by the same factor; of course, the longer the orbital periods, the narrower the eclipses, which works to limit the benefits of the increased number of visits. Because of this interplay, we expect the detection sensitivity to increase from orbital periods

<sup>85</sup> <https://www.lsst.org/submitted-whitepaper-2018>

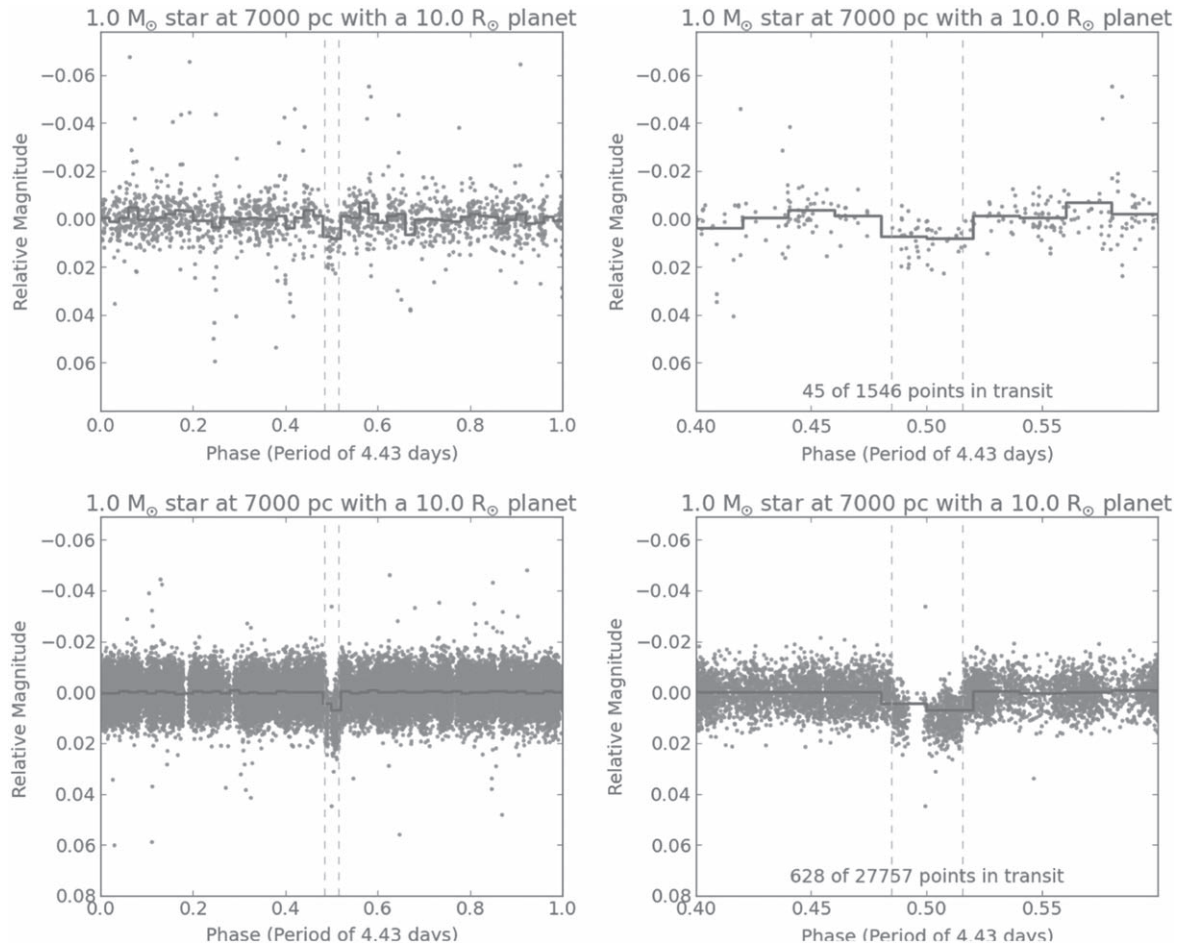


**Figure 25.** Light curve for a  $10 R_{\oplus}$  planet in a 4.43 days orbit around a  $1.0 M_{\odot}$  star at 7000 pc. The top two plots show a regular Rubin LSST field and the bottom two plots show a Rubin LSST Deep Drilling Field. The plots on the left show the full phase, and the plots on the right zoom in on the transit. Black lines are binned data of the light curve. Reproduced from Lund et al. (2015). © IOP Publishing Ltd. All rights reserved.

of  $\sim 2.5$  days of the main survey to about 10 days for Deep Drilling Fields (Kirk et al. 2016).

(b) **Increased sensitivity to intrinsic phenomena**

In addition to extending the orbital period sensitivity, increased cadence will enable observations of intrinsic time-variable phenomena such as spots, pulsations and other surface prominences, extrinsic phenomena such as extraneous body interactions (stars, circumbinary planets), and component interactions such as mass transfer or mass loss. Of course, we should maintain realistic expectations: the cadence of the Deep Drilling Fields do not provide the same orbital coverage as Kepler or TESS.

2. Pie in the sky

(a) **Increase in precision for all eclipsing binary science cases**

We will be able to undertake all analyses mentioned in Section 3.3.2, but to a higher

precision—thanks to the increased cadence. The number of eclipsing systems in Deep Drilling Fields will of course be vastly smaller than from the main survey, but it will give us an opportunity to assess the amount of information loss due to limited cadence.

### 4.3. Intrinsic Galactic and Local Universe Transients and Variables

#### 4.3.1. Pulsating Stars

The measurement of stellar pulsations enables the study of stellar interior structures and the determination of global stellar properties as described in Section 3.4.1. Deep Drilling Fields will deliver additional science results as the observations will be obtained with different observing strategies. In the Deep Drilling Fields, the location and strength of aliases and the

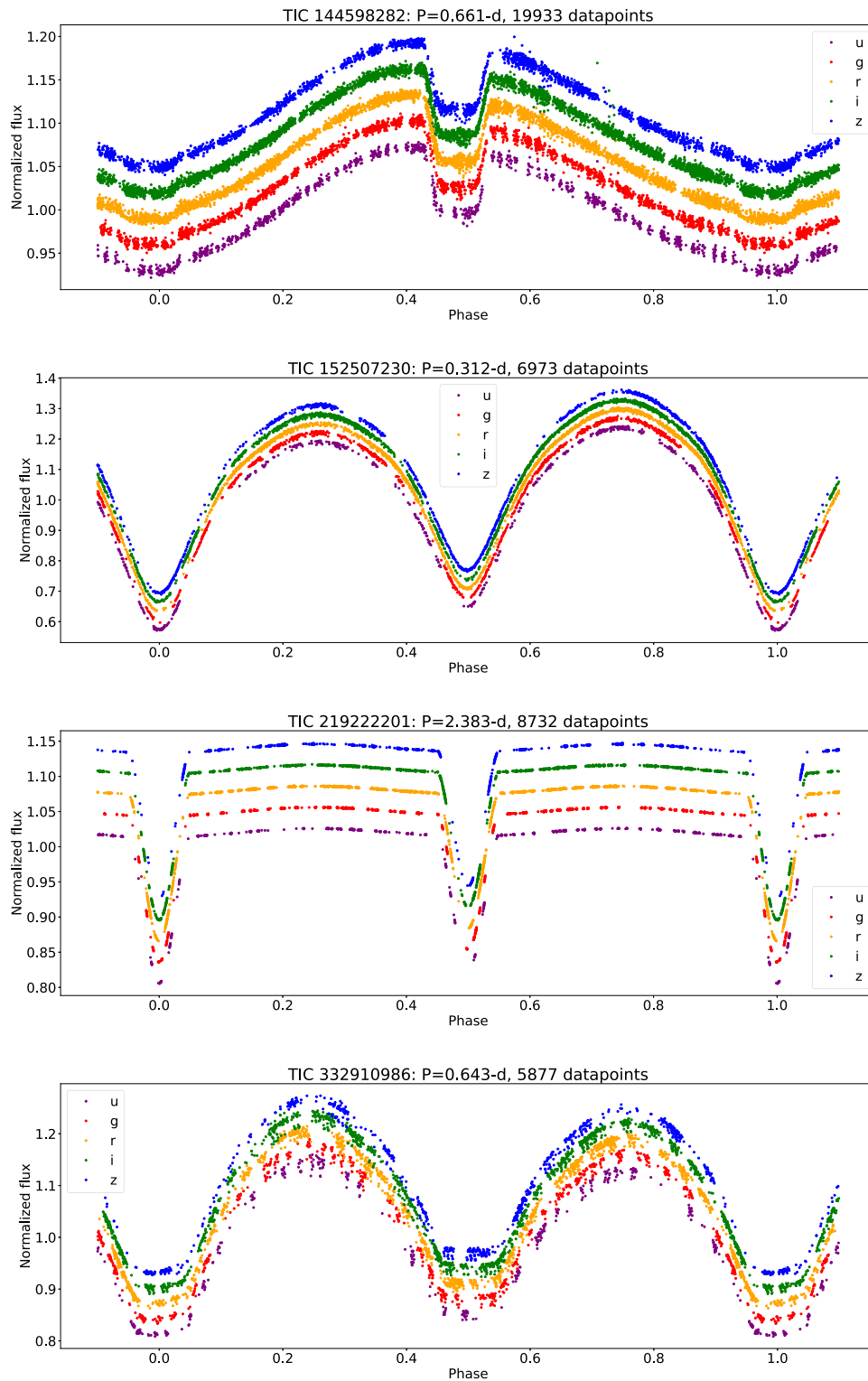


**Figure 26.** Simulated Deep Drilling Field light curves of eclipsing binaries, top to bottom: TIC 144598282, TIC 152507230, TIC 219222201 and TIC 332910986. Individual passbands are offset for clarity.



signal detection threshold will be different (and often better) than for the main survey.

A detailed introduction to pulsating stars science cases can be found in Section 3.4.1. Here we discuss pulsating star science in the Deep Drilling Fields.

## 1. Low hanging fruit

### (a) Observations of short-period/multi-periodic pulsators

If the Deep Drilling Field observations are carried out at a higher (possibly continuous Bell & Hermes 2018) cadence, accurate period solutions could be obtained for many shorter-period and multi-periodic variables (including  $\delta$  Scuti stars and  $\gamma$  Dor stars, to name a few). Astroseismic analysis could potentially constrain the internal structures of these objects. Further, these well characterized variables could provide a reliable sample for training machine learning models to classify variables in the main survey.

For the purpose of asteroseismology, radial velocity follow-up observations will provide a more detailed look into the pulsational nature of the objects and will allow for thorough pulsational modeling. The required spectroscopy must be of high resolution with high cadence (to obtain several spectra per pulsational cycle). This becomes significantly more difficult for higher frequency pulsations, as shorter exposures are required and thus the largest telescopes will be needed to reach the faint magnitude limits of Rubin LSST. For known pulsating stars in the field, spectroscopic observations can begin prior to the commencement of the survey observations.

## 2. Pie in the sky

### (a) Observations of the RR Lyrae Blazhko effect

The properties of RR Lyrae stars, including their period, color, period variations, and the detection of modulations in their light curves may be visible in the Deep Drilling Fields. The Blazhko effect is the cyclical period and amplitude modulation of RR Lyrae pulsations. Given the large-area and depth of the Deep Drilling Fields, we expect to obtain statistics on the occurrence rate of Blazhko modulations, which would be highly beneficial, since their origin is still heavily debated. The identification of multi-mode pulsations (RRd, double- and triple-mode Cepheids) will also be relatively easy in the Deep Drilling Fields. Additionally, other dynamical phenomena (like period doubling) may be observable depending on the selected cadence.

### (b) Pulsating stars in binary systems

The discovery of Cepheids and RR Lyrae stars in binary or even eclipsing systems would be of

particular importance to derive their masses and radii, and other physical parameters. The chance of finding them is low, especially for RR Lyrae stars because of binary evolutionary constraints, but the potential gain is high. To obtain the fundamental parameters from such objects, follow-up spectroscopy would be required so that the radial velocities of the stellar components could be determined.

### (c) The asteroseismology of red giant stars

Red giant stars are stochastic pulsators. They pulsate with periods on the order of days to hours. Studies will have to evaluate how reliably the global seismic parameters  $\nu_{\max}$  (frequency of maximum oscillation power) and  $\delta\nu$  (large separation between radial overtones) can be determined given the aliasing caused by sparse and structured observing times.

The Rubin LSST color measurements of red giants will provide temperatures which are necessary for the determination of radii and masses from the use of scaling relations. By considering red giants from several mini-surveys, population studies of red giants can be performed, including the consideration of their fundamental parameters. An assessment of the scaling relations as a function of location and thus metallicity can also be performed. If this is possible, it will require the complete data acquisition period because of the need for a long observational baseline. With a 10 yr baseline, it may be possible to detect solar-like oscillators that have frequencies of maximum oscillation power lower than those detected by the Kepler satellite.

Studying the aliasing caused by the observational window function of different survey strategies will inform the realistic limitations for asteroseismology in these better studied fields. Ideally, the Deep Drilling Fields will be designed to minimize aliasing. Specifically, the timing of future field visits could be based on past field visits to strategically reduce aliases (Bell et al. 2018).

Information on adopted Deep Drilling Field strategies will enable more specific preparation for science results and the associated tools and resources that they will require. The classification will commence with the first data release and will continue incrementally as the data are released. Infrastructure to store and host a pulsating star catalog is required. Furthermore, the creation of an online catalog to provide the data to the community in a user-friendly format is desirable.

### 4.3.2. Brown Dwarfs

The possibilities for brown dwarf science are similar to those for the main survey, as stated in Section 3.4.5. However, the higher cadence for Deep Drilling Fields will allow us to better characterize the photometric variabilities in brown dwarfs.

## 1. Low hanging fruit

(a) **Analysis of the evolution of weather on brown dwarfs**

High-cadence long-term observations of brown dwarfs will help us to probe the atmosphere dynamics over several brown dwarf rotation periods, detect long term weather evolution Hitchcock et al. (2020) and possible planetary wave patterns Apai et al. (2021). See Section 3.4.5 for more details.

## 2. Pie in the sky

(a) **Observe extremely short scale variability in brown dwarfs**

This science case is outline in Section 3.4.5. However, studying possible short-term variability effects including lightning and auroral activities may be achievable with the Deep Drilling Field high-cadence data.

(b) **Identification of transiting planets around brown dwarfs**

A favorable alignment between a potential planetary orbit and the observer's line of sight could also cause a periodic transit-shaped signal in the brown dwarf host star (details on transiting planets can be found in Section 3.3.1). This is more likely to be observed in the Deep Drilling Fields due to the (anticipated) higher cadence and larger number of observations.

In Section 3.4.5 we have outlined the possible telescope and computational resources, which will be helpful for studying variabilities in brown dwarfs.

4.3.3. *Compact Binaries: AM CVn and Ultracompact Binaries*

Ultra-compact binary systems have orbital periods less than  $\sim 80$  minutes, which implies they have non-main sequence degenerate or semi-degenerate secondaries. Although ultra-compact binary systems are predicted to have a high Galactic spatial density (e.g., Nelemans et al. 2001, 2004), there are only  $\sim 60$  of these systems currently known (Ramsay et al. 2018), with periods ranging from 5 to 65 minutes. It is therefore not clear if the models seriously over estimate their number, or if many more systems await discovery. The Zwicky Transient Facility has so far discovered several new ultra-compact binary systems (Coughlin et al. 2020). Rubin LSST Deep Drilling Fields with sufficient cadence (ideally 15 s), would result in the discovery of many new examples and therefore constrain their spatial density. Rubin LSST Deep Drilling Fields will enable the following science for compact binaries:

## 1. Low Hanging fruit

(a) **Testing binary evolution models and the common envelope phase**

This will be performed through the comparison of

the observed population with common envelope phase evolution models (e.g., Nelemans & Tout 2005). This will require a large homogeneous sample, as only Rubin LSST can provide, and will allow a more complete determination of their chemical compositions, masses, and orbital variability. These parameters are critical inputs to test theoretical predictions, such as temperatures and disk instability properties, (e.g., Deloye et al. 2005; Bildsten et al. 2006).

(b) **Discovering all of the ultra-compact binary systems in the solar neighborhood**

With a significant number of ultra-compact binary systems, we will determine their orbital periods and space densities, which is crucial for developing algorithms for detecting sources in LISA data. Ultra-compact binary systems and short period detached white dwarf binaries are predicted to be the dominant source of low frequency (mHz) persistent gravitational wave sources detectable by the new space-based gravitational wave observatories of the future, such as LISA (Stroeer & Vecchio 2006). The significance of ultra-compact binary systems is highlighted in the LISA science case.<sup>86</sup>

Many identified ultra-compact binary systems will have very short orbital periods ( $\sim 10$  minutes), and are typically very faint ( $g > 21$ ). Depending on the cadence, they may be detectable in the Rubin LSST Deep Drilling Fields, where observations of  $\sim 1$  hour or more with a 10–30 s cadence in a single filter would lead to the detection of eclipses or orbital modulations. Rubin LSST, with its huge etendue and ability to undertake high cadence observations continuously for up to several hours, will be crucial in discovering faint ultra-compact binary systems, including short period ( $< 80$  minutes) detached binaries with white dwarfs. There is no doubt that Rubin LSST will succeed in detecting these intrinsically faint objects. As an example, the Faint Sky Variability Survey undertaken with the Wide Field Camera on the 2.5-m Isaac Newton Telescope, was easily sensitive to variations on timescales of 10 minutes and longer (Groot et al. 2003).

4.3.4. *Compact Binaries: Neutron Star Binaries*

Deep Drilling Fields in the context of low mass X-ray binaries, milli-second pulsars and transitional milli-second pulsars will work similarly to the Rubin LSST main survey, although the cadence, filter choice and sequence will be different. Hence, DDF data could produce additional alerts (see Time Critical Science Section 2.4.3) and, more importantly, higher cadence light curves in multiple colors (see non-Time-Critical Science Section 3.4.8). Here we detail the science that

<sup>86</sup> <https://www.elisascience.org/articles/lisa-mission/gravitational-universe-science-case-lisa/ultra-compact-binaries-milky-way>

we hope to achieve given the higher cadence of the Deep Drilling Fields.

#### 1. Low hanging fruit

##### (a) **Perform period analysis for known and newly discovered accreting neutron stars**

The higher cadence foreseen for Deep Drilling Fields will enable complementary science/analysis with respect to the Rubin LSST main survey. In particular, they will allow period searches to be performed (especially for the orbital periods) of the monitored systems, once a sufficient number of data points have been acquired.

##### (b) **A census of accreting neutron stars in crowded fields**

The different stellar environments explored by the Deep Drilling Field surveys will enable the comparison of multiple accreting neutron star populations, which will provide insight into how they are affected by their environment (including star density and metallicity).

##### (c) **Change of states and outburst alerts:**

Alerts from Deep Drilling Field surveys are, in principle, possible and will enable us to trigger follow-up observations for accreting neutron star binaries. We plan to focus on neutron star binaries in states that allow us to probe the binary parameters and/or physical mechanisms responsible for their observed phenomenology. The combination of spectroscopy and high-cadence Deep Drilling Field light curves will enable a more detailed analysis of these exotic objects.

#### 4.3.5. *Intermediate Luminosity Optical Transients*

For a general introduction about Intermediate Luminosity Optical Transients (ILOTs), see Section 2.5.2. In the investigation of the physical mechanisms responsible for the different types of ILOTs, detection of the earliest stages of an outburst is priceless. This is especially true because ILOTs differ from each other in the early development of their light curves and theoretical models predict different light curve morphologies, depending on the progenitor. In view of their higher cadence, Deep Drilling Fields should offer better monitoring than that of the main Rubin LSST survey. For the case of extra-galactic Deep Drilling Fields, ILOTs will be too faint to allow for proper follow-up. Specifically, Deep Drilling Fields focused on the Galactic Plane and nearby galaxies in the Local Universe will allow us to characterize ILOT variability with good cadence and to a higher precision than that provided by the main survey. This may also enable the analysis of shorter duration variability (e.g., that produced by erratic stellar flares) and quasi-periodic variability due to close binary interactions, possibly associated with the ILOT's progenitor.

#### 1. Low hanging fruit

##### (a) **The discovery of ILOTs in their early phases**

Deep Drilling Fields will enable the discovery of ILOTs at very early phases. A higher, multi-band cadence allows us to characterize the stellar variability, and (including the data obtained with the main survey) constrain the variability history and nature of the progenitor system. This strategy allowed the OGLE survey to detect the famous red nova V1309 Sco, which was determined to be a stellar merger event (Mason et al. 2010; Tytenda et al. 2011).

#### 2. Pie in the sky

##### (a) **The search for luminous red nova precursor candidates**

The photometric monitoring of new and/or known contact binaries will allow us to find new luminous red nova precursor candidates (e.g., the claimed KIC 9832227; Molnar et al. 2017). The identification of binary systems that show a photometric period decline with time can indicate inspiraling motions, which can lead to a common envelope ejection. The common envelope may rearrange the geometry of the stellar system or cause the two stars to merge. The monitoring of such stellar systems would require a cadence of one exposure every several hours.

##### (b) **The identification of smaller-amplitude/shorter timescale variability**

High-precision photometry of bright objects is crucial to identify lower-contrast modulations superimposed on the well-known larger variability of luminous blue variables. This is a key step to observing luminous blue variables with binary companions.

##### (c) **Observations of fast evolving transients**

High-cadence observations reveal fast-evolving transients, which could include new species of ILOTs and faint, fast-evolving SNe. In particular, studying the rapid photometric evolution of some types of ILOTs (e.g., putative SNe impostors or intermediate luminosity red transients) during the very early phases may reveal shock-breakout signatures, which may enable us to unequivocally discriminate terminal (faint) SN explosions from non-terminal outbursts.

#### 4.4. *Intrinsic/Extrinsic Extragalactic Transients*

##### 4.4.1. *Blazars*

With their denser sampling, Deep Drilling Fields would allow us to study blazar variability in more detail, in particular at shorter time scales than the Main Survey. As discussed in Raiteri et al. (2022), we may expect that Rubin LSST will observe about 150 blazars in the six planned Deep Drilling Fields (see Figure 27).

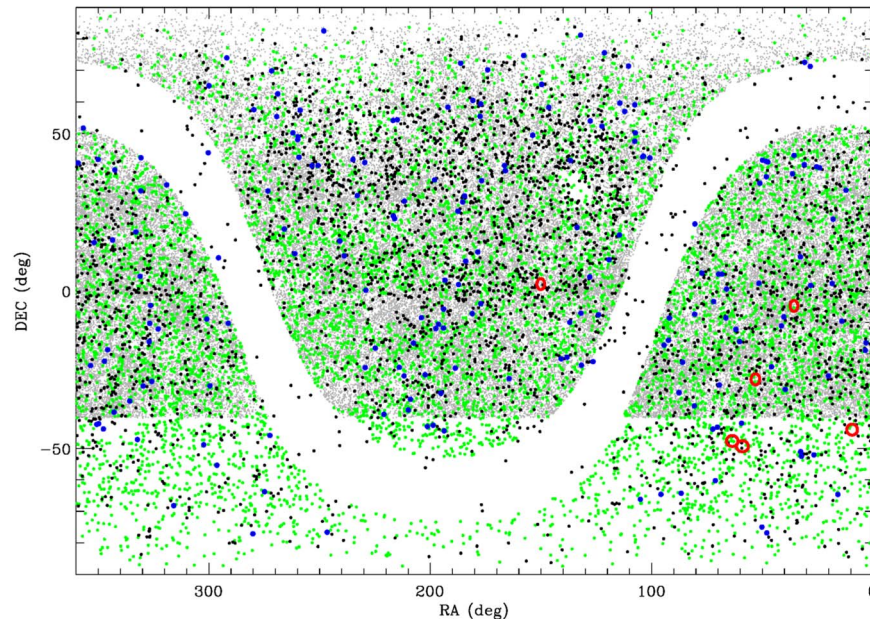


**Figure 27.** The distribution of blazars in the sky according to the BZCAT5 (black symbols), BROS (gray), and CRATES (green) blazar catalogs. Blue circles mark the BZCAT5 objects whose  $R$ -band catalog magnitude is brighter than 15.5 and can thus be affected by saturation problems. Red lines represent the planned Deep Drilling Fields. From North to South: COSMOS, XMM-LSS, EDFS, ELAIS S1, and the double field EDFS. Reproduced from Raiteri et al. 2022. CC BY 4.0.

The majority of them will likely be detectable with single exposures. These sources will constitute a small golden sample, whose monitoring will be highly valuable, especially if multiband intra-night observations are performed to follow flux and spectral variability on hour-long time scales.

#### 1. Low hanging fruit

##### (a) Analyse the fast variability of blazars

Variability at higher cadences can reveal different emission mechanisms with respect to those that are seen on longer time scales. Fast variability is a distinctive signature of the non-thermal jet emission contribution, and is likely due to intrinsic, energetic processes. On longer time scales, we may see the result of changes in the jet orientation (see Section 2.5.4). Moreover, in flat-spectrum radio quasars (FSRQs), time scales of the order of weeks to months also characterize the variability due to the thermal nuclear emission, which is due to the quasar core (e.g., Raiteri et al. 2019).

#### 2. Pie in the sky

##### (a) Push the study of the environment of the blazar host galaxies to higher redshifts

As mentioned in Section 3.5.1, deeper and deeper photometry is required as we proceed to higher redshifts. This will be provided by the Deep Drilling Fields. Moreover, the Deep Drilling Field observations will increase the environment richness at low

redshifts, through a better sampling of the faintest galaxies.

Precursor optical monitoring of Deep Drilling Fields would improve detection of unknown sources (including blazars, but also active galactic nuclei in general) based on variability at the beginning of the survey, creating a longer monitoring baseline. Moreover, it would extend the timeline for blazar variability studies and further, enable earlier diagnostic testing for blazar identification.

## 5. Minisurvey and Microsurvey Science Cases

### 5.1. Introduction

The third category of survey strategy proposed for Rubin LSST is “minisurveys” and “microsurveys.” These represent proposals for novel survey strategies of small regions, though typically larger than that of a Deep Drilling Field, and often located outside the main Wide-Fast-Deep footprint. The survey cadence and filter selection for these surveys is (commonly) specific to the science case that motivated it, as described in 2018 survey strategy White Papers,<sup>87</sup> and in the following sections. The majority of these strategies are referred to as “microsurveys,” as they require a relatively small telescope time commitment (<3% of total survey time) to generate a significant scientific return. However, numerous White Paper authors presented scientific motivations for increasing the

<sup>87</sup> <https://www.lsst.org/submitted-whitepaper-2018>

number of visits Rubin dedicates to the Galactic Plane (Gonzalez et al. 2018; Lund et al. 2018a, 2018b; Prisinzano et al. 2018; Strader et al. 2018; Street et al. 2018b) relative to the original implementation. The survey regions and cadence strategies proposed by these authors overlapped sufficiently well to motivate the exploration of a common strategy for the time-series monitoring of a significant area in the Galactic Plane. As this region will serve a range of science goals, it is referred to as a “minisurvey.” Additional minisurveys include the North Ecliptic Spur and the Southern Celestial Pole. Currently, the minisurveys proposed have either similar cadence to the main survey (Ecliptic Spur) or 5 times fewer observations with respect to the main survey (Galactic Plane and Southern Ecliptic Pole). In this section, we describe the science anticipated from each category of survey.

## 5.2. Extrinsic Transients and Variables

### 5.2.1. Microlensing

A general introduction to microlensing can be found in the time-critical section, Section 2.3.1 and in the non-time critical section, Section 3.3.3. Here we discuss microlensing science in the minisurveys.

One of our most powerful tools for understanding planetary formation is to compare the actual planet population with that predicted by simulations, but there remain important gaps in our planet census. Low-mass planets in orbits between  $\sim 1\text{--}10$  au are of particular interest, because the core accretion mechanism predicts a population of icy bodies (e.g., Ida et al. 2013) in this region. Evolutionary models further predict that gravitational interactions between migrating protoplanets should result in some being ejected from their systems (Chatterjee et al. 2008; Mustill et al. 2015). However, this parameter space coincides with a gap in the sensitivity of the planet-hunting techniques used to date, leading to it being sparsely sampled. Microlensing offers a way to test both of these predictions, being capable of detecting planets down to  $\sim 0.1 M_{\oplus}$  at orbital separations of  $\sim 1\text{--}10$  au. It is also capable of detecting free-floating planets that have been ejected from their parent star systems. The effectiveness of this technique has now been demonstrated by the discovery of three candidate free-floating planet events (Mróz et al. 2018).

#### 1. Low hanging fruit

##### (a) Exoplanets in the Bulge

A survey of the Galactic Bulge region, where the rate of microlensing events is highest, is one of the main goals of NASA’s Roman Space Telescope (previously WFIRST) Mission (Spergel et al. 2015). The spacecraft will discover  $\sim 1400$  bound planets and will provide a dataset that is ideal for detecting free-floating planets (Penny et al. 2019). The physical properties of bound planets can be constrained

through the direct measurement of the light from the lensing system, but this technique cannot be applied for free-floating planets. Unfortunately, microlensing models suffer from a number of degeneracies and the physical properties of the lens are extremely hard to measure without the additional constraint of the event parallax. For long timescale events ( $>30$  days) this can be derived from a single light curve (thanks to the orbital motion of the observer) but Roman data alone cannot measure the parallax for short timescale ( $t_E \leq 30$  days) events. Thanks to the  $\sim 0.01$  au separation between Rubin and Roman (at L2), the observatories will measure different magnifications and times of maximum, enabling us to derive the physical and dynamical properties of short timescale events.

Rubin LSST will substantially improve constraints on the lens properties, specifically the free-floating planet mass function, distances and kinematics, by performing regular multi-band imaging of the Roman survey of the Bulge region during the periods when the field is visible to both Rubin and Roman observatories simultaneously. By continuing to monitor the Bulge during the multi-month gaps in the Roman survey, Rubin LSST will also complete event light curves that remain partially sampled by Roman. Roman will observe  $i \sim 19\text{--}25$  mag stars in the Bulge for a total of  $\sim 432$  days spread over 6 ‘seasons’. But the spacecraft can only monitor the field for  $\sim 72$  days at a time, due to pointing constraints. Since microlensing events can peak at any time, and have durations  $t_E \sim 1\text{--}100$  days, many Roman light curves will be incompletely sampled. This will make it difficult to measure the parallax (and hence physical properties) for long timescale events, and raises the probability that anomalous features (and lens companions) will be missed in the inter-season gaps.

Originally, the Roman Galactic Exoplanet Survey region was proposed as a Deep Drilling Field in a 2018 white paper. While this was not selected, it was later incorporated into a minisurvey that covers the Galactic Plane and Magellanic Clouds. To prepare for this science, it will be necessary to cross-match all Rubin LSST Difference Imaging Analysis Sources with the Roman catalog. This will require access to the full Difference Imaging Analysis Source catalogs for an extremely star-rich field; Penny et al. (2019) predicts that Roman will detect  $\sim 240 \times 10^6$  stars with  $W149 < 25$  mag—and thus this substantial task will necessarily be accomplished within the Rubin Science Platform.<sup>88</sup> For brighter objects, it will be advantageous to cross-match against additional

<sup>88</sup> <https://data.lsst.cloud>

catalogs, including the OGLE Variable Star catalogs (e.g., Soszyński et al. 2018, 2019), and the VISTA Variables in the Vía Lactea (VVV) Survey (Medina et al. 2019) as well as the Gaia catalog, where available. The combination of optical and near infrared photometry will enable us to determine the spectral types of source stars, estimate their distances, and in some cases place constraints on blending. The astrometric information will also help to constrain microlensing models.

Although NASA are developing a pipeline for Roman that will independently detect microlensing events within that dataset, it is highly desirable to combine the full timeseries photometry for all stars detected by both Roman and Rubin LSST within this minisurvey. Since Rubin LSST will fill in the gaps in Roman’s light curves, this combined analysis is likely to reveal additional events, to substantially improve the classification of all other events and to detect previously-unseen anomalies. Since this will require the combination of two very substantial data sets, this analysis is likely to take place within the Rubin LSST Science Platform and/or a NASA Archive. The resulting data products will then be used to select subsets of events for more detailed analysis, which could be done either within the Rubin Science Platform or at the researcher’s home institution.

### 5.2.2. Eclipsing Binary Stars

The impact of minisurveys on eclipsing binary science is unlikely to be fundamentally different from the main survey: minisurveys feature a different cadence to reach their respective science goals, but that does not mean deeper/more visits. While the details of the impact will depend on the minisurvey at hand, the main driver for EB science remains overall cadence. If there is no appreciable increase in field visits, science yield will be similar to that of the main survey discussed in Section 3.3.2.

#### 1. Pie in the sky

##### (a) Binary stars in the Magellanic Clouds

The Magellanic Clouds have been a target of many variability studies, so we have a healthy set of (mostly early-type) eclipsing binaries known to date. The main power of Rubin LSST LMC/SMC minisurvey will be to follow-up and calibrate those systems. We can certainly expect color calibration and, in turn, improved spectral type/luminosity class determinations. Additionally, for binaries that undergo changes to light curve shapes and times of arrival compared to archival data will be visible.

### 5.2.3. Interstellar Scintillation Toward the Magellanic Clouds

Stars twinkle because their light propagates through the Earth’s turbulent atmosphere. Approximately one percent of this light modulation is also expected to happen on timescales

of a few minute when remote stars are observed through an interstellar turbulent cloud (although, it has never been observed at optical wavelengths). The timescales of the weak optical intensity fluctuations resulting from the wave distortions induced by a turbulent medium (visible nebulae or hidden molecular gas) are only now accessible to the current technology. Rubin LSST is the ideal setup to search for this signature of gas, thanks to the fast readout, and the wide and deep field. As a first result, the detection of such a signal would provide a new tool to measure the inhomogeneities and the dynamics of nebulae. Our long term objective is to search for *cold transparent* molecular  $H_2$  *dust-free* clouds, which are the last possible candidates for the missing baryons (Pfenniger et al. 1994; Pfenniger & Revaz 2005) representing  $\sim 50\%$  of the Milky Way baryons (McGaugh et al. 2009).

We propose to take a long series of consecutive images of the same field toward the LMC or SMC during two nights through the “moving mode.” This “micro-survey” could be done during the commissioning of the camera, but does not need all the mechanical functionalities of the telescope mount, since the telescope should point in the same direction during each full night.

It has been suggested that the hierarchical structure of cold  $H_2$  could fill the Galactic thick disk (Pfenniger et al. 1994) or halo, providing a solution for the Galactic dark matter problem. This gas should form transparent (dust-free) “clumpuscles” of 10 au size, with a column density of  $10^{24}$ – $10^{25}$   $\text{cm}^{-2}$ , and a surface filling factor smaller than 1%. Such clumpuscles are not directly observable since they do not emit or absorb light, but only increase the total optical path of the light by 5–50 cm; as a consequence, the diffractive and refractive scintillation caused by their turbulence—similarly to the well known radio scintillation—is the only way to detect them.

Figure 28 shows how refraction through an inhomogeneous transparent cloud produces irregular illumination on Earth (Moniez 2003; Habibi et al. 2010). The turbulence strength of the refractive medium is quantified by the diffraction radius  $R_{\text{diff}}(\lambda)$ , defined as the transverse separation for which the route-mean-square of the phase difference is 1 radian at  $\lambda$ . Assuming that the cloud turbulence is isotropic and is described by the Kolmogorov theory up to the largest cloud’s scale  $L_z$ ,  $R_{\text{diff}}$  can be expressed as:

$$R_{\text{diff}}(\lambda) = 263 \text{ km} \times \left[ \frac{\lambda}{1 \mu \text{ m}} \right]^{\frac{6}{5}} \times \left[ \frac{L_z}{10 \text{ au}} \right]^{-\frac{1}{5}} \left[ \frac{\sigma_{3n}}{10^9 \text{ cm}^{-3}} \right]^{-\frac{6}{5}}, \quad (5)$$

where  $\sigma_{3n}$  is the cloud’s molecular number density dispersion. Here, we assume that the cloud is a mix of 76% of  $H_2$  and 24% of He by mass. The refractive medium, located at distance  $z_0$  from Earth, and moving with transverse velocity  $V_T$  relative to

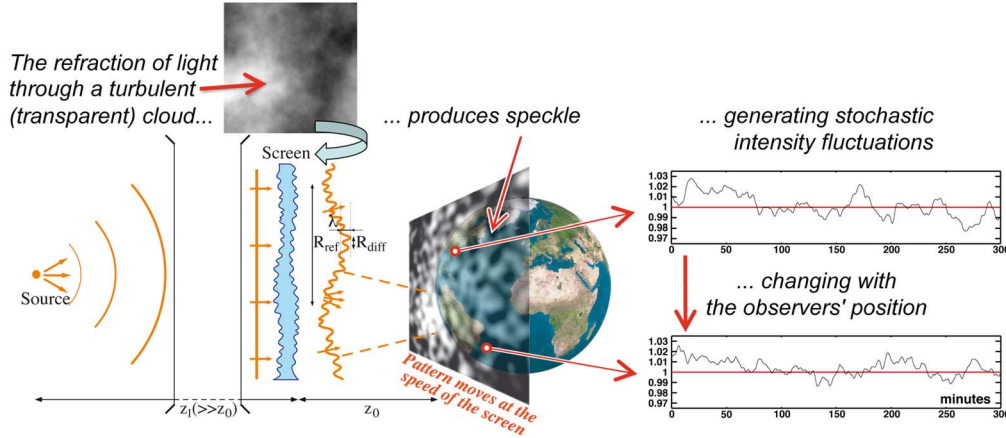


**Figure 28.** Upper region: A simulation of a 2D stochastic phase delay (gray scale) caused by a column of gas affected by Kolmogorov-type turbulence. Lower region: The propagation of light from a stellar source (left) after crossing the cloud (represented as a phase screen) and the resulting illumination pattern on Earth. The distorted wave front produces structures on the scale of:  $R_{\text{ref}} = 3086 \text{ km} \times [\lambda/1\mu \text{ m}][z_0/100 \text{ pc}][R_{\text{diff}}/1000 \text{ km}]^{-1}$ . As a consequence, two telescopes separated by a few thousand kilometers are differently illuminated at a given time. These structures sweep the Earth at the transverse speed of the screen (typically a few tens of  $\text{km s}^{-1}$ ), producing uncorrelated illumination fluctuations over time scales of minutes. The configuration simulated here corresponds to a scintillating star that is half the size of the Sun, located 1 kpc away, as seen through a turbulent cloud. The cloud is 160 pc from Earth with a diffraction radius of  $R_{\text{diff}} = 1000 \text{ km}$  and a translation velocity of  $V_T \sim 17 \text{ km s}^{-1}$  (with respect to the line of sight). The two telescopes are separated by 10,000 km (the GEMINI telescopes are separated by a linear distance of 9430 km).

the line of sight, is responsible for the stochastic intensity fluctuations of the light received from the star at the typical characteristic timescale of a few minutes, scaling as:

$$t_{\text{ref}}(\lambda) = 5.2 \text{ min} \left[ \frac{\lambda}{1\mu \text{ m}} \right] \left[ \frac{z_0}{100 \text{ pc}} \right] \times \left[ \frac{R_{\text{diff}}(\lambda)}{1000 \text{ km}} \right]^{-1} \left[ \frac{V_T}{10 \text{ km s}^{-1}} \right]^{-1}, \quad (6)$$

with a typical intensity modulation index  $m_{\text{scint.}} = \sigma_I / \langle I \rangle$  of a few percent, limited by the source's spatial coherence, thus decreasing when the angular stellar radius ( $\theta_r$ ) increases, according to:

$$m_{\text{scint.}} = 0.05 \left[ \frac{\lambda}{1\mu \text{ m}} \right] \left[ \frac{z_0}{100 \text{ pc}} \right]^{-1/6} \left[ \frac{R_{\text{diff}}(\lambda)}{1000 \text{ km}} \right]^{-5/6} \times \left[ \frac{\theta_r}{\theta(\text{Sun at 10kpc})} \right]^{-7/6}. \quad (7)$$

Since the illumination that is observed on Earth depends on the position (see the right panel of Figure 28), we expect variations of the observed light curves from two telescopes to decorrelate when their distance increases. This signature—incompatible with an intrinsic source variability—points to a propagation effect.

One should notice that the signal cannot be confused with atmospheric scintillation or atmospheric absorption fluctuations. Atmospheric scintillation induces fast point-spread function variations concurrent with negligible intensity variations within a large aperture (Dravins et al. 1997a, 1997b, 1998). Atmospheric absorption fluctuations can be precisely taken into

account in the analysis, by the simultaneous monitoring of all stars in the field.

## 1. Low hanging fruit

### (a) Searching for scintillation signals

Using Rubin LSST (either with a neutral filter, to provide the maximum amount of light or with the  $g$ -band filter), two observing runs of a few hours toward a given direction (LMC or SMC to benefit from the wide field), taking series of 15 s consecutive exposures, will produce a few tens of millions of light curves with 1–2 thousand measurements each. This would satisfy the requested, high sampling rate of  $\sim 3$  per minute and the requested photometric precision of better than 1% for stars with  $M_V = 20.5$ , which is necessary for this science case. Such a harvest of data would enable an efficient search for scintillation signals down to an optical depth of  $\sim 10^{-6}$ .

If no scintillation is discovered, a strong upper limit of the molecular gas contribution to the Galactic mass will be established (following the analysis of Habibi et al. 2010). If a scintillation signal is suspected, it could be confirmed during the second night of observations (which do not need to be consecutive). Moreover, if a trigger is available at the time of observations (based on simple peak-to-peak variation threshold), complementary observations could be simultaneously done with remote telescopes, allowing the decorrelation of the stochastic fluctuations between distant locations to be assessed. If

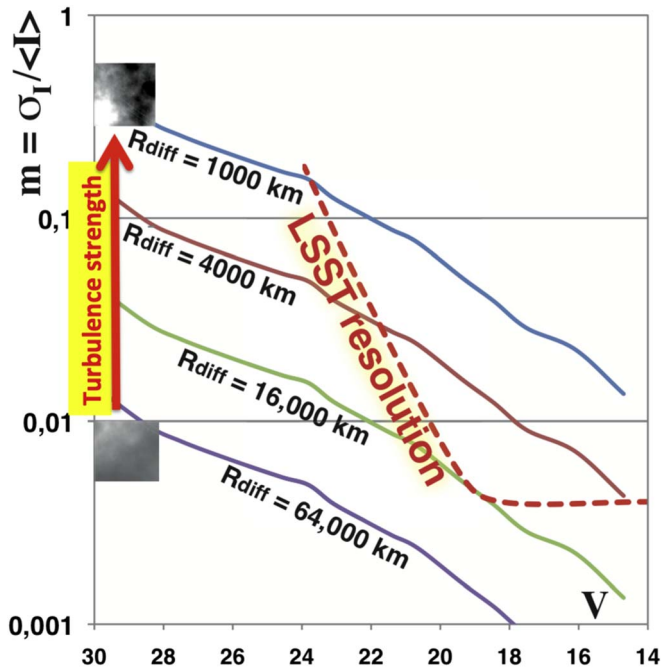


**Figure 29.** The expected modulation index  $m$  in  $I$ -band, as a function of the source’s apparent magnitude  $V$ , for four different turbulence strength parameters  $R_{\text{diff}}$  (smaller  $R_{\text{diff}}$  corresponds to stronger turbulence). The screen is at  $z_0 = 1\text{Kpc}$  (typical for an invisible halo clump) and the source is in the Large Magellanic Cloud. The instrumental photometric precision (dashed line) is taken from the Rubin LSST science book (Abell et al. 2009). We see that observations with a precision of a few percent are already sensitive to a medium that has relatively low strength turbulence, characterized by ( $R_{\text{diff}} < 16,000$  km). Such turbulence should induce scintillation that is detectable for stars with  $16 < V < 22$ .

enough twinkling stars are discovered, we will aim to measure the decrease of the modulation index as the size of the source increases could, enabling a check of the properties of the scintillation process.

Figure 29 shows the configurations (source magnitude and turbulence strength, expressed in  $R_{\text{diff}}$ ) that should produce detectable scintillation with Rubin LSST observations (upper-right region). The ultimate sensitivity corresponds to  $R_{\text{diff}} \sim 16,000$  km, which is typically associated to a medium with density fluctuations as low as  $2 \times 10^7 \text{cm}^{-3}$ .

The database of observations that will be produced by the proposed “movie mode” will certainly be useful for many other science subjects, including: the search for planetary transits; the detailed study of eclipsing binaries (e.g., to refine the knowledge of the LMC distance, Muraveva et al. 2014); the search for hidden, very low mass compact objects using microlensing; and for observations of caustic crossing microlensing events, if observations are coordinated with microlensing networks.

### 5.3. Intrinsic Galactic and Local Universe Transients and Variables

#### 5.3.1. RR Lyrae Stars

Despite all the efforts so far, we still lack a clear knowledge of the old stellar population in the Galactic Inner Bulge, mainly because of strong reddening. Observations of RR Lyrae stars in the Galactic Inner Bulge promise to improve our knowledge of this highly populated region. RR Lyrae stars are well-known pulsating stars that form a representative sample of the old stellar population. They are further sound standard candles, since they follow well-defined near-infrared period–luminosity relations. As standard candles, in the GAIA DR3 era, they can provide individual distances with an accuracy better than 3%. Moreover, they follow reddening-free Wescheneit functions, which enable accurate distance determination in environments affected by strong and/or differential reddening. With these tools, we can measure the density profile of the old population, the 3D structure of the bulge and of the bar, and obtain fundamental observables to constrain the Milky Way formation models. The use of the  $i$ -,  $z$ - and  $y$ -band measurements, together with  $J$ -,  $H$ - and  $K$ -band measurements from the VVV (VISTA Variables in the Via Láctea) survey, will enable the determination of new individual estimates for distance, reddening and metallicity.

#### 1. Low hanging fruit

##### (a) The determination of individual distances for RR Lyrae stars in the Galactic Bulge

As in Section 3.4.2, we plan to obtain distances to the RR Lyrae stars in the Galactic Bulge. As an additional objective, we will also determine distances to SX Phe and Anomalous Cepheid stars. The crowding in the bulge will require the extraction of accurate photometry from point sources. While Rubin LSST will provide differential photometry of the bulge as a data product, for this project, point-spread function (PSF) photometry will be necessary.

#### 2. Pie in the sky

##### (a) The comparison of results with theory

The collected database of individual distances, and reddening and metallicity estimates for RR Lyrae stars in the Galactic Inner Bulge will allow us to: (1) Put constraints on the 3D model and density profile of the old population in the Inner Galactic Bulge and (2) Compare the derived profiles with the results from other stellar population tracers (red clump stars, etc.), and with the theoretical models that describe the formation of the Bulge.

The effective detection and robust characterization of the aforementioned pulsating variables will be essential to understanding the old population of stars in the bulge. To obtain



these goals, we plan to use variability criteria that have been widely tested in the literature, most of them being implemented in the VaST software (<http://scan.sai.msu.ru/vast/>). This software is freely available, and it does not have special hardware requirements or software dependencies. The required characterization involves the evaluation of all the relevant pulsational properties of the candidate variables, including: periods, mean magnitudes and amplitudes. The characterization of the candidate variables will be accomplished with two different approaches: during the first year, when only a few data points per source are available, the characterization will be performed by comparing the observations with available templates. When at least 15–20 data points are available, the evaluation can be performed directly on the observed data, with well tested methods.

As previously mentioned, we will only require Rubin LSST data for our scientific goals. However, where possible, cross-matching our objects with Gaia (for the positions, proper motions and parallaxes), OGLE-IV (for the classification and very-long term characterization) and VVV (for the near-infrared measurements) will provide useful, complementary information.

### 5.3.2. Brown Dwarfs

A general introduction to brown-dwarf science can be found in Section 3.4.5. Already, during the commissioning phase, several test surveys will be conducted to assess the performance of the Vera Rubin Observatory and all its systems. Those test surveys are designed to simulate 10 and 20 years of survey operations within a few months. To do this, a small region of the sky will be observed with high cadence, which will provide an excellent data set to study the variability of brown dwarfs. An additional minisurvey has been submitted that proposes to observe fields that overlap with those that will be observed by the Roman Space Telescope (aka WFIRST). Further, Deep Drilling Fields are usually sparse fields that do not contain a large number of brown dwarfs. Choosing crowded fields, e.g., in the Galactic Plane, for mini/microsurveys will allow us to probe those denser regions for brown dwarfs.

#### 1. Pie in the sky

##### (a) Probe the space density and sub-stellar mass function in crowded fields

We hope to extend and improve our understanding of the initial mass function for brown dwarfs in dense regions. These regions have been avoided in the past due to crowding and increased confusion with other objects, e.g., ‘O’-rich and ‘C’-rich long-period variables; asymptotic giant branch stars; distant, highly-reddened luminous early-type main-sequence/giant branch stars; and Young Stellar Objects. Therefore, only few limited searches for

brown dwarfs in the galactic plane have been conducted (see, e.g., Phan-Bao et al. 2003; Reid 2003; Folkes et al. 2012). While the minisurvey of the galactic plane will have a reduced number of observations with respect to the main survey ( $\sim 1/5$ ), we hope to obtain a first glimpse of brown dwarf science through these observations.

In Section 3.4.5 we have outlined the possible telescope and computational resources that would be helpful for studying variabilities in brown dwarfs. The main Wide-Fast-Deep Survey will provide additional information on proper motion and parallaxes, which will help us to place our objects on the color–magnitude diagram and improve their spectral type characterization.

### 5.3.3. Variables Stars

The Magellanic Clouds contain a large range of variables and transients, all at the same distance, with low extinction and low metallicity. Thus, the minisurvey of the Clouds provides the ability to collect a large statistical sample of both known and unknown variability types. To obtain light curves covering the full range of periodic variability from 30 s to 10 yr, as well as transient and eruptive objects, would require a diverse range of observations. These would range from continuous, 15-s exposures in a single filter (to catch short period variables such as  $\delta$  Scuti stars and pulsating white dwarfs) to multiple (30–300) visits in the  $g$ -,  $r$ - and  $i$ -band filters, depending on the type of variable, and to catch transient or eruptive variables. Current simulations of the proposed cadence include a minisurvey of the Large Magellanic Cloud and Small Magellanic Cloud with five times fewer observations than the main survey. However, a microsurvey has been proposed to observe 10 local volume galaxies in a higher cadence in  $g$ -band. It has been recommended by the Survey Cadence Optimization Committee that the cadence for the minisurveys and microsurveys should be finalized during the first year of operations. As some variables will benefit from multiwavelength (X-ray, ultraviolet, infrared) observations, the dates of Rubin LSST observations of the Clouds should be advertised to facilitate simultaneous or contemporaneous observations of the Rubin LSST fields. During the first survey year, most of the short period (periodic) variables will likely be discovered (given a high-enough cadence for the variability type). At three years, there will start to be enough data to identify new, long-period variables. By the end of the survey, we should have a complete list of variability in the Clouds.

#### 1. Low hanging fruit

##### (a) Fully characterize variable stars in the Magellanic Clouds

A much higher cadence of observations, with respect to the main survey, in  $g$ -band and/or  $r$ -band filters will enable us to observe variable objects with

periods between 15 s and 3 days that are missed in the main survey.

(b) **Absolute magnitude limited period determination of all variables in the Clouds**

We plan to determine accurate periods for all regularly variable objects down to an approximate absolute magnitude of 6.5 (assuming a limit for variability of apparent magnitude of 25).

(c) **Study the effect of metallicity on novae occurrences**

We plan to analyze novae observations in the Magellanic Clouds to determine how the differences in metallicity affect the rate and location of novae. We will do this by comparing novae in the Magellanic Clouds with those in the Milky Way.

(d) **Search for the progenitors of SN Ia**

Recurrent novae are the best candidates for SN Ia progenitors. Through the observation of known and new novae, we will determine the number of short period recurrent novae, which we will compare with expected numbers for SNe.

2. Pie in the sky

(a) **Analyze all non-periodic variables in the Clouds**

By identifying non-periodic variables in the Magellanic Clouds, we will be able to probe the cause of their variability. This will require machine-learning to characterize known variables and theoretical work to understand the variability mechanisms for previously unknown types of variables.

### 5.3.4. Compact Binaries: Neutron Star Binaries

Minisurveys will support and serve our studies of binary neutron stars, specifically: low-mass X-ray binaries, milli-second pulsars and transitional milli-second pulsars. This will be identical to the main Rubin LSST Survey and Deep Drilling Fields but for different patches of sky. Importantly, the minisurvey of the Galactic Bulge and Magellanic Clouds will probe different stellar environments compared to the Rubin LSST Main Survey and the Deep Drilling Fields (see Sections 2.4.3, 3.4.8 and 4.3.4). The smaller total number of visits foreseen for the minisurveys, will however produce more sparsely sampled light curves and less timely alerts.

1. Low hanging fruit

(a) **Change of states and outbursts alerts**

Alerts from a minisurvey are in principle possible. These alerts can trigger follow-up observations of accreting neutron star binaries. For follow-up observations, we plan to focus on neutron star binaries that enter a state where we can probe the binary parameters and/or physical mechanisms that are responsible for the observed phenomenology. The proposed science case is identical to that described in

earlier neutron star binary sections, however, will probe a different region of the sky.

### 5.3.5. Intermediate Luminosity Optical Transients

In the investigation of the physical mechanisms responsible for the different types of intermediate luminosity optical transients (ILOTs), detection of the earliest stages of an outburst is priceless. Especially because subclasses of ILOTs differ from each other in the early development of their light curves and theoretical models predict different light curves depending on the progenitor. Hence, microsurveys that have a higher cadence than the main survey will enable a detailed investigation into the various ILOT progenitors. Unfortunately, Deep Drilling Fields (with the highest Rubin LSST cadence) will monitor variability in the distant Universe, where ILOTs are too dim for follow-up observations. Instead, the higher-cadence observations of some proposed microsurveys will provide an important tool to study nearby ILOTs. Specifically, if the microsurveys of individual galaxies and the Local Universe have higher cadence than the main survey, this will allow us to characterize the ILOT variability with the option for follow-up observations. This may also enable constraints to be placed both shorter duration variability that is produced by erratic stellar flares and (quasi)-periodic variability that is caused by close binary interaction, possibly associated with the ILOTs' progenitors.

1. Low hanging fruit

(a) **ILOTs observed in their early phases**

As with the Deep Drilling Field observations, high-cadence microsurveys that targeting the Local Universe, Large and Small Magellanic Clouds, and crowded fields in the Milky Way can discover ILOTs during their very early phases.

(b) **Determination of occurrence rates**

Reliable rate estimates for the different ILOT types are still incomplete, or have not been established. With the minisurveys of the Galactic Bulge and Local Group, we aim to precisely constrain the frequency with which the different families of transients occur different environments (in particular, Milky Way, SMC, LMC and M31).

2. Pie in the sky

(a) **Understanding luminous blue variable companions**

As with the Deep Drilling Fields, dedicated microsurveys of nearby galaxies (within 30 Mpc), with a higher cadence, can will enable the identification of lower-contrast modulations that are superimposed on the well-known larger variability of luminous blue variables. This is a key step to constraining the presence of the binary companions of luminous blue variables.

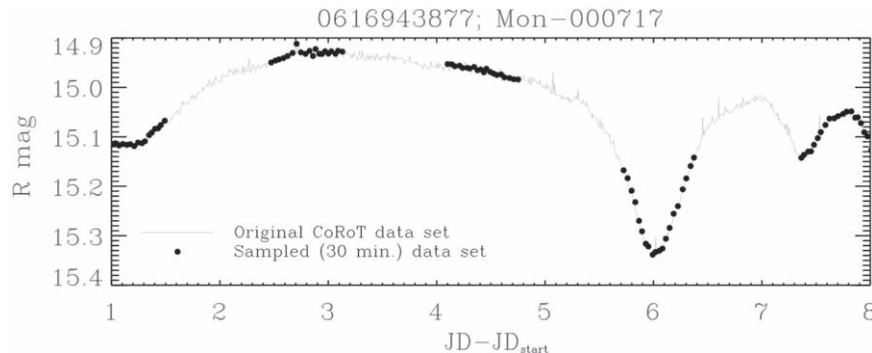


**Figure 30.** The CoRoT light curve of a young star showing short-term variability, manifested as a flux dip due to the presence of a warped inner disk (see also McGinnis et al. 2015). Black dots mark the 10 hr nightly observing periods over a total of 7 days with 30 minutes cadence (as discussed in the text). Reproduced with permission from Bonito et al. (2018).

### 5.3.6. Young Stellar Objects

For an introduction to young stars, particularly EXor and FUor stars, see Section 2.4.1. Here we discuss young stars in the context of minisurveys and micros surveys. We aim to investigate stellar variability of single objects or statistically in stellar clusters. We plan to analyze the variability induced by several mechanisms, including stellar activity, the disk accretion process (which can also occur in eruptive bursts, e.g., FUors and EXors), and rotation. Our goals include identifying specific regions in the sky, selecting suitable targets, and determining the appropriate cadence to pursue the study of variability for young stars in general. We plan to take advantage of data collected in existing surveys and previous programs (e.g., the Gaia-ESO Survey and Chandra) to characterize interesting fields and objects, also using a multi-wavelength approach. Indeed, stellar variability is a panchromatic phenomenon, with distinctive features on all timescales from hours to years (e.g., Fischer et al. 2022). While long-term variability can be optimally traced with the Wide-Fast-Deep approach, studies of shorter-term variability, driven by inner disk dynamics, will benefit from a denser cadence, which will also enable the exploration of the impact of different properties, e.g., ages, metallicity, and environment. The Galactic Plane, and in particular, select star-forming regions, should therefore be investigated with a cadence higher than that of the main survey to follow the variability of stars on short time scales (hours and days; see Figure 30). Analysis of available data from previous surveys, as well as the development of diagnostic tools, will be undertaken to lay the groundwork for the proposed science cases.

#### 1. Low hanging fruit

##### (a) Analyzing short term variability in young stellar objects

Photometric variability, on short timescales (hours), mid-length timescales (days to months), and

long timescales (years), is part of the definition of classical T Tauri stars (Joy 1945). Young stellar objects are characterized by photometric variability caused by several distinct physical processes: mass accretion events from circumstellar disks; the presence of warps in envelopes and disks; the creation of new knots in stellar jets; stellar rotation; starspots; magnetic cycles; and flares. We can study all these phenomena if we acquire both short-term and long-term light curves of a statistically significant sample of young stellar objects. The analysis of “static” color-magnitude diagrams in Rubin LSST filters, such as  $r$  versus  $g - r$  or  $r$  versus  $u - r$ , will allow us to identify weak-line T Tauri stars (non-accreting) within the observed clusters. Although, the bulk of classical T Tauri star members are typically spread out at bluer colors than the cluster sequence traced by weak-line T Tauri stars, which is a result of the short-wavelength color excess related to the accretion activity that is only present in classical T Tauri stars (e.g., Venuti et al. 2014). For this reason, it is important that the selected fields be observed in both bluer and redder bands so that we are able to discriminate between weak-line T Tauri stars and classical T Tauri stars.

We have data from previous programs, such as DECam observations of Carina at the CTIO 4-m, that reached depths similar to those expected for Rubin LSST. We will also take advantage of data collected in existing surveys and data from previous programs (for instance, many team members are involved in the Gaia-ESO Survey, Chandra, etc.) to characterize fields and objects of interest, using a multi-wavelength approach. Minisurveys or micros surveys that overlap with these cluster observations will provide an in-depth look at young stars in clusters, as well as a significantly extended the baseline over which the

inner disk processes can be tracked and characterized.

For those stars identified as young stars, classifications based on photometric colors can be confirmed spectroscopically with, for example, FLAMES observations of the H  $\alpha$  emission line (see also Bonito et al. 2013, 2020).

## 2. Pie in the sky

### (a) Dense coverage of star-forming regions

As mentioned above, young stars exhibit short-term photometric variability caused by mass accretion events from: circumstellar disks; the presence of dusty warps within the inner disks; heterogeneous starspot coverage across the stellar surface; and flares. Some of these processes (e.g., accretion bursts and stellar flares) develop on timescales as short as a few hours (e.g., Stauffer et al. 2014; Cody et al. 2017; Getman & Feigelson 2021), while others exhibit characteristic timescales of variability comparable to the stellar rotation rates ( $\lesssim 7$  days; e.g., Venuti et al. 2017, 2021). Therefore, adopting a denser observing cadence (e.g., one datapoint every 30 minutes each night for one week per year) in star-forming regions is necessary to follow the evolution of each process and clarify the nature of short-term variability for thousands of young stars. This would complement the long-term observations that will be accumulated over the course of the Main Survey. More details can be found in (Bonito et al. 2018; Bonito et al. 2023; Prisinzano et al. 2023).

This approach will allow us to relate the observed variability to stellar properties, such as mass, age, binarity, and to environmental properties such as location within or exterior to the H II region, and to the presence or absence of an av circumstellar disk. Large samples are needed to quantify how the various physical processes depend upon stellar properties, environmental conditions, and the evolutionary stages of the stars. Rubin LSST will allow us to survey an extensive collection of star-forming regions in the Southern hemisphere: the closest low-mass populations, the intermediate-mass populations, and massive (like Carina) star formation regions. Therefore, in our white paper, we proposed to target one major star-forming region every year. We plan to start with observations of the Carina Nebula, which is well-placed for observations from Chile with Rubin LSST, and guarantees a large number of sources (11,000 members identified; Townsley et al. 2011).

Different causes of variability (e.g., stellar flares, accretion bursts, absorption due to warped disks, rotational modulation due to spots) can be discriminated on the basis of their significantly differing observational characteristics. A dense coverage of star

formation regions with Rubin LSST will allow us to characterize different classes of light curves (see Figure 1 of Bonito et al. 2018), including light curves dominated by accretion bursts (Stauffer et al. 2014), or periodic or quasi-periodic flux dips (associated with rotating inner disk warps partly occulting the stellar photosphere; see, e.g., Bouvier et al. 2007; Alencar et al. 2010).

As young stars with variability undergo significant and rapid color changes owing to both accretion processes and extinction variations, it is important to include multiple filters in any dense coverage campaign, e.g., *g*-, *r*-, and *i*-bands. Data in each band (changing every 30 minutes between *g*-, *r*-, and *i*-filters, and possibly also the *u*-band) will provide their own light curves, making it possible to follow how the stellar colors vary with phase: 140 photometric points in each filter (corresponding to a 30-minute observing cadence implemented for one week, assuming 10 hr long observing nights) should be collected in order to populate the phases well enough. Variability in different colors helps to discriminate between hot spots, cold spots, and circumstellar extinction (e.g., Venuti et al. 2015). Flaring in weak-line T Tauri stars can also be monitored, though the rapid decline of chromospheric flares requires a rapid cadence to capture the necessary details. Monitoring the accretion events will be pivotal to trigger an alert to observe the same objects with other instruments and in different bands (from X-rays to infrared wavelengths).

At the beginning of Rubin LSST operations, we argue that a targeted test field (Carina Nebula) should be observed in the above manner to illustrate what can be done with Rubin LSST in this mode. In subsequent years, we would then either choose a different region or possibly return to the same regions to monitor slow changes in periods or amplitudes that may arise from differential rotation or starspot cycles. Combining a densely-packed short-interval dataset with a sparse but long-baseline study maximizes the scientific return for both methods, and allows Rubin LSST to address all of the accretion and rotational variability associated with young stars, and to bridge the knowledge gap between short-term and long-term behaviors documented for young stellar objects.

The analysis of variability in young stellar objects described here will be based on Rubin LSST data, but for a complete description of these complex systems (consisting of a central young star, the surrounding disk, the accretion streams, the jets, and the shocks formed at the stellar surface and at the intersection with the ambient medium) it will be crucial to also

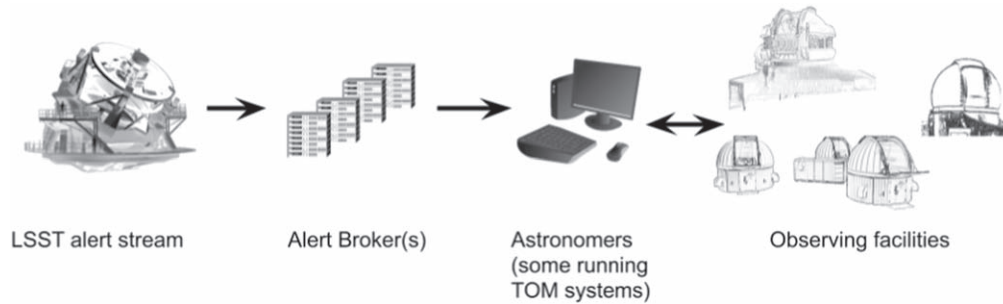


**Figure 31.** Overview of the Rubin LSST follow-up ecosystem; the chain of services and facilities necessary for Rubin LSST discoveries to be: categorized, selected for further study and for additional characterization observations to be made, where necessary.

take advantage of additional data from existing surveys (e.g., the Gaia-ESO Survey) or through synergies with new observations and surveys (e.g., with 4MOST, WEAVE and eROSITA).

In particular, spectroscopic follow-up data will be used to investigate variable young stellar objects showing accretion/ejection activity. FLAMES, 4MOST, WEAVE, eROSITA and SoXS are a few examples of facilities that we plan to use for follow-up and additional new observations.

Detailed 3D magnetohydrodynamic (MHD) models of the infalling material have been developed to investigate the accretion processes in young stars. These models account also for the observed variability in the inverse P-Cygni line profiles as we view accretion streams along the line of sight to the star (Kurosawa & Romanova 2013; Bonito et al. 2014; Revet et al. 2017). Models suggest an accretion cooling timescales of 30 minutes to several hours, in accordance with observations of the shortest bursts in BP Tau (0.6 hr; see discussion in Siwak et al. 2018).

This study will additionally require the development of software dedicated to the analysis of variability related to accretion/ejection activity in young stellar objects. In more detail, this software will be necessary to characterize the light curves, discriminate the physical processes behind the light curves and further to investigate the color–magnitude diagrams to distinguish classical T Tauri stars from weak-line T Tauri stars. This will be developed in collaboration with the Italian National Institute of Astrophysics—Observatory of Palermo and the team already working on this topic of young stellar objects and young clusters.

Our current hardware resources are not suited to handle the Rubin LSST data volume. Therefore, updated computational resources are required to keep up with the increased data-flow rate (already seen with Gaia).

With its unprecedented sensitivity, spatial coverage, and observing cadence, Rubin LSST will allow us to employ a statistical approach for the first time to achieve a comprehensive view of the process of star formation.

## 6. Methodology and Infrastructure

### 6.1. Infrastructure Required for Time-Critical Science

The promise that we will discover new transient phenomena occurring on short timescales has motivated a rapid response to fully characterize the objects in question, while we have the chance. In some cases, the window of opportunity for follow-up observations may be  $<1$  day. This drives the most stringent technical demands of any program following-up on Rubin LSST discoveries, particularly since the high data volume and data rate produced by Rubin LSST effectively mandates a reliance on software infrastructure at all stages. In this section, the requirements that these science use-cases will place on all astronomical facilities involved are examined within the context of the infrastructure presented in Figure 31.

#### 6.1.1. Rubin LSST Prompt Data Products and Alert Stream

An informal survey of TVS members was used to gauge the maximum tolerable delay between new alerts being produced by the Rubin LSST Data Management system and the alert information being made available to the community (responses are presented in Figure 32). 30% of respondents preferred to have access to that information within 1 hr of alert production, while 75% indicated a maximum delay of 24 hr. The primary scientific drivers behind this requirement were the follow-up of gravitational wave detections and early-time SNe.

It is expected that the Rubin LSST Data Management system will meet this requirement by producing real-time photometry and alerts for every image within  $\sim 1$  minutes of shutter-close. Current designs for the alert handling infrastructure will immediately serve the alert data publicly in the form of a Kafka event stream.

#### 6.1.2. Rubin LSST Alert Brokers

Owing to the high data rate and volume of the full Rubin LSST alert stream (approximately 10 million alerts per night), it is not envisioned that individual science users will subscribe to it directly, but rather that it will be sent to several

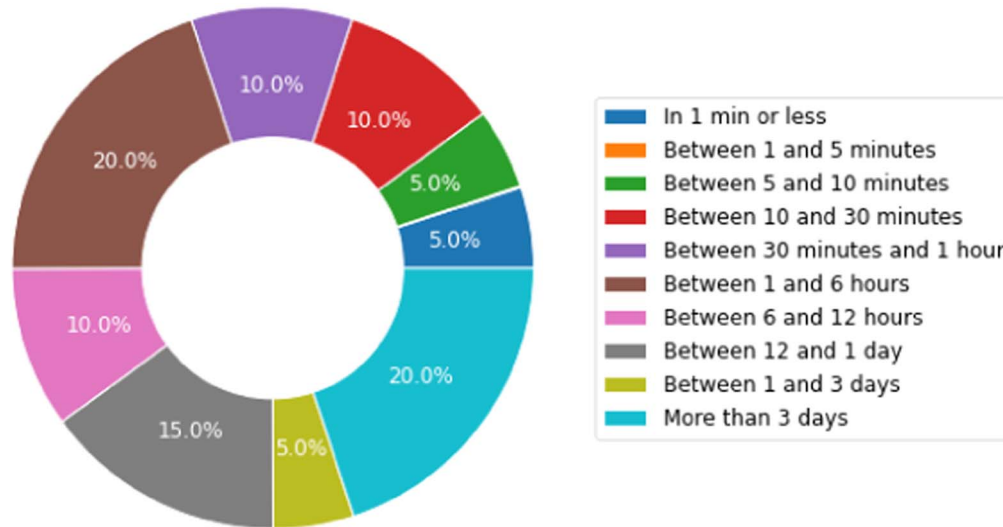


**Figure 32.** The breakdown of TVS scientists' responses to the question: "What is the maximum time delay tolerable between new alerts being produced by the Rubin LSST data reduction and the alert information becoming available through a broker service?" In this context "tolerable" means that you would still be able to complete your scientific goals.

Community Brokers. These services are expected to collate the available alert data and serve it to their communities online. Brokers also provide value-added services, for example, they might aggregate data from multiple survey alert streams and existing data catalogs, and they also may attempt to classify the alerts by astrophysical type. Some also provide additional science-specific modeling such as orbit-linking for solar system objects.

Due to the anticipated high bandwidth of the Rubin Observatory alert stream, only a limited number of brokers will receive the alert stream directly from Rubin Observatory. In May 2019, the broker selection process was started with Letters of Intent (LOI) submitted from 15 teams, after which, in August 2019, the Science Advisory Committee (SAC)<sup>89</sup> announced that all LOI teams were encouraged to submit full proposals. From the nine full proposals submitted by December 2020, the SAC recommended that seven brokers should receive direct access to the full alert stream, with the remaining two brokers acting as downstream brokers, getting their input stream from another broker.

Currently, these brokers are under development, being tested on the alert stream delivered by ZTF (Patterson et al. 2019). Also, for testing purposes, an archive of ZTF alerts is available from the University of Washington.

To facilitate the development of the brokers, the alert broker teams held a two-part virtual workshop, which consisted of two LSST Corporation (LSSTC) Enabling Science Broker

Workshops, one in 2020 and one in 2021. The recordings, slides and collaborative products are available online.<sup>90</sup>

These services are expected to be the primary point of contact for astronomers accessing the Rubin LSST Prompt Data Products in real-time. This is especially important for TVS science where rapid access to alert data is critical for many science cases.

*Overview of existing Brokers.* The list of Rubin Observatory Full-Stream Alert Brokers is as follows:

1. ALeRCE ( <http://alerce.science/>)
2. AMPEL ( <https://ampelproject.github.io/>)
3. ANTARES ( <https://antares.noirlab.edu/>)
4. Baba-Mul
5. Fink ( <https://fink-broker.org/>)
6. Lasair ( <https://lasair-ztf.lsst.ac.uk/>)
7. Pitt-Google ( <https://pitt-broker.readthedocs.io>)

The list of Rubin Observatory Downstream Alert Brokers is as follows:

1. SNAPS
2. POI: Variables (a downstream broker from ANTARES)

In the following, we give an overview of the technical specifications, especially regarding the classification capabilities, of these brokers.

*ALeRCE.* The ALeRCE broker (Carrasco-Davis et al. 2021; Förster et al. 2021; Sánchez-Sáez et al. 2021) is a Chilean-led initiative to build a community broker for ZTF, Rubin LSST,

<sup>89</sup> <https://project.lsst.org/groups/sac/welcome>

<sup>90</sup> <https://github.com/broker-workshop>

and other large etendue survey telescopes. Its goal is to facilitate the study of variable and transient objects, while using its classification to connect survey and follow-up resources in Chile and abroad.

ALeRCE’s classification is implemented by both a stamp classifier and a light curve classifier. The stamp classifier is implemented with a convolutional neural network (Carrasco-Davis et al. 2021). The light curve classifier utilizes a Hierarchical Random Forest Classifier for light curves with at least 6 observations (Sánchez-Sáez et al. 2021).

ALeRCE will help with answering science questions regarding transients (especially regarding the progenitors of stellar explosions and explosion physics), variable stars (including low-mass microlensing events, mode-changing stellar pulsators, eclipsing events and eruptive events) and supermassive black holes (including changing state AGNs, the detection of intermediate mass black holes, tidal disruption events and reverberation mapping studies).

The developers demonstrate use cases in a series of Jupyter notebooks available at <https://github.com/alercebroker/usecases>. The ALeRCE broker web interface is available at <http://alerce.science/> with the ZTF Explorer (<http://alerce.online>) and the SN Hunter (<http://snhunter.alerce.online>).

*AMPEL*. AMPEL (Nordin et al. 2019a) is a modular and scalable platform with explicit provenance tracking, suited for the real-time processing of large astronomical data sets, but also potentially other heterogeneous data streams.

The goal of the AMPEL broker is to answer science questions regarding multi-messenger science (such as real-time comparisons between optical and gravitational wave events, neutrino and GRB alerts), autonomous transient selection (triggering immediate follow-up observations, for example for SNe) and complex light curve evaluation (with the application of domain-specific algorithms that allow e.g., the detection of tidal disruption events; van Velzen et al. 2021). The AMPEL repository is available at <https://ampelproject.github.io/>.

*ANTARES*. ANTARES (Matheson et al. 2021) is a real-time broker system under development at NOIRLab. ANTARES applies filters to the alert stream, which it ingests in real-time. Filters are Python functions that flag loci (each locus is a compilation of alerts, possibly from different surveys) for distribution via various output streams, depending on their properties (called *tags*). The filters also produce classifications. Users can write their own filters in Python and submit them to run on ANTARES. The ANTARES client can be used by the community to communicate with the broker for both listening to an alert sub-stream, and for archival loci requesting. ANTARES can also cross-matching results with external catalogs and is open to adding new catalogs, as needed by science community.

ANTARES provides a built-in light-curve feature extraction filter as well as a number of filters contributed by the broker

team, including anomaly detection filters for weird Galactic and extra-galactic transients.

The ANTARES broker web interface is available at <https://antares.noirlab.edu/>.

*Baba-Mul*. Baba-Mul is a broker developed at Caltech (PI: Matthew Graham). In contrast with the other brokers, which are designed around a centralized service operated by the broker developers, Baba-Mul proposes a decentralized network of smaller brokers. The Baba-Mul team proposed to make available a public repository with the code for the broker packaged as a containerized instance, enabling users to deploy their own instance of the software, and customize it for their own science case. The software, which makes use of the TensorFlow<sup>91</sup> machine learning tools, is optimized to run on inexpensive Coral Edge TPUs, as a means of making these powerful tools easily available to users.

*Fink*. Fink (Möller et al. 2021) is a community-driven broker that processes time-domain alert streams and connects them with follow-up facilities and science teams. The goal of Fink is to enable discovery in many areas of time-domain astronomy. It has been designed to be flexible and can be used for a variety of science cases, from stellar microlensing, to extra-galactic transients. It currently processes the ZTF public alert stream and has been extensively tested for deployment with Rubin LSST.

Fink is built on high-end technology that enables real-time selection of transients and variable sources in big data. To achieve this, it enriches alert data with existing catalogs, multi-wavelength and messenger detections, as well as machine learning algorithms to select promising candidates for a variety of science cases. Selected events are communicated in real-time for follow-up coordination using customizable filtering; as well as through access to the data through a web-portal and a REST API (<http://fink-portal.org/>). Example user cases and tutorials can be found in a series of Jupyter Notebooks at <https://github.com/astrolabsoftware/fink-tutorials>.

Fink aims to provide classification scores for a wide-range of science cases. These classification scores are and can be used for customizable selection of events with partial and complete data. Current algorithms include filters for: early SN (Leoni et al. 2022), early and complete SN (Möller & de Boissière 2019), kilonovae (Biswas et al. in prep), microlensing (Godines et al. 2019), and satellite glints (Karpov & Peloton 2022). Algorithms are based in many techniques ranging from Active Learning to Supervised Learning algorithms such as Random Forests and Recurrent Neural Networks. Further information on Fink, can be found at <https://fink-broker.org/>.

*Lasair*. The Lasair broker (Smartt 2021) will cross-match the alert stream with observations and objects from astronomical catalogs, such as stars, galaxies, active galactic nuclei and

<sup>91</sup> <https://www.tensorflow.org/>

cataclysmic variables. The selected catalogs include photometric as well as spectroscopic redshift catalogs. In addition, the Lasair broker will cross-match sources with gravitational waves, gamma rays, and neutrino observations. Further information on Lasair can be found at <https://lasair-ztf.lsst.ac.uk/>.

*Pitt-Google.* The Pitt-Google Broker is a scalable broker system designed to maximize the availability and usefulness of the Rubin LSST alert data by combining cloud-based analysis opportunities with value-added data products. It utilizes publicly available classifiers and a Bayesian belief network meta-classifier. Further information on Pitt-Google can be found at <https://pitt-broker.readthedocs.io>.

*SNAPS.* SNAPS, The Solar System Notification Alert Processing System, is a downstream alert broker targeted toward asteroid detection and classification. At present, nearly 800,000 asteroids are known, with the number expected to increase with Rubin LSST, i.e., more than 5 million main-belt asteroids are expected to be observed. Asteroids are tracers of the solar system’s dynamical and physical evolution, they contain the intrinsic material properties of primitive solar system bodies, and finally, as they brought the water and organic material to Earth when it was in its earlier stages, they provide information about the origin of life on Earth. To fulfill the goal of asteroid detection, astronomical data, such as those gathered by the Vera C. Rubin Observatory, must be converted into the physical properties of solar system objects. SNAPS will provide the tools necessary to derive those physical properties.

*POI:Variables.* The Point of Interest broker (PI: Nina Hernitschek) is tailored toward the needs of astronomers looking for updated observations of variable stars in specific on-sky regions. Stellar streams, as well as their progenitors—dwarf galaxies and globular clusters—are of great interest because their orbits are sensitive tracers of galaxy formation and the gravitational potential. Many of these regions of interests can be traced by periodic variable stars, e.g., RR Lyrae and Cepheid stars. Additional attributes of these variable objects include that they are quite easily detectable due to their periodicity and further, their distances can be constrained by period–luminosity–metallicity relations.

The POI alert broker will provide users with updates on variable star observations within regions of interest. The output consists mainly of the light curves of machine-learning identified pulsating variable stars (RR Lyrae and Cepheid stars), and their derived light curve features such as periods and phase offsets (once LSST has reached the point of sufficient revisits). Depending on the classification result, further information, such as the pulsation modulations (the Blazhko effect), which are shown by some RR Lyrae stars, or a distance estimates, can be additionally quantified.

The Point of Interest broker is a downstream broker from ANTARES.

### 6.1.3. Managing Follow-up Programs

Studying astrophysical phenomena in real-time can be an extremely demanding task. For many of the science cases described in this document, once the targets are selected, astronomers will need to compile and analyze data from Rubin LSST and a number of other sources, often involving science-specific modeling. Additional follow-up observations may also be required. For time-critical science, these will often need to be taken very rapidly (within days, at most) of discovery, sometimes from multiple facilities. This creates a need to share data efficiently between team members and to coordinate their efforts, as well as to manage the observations themselves and the data products and analyses they entail. These issues become especially acute when subject to the data rate of Rubin LSST.

Target and Observation Manager systems (TOMs) are often used to manage the workload of follow-up programs, particularly in time-critical science areas. These database-driven systems harvest information on targets of interest, and provide display and visualization tools for teams to share and discuss the information online. They also offer programmatic interfaces to observing facilities so that observations can be planned and requested, and so that the data products can be shared. TOMs often make extensive use of APIs to automate many or even all aspects of their operation and to ensure the most rapid response possible to an alert.

Though TOMs generally need to be customized to the needs of each specific science use-case, open-source packages now exist (Street et al. 2018a) to make them easier to develop and maintain.

*Observing Facilities.* Perhaps counter-intuitively, time-critical science often requires that follow-up observations be made across a range of timescales. In many cases, such as for a gravitational wave events, there is the obvious need to observe as soon as possible, often with many different ground- and space-based facilities operating at different wavelengths and with a range of instrumentation. With this in mind, many observing facilities offer a Target-of-Opportunity override mode of operation. However, the way targets behave over the longer term (days, months or even years) can be equally diagnostic, for example in order to establish SNe type, or to look for stellar accretion events or outbursts. The traditional block-scheduling of telescope facilities, where consecutive hours or nights of time are allocated months in advance, does not adequately support the needs of these “monitoring” observations. For our purposes, queue-scheduling is preferred.

Though technically challenging, programmatic access to a follow-up telescope facilitates rapid follow-up observations strongly enhances an astronomer’s ability to conduct effective follow-up observations of time-critical targets. By requesting observations via a software interface, and receiving information about the status of those observations and the facilities themselves, astronomers are able to respond quickly and



efficiently to new alerts, which in-turn leads to more efficient use of limited follow-up resources.

*Data Archives.* It is often necessary to access and analyze the data obtained from follow-up observations rapidly (in many cases, as rapidly as the initial alert data). Since the purpose of follow-up data is usually to characterize a target, the results of the analysis provide an updated assessment of the target. This new information can often determine whether further observations are required, and if so, how many. It may also inform the types of observations necessary.

For this reason, it is a priority for time-critical science programs to be able to access data products from follow-up facilities rapidly via an online data archive. Making these data products accessible via an application programming interface (API) is the final step in the ‘follow-up chain’, as it enables astronomers to fully automate a time-critical science program, from discovery to characterization, and thus represents the most-efficient possible response to the Rubin LSST alert stream.

## 6.2. Classification

The classification of transient objects is vital for answering the science questions that Rubin LSST endeavours to address: understanding the nature of Dark Matter and Dark Energy (for which tracers, such as quasars and SNe, are vital), cataloging the solar system (which incorporates the detection of asteroids and other small bodies as well as calculating accurate ephemerides), exploring the changing sky (which refers to the detection and analysis of transients and variable stars in general), and understanding the structure and formation of our Milky Way (which draws heavily on distance calculations and population studies relying on variable stars such as Cepheids and RR Lyrae). Within TVS, we aim to classify variable stars, or variable objects in general, as well as other transients.

Given the large number of transients and variable stars that will be detected by Rubin LSST, up to 10 million detections per night, it is imperative to develop classification algorithms using only the photometric data from Rubin LSST, as spectroscopic classification will be available only for a very small fraction of events.

Classification algorithms are crucial for TVS science to: (1) identify new and richer samples of known transients and variables, (2) identify samples of unknowns or barely characterized objects, and (3) early (with partial information) selection of promising transients and variables that would benefit from follow-up observations. The latter is a particular focus of the classification efforts by Rubin LSST Community Brokers, which will analyze Rubin LSST detections in real-time.

In the following, we give more detailed descriptions of recent projects regarding the classification of sources in the LSST main-survey data. We note that classification is one of

many objectives that the Informatics and Statistics Science Collaboration<sup>92</sup> are working on in parallel, and that several TVS members are also members of the Informatics and Statistics Science Collaboration. Here we focus on the classification of Transient and variable objects that are relevant to the science goals of TVS.

### 6.2.1. The Classification of Periodic Variables

A classification algorithm to classify periodic variables is currently being constructed. Assuming several groups will select and investigate transient phenomena, the primary goal of this project is to identify and classify non-transient variable stars. In order to classify periodic variables (e.g., pulsating stars and eclipsing binaries), first we need to identify them and obtain an estimate of their periods. For our purposes, we assume that these pieces of information are available. By classification we mean assigning major variable star classes to individual objects, which later (as more and more data come in) can be further refined into subclasses.

*Methods.* For classification, Convolutional Neural Networks (CNN) are used, which can identify the features of several variable classes. Convolution is a powerful tool that can identify high- and low-level features. We have performed extensive tests based on the OGLE-III and OGLE-IV variable star catalogs (several hundred thousand variable stars, each with several thousand individual photometric measurements). These light curves have proved to be suitable as a training set for these methods.

Data augmentation is a key process before the training phase because the number of stars within each class has to be balanced. With this step and with a judiciously planned neural network we are able to avoid over-fitting the model.

Our preliminary tests show a high level of precision (above 80% Szklennar et al. 2020), but these tests were based on well-sampled OGLE light curves, each with several thousand of data points and known periods. We anticipate that the more sparsely sampled Rubin LSST light curves, which will contain significant number of newly discovered variable stars, will be quite different. Clearly, more work is needed to test these methods with Rubin LSST-like data sets.

*Future Developments.* One future goal is to apply our current pipeline to light curves sampled by the Rubin LSST observing strategy. The OGLE database can be further used for benchmarking, because it features high quality light curve coverage in the *I*-band filter with significantly lower coverage in the *V*-band filter. The latter could be used as a proxy for Rubin LSST data.

Another direction is to exploit the inherently multi-color Rubin LSST observations. Multi-color light curves and color curves will provide an extra source of information that can be

---

<sup>92</sup> <https://issc.science.lsst.org/>

fed into the neural network to balance the lower sampling rate and to improve the accuracy of the classification.

### 6.2.2. *Transient and Anomalies Classification Algorithms*

Transients provide information on the extreme and fundamental physics of the Universe. However, for many of them, their progenitors, explosion mechanisms and diversity remain unknown. These transient phenomena include SNe and the recently detected (for the first time) kilonovae. Additionally, perhaps the greatest promise of Rubin LSST is its potential to discover entirely new phenomena, never seen before or even predicted from theory. The ability of Rubin LSST to deliver on this promise and the details of the algorithms that enable these discovery cannot be finalized until the Rubin LSST survey strategy itself is finalized (see (Li et al. 2021) for a study of the effectiveness of different Rubin LSST strategies in enabling anomaly detection).

Classification algorithms already exist that can be applied to select transients to address LSST science questions. Here we discuss some of the projects that we plan to undertake:

#### 1. **Explore SNe diversity**

There are already a significant number of classification algorithms for SNe using their light-curves (Muthukrishna et al. 2019; Möller & de Boissière 2019). These algorithms allow us to obtain the largest number and most diverse sample of SNe across cosmic time. Additionally early classifiers can allow us to trigger follow-up to obtain additional follow-up observations such as spectra (Leoni et al. 2022). This will allow us to characterize SNe rates, population properties and determine sub-classes boundaries.

#### 2. **Classification of transients**

Most of the existing transient classification algorithms assume some pre-filtering of objects to be done to select transient-like light-curves before they consume the light curves and contextual information. If no relevant contextual data is available (such as a close galaxy or variability catalog match) a relatively fast classification algorithm can be used for this purpose, for example a stamp classifier or light-weight variability time-series feature classifier. The successful usage of both approaches was presented by the ALerCE broker team (Carrasco-Davis et al. 2021; Sánchez-Sáez et al. 2021). To help with classification, some community brokers for ZTF and Rubin LSST broadcast a set of light-curve features as a part of alert package (see DMTN-118) with community driven solutions, such as a light-curve toolkit (Malanchev 2021).

#### 3. **Anomalies**

With billions of transients to be detected by Rubin LSST, new classes are essentially guaranteed. Some classification algorithms based on Isolation Forests and

other methods are already designed for anomaly detection and have been applied to current data sets (Pruzhinskaya et al. 2019; Malanchev et al. 2021; Martínez-Galarza et al. 2021) and will be adapted to Rubin LSST data, once available. A combination of anomaly detection and active learning could be used for expert-driven anomaly detection and active classification tasks (Ishida et al. 2021; Lochner & Bassett 2021).

#### 4. **Multi-survey astronomy**

The early identification of transients, such as SNe or potential afterglows, will allow joint analyses in multiple wavelengths as well as follow-up optimization. Later classification can incorporate new and additional information to further classify objects into their relative sub-types.

*Challenges for Classification Algorithms in the Rubin LSST Era.* Here we present the known challenges for classification given the characteristics of Rubin LSST data and the challenges of classification in general.

#### 1. **Event-dependent baselines**

Different transients and variables require different light-curve spans for accurate classification, e.g., yearly or multi yearly for microlensing and RR Lyrae, and weeks to months for kilonovae and SNe. It will be useful to continue developing algorithms that can accurately classify all different classes using the same data and/or designing hierarchical mechanisms that allow a distinction between object type (e.g., from the light curves submitted as part of the Rubin LSST PLAsTiCC classification challenge (Kessler et al. 2019) and as part of the current Rubin LSST alert stream challenge ELAsTiCC).

#### 2. **Incomplete data**

Rubin LSST's observing strategy will provide non-homogeneous light-curve sampling. Classification methods are being developed to tackle this, which use Recurrent Neural Networks with uneven time sampling (Möller & de Boissière 2019), model or gaussian process extrapolation (Boone 2019) and wavelength/sampling-agnostic classifiers (Qu et al. 2021). It is imperative to make these classifiers more robust to all transient classes to eliminate biases.

#### 3. **Training sets for supervised learning algorithms**

Current training sets, whether simulated or survey data, are an incomplete representation of our transient and variable Universe. We need to explore methods to improve training sets such as through the augmentation and optimization of spectroscopic follow-up using Active Learning (Ishida et al. 2019; Leoni et al. 2022; Boone 2019).

## 7. Equity and Inclusivity in the Transient and Variable Stars Science Collaboration

### 7.1. Introduction and Current State

The Transiting and Variable Stars Science Collaboration (TVS SC) is designed to be a collaborative environment to advance the science potential of the Rubin Legacy Survey of Space and Time. Through the TVS SC, the community can prepare to turn the Rubin LSST data into discoveries about the Universe. The TVS SC encourages its members to advocate for science-driven decisions that can enhance the power of Rubin LSST to explore and advance our knowledge of the transient and variable Universe.

The TVS members and leadership believe that the maximization of the potential of Rubin LSST will only happen if we create a supportive and inclusive environment for all our members and if we strive to make our community inclusive.

In the wake of the COVID-19 pandemic, which brought to light and amplified established social inequities, and with the racial reckoning following the murder of George Floyd, Breonna Taylor, and many other people of color, killed by authorities in the USA, we have renewed our commitment to advance equity and justice within our organization and to promote equitable and fair scientific practices. In June 2020, the TVS released its first statement of values, and a Code of Conduct. The Statement of Values was open for collaborative editing by all TVS members and was adopted by consensus by all TVS members. The original statement of value is reported here in full:

The goal of the LSST TVS SC is to advance our understanding of the Universe through science and to create and sustain a research environment in which all members can thrive. Supporting an equitable space, free of discrimination is first and foremost a matter of social justice. We recognize that academia is embedded within, and takes advantage of, systemic racism that perpetuates white supremacy and suppresses non-white voices and the voices of diverse scholars along other axes or privilege. We, as an organization, renew our commitment to be proactive in order to fix and stop this “status quo” in our corner of the Universe. The TVS SC is inherently a multinational organization with members from a wide range of cultures and this diversity strengthens our research by bringing in different perspectives and expertise. We seek to enhance our diversity of membership and to create an educational and research culture that is welcoming and supportive for all members. We encourage people to apply and be an active part of the TVS SC, regardless of their race, color, country of origin, sex, age, national origin, religion, sexual orientation, gender identity and/or expression, disability or veteran status. We have an ongoing commitment to a range of initiatives to make our organization more equitable and just, undertaken with the guidance of the Justice, Equity, Diversity, and Inclusion (JEDI) group of the TVS SC. More information

on these activities can be found in our TVS call to action (see Section 7.1.1). The leadership of the TVS SC and JEDI are responsible for, and all members are empowered to, ensure full support for these activities. Accountability metrics are explicitly included in the same document.

A specific roadmap to fulfill our commitment to equity should be created in the framework of Change Management to ensure its feasibility and sustainability (James et al. 2019). For now, the TVS SC has established a “Call to Action” (see Section 7.1.1) with several equity focused items which are discussed in the next section.

A note on western-centric bias is in order: while we are a highly international organization, we work alongside a US/Chilean National facility, and our composition reflects the statistics of the STEM population in general. Our members’ composition is primarily white, and primarily from Western countries. It is natural for us to focus on US and Europe-based rights issues and sociopolitical events in the US, Europe, and other “developed” countries that have traditionally been involved in large international STEM collaborations. For example, as discussed below, we strove to collect resources in support of members impacted by the Ukraine war, and by police violence, gun violence, and the right to health-care services in the US. However, we recognize we are likely to overlook international events that are just as impactful, if not involving directly as many of our members. As part of our path to truly becoming an equitable organization, and as we accrue more international members from different countries, we recognize we need to educate ourselves and pay closer attention to international and global events and learn how to support members across cultures. This will require self-education and working closely with members from different communities, while striving not to burden them with the obligation to help those of us in dominant cultures to expand our perspectives.

We emphasize that equity-focused work is time consuming and emotionally draining. Unfortunately, most of this work in academic and STEM-focused organizations is also done on a volunteer basis and with little to no academic recognition. While several TVS members routinely engage in equity-focused work, to truly ensure the sustainability of this effort and the continuing progress of TVS toward equity and justice, support for these activities needs to be secured. In 2021 the Heising-Simons Foundation generously awarded \$900,000 to three Science Collaborations, the TVS SC, the Stars, Milky Way, and Local Volume Science Collaboration, and the Solar System Science Collaborations.<sup>93</sup> This grant supported many equity-focused activities, as described below. This grant ended in August 2022.

<sup>93</sup> <https://lco.global/news/heising-simons-foundation-grant-will-fund-equity-and-excellence-in-science>

### 7.1.1. TVS Call for Action: Current Progress and Future Commitments

In June 2020 TVS released a “Call to Action”<sup>94</sup> and established the Justice, Equity, Diversity, and Inclusion (JEDI) group. The Call to Action included several areas of activities, the current status of which is reported here:

1. **Create a Justice, Equity, Diversity, and Inclusion group.** Status: completed.
2. **Collect, retain, and publicly release anonymized TVS demographic data.** Status: ongoing. A demographic assessment requires: (1) formulation of a survey; (2) distribution of the survey; (3) aggregation of the responses to ensure anonymization; (4) analysis of the responses and formulation of an action plan to address concerns. At the time of writing, a census of the TVS SC has been formulated and released (phase 1), and the demographic data has been collected (phase 2). At the time of writing, we are in the process of analyzing the results and plan to release a document detailing our findings soon. We project the census will be reissued every two years.
3. **Establish formal, structured mentoring relationships to pair senior members with new members, particularly students, and ensure that all members have the support and preparation they need to be successful.** Status: while steps to improve on-boarding procedures have been taken, a formal mentoring structure is yet to be established. The volunteer nature of our organization, which is not supported by any stable source of funding at this time, makes recruitment of members for these kind of activities difficult. One project, which focused on mentoring, involved pairing 4 faculty members with students from minority serving institutions. For this purpose, a grant has been awarded by a 2021–2022 Heising-Simons Foundation.<sup>95</sup> *Action: fundraising to support this activity may be necessary.*
4. **Recruit diverse cohorts of members, especially junior members.** Status: the process to expand our membership through targeted recruitment is ongoing. This process was actively supported by a 2021–2022 Heising-Simons Foundation grant awarded to the TVS SC, the Stars Milky Way Science Collaboration, and Local Volume, and the Solar System Science Collaboration. A fraction of the funds from this grant were used to support kickstarter programs that focused on partnerships between research-focused institutions (with ongoing Rubin LSST programs and access to research funds), and primarily teaching and/or minority serving institutions to establish Rubin-

related research programs that cater to a broader and more diverse community.<sup>96</sup> *Action: The sustainability of this effort will depend on our ability to secure additional funds.*

5. **Raise funds to advertise our organization at meetings and also at conferences directed at underrepresented groups and identities.** Status: TVS has honored its commitment to increase its visibility by participating in STEM URM-focused conferences/organizations. In the US, TVS purchased booths at the National Society of Black Physicist annual conference (2020), the Blacks in Physics conference (2020), and has advertised TVS opportunities by supporting the participation of its members at relevant meetings, for example at the SACNAS (Society for the Advancement of Chicanos/Hispanics and Native Americans in Science) meeting. At this stage, however, there is no clear throughput from these activities. It is possible that engaging in these activities while the meetings were held remotely was ineffective. We are hopeful that in person participation will be more effective.

Additionally, the TVS has recently been successful at involving communities in Africa. Notably, South African astronomers have long been members of TVS (and contributors to this roadmap). But until recently, South Africa was the only country in Africa represented in our membership. In March 2022, as a members of TVS SC, the “SER-SAG” in-kind team<sup>97</sup> organized a one day training session for students from several Ethiopian and Serbian universities and research institutions. The workshop was entitled: “Student intro training on Python for data processing of AGN variability within the LSST.”<sup>98</sup> The workshop was aimed to raise staff and student awareness of scientific and cooperation opportunities within the LSST. Riding on the tail wind of this initiative, TVS has recruited members of the Ethiopian community to become members of our Science Collaboration and encouraged participation in an intermediate software development skills training workshop, that was held in July 2022. This workshop, supported through a Heising-Simons Foundation grant, provided access to training materials written by the Software Carpentries and presented by the Software Sustainability Institute. It was deliberately designed to be fully virtual and largely asynchronous, structured to enable participation from different timezones and from different levels of connectivity. These workshops form a promising option to expand our presence and offer opportunities in areas not traditionally connected with large astrophysical

<sup>94</sup> <https://lsst-tvssc.github.io/calltoaction.html>

<sup>95</sup> <https://lco.global/news/heising-simons-foundation-grant-will-fund-equity-and-excellence-in-science>

<sup>96</sup> [https://lsst-sci-prep.github.io/kickstarter\\_grants.html](https://lsst-sci-prep.github.io/kickstarter_grants.html)

<sup>97</sup> <http://147.91.204.57/index.html>

<sup>98</sup> <https://github.com/LSST-sersag/dle/tree/main/activities/workshop>

programs.

As mentioned earlier, we acknowledge and regret that our structure and composition leads naturally to a western-centric bias. As we continue to work to mitigate this, we are discovering the many ways in which the opportunities we offer are not suitable for everyone. For example, when Rubin LSST begins operations, the accessibility of computing resources may very well be one of the most important disparities that will exist. While Rubin will offer a platform for processing data, connectivity may be a bottleneck. Groups within the TVS SC—including groups offering in-kind contributions from the Astronomical Observatory—Belgrade (AOB) and University of Belgrade—Faculty of Mathematics (UB-MatF)—are working to address this by offering to execute a pipeline on available HPC platforms on behalf of users. More solutions for securing missing resources and enabling the participation of under-resourced communities to undertake scientific discovery through Rubin LSST are clearly needed. Fund-raising through agencies and foundations, as well as leveraging in-kind resources from international communities seeking access to Rubin LSST data<sup>99</sup> are all viable paths that our SC should commit to. *Action: A more comprehensive strategy to increase our visibility in the broader (more diverse) community needs to be developed.*

6. **Keep our webpage up to date and make it more accessible to all, taking into consideration the needs of differently-abled members and prospective members of our organization.** Status: The TVS website<sup>100</sup> was redesigned in 2020 to enhance accessibility, information retrieval, transparency, and now has a space to elevate the work and achievements of TVS members. In the wake of the Ukraine crisis, the JEDI group has also collected information to support our colleagues that are suffering due to the ongoing war, such as opportunities for scientists from Ukraine and Russian dissidents to be hosted at international locations. This information has been shared on the TVS website.

The sustainability of this work will only be ensured if TVS can recruit members to serve as web-masters and perform website maintenance on an ongoing basis. Ensuring service work such as this is recognized will be a necessary step to recruiting a web-master. Furthermore, TVS intends to provide support to its community through the national and international crisis leveraging of its large international network of members. This will be done in the future through the TVS JEDI as well as a new

(at the time of writing) Diversity Equity and Inclusion (DEI) Council of the Science Collaborations. *Action: this work requires ongoing involvement from all TVS members to support each other which, in turn, requires the continued reinforcement of ethically-focused collaborative practices, which is a responsibility of the TVS leadership and JEDI.*

7. **Create a Slack channel where questions about TVS can be asked. Assign primary members to the channel to make sure that the questions are answered.** A SLACK channel #tvsvhos-in-the-what-now has been added to the LSST Corporation (LSSTC) SLACK Workspace, the primary communication venue for the Rubin TVS SC and all SCs (alongside Rubin Community<sup>101</sup>). *Action: The usage has been limited since its creation. This could be due to poor advertising of this venue, or to inherent ineffectiveness. A review of the usefulness of this feature should be initiated.*
8. **Create a speaker's bureau that ensures the representation of TVS at conferences and meetings is diverse.** Status: On hold. The TVS Chairs, however, have committed to increase the visibility of junior members by directly recruiting speakers for talks and speaking engagements.
9. **Develop and collect bystander intervention training resources for our members.** The TVS has shared information and supported the participation of its members at bystander virtual training workshops. The TVS leadership and JEDI have been and continue to be involved in the organization of facilitated events toward DEI for TVS and the Rubin community. These events include anti-racism and bystander training at the 2021 Rubin Project Community Workshop, and involvement in other Rubin meetings and in ad-hoc TVS-specific sessions. The JEDI team was awarded a \$9000 grant (as part of the 2021–2022 Heising-Simons Foundation grant to support the Science Collaborations<sup>102</sup>) to provide training on DEI topics to members of the SCs. *Action: the JEDI will continue to engage in the organization of equity-focused training. Further fundraising to support our training will be necessary.*
10. **Enable and reward mentor training that is targeted at mentoring minority students by senior members.** Status: on hold. *Action: appropriate training opportunities need to be identified or created.*
11. **Commit to hosting meetings only in places that are near minority serving institutes and in areas where police practices are progressive and do not make our members and guests unsafe.** Status: this action has been

<sup>99</sup> See <https://community.lsst.org/t/international-in-kind-contribution-evaluation-committee-cec-update-charge-and-science-collaboration-representation/3998>.

<sup>100</sup> The TVS website is accessible at <https://lsst-tvssc.github.io/>.

<sup>101</sup> [community.lsst.org](https://community.lsst.org)

<sup>102</sup> <https://lco.global/news/heising-simons-foundation-grant-will-fund-equity-and-excellence-in-science>

on hold since the creation of our Call for Action as no in-person meetings have been organized due to COVID-19. Additionally, in the changing political and social landscape, further aspects should be considered in the selection of venues. These include: the access to and criminalization of pregnancy-related medical procedures that may put pregnant meeting members at risk; concealed-carrying laws; ability to impose COVID-related precautions such as mask-wearing. Furthermore, the TVS leadership has committed to provide remote access to all its meetings going forward, explicitly working to ensure a quality experience for the remote attendees, in order to better support the needs of TVS members that cannot or prefer not to engage in person. Currently, this may be a common choice because of the ongoing pandemic, but TVS commits to continue to enable remote meeting attendance past the pandemic. Circumstances that will continue to make remote attendance the preferred mode of participation, identified by the TVS, include family and care-taking responsibilities, lack of flexibility in work engagements, or neurodiversities. The JEDI should compile information on all potential venues and, on an ongoing basis, continue to keep statistics up-to-date on all sites where members of the TVS SC are located, including statistics on policing, weapons laws and abortion laws. This is time consuming and complex work. Structures within the Rubin larger ecosystem, such as the Diversity Equity and Inclusion Council of the Science Collaborations, may be able to support this work.

## 7.2. Increasing Accessibility to Rubin Data

The TVS has recently instantiated a subgroup for Data Visualizations and Representations dedicated to conceptualize, foster, and prototype ways to access Rubin LSST data that will enable all members, including members with vision impairments, to participate in Rubin LSST-driven discovery.

Astronomy is a highly visual science. However, Rubin LSST's commitment to equity would not be complete if it did not enable Blind and Visually Impaired (BVI) users to explore its rich, scientific data. Ways to enable access to the BVI community include (see Astrobite article: enabling *tactile access*<sup>103</sup>): “using the sense of touch to explore a model. One example of a tactile model is a skymap that can be touched.” *Enabling auditory access*: Through “sonifications” by mapping Rubin LSST data features to sounds, and “Using audio descriptions for images or videos.”

As the Rubin LSST data will be accessed through the Rubin Science Platform, BVI users will not have the opportunity to use tools for its analysis on their own devices if the only data

representation enabled is visualization-based. Furthermore, the jupyter notebook environment requires specific tweaks to enable integration with a Smart Reader (Geetha et al. 2020), so the integration of sonification has to happen at the Rubin Science Platform level. Without such efforts, we run the risk of inadvertently locking BVI users out of the process of scientific discovery.

### 7.2.1. Sonification

Sonification is the practice of giving an audible representation of information and processes (Kramer 1994). While visualizations are the traditional means of making data accessible to scientists as well as to the public, sonification is a less common but powerful alternative. In scientific visualizations, specific data properties are mapped to visual elements such as color, shape, or position in a plot. Similarly, data properties can be matched to sound properties, such as pitch, volume, timbre, etc. In order to successfully convey information, both visualization and sonification need to be systematic, reproducible, and avoid distorting the data.

Today, more and more examples of discovery through sound are emerging across disciplines.<sup>104</sup> This is further addressed in the TED talk by Wanda Diaz Merced “How a blind astronomer found a way to hear the stars.”<sup>105</sup> While sonification is generally considered a “potentially useful alternative and complement to visual approaches, it has not reached the same level of acceptance” (de Campo 2009). Nevertheless, Zanella et al. 2022 report an exponential growth of sonification over the last 10 years and discuss the application of sonification to research, education, and public engagement. Compared to visualization, the sonification of scientific data is rare, despite the fact that the differences in the processing of visual and auditory stimuli imply that sonification, by emphasizing complementary relationships in the data, can reveal properties that are missed in visualizations. Compared to the human eye the ear is orders of magnitude more sensitive to changes in signal intensity and frequency, can pick out low signal-to-noise sources better than computer code, can respond and identify aspects of the data faster (e.g., alarms), can determine variable source periods faster and more accurately, and can reach new regimes using sound quality and higher-order harmonics to convey and interpret a large number of parameters at once (Cooke et al. 2017; Treasure 2011). Data plotted visually in more than three-dimensions are too difficult and much harder to interpret compared to sound.

We argue that integrating sonification in the workflow of Rubin LSST data analyses serves three important purposes. First, it is an issue of equity and research inclusion. Rubin's

<sup>103</sup> <https://astrobites.org/2022/07/17/>

<sup>104</sup> Exempla gratia <https://sonification.design/> and <https://eos.org/articles/set-to-music-exoplanets-reveal-insight-on-their-formation>.

<sup>105</sup> [https://www.ted.com/talks/wanda\\_diaz\\_merced\\_how\\_a\\_blind\\_astronomer\\_found\\_a\\_way\\_to\\_hear\\_the\\_stars?language=en](https://www.ted.com/talks/wanda_diaz_merced_how_a_blind_astronomer_found_a_way_to_hear_the_stars?language=en)

commitment to equity would not be complete if it did not enable BVI users to explore its rich, scientific data. As the Rubin data will be accessed through the Rubin Science Platform,<sup>106</sup> BVI users will not have the opportunity to use tools for its analysis on their own devices, so the integration of sonification has to happen at the Rubin Science Platform level. Access to such data also enables real BVI scientific contributions and will promote STEM careers for the large BVI community that would otherwise be missed. Second, we argue that sonification will enable alternative and complementary ways to explore Rubin LSST data in all its complexity and high dimensionality, and that it will provide a tremendous benefit to the Rubin community as an extension of the representation of data beyond visual elements. Just as Rubin will open up the parameter space for astrophysical discovery with its rich dataset, investment in sonification strategies has the potential to expand the representation space, ultimately benefiting the entire scientific community. Finally, sonification provides a means of verification for the detections and discoveries identified in the data via software or visual methods, in particular for the low signal-to-noise sources and events that are often the most important and impactful. We believe the integration of sonification into the Rubin data access and analysis workflow is achievable, and even may be considered a “Low hanging fruit.” For this ambitious goal to come to fruition, dedicated resources will be required, including funding support for the community activities that are required to establish a sonification standard for Rubin LSST data, and for the Rubin Observatory to implement technical solutions that are out of scope at the moment.

Considerations when working toward the sonification of Rubin LSST data include:

1. Because Rubin LSST data are complex, they can benefit tremendously from the extension of the representation of the data beyond visual elements. But the sound representation of a source is only scientifically effective if a deliberate sonification design scheme is created for the complexity and richness of the Rubin LSST dataset, with perceptive effectiveness and clarity (Walker & Kramer 2005). Sonification is relatively common in astronomy to represent (1) 1D time-series, typically evenly sampled (e.g., Kepler data<sup>107</sup>) and spectra, and (2) 2D images (e.g., Chandra images<sup>108</sup>) and 3D spectroscopic integral field unit (IFU) collapsed data cubes. Yet, the effective sonification of 6-bands of unevenly spaced light curves *and the corresponding metadata* is essentially an uncharted territory (however, see also Cooke et al. 2017). The very first step to enabling the sonification of Rubin LSST data is to establish an effective standard for the

mapping of Rubin LSST features to sound properties (see Figure 33). Early work in this direction was supported by the Preparing for Astrophysics with LSST Program, funded by the Heising-Simons Foundation.<sup>109</sup> The proposed mapping will have to be vetted by user communities in controlled experiments, likely with separated experiments for members of the BVI community. This effort will require time and resources.

2. Sonification software tools, including tools specifically created for the sonification of astrophysical data exist and are proliferating, e.g., *astronify*,<sup>110</sup> *SonoUno* (Cooke et al. 2017), *soni-py*,<sup>111</sup> *StarSound* and *VoxMagellan*.<sup>112</sup> However, it is likely that the complexity of the Rubin LSST data will require additional capabilities if we truly want to enhance data interaction through sound. For example: the sonification of the data (numerical data such as time series) without the metadata (e.g., categorical information such as galaxy association) would provide an incomplete picture. Interaction with engineers building sonification software will be required.
3. Issues of accessibility need to be considered early in the design of the Rubin Science Platform<sup>113</sup> to be embedded as natural solutions instead of ad-hoc workarounds. For example, while the emphasis Rubin Science Platform places on Jupyter notebooks is welcome as an effective and popular coding platform, these benefits must be weighted against accessibility issues: Jupyter notebooks do not work with screenreaders, for example. This issue of accessibility has been noted by the NASA Mikulski Archive for Space Telescopes<sup>114</sup> (MAST). The MAST archive is implementing a workaround to convert notebooks to HTML so they are accessible with screenreaders. Enabling similar solutions will require close collaboration with the Rubin Project and Operation teams.

### 7.2.2. 3D Rendering of Rubin Data

To increase accessibility to Rubin LSST’s scientific results for BVI students and researchers, we can develop 3D models of astrophysical objects observed by Rubin LSST and utilize these models to print 3D renderings.

3D models can be useful in the research dissemination, increase accessibility for the BVI community, and support sighted astronomers in research: 3D printed models allow us to better understand the complexity of astrophysical systems. For example, we aim at investigating the stellar variability on a wide range of

<sup>106</sup> <https://data.lsst.cloud>

<sup>107</sup> <https://starsounder.space>

<sup>108</sup> <https://chandra.si.edu/sound/>

<sup>109</sup> The project website can be found at <https://lsst-tvssc.github.io/RubinRhapsodies>.

<sup>110</sup> <https://astronify.readthedocs.io>

<sup>111</sup> <http://www.sonification.com.au/sonipy>

<sup>112</sup> <https://www.jeffreyhannam.com/starsound>

<sup>113</sup> <https://data.lsst.cloud>

<sup>114</sup> <https://archive.stsci.edu>

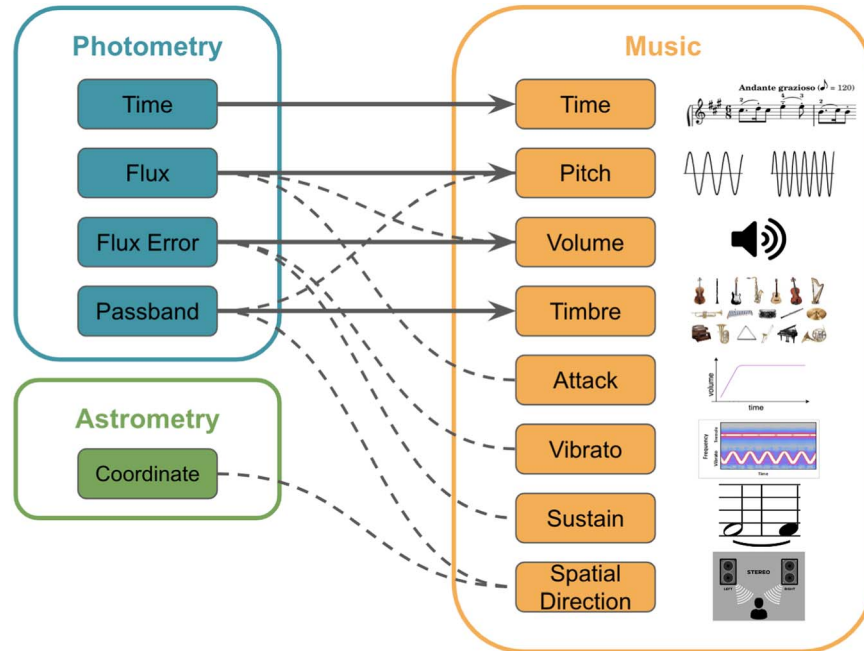


**Figure 33.** Example of potential parameter mapping schemes for Rubin LSST data sonification: on the left are Rubin LSST time-domain data features, on the right sound parameters (and a graphical representation of their meaning). Arrows represent potential mapping, in gray are the mappings that have been tested (results from preliminary interdisciplinary studies involving musicians and TVS members can be found on the TVS website).

timescales (from hours to years), exploiting the full capability that will be available with Rubin LSST data. We will analyze the light curves of a very diverse range of physical processes leading to variability detections, as discussed in several sections of this document. Producing 3D renderings of these astrophysical objects, and the associated 3D printing kits, will enhance Rubin LSST science accessibility and inclusiveness, and help develop understanding of these systems which consist of multiple components.

We note that in addition to 3D renderings, Virtual Reality experiences relating to the physical processes we study can be produced based on the same 3D physical models (see Orlando et al. 2019). While not aimed at increasing accessibility to differently-abled scientists and communities, this is also a method of dissemination and will build awareness and excitement about Rubin LSST science. We note that while virtual reality sets have historically been expensive, free platforms, such as Sketchfab<sup>115</sup> and low-cost visors (e.g., cardboard visors that can even be made at home) are becoming more common, mitigating equity issues and concerns in devoting resources to scientific communication accessible to only a subset of the population.

The 2021–2022 Heising-Simons Foundation grant that was awarded to the Science Collaborations<sup>116</sup> has supported a pilot project to produce 3D models and 3D printed kits as described

here, focusing on young stellar objects (see Section 2.4.1). To make our scientific results more accessible, we are creating publicly available interactive 3D graphics and 3D printed kits based on our interpretation of a diverse range of physical processes causing photometric stellar variability.

To make the 3D modeling and rendering of physical systems, whose study is aided by Rubin LSST data (from prototype to a final product that is an integral element of the Rubin research and dissemination workflow), the following steps are needed:

1. A path for accessing virtual reality renderings and experiences: free and low cost resources to enable virtual reality access are becoming more common and TVS will be able to take advantage of this increased accessibility
2. The transfer-of-knowledge regarding 3D modeling/rendering to the scientific community (including students) so that they may develop 3D models that can be both: (i) printed in 3D for a more accessible dissemination of Rubin LSST results (including to the BVI community) and (ii) converted into virtual reality experience through repositories focused on astrophysical objects that are of interest to the TVS members and beyond, using platforms such as Sketchfab.

Members of TVS developing 3D models will make them available as printable files or 3D printed kits. Although the previous items are easily achievable, to truly advance this data

<sup>115</sup> <https://sketchfab.com>

<sup>116</sup> <https://lco.global/news/heising-simons-foundation-grant-will-fund-equity-and-excellence-in-science/>



representation method and make it common practice, additional resource will be needed. These include:

1. Advanced laptops for 3D visualization equipped with virtual reality visors. Further, 3D printers should be provided for every team engaging in 3D rendering work for a variety of physical phenomena whose modeling is aided by Rubin LSST data.
2. Advanced laptops for 3D visualization equipped with virtual reality visors would also be needed to enable the teams developing the 3D models to share the virtual reality experience at meetings and conferences, when engaging with the community of researchers and students, as well as for outreach and education related to the exploitation of future Rubin LSST data.
3. Collaboration with experts to develop standalone applications<sup>117</sup> to fully exploit the virtual reality experience. This would enable an immersive investigation of 3D models of astrophysical objects, which could allow an higher degree of engagement of the community.

## 8. Summary and next steps

This document has been in the making for several years, during which time the Rubin Legacy Survey of Space and Time (LSST) Transients and Variable Stars Science Collaboration (TVS SC) has doubled in size, and expanded the scope of its science. Additionally, time domain science itself has changed with discoveries of new classes of object, a growing emphasis on Multi-Messenger Astronomy, and a renewed energy as the start of the Rubin LSST approaches, with its potential to revolutionize our science.

The plans for Rubin LSST have been continue to be refined, with: the growing knowledge of the system as it is built; a transition from constructions to operations; changes in the paths available to acquire data rights; and, notably, with the survey strategy decisions still being finalized as we write this Roadmap. Rubin LSST cadence decisions are being made through a process that involves the community at-large and, in particular the Science Collaborations, to an unprecedented degree (Bianco et al. 2022). The TVS SC has contributed to the cadence optimization process with over 20 white papers and peer reviewed publications (most of them collected in the Rubin LSST Survey Strategy Optimization Special Issue of the Astrophysical Journal Supplements;<sup>118</sup> see: Li et al. 2021; Raiteri et al. 2021; Hernitschek & Stassun 2021; Andreoni et al. 2021; Bellm et al. 2022). Our roadmap to science depends inextricably on the final survey strategy that Rubin will implement.

<sup>117</sup> See for example <http://www.pharos.ice.csic.es/star-blast>, PI M. Miceli.

<sup>118</sup> [https://iopscience.iop.org/journal/0067-0049/page/rubin\\_cadence](https://iopscience.iop.org/journal/0067-0049/page/rubin_cadence)

As a result of this ever evolving landscape, we recognize that our roadmap will have to be responsive, adapting to changes in our science domain and Science Collaboration composition. With this publication, we wish to benchmark our roadmap, roughly a year prior to the start of Rubin LSST commissioning, and share with the world our plan to support and leverage Rubin Observatory in the discovery of the ever-changing sky.

Updates to this document will be posted on the TVS website.<sup>119</sup>

## Acknowledgments

This work was produced in the nursery of the Rubin LSST Transient and Variable Star Collaboration (TVS SC). TVS SC particularly acknowledges the support of the LSST Corporation<sup>120</sup> and its commitment to securing and directing private funds toward activities that have supported the work of the TVS SC over the years.

This work was supported by the Preparing for Astrophysics with Rubin LSST Program, funded by the Heising Simons Foundation through grant 2021-2975, and administered by Las Cumbres Observatory.


We thank the external reviewers: Maurizio Paolillo, Massimo Villata, Dan Holdsworth, Olivier Perdereau.

K.M.H. acknowledges support through NASA ADAP grant 80NSSC19K0594. K.C.D. acknowledges funding from the Natural Sciences and Engineering Research Council of Canada (NSERC), and fellowship funding from the McGill Space Institute. This work was performed in part at Aspen Center for Physics, which is supported by National Science Foundation grant PHY-1607611. X.L. and F.B.B. were partially supported by the National Science Foundation grant No. 2108841 and University of Delaware General University Research grant GUR20A00782. A.R. acknowledges support from ANID BECAS/DOCTORADO NACIONAL 21202412. K.B.B. and A.G. acknowledge the financial support from the Slovenian Research Agency (P1-0031, I0-0033, J1-8136, J1-2460). A.G. acknowledges the support from the Fulbright Visiting Scholars program. R.B. acknowledges financial support from the project PRIN-INAF 2019 “Spectroscopically Tracing the Disk Dispersal Evolution.”

## ORCID iDs

Kelly M. Hambleton  <https://orcid.org/0000-0001-5473-856X>

Federica B. Bianco  <https://orcid.org/0000-0003-1953-8727>

Rachel Street  <https://orcid.org/0000-0001-6279-0552>

Keaton Bell  <https://orcid.org/0000-0002-0656-032X>

David Buckley  <https://orcid.org/0000-0002-7004-9956>

Melissa Graham  <https://orcid.org/0000-0002-9154-3136>

<sup>119</sup> <https://lsst-tvssc.github.io/roadmap.html>

<sup>120</sup> The LSST Corporation a not-for-profit 501(c)3 corporation formed to initiate the LSST Project and advance the science of astronomy and physics <https://www.lsstcorporation.org>.

Nina Hernitschek <https://orcid.org/0000-0003-1681-0430>  
 Michael B. Lund <https://orcid.org/0000-0003-2527-1598>  
 Elena Mason <https://orcid.org/0000-0003-3877-0484>  
 Joshua Pepper <https://orcid.org/0000-0002-3827-8417>  
 Andrej Prša <https://orcid.org/0000-0002-1913-0281>  
 Markus Rabus <https://orcid.org/0000-0003-2935-7196>  
 Claudia M. Raiteri <https://orcid.org/0000-0003-1784-2784>  
 Róbert Szabó <https://orcid.org/0000-0002-3258-1909>  
 Paula Szkody <https://orcid.org/0000-0003-4373-7777>  
 Igor Andreoni <https://orcid.org/0000-0002-8977-1498>  
 Eric Bellm <https://orcid.org/0000-0001-8018-5348>  
 Rosaria Bonito <https://orcid.org/0000-0001-9297-7748>  
 Enzo Brocato <https://orcid.org/0000-0001-7988-8177>  
 Katja Bučar Bricman <https://orcid.org/0000-0001-6494-9045>  
 Maria Isabel Carnerero <https://orcid.org/0000-0001-5843-5515>  
 Ryan Chornock <https://orcid.org/0000-0002-7706-5668>  
 Phil Cowperthwaite <https://orcid.org/0000-0002-2478-6939>  
 Antonino Cucchiara <https://orcid.org/0000-0001-6455-5660>  
 Filippo D'Ammando <https://orcid.org/0000-0001-7618-7527>  
 Kristen C. Dage <https://orcid.org/0000-0002-8532-4025>  
 Massimo Dall'Ora <https://orcid.org/0000-0001-8209-0449>  
 James R. A. Davenport <https://orcid.org/0000-0002-0637-835X>  
 Domitilla de Martino <https://orcid.org/0000-0002-5069-4202>  
 Michele Fabrizio <https://orcid.org/0000-0001-5829-111X>  
 Giuliana Fiorentino <https://orcid.org/0000-0003-0376-6928>  
 Poshak Gandhi <https://orcid.org/0000-0003-3105-2615>  
 Teresa Giannini <https://orcid.org/0000-0002-7035-8513>  
 Andreja Gomboc <https://orcid.org/0000-0002-0908-914X>  
 Laura Greggio <https://orcid.org/0000-0003-2634-4875>  
 Patrick Hartigan <https://orcid.org/0000-0002-5380-549X>  
 Markus Hundertmark <https://orcid.org/0000-0003-0961-5231>  
 Michael Johnson <https://orcid.org/0000-0002-5566-6147>  
 Konstantin Malanchev <https://orcid.org/0000-0001-7179-7406>  
 Raffaella Margutti <https://orcid.org/0000-0003-4768-7586>  
 Anais Möller <https://orcid.org/0000-0001-8211-8608>  
 Iliaria Musella <https://orcid.org/0000-0001-5909-6615>  
 Chow-Choong Ngeow <https://orcid.org/0000-0001-8771-7554>  
 Andrea Pastorello <https://orcid.org/0000-0002-7259-4624>  
 Silvia Piranomonte <https://orcid.org/0000-0002-8875-5453>  
 Fabio Ragosta <https://orcid.org/0000-0003-2132-3610>  
 Andrea Reguitti <https://orcid.org/0000-0003-4254-2724>  
 Liliana Rivera Sandoval <https://orcid.org/0000-0002-9396-7215>

Keivan G. Stassun <https://orcid.org/0000-0002-3481-9052>  
 Michael Stroh <https://orcid.org/0000-0002-3019-4577>  
 Giacomo Terreran <https://orcid.org/0000-0003-0794-5982>  
 Yiannis Tsapras <https://orcid.org/0000-0001-8411-351X>  
 Laura Venuti <https://orcid.org/0000-0002-4115-0318>  
 Jorick S. Vink <https://orcid.org/0000-0002-8445-4397>

## References

- Aartsen, M., Ackermann, M., Adams, J., et al. 2018, *Sci*, 361, 6398  
 Aartsen, M. G., Ackermann, M., Adams, J., et al. 2019, *EPJC*, 79, 234  
 Abbott, B. P., Abbott, R., Abbott, T. D., et al. 2016, *PhRvL*, 116, 061102  
 Abbott, B. P., Abbott, R., Abbott, T. D., et al. 2017, *ApJ*, 851, L35  
 Abbott, B. P., Abbott, R., Abbott, T. D., et al. 2017a, *ApJL*, 848, L13  
 Abbott, B. P., Abbott, R., Abbott, T. D., et al. 2017b, *ApJL*, 848, L12  
 Abbott, B. P., Abbott, R., Abbott, T. D., et al. 2020, *ApJL*, 892, L3  
 Abell, P., et al. 2009, LSST Science Book Version 2.0 Tech. Rep., Fermi National Accelerator Lab.  
 Ackermann, M., Ajello, M., Albert, A., et al. 2015, *ApJL*, 813, L41  
 Adams, S. M., Kochanek, C. S., Prieto, J. L., et al. 2016, *MNRAS*, 460, 1645  
 Aghanim, N., Akrami, Y., Arroja, F., et al. 2020, *A&A*, 641, A1  
 Akras, S., Guzman-Ramirez, L., Leal-Ferreira, M. L., & Ramos-Larios, G. 2019, *ApJS*, 240, 21  
 Alencar, S. H. P., Teixeira, P. S., Guimarães, M. M., et al. 2010, *A&A*, 519, A88  
 Alpar, M. A., Cheng, A. F., Ruderman, M. A., & Shaham, J. 1982, *Natur*, 300, 728  
 Alvarez, R., Jorissen, A., Plez, B., et al. 2001, *A&A*, 379, 288  
 Ambrosino, F., Pappitto, A., Stella, L., et al. 2017, *NatAs*, 1, 854  
 Andreoni, I., Ackley, K., Cooke, J., et al. 2017, *PASA*, 34, e069  
 Andreoni, I., Coughlin, M. W., Almualla, M., et al. 2021, *ApJS*, 258, 5  
 Andreoni, I., Coughlin, M. W., Almualla, M., et al. 2022b, *ApJS*, 258, 5  
 Andreoni, I., Margutti, R., Salafia, O. S., et al. 2022a, *ApJS*, 260, 18  
 Andrews, J. E., Jencson, J. E., Van Dyk, S. D., et al. 2021, *ApJ*, 917, 63  
 Antokhina, E. A., & Cherepashchuk, A. M. 1997, *AstL*, 23, 773  
 Antonucci, S., Arkharov, A. A., Paola, A. D., et al. 2014b, *A&A*, 565, L7  
 Antonucci, S., López, R. G., Nisini, B., et al. 2014a, *A&A*, 572, A62  
 Apai, D., Nardiello, D., & Bedin, L. R. 2021, *ApJ*, 906, 64  
 Arcavi, I., Hosseinzadeh, G., Howell, D. A., et al. 2017, *Natur*, 551, 64  
 Arcavi, I., et al. 2014, *ApJ*, 793, 38  
 Archibald, A. M., Bogdanov, S., Patruno, A., et al. 2015, *ApJ*, 807, 62  
 Archibald, A. M., Stairs, I. H., Ransom, S. M., et al. 2009, *Sci*, 324, 1411  
 Arellano Ferro, A., Bramich, D. M., Figuera Jaimes, R., et al. 2013, *MNRAS*, 434, 1220  
 Arnold, L. 2005, sf2a, 207  
 Atri, P., Miller-Jones, J. C. A., Bahramian, A., et al. 2019, *MNRAS*, 489, 3116  
 Audard, M., Ábrahám, P., Dunham, M. M., et al. 2014, *Protostars and Planets VI* (Tucson, AZ: Univ. Arizona Press), 944  
 Bailey, R. L., Helling, C., Hodosán, G., Bilger, C., & Stark, C. R. 2014, *ApJ*, 784, 43  
 Barret, D., den Herder, J.-W., Trong, T. L., Piro, L., & Cappi, M. 2018, *Proc. SPIE*, 10699, 106991G  
 Bassa, C. G., Patruno, A., Hessels, J. W. T., et al. 2014, *MNRAS*, 441, 1825  
 Beck, P. G., Hambleton, K., Vos, J., et al. 2014, *A&A*, 564, A36  
 Bell, K. J., Hambleton, K. M., Lund, M. B., & Szabó, R. 2018, arXiv:1812.03142  
 Bell, K. J., & Hermes, J. J. 2018, arXiv:1812.03143v1  
 Bellm, E., et al. 2018, *Plans and Policies for LSST Alert Distribution*, *ls.st/LDM-612*  
 Bellm, E. C., Burke, C. J., Coughlin, M. W., et al. 2022, *ApJS*, 258, 13  
 Belloni, D., & Rivera Sandoval, L. 2021, *The Golden Age of Cataclysmic Variables and Related Objects V*, 2-7, 13  
 Benford, J. N., & Benford, D. J. 2016, *ApJ*, 825, 101  
 Berger, E., Soderberg, A. M., Chevalier, R. A., et al. 2009, *ApJ*, 699, 1850  
 Bernardini, F., Russell, D. M., Shaw, A. W., et al. 2016, *ApJ*, 818, L5  
 Bhalerao, V., Kasliwal, M. M., Bhattacharya, D., et al. 2017, *ApJ*, 845, 152  
 Bianco, F. B., Ivezić, Ž., Jones, R. L., et al. 2022, *ApJS*, 258, 1

- Bildsten, L., Townsley, D. M., Deloye, C. J., & Nelemans, G. 2006, *ApJ*, **640**, 466
- Blagorodnova, N., Klencki, J., Pejcha, O., et al. 2021, *A&A*, **653**, A134
- Blagorodnova, N., Kotak, R., Polshaw, J., et al. 2017, *ApJ*, **834**, 107
- Blagorodnova, N., et al. 2017, *ApJ*, **844**, 46
- Blaineau, T., Moniez, M., Afonso, C., et al. 2022, arXiv:2202.13819
- Bond, H. E., Bedin, L. R., Bonanos, A. Z., et al. 2009, *ApJL*, **695**, L154
- Bond, I. A., Abe, F., Dodd, R. J., et al. 2001, *MNRAS*, **327**, 868
- Bond, I. A., Udalski, A., Jaroszyski, M., et al. 2004, *ApJL*, **606**, L155
- Bonito, , Hartigan, P., Venuti, L., et al. 2018, arXiv:1812.03135
- Bonito, R., Orlando, S., Argiroffi, C., et al. 2014, *ApJ*, **795**, L34
- Bonito, R., Prisinzano, L., Guarcello, M. G., & Micela, G. 2013, *A&A*, **556**, A108
- Bonito, R., Prisinzano, L., Venuti, L., et al. 2020, *A&A*, **642**, A56
- Bonito, R., Venuti, L., Ustamujic, S., et al. 2023, *ApJS*, **265**, 27
- Prisinzano, L., Bonito, R., Mazzi, A., et al. 2023, *ApJS*, **265**, 39
- Bonnerot, C., Rossi, E. M., & Lodato, G. 2017, *MNRAS*, **464**, 2816
- Bono, G., Caputo, F., Fiorentino, G., Marconi, M., & Musella, I. 2008, *ApJ*, **684**, 102
- Bono, G., Caputo, F., Marconi, M., & Musella, I. 2010, *ApJ*, **715**, 277
- Bono, G., Marconi, M., & Stellingwerf, R. F. 1999, *ApJS*, **122**, 167
- Boone, K. 2019, *AJ*, **158**, 257
- Borucki, W. J., Koch, D., Basri, G., et al. 2010, *Sci*, **327**, 977
- Böttcher, M., Reimer, A., Sweeney, K., & Prakash, A. 2013, *ApJ*, **768**, 54
- Botticella, M., Cappellaro, E., Greggio, L., et al. 2017, *A&A*, **598**, A50
- Botticella, M. T., Pastorello, A., Smartt, S. J., et al. 2009, *MNRAS*, **398**, 1041
- Bouvier, J., Alencar, S. H. P., Bouletier, T., et al. 2007, *A&A*, **463**, 1017
- Boyer, M. L., McQuinn, K. B. W., Barmby, P., et al. 2014, *ApJS*, **216**, 10
- Bricman, K., & Gomboc, A. 2020, *ApJ*, **890**, 73
- Brown, T. M. 2003, *ApJL*, **593**, L125
- Brumback, M. C., Hickox, R. C., Fürst, F. S., et al. 2020, *ApJ*, **888**, 125
- Bryson, S., Coughlin, J., Batalha, N. M., et al. 2020, *AJ*, **159**, 279
- Buchner, J., Georgakakis, A., Nandra, K., et al. 2014, *A&A*, **564**, A125
- Buenzli, E., Saumon, D., Marley, M. S., et al. 2015, *ApJ*, **798**, 127
- Butler, N. R., & Bloom, J. S. 2011, *AJ*, **141**, 93
- Cai, Y.-Z., Pastorello, A., Fraser, M., et al. 2019, *A&A*, **632**, L6
- Cai, Y.-Z., Pastorello, A., Fraser, M., et al. 2021, *A&A*, **654**, A157
- Cai, Y. Z., Pastorello, A., Fraser, M., et al. 2022, arXiv:2207.00734
- Cantrell, A. G., Baily, C. D., Orosz, J. A., et al. 2010, *ApJ*, **710**, 1127
- Capetti, A., & Raiteri, C. M. 2015a, *MNRAS*, **449**, L128
- Capetti, A., & Raiteri, C. M. 2015b, *A&A*, **580**, A73
- Cappellaro, E., Botticella, M. T., Pignata, G., et al. 2015, *A&A*, **584**, A62
- Caproni, A., Abraham, Z., Motter, J. C., & Monteiro, H. 2017, *ApJL*, **851**, L39
- Carrasco-Davis, R., Reyes, E., Valenzuela, C., et al. 2021, *AJ*, **162**, 231
- Casaes, J., & Jonker, P. G. 2014, *SSRv*, **183**, 223
- enko, S. B., Urban, A. L., Perley, D. A., et al. 2015, *ApJL*, **803**, L24
- Chang, Y. L., Arsioli, B., Giommi, P., Padovani, P., & Brandt, C. H. 2019, *A&A*, **632**, A77
- Charles, P. A., & Coe, M. J. 2006, *Compact Stellar X-ray Sources*, Vol. 39 (Cambridge: Cambridge Univ. Press), 215
- Charnock, T., Perreault-Levasseur, L., & Lanusse, F. 2020, arXiv:2006.01490
- Chatterjee, S., Ford, E. B., Matsumura, S., & Rasio, F. A. 2008, *ApJ*, **686**, 580
- Childress, M. J., Hillier, D. J., Seitzzahl, I., et al. 2015, *MNRAS*, **454**, 3816
- Chornock, R., Berger, E., Fox, D. B., et al. 2013, *ApJ*, **774**, 26
- Chornock, R., et al. 2014, *ApJ*, **780**, 44
- Clark, J. S., Crowther, P. A., Larionov, V. M., et al. 2009, *A&A*, **507**, 1555
- Cody, A. M., Hillenbrand, L. A., David, T. J., et al. 2017, *ApJ*, **836**, 41
- Cohn, H. N., Lugger, P. M., Couch, S. M., et al. 2010, *ApJ*, **722**, 20
- Collins, K. A., Collins, K. I., Pepper, J., et al. 2018, *AJ*, **156**, 234
- Cooke, J., Díaz-Merced, W., Foran, G., Hannam, J., & Garcia, B. 2017, *Proc. IAU*, **14**, 251
- Corral-Santana, J. M., Casaes, J., Muñoz-Darias, T., et al. 2016, *A&A*, **587**, A61
- Cortés, J., & Kipping, D. 2019, *MNRAS*, **488**, 1695
- Coughlin, M. W., Burdge, K., Phinney, E. S., et al. 2020, *MNRAS*, **494**, L91
- Coulter, D. A., Foley, R. J., Kilpatrick, C. D., et al. 2017, *Sci*, **358**, 1556
- Cowperthwaite, P. S., Berger, E., Villar, V. A., et al. 2017, *ApJL*, **848**, L17
- Cowperthwaite, P. S., Villar, V. A., Scolnic, D. M., & Berger, E. 2019, *ApJ*, **874**, 88
- Di Criscienzo, M. D., Dell'Agli, F., Ventura, P., et al. 2013, *MNRAS*, **433**, 313
- Di Criscienzo, M. D., Marconi, M., & Caputo, F. 2004, *ApJ*, **612**, 1092
- Di Criscienzo, M. D., Marconi, M., Musella, I., Cignoni, M., & Ripepi, V. 2012, *MNRAS*, **428**, 212
- Cucchiara, A., Fumagalli, M., Rafelski, M., et al. 2015, *ApJ*, **804**, 51
- Cucchiara, A., Levan, A. J., Fox, D. B., et al. 2011, *ApJ*, **736**, 7
- Cucchiara, A., Prochaska, J. X., Perley, D., et al. 2013, *ApJ*, **777**, 94
- D'Abrusco, R., Álvarez Crespo, N., Massaro, F., et al. 2019, *ApJS*, **242**, 4
- Dage, K. C., Brumback, M., Neilsen, J., et al. 2022, *MNRAS*, **514**, 5457
- D'Angelo, C. R., & Spruit, H. C. 2010, *MNRAS*, **406**, 1208
- Davenport, J. R. A. 2019, arXiv:1907.04443
- de Campo, A. 2009, *Science by Ear: An Interdisciplinary Approach to Sonifying Scientific Data*, Univ. of Music and Performing Arts
- De Cia, A., Ledoux, C., Fox, A. J., et al. 2012, *A&A*, **545**, A64
- de Martino, D., Belloni, T., Falanga, M., et al. 2013, *A&A*, **550**, A89
- de Martino, D., Falanga, M., Bonnet-Bidaud, J. M., et al. 2010, *A&A*, **515**, A25
- de Martino, D., Papitto, A., Belloni, T., et al. 2015, *MNRAS*, **454**, 2190
- De Martino, S., & De Siena, S. 2010, arXiv:1012.4975
- de Mink, S. E., & King, A. 2017, *ApJL*, **839**, L7
- de Mink, S. E., Sana, H., Langer, N., Izzard, R. G., & Schneider, F. R. N. 2014, *ApJ*, **782**, 7
- De Somma, G., Marconi, M., Molinaro, R., et al. 2020, *ApJS*, **247**, 30
- Dell'Agli, F., Valiante, R., Kamath, D., Ventura, P., & García-Hernández, D. A. 2019, *MNRAS*, **486**, 4738
- Deloye, C. J., Bildsten, L., & Nelemans, G. 2005, *ApJ*, **624**, 934
- Dermer, C. D., Chiang, J., & Böttcher, M. 1999, *ApJ*, **513**, 656
- Dietrich, T., Coughlin, M. W., Pang, P. T. H., et al. 2020, *Sci*, **370**, 1450
- Dobbie, P. D., Burleigh, M. R., Levan, A. J., et al. 2005, *MNRAS*, **357**, 1049
- Dong, S., Shappee, B. J., Prieto, J. L., et al. 2016, *Sci*, **351**, 257
- Dravins, D., Lindegren, L., Mezey, E., & Young, A. T. 1997a, *PASP*, **109**, 173
- Dravins, D., Lindegren, L., Mezey, E., & Young, A. T. 1997b, *PASP*, **109**, 725
- Dravins, D., Lindegren, L., Mezey, E., & Young, A. T. 1998, *PASP*, **110**, 1118
- Drout, M. R., Piro, A. L., Shappee, B. J., et al. 2017, *Sci*, **358**, 1570
- Dunham, M. M., Allen, L. E., II, N. J. E., et al. 2015, *ApJS*, **220**, 11
- Edelson, R. A., & Krolik, J. H. 1988, *ApJ*, **333**, 646
- Eichler, D., Livio, M., Piran, T., & Schramm, D. N. 1989, *Natur*, **340**, 126
- Eriksson, S. C., Janson, M., & Calissendorff, P. 2019, *A&A*, **629**, A145
- Evans, C. R., & Kochanek, C. S. 1989, *ApJL*, **346**, L13
- Evans, N. J. I., Dunham, M. M., Jørgensen, J. K., et al. 2009, *ApJS*, **181**, 321
- Feigelson, E. D., Babu, G. J., & Caceres, G. A. 2018, *FrP*, **6**, 80
- Fender, R. P., Belloni, T. M., & Gallo, E. 2004, *MNRAS*, **355**, 1105
- Filippenko, A. V. 2003, in *From Twilight to Highlight: The Physics of Supernovae*, ed. W. Hillebrandt & B. Leibundgut (Berlin: Springer), 171
- Finn, K., Bianco, F. B., Modjaz, M., Liu, Y.-Q., & Rest, A. 2016, *ApJ*, **830**, 73
- Fiorentino, G., Caputo, F., Marconi, M., & Musella, I. 2002, *ApJ*, **576**, 402
- Fiorentino, G., Marconi, M., Musella, I., & Caputo, F. 2007, *A&A*, **476**, 863
- Fiorentino, G., Musella, I., & Marconi, M. 2013, *MNRAS*, **434**, 2866
- Fischer, W. J., Hillenbrand, L. A., Herczeg, G. J., et al. 2022, arXiv:2203.11257
- Fishman, G. J., & Meegan, C. A. 1995, *ARA&A*, **33**, 415
- Folkes, S. L., Pinfield, D. J., Jones, H. R. A., et al. 2012, *MNRAS*, **427**, 3280
- Foreman-Mackey, D., Agol, E., Angus, R., & Ambikasaran, S. 2017, *AJ*, **154**, 220
- Foreman-Mackey, D., Hogg, D. W., Lang, D., & Goodman, J. 2013, *PASP*, **125**, 306
- Förster, F., Cabrera-Vives, G., Castillo-Navarrete, E., et al. 2021, *AJ*, **161**, 242
- Fortson, L., Masters, K., Nichol, R., et al. 2012, *Advances in Machine Learning and Data Mining for Astronomy*, **2012**, 213
- Foucart, F., Hinderer, T., & Nissanke, S. 2018, *PhRvD*, **98**, 081501
- Fraser, M., Inarra, C., Jerkstrand, A., et al. 2013, *MNRAS*, **433**, 1312
- Fraser, M., Stritzinger, M. D., Brennan, S. J., et al. 2021, arXiv:2108.07278
- French, K. D., Arcavi, I., & Zabludoff, A. 2016, *ApJL*, **818**, L21
- French, K. D., & Zabludoff, A. I. 2018, *ApJ*, **868**, 99
- Fryer, C. L., Woosley, S. E., & Hartmann, D. H. 1999, *ApJ*, **526**, 152
- Gaia Collaboration, Creevey, O. L., Sarro, L. M., et al. 2022, arXiv:2206.05870
- Gaia Collaboration et al. 2017, *A&A*, **605**, A79
- Gaia Collaboration et al. 2021, *A&A*, **649**, A1

- Gal-Yam, A., Bruch, R., Schulze, S., et al. 2022, *Natur*, **601**, 201
- Gal-Yam, A., Leonard, D. C., Fox, D. B., et al. 2007, *ApJ*, **656**, 372
- Gandhi, P., Bachetti, M., Dhillon, V. S., et al. 2017, *NatAs*, **1**, 859
- Gandhi, P., Rao, A., Johnson, M. A. C., Paice, J. A., & Maccarone, T. J. 2019, *MNRAS*, **485**, 2642
- Gatto, A., Walch, S., Naab, T., et al. 2017, *MNRAS*, **466**, 1903
- Geetha, M. N., Sheethal, H. V., Sindhu, S., Siddiqua, J. A., & Chandan, H. C. 2020, Smart Reader for Blind and Visually Impaired (BVI), EasyChair Preprint no. 3936
- Getman, K. V., & Feigelson, E. D. 2021, *ApJ*, **916**, 32
- Gezari, S., Chornock, R., Rest, A., et al. 2012, *Natur*, **485**, 217
- Giannini, T., Giunta, A., Lorenzetti, D., et al. 2020, *A&A*, **637**, A83
- Giannini, T., Lorenzetti, D., Antonucci, S., et al. 2016a, *ApJ*, **819**, L5
- Giannini, T., Lorenzetti, D., Harutyunyan, A., et al. 2016b, *A&A*, **588**, A20
- Giannini, T., Munari, U., Antonucci, S., et al. 2018, *A&A*, **611**, A54
- Godines, D., Bachelet, E., Narayan, G., & Street, R. A. 2019, *A&C*, **28**, 100298
- Gomboc, A., & Čadež, A. 2005, *ApJ*, **625**, 278
- Gomez, S., Berger, E., Nicholl, M., et al. 2019, *ApJ*, **881**, 87
- Gonzalez, O. A., Clarkson, W., Debattista, V. P., et al. 2018, arXiv:1812.08670
- Goodfellow, I. J., Pouget-Abadie, J., Mirza, M., et al. 2014, in Proc. 27th Int. Conf. Neural Information Processing Systems—Vol. 2, NIPS'14 (Cambridge, MA: MIT Press), 2672
- Goodman, J. 1986, *ApJL*, **308**, L47
- Goranskij, V. P., Barsukova, E. A., Spiridonova, O. I., et al. 2016, *AstBu*, **71**, 82
- Gould, A. 2000, *ApJ*, **542**, 785
- Gräfenor, G., Owocki, S. P., & Vink, J. S. 2012, *A&A*, **538**, A40
- Grassitelli, L., Langer, N., Mackey, J., et al. 2021, *A&A*, **647**, A99
- Graur, O., Bianco, F., & Modjaz, M. 2015, *MNRAS*, **450**, 905
- Graur, O., et al. 2018, *ApJ*, **853**, 39
- Greene, J. E., Strader, J., & Ho, L. C. 2020, *ARA&A*, **58**, 257
- Greggio, L. 2005, *A&A*, **441**, 1055
- Greggio, L. 2010, *MNRAS*, **406**, 22
- Greggio, L., & Cappellaro, E. 2009, Probing Stellar Populations Out to the Distant Universe: Cefalu 2008 in AIP Conf. Ser. 1111, ed. G. Giobbi et al., 477
- Greggio, L., & Cappellaro, E. 2019, *A&A*, **625**, A113
- Grinin, V. 1988, *SvAL*, **14**, 27
- Groh, J. H., Hillier, D. J., Daminieli, A., et al. 2009, *ApJ*, **698**, 1698
- Groot, P. J., Vreeswijk, P. M., Huber, M. E., et al. 2003, *MNRAS*, **339**, 427
- Guillochon, J., & Loeb, A. 2015, *ApJ*, **811**, L20
- Guillochon, J., Manukian, H., & Ramirez-Ruiz, E. 2014, *ApJ*, **783**, 23
- Guillochon, J., Nicholl, M., Villar, V. A., et al. 2018, *ApJS*, **236**, 6
- Guillochon, J., & Ramirez-Ruiz, E. 2013, *ApJ*, **767**, 25
- Guo, W., Zhang, F., Meng, X., et al. 2008, *ChJAA*, **8**, 63
- Gupta, R. R., Kuhlmann, S., Kovacs, E., et al. 2016, *AJ*, **152**, 154
- Guy, L. P., Cuillandre, J.-C., Bachelet, E., et al. 2022, Rubin-Euclid Derived Data Products?Initial Recommendations, v1.0, Zenodo, doi:10.5281/zenodo.5836022
- Habibi, F., Moniez, M., Ansari, R., & Rahvar, S. 2010, *A&A*, **525**, A108
- Hallinan, G., Littlefair, S. P., Cotter, G., et al. 2015, *Natur*, **523**, 568
- Hartmann, L., & Kenyon, S. J. 1985, *ApJ*, **299**, 462
- Hawley, S. L., Covey, K. R., Knapp, G. R., et al. 2002, *AJ*, **123**, 3409
- Healey, S. E., Romani, R. W., Taylor, G. B., et al. 2007, *ApJS*, **171**, 61
- Heller, R., & Pudritz, R. E. 2016, *AsBio*, **16**, 259
- Helling, C., Jardine, M., Stark, C., & Diver, D. 2013, *ApJ*, **767**, 136
- Herbig, G. 1989, in ESO Workshop on Low Mass Star Formation and Pre-Main Sequence Objects, 233
- Hermitschek, N., & Stassun, K. G. 2021, *ApJS*, **258**, 4
- Hitchcock, J. A., Helling, C., Scholz, A., et al. 2020, *MNRAS*, **495**, 3881
- Ho, A. Y. Q., Perley, D. A., Gal-Yam, A., et al. 2021, arXiv:2105.08811
- Hodosán, G., Rimmer, P. B., & Helling, C. 2016, *MNRAS*, **461**, 1222
- Höfner, S., & Olofsson, H. 2018, *A&ARv*, **26**, 1
- Holoien, T. W. S., Huber, M. E., Shappee, B. J., et al. 2019, *ApJ*, **880**, 120
- Holoien, T. W. S., Kochanek, C. S., Prieto, J. L., et al. 2016, *MNRAS*, **463**, 3813
- Holoien, T. W. S., Prieto, J. L., Bersier, D., et al. 2014, *MNRAS*, **445**, 3263
- Holoien, T. W. S., Valley, P. J., Auchettl, K., et al. 2019, *ApJ*, **883**, 111
- Hopkins, A. M., & Beacom, J. F. 2006, *ApJ*, **651**, 142
- Howell, S. B., Sobek, C., Haas, M., et al. 2014, *PASP*, **126**, 398
- Howitt, G., Stevenson, S., Vigna-Gómez, A., et al. 2020, *MNRAS*, **492**, 3229
- Hu, C.-P., Mihara, T., Sugizaki, M., Ueda, Y., & Enoto, T. 2019, *ApJ*, **885**, 123
- Huang, C. D., Riess, A. G., Hoffmann, S. L., et al. 2018, *ApJ*, **857**, 67
- Huang, C. D., Riess, A. G., Yuan, W., et al. 2020, *ApJ*, **889**, 5
- Hubble, E., & Sandage, A. 1953, *ApJ*, **118**, 353
- Hufnagel, B. R., & Bregman, J. N. 1992, *ApJ*, **386**, 473
- Hughes, P. A., Aller, H. D., & Aller, M. F. 1992, *ApJ*, **396**, 469
- Humphreys, R. M., Bond, H. E., Bedin, L. R., et al. 2011, *ApJ*, **743**, 118
- Humphreys, R. M., & Davidson, K. 1994, *PASP*, **106**, 1025
- Humphreys, R. M., & Davidson, K. 1994, *PASP*, **106**, 1025
- Humphreys, R. M., Davidson, K., Van Dyk, S. D., & Gordon, M. S. 2017, *ApJ*, **848**, 86
- Hung, T., et al. 2018, *ApJS*, **238**, 15
- Ida, S., Lin, D. N. C., & Nagasawa, M. 2013, *ApJ*, **775**, 42
- Ilkiewicz, K., Mikolajewska, J., Shara, M. M., et al. 2018, arXiv:1811.06696
- Ishida, E. E. O., Beck, R., González-Gaitán, S., et al. 2019, *MNRAS*, **483**, 2
- Ishida, E. E. O., Kornilov, M. V., Malanchev, K. L., et al. 2021, *A&A*, **650**, A195
- Itoh, R., Utsumi, Y., Inoue, Y., et al. 2020, *ApJ*, **901**, 3
- Jacklin, S., Lund, M. B., Pepper, J., & Stassun, K. G. 2015, *AJ*, **150**, 34
- Jacklin, S. R., Lund, M. B., Pepper, J., & Stassun, K. G. 2017, *AJ*, **153**, 186
- Jacobson-Galán, W., Dessart, L., Jones, D., et al. 2022, *ApJ*, **924**, 15
- Jake VanderPlas 2014, in Proc. 13th Python in Science Conf., ed. Stéfan van der & James Bergstra, 93
- James, M., Bertschinger, E., Beckford, B., et al. 2019, The Time is Now: Systemic Changes to Increase African Americans with Bachelor's Degrees in Physics and Astronomy Tech. Rep. MSU-CSE-06-2, AIP National Task Force to Elevate African
- Jeffery, C. S., Kurtz, D., Shibahashi, H., et al. 2015, *MNRAS*, **447**, 2836
- Jiménez, N., Tissera, P. B., & Matteucci, F. 2015, *ApJ*, **810**, 137
- Johnson, M. A. C., Gandhi, P., Chapman, A. P., et al. 2018, *MNRAS*, **484**, 19
- Joy, A. H. 1945, *ApJ*, **102**, 168
- Jurić, M., Ciardi, D., & Dubois-Felsmann, G. 2017, LSST Science Platform Vision Document, [ls.st/LSE-319](https://www.lsst.org/lsst/lse/319)
- Jurić, M., et al. 2018, LSST Data Products Definition Document, [ls.st/dpdd](https://www.lsst.org/lsst/dpdd)
- Ivezić, Ž., Kahn, S. M., Tyson, J. A., et al. 2008, arXiv:0805.2366
- Ivezić, Ž., Kahn, S. M., Tyson, J. A., et al. 2019, *ApJ*, **873**, 111
- Kalari, V. M., Vink, J. S., Dufton, P. L., & Fraser, M. 2018, *A&A*, **618**, A17
- Kann, D. A. 2012, PhD thesis, Friedrich Schiller Univ. Jena
- Kann, D. A., Klose, S., Zhang, B., et al. 2010, *ApJ*, **720**, 1513
- Karalidi, T., Apai, D., Marley, M. S., & Buenzli, E. 2016, *ApJ*, **825**, 90
- Karczmarek, P., Pietrzyński, G., Górski, M., Gieren, W., & Bersier, D. 2017, *AJ*, **154**, 263
- Karpov, S., & Peloton, J. 2022, arXiv:2202.05719
- Kasliwal, M. M. 2012, *PASA*, **29**, 482
- Kasliwal, M. M. 2013, Binary Paths to Type Ia Supernovae Explosions in IAU Symp., **281**, 9
- Kasliwal, M. M., Kulkarni, S. R., Arcavi, I., et al. 2011, *ApJ*, **730**, 134
- Kasliwal, M. M., Nakar, E., Singer, L. P., et al. 2017, *Sci*, **358**, 1559
- Kelly, B. C., Becker, A. C., Sobolewska, M., Siemiginowska, A., & Uttley, P. 2014, *ApJ*, **788**, 33
- Kesden, M. 2012, *PhRvD*, **85**, 024037
- Kessler, R., Narayan, G., Avelino, A., et al. 2019, *PASP*, **131**, 094501
- Kessler, R., Narayan, G., Avelino, A., et al. 2019, *PASP*, **131**, 094501
- Khakpash, S., Pepper, J., Penny, M., Gaudi, B. S., & Street, R. 2021, *AJ*, **161**, 132
- Kipping, D. M., & Teachey, A. 2016, *MNRAS*, **459**, 1233
- Kirk, B., Conroy, K., Prša, A., et al. 2016, *AJ*, **151**, 68
- Kirkpatrick, J. D., Gelino, C. R., Faherty, J. K., et al. 2021, *ApJS*, **253**, 7
- Klebesadel, R. W., Strong, I. B., & Olson, R. A. 1973, *ApJL*, **182**, L85
- Kochanek, C. S. 1994, *ApJ*, **422**, 508
- Kochanek, C. S. 2016, *MNRAS*, **461**, 371
- Kochanek, C. S., Adams, S. M., & Belczynski, K. 2014, *MNRAS*, **443**, 1319
- Koljonen, K. I. L., Russell, D. M., Corral-Santana, J. M., et al. 2016, *MNRAS*, **460**, 942
- Konigl, A. 1981, *ApJ*, **243**, 700
- Kotyla, J. P., Chiaberge, M., Baum, S., et al. 2016, *ApJ*, **826**, 46
- Kouveliotou, C., Meegan, C. A., Fishman, G. J., et al. 1993, *ApJL*, **413**, L101

- Kovács, G., Zucker, S., & Mazeh, T. 2002, *A&A*, **391**, 369
- Kramer, G. 1994, Auditory Display-sonification, Audification and Auditory Interfaces (Boca Raton, FL: Chemical Rubber Company (CRC Press)), 1
- Krolik, J., Piran, T., Svirski, G., & Cheng, R. M. 2016, *ApJ*, **827**, 127
- Kulkarni, S. R., Ofek, E. O., Rau, A., et al. 2007, *Natur*, **447**, 458
- Kupfer, T., Bauer, E. B., Burdge, K. B., et al. 2019, *ApJL*, **878**, L35
- Kurosawa, R., & Romanova, M. M. 2013, *MNRAS*, **431**, 2673
- Lasota, J.-P. 2001, *NewAR*, **45**, 449
- Law, N. M., Fors, O., Ratzloff, J., et al. 2015, *PASP*, **127**, 234
- Law-Smith, J., et al. 2017, *ApJ*, **850**, 22
- Lehto, H. J., & Valtonen, M. J. 1996, *ApJ*, **460**, 207
- Leitherer, C., Appenzeller, I., Klare, G., et al. 1985, *A&A*, **153**, 168
- Leloudas, G., Fraser, M., Stone, N. C., et al. 2016, *NatAs*, **1**, 0002
- Leloudas, G., et al. 2016, *NatAs*, **1**, 0002
- Lemarchand, G. A. 1994, *Ap&SS*, **214**, 209
- Lenz, P., & Breger, M. 2005, *CoAst*, **146**, 53
- Lenz, P., & Breger, M., 2014 Period04: Statistical analysis of large astronomical time series, Astrophysics Source Code Library, ascl:1407.009
- Leoni, M., Ishida, E. E. O., Peloton, J., & Möller, A. 2022, *A&A*, **663**, A13
- Li, X., Ragosta, F., Clarkson, W. I., & Bianco, F. B. 2021, *ApJS*, **258**, 2
- Li, X., Bianco, F. B., Dobler, G., et al. 2022, *AJ*, **164**, 250
- Lico, R., Liu, J., Giroletti, M., et al. 2020, *A&A*, **634**, A87
- Lipunov, V. M., Gorboskovy, E., Kornilov, V. G., et al. 2017, *ApJL*, **850**, L1
- Lochner, M., & Bassett, B. A. 2021, *A&C*, **36**, 100481
- Lodato, G., King, A. R., & Pringle, J. E. 2009, *MNRAS*, **392**, 332
- Loeb, A. 2016, *ApJL*, **819**, L21
- Loeb, A., & Ulmer, A. 1997, *ApJ*, **489**, 573
- Loewenstein, M., Loewenstein, M., & Loewenstein, M. 2006, *ApJ*, **648**, 230
- LSST Dark Energy Science Collaboration 2012, Large Synoptic Survey Telescope: Dark Energy Science Collaboration, arXiv:1211.0310
- Lucy, A. B., Knigge, C., & Sokoloski, J. L. 2018, *MNRAS*, **478**, 568
- Lund, M. B., Pepper, J., & Stassun, K. G. 2015, *AJ*, **149**, 16
- Lund, M. B., Pepper, J. A., Shporer, A., & Stassun, K. G. 2018a, arXiv:1809.10900
- Lund, M. B., Stassun, K. G., Farihi, J., et al. 2018b, arXiv:1812.03148
- Maccarone, T., & Knigge, C. 2007, *A&G*, **48**, 5.12
- Madau, P., & Dickinson, M. 2014, *ARA&A*, **52**, 415
- Magliocchetti, M., Popesso, P., Brusa, M., & Salvato, M. 2018, *MNRAS*, **478**, 3848
- Magorrian, J., & Tremaine, S. 1999, *MNRAS*, **309**, 447
- Makovetskii, P. 1977, *AZh*, **54**, 449
- Malanchev, K., 2021 Light-curve: Light curve analysis toolbox, Astrophysics Source Code Library, ascl:2107.001
- Malanchev, K. L., Pruzhinskaya, M. V., Korolev, V. S., et al. 2021, *MNRAS*, **502**, 5147
- Maoz, D., Mannucci, F., & Nelemans, G. 2014, *ARA&A*, **52**, 107
- Marconi, M., Bono, G., Caputo, F., et al. 2011, *ApJ*, **738**, 111
- Marconi, M., Caputo, F., Criscienzo, M. D., & Castellani, M. 2003, *ApJ*, **596**, 299
- Marconi, M., Cignoni, M., Criscienzo, M. D., et al. 2006, *MNRAS*, **371**, 1503
- Marconi, M., Coppola, G., Bono, G., et al. 2015, *ApJ*, **808**, 50
- Marconi, M., Molinaro, R., Bono, G., et al. 2013, *ApJL*, **768**, L6
- Marconi, M., Molinaro, R., Dall’Ora, M., et al. 2022, arXiv:2206.06470
- Marconi, M., Molinaro, R., Ripepi, V., et al. 2017, *MNRAS*, **466**, 3206
- Marconi, M., Molinaro, R., Ripepi, V., Musella, I., & Brocato, E. 2013, *MNRAS*, **428**, 2185
- Marconi, M., Musella, I., & Fiorentino, G. 2005, *ApJ*, **632**, 590
- Marconi, M., Musella, I., Fiorentino, G., et al. 2010, *ApJ*, **713**, 615
- Marengo, M., Hulsebus, A., & Willis, S. 2015, *ApJL*, **814**, L15
- Margutti, R., & Chornock, R. 2021, *ARA&A*, **59**, 155
- Margutti, R., Milisavljevic, D., Soderberg, A. M., et al. 2014, *ApJ*, **780**, 21
- Martley, M. S., Saumon, D., & Goldblatt, C. 2010, *ApJL*, **723**, L117
- Martínez-Galarza, J. R., Bianco, F. B., Crake, D., et al. 2021, *MNRAS*, **508**, 5734
- Mason, E., Diaz, M., Williams, R. E., Preston, G., & Bensby, T. 2010, *A&A*, **516**, A108
- Massaro, E., Giommi, P., Leto, C., et al. 2009, *A&A*, **495**, 691
- Matheson, T., Stubens, C., Wolf, N., et al. 2021, *AJ*, **161**, 107
- Matsumoto, T., & Metzger, B. D. 2022, arXiv:2202.10478
- Matteucci, F. 2010, Progenitors and Environments of Stellar Explosions in IAP Annual Coll., **16**, 63
- Mattila, S., Dahlen, T., Efstathiou, A., et al. 2012, *ApJ*, **756**, 111
- McGaugh, S. S., Schombert, J. M., de Blok, W. J. G., & Zagursky, M. J. 2009, *ApJ*, **708**, L14
- McGinnis, P. T., Alencar, S. H. P., Guimarães, M. M., et al. 2015, *A&A*, **577**, A11
- McKernan, B., Ford, K. E. S., Bellovary, J., et al. 2018, *ApJ*, **866**, 66
- Medina, N., Borissova, J., Bayo, A., et al. 2019, *yCat*, **864**, 11
- Merc, J., Gális, R., & Wolf, M. 2019, *RNAAS*, **3**, 28
- Merloni, A., Predehl, P., Becker, W., et al. 2012, arXiv:1209.3114
- Mészáros, P., & Rees, M. J. 1997, *ApJL*, **482**, L29
- Metchev, S. A., Heinze, A., Apai, D., et al. 2015, *ApJ*, **799**, 154
- Metzger, B. D., Bauswein, A., Goriely, S., & Kasen, D. 2015, *MNRAS*, **446**, 1115
- Mikolajewska, J., Kolotilov, E. A., Shugarov, S. Y., & Yudin, B. F. 2002, *A&A*, **392**, 197
- Mirhosseini, A., & Moniez, M. 2018, *A&A*, **618**, L4
- Mockler, B., Guillochon, J., & Ramirez-Ruiz, E. 2019, *ApJ*, **872**, 151
- Modjaz, M., Bianco, F. B., Siwek, M., et al. 2020, *ApJ*, **892**, 153
- Möller, A., & de Boissière, T. 2019, *MNRAS*, **491**, 4277
- Möller, A., Peloton, J., Ishida, E. E. O., et al. 2021, *MNRAS*, **501**, 3272
- Molnar, L. A., Van Noord, D. M., Kinemuchi, K., et al. 2017, *ApJ*, **840**, 1
- Moniez, M. 2003, *A&A*, **412**, 105
- Moniez, M. 2010, *GRGr*, **42**, 2047
- Moniez, M., Sajadian, S., Karami, M., Rahvar, S., & Ansari, R. 2017, *A&A*, **604**, A124
- Mróz, P., & Poleski, R. 2018, *AJ*, **155**, 154
- Mróz, P., Ryu, Y. H., Skowron, J., et al. 2018, *AJ*, **155**, 121
- Muraveva, T., Clementini, G., Maceroni, C., et al. 2014, *MNRAS*, **443**, 432
- Musella, I. 2022, *Univ*, **8**, 335
- Musella, I., Marconi, M., Molinaro, R., et al. 2021, *MNRAS*, **501**, 866
- Mustill, A. J., Davies, M. B., & Johansen, A. 2015, *ApJ*, **808**, 14
- Muthukrishna, D., Narayan, G., Mandel, K. S., Biswas, R., & Hložek, R. 2019, arXiv:1904.00014
- Nanni, A., Bressan, A., Marigo, P., & Girardi, L. 2014, *MNRAS*, **438**, 2328
- Narayan, G., Zaidi, T., Soraisam, M. D., et al. 2018, *ApJS*, **236**, 9
- Neilsen, B. 2018, *AcA*, **68**, 351
- Nelemans, G., Portegies Zwart, S. F., Verbunt, F., & Yungelson, L. R. 2001, *A&A*, **368**, 939
- Nelemans, G., & Tout, C. A. 2005, *MNRAS*, **356**, 753
- Nelemans, G., Yungelson, L. R., & Portegies Zwart, S. F. 2004, *MNRAS*, **349**, 181
- Ngeow, C.-C., Liao, S.-H., Bellm, E. C., et al. 2021, *AJ*, **162**, 63
- Nordin, J., Brinnel, V., van Santen, J., et al. 2019b, arXiv:1904.05922
- Nordin, J., Brinnel, V., van Santen, J., Bulla, M., & Feindt, U. 2019a, *A&A*, 161
- Ofek, E. O., Sullivan, M., Shaviv, N. J., et al. 2014, *ApJ*, **789**, 104
- Offner, S. S. R., & McKee, C. F. 2011, *ApJ*, **736**, 53
- Ogilvie, G. I., & Dubus, G. 2001, *MNRAS*, **320**, 485
- Oluseyi, H. M., Becker, A. C., Culliton, C., et al. 2012, *AJ*, **144**, 9
- Orlando, S., Pillitteri, I., Bocchino, F., Daricello, L., & Leonardi, L. 2019, *RNAAS*, **3**, 176
- Paczynski, B. 1986, *ApJ*, **304**, 1
- Paggi, A., Bonato, M., Raiteri, C. M., et al. 2020, *A&A*, **641**, A62
- Pala, A. F., Gänsicke, B. T., Belloni, D., et al. 2022, *MNRAS*, **510**, 6110
- Panahi, A., & Zucker, S. 2021, *PASP*, **133**, 024502
- Panaiteescu, A., & Kumar, P. 2002, *ApJ*, **571**, 779
- Papitto, A., Ambrosino, F., Stella, L., et al. 2019, *ApJ*, **882**, 104
- Papitto, A., de Martino, D., Belloni, T. M., et al. 2015, *MNRAS*, **449**, L26
- Papitto, A., Ferrigno, C., Bozzo, E., et al. 2013, *Natur*, **501**, 517
- Papitto, A., & Torres, D. F. 2015, *ApJ*, **807**, 33
- Papitto, A., Torres, D. F., & Li, J. 2014, *MNRAS*, **438**, 2105
- Pastorello, A., Botticella, M. T., Trundle, C., et al. 2010, *MNRAS*, **408**, 181
- Pastorello, A., Cappellaro, E., Inserra, C., et al. 2013, *ApJ*, **767**, 1
- Pastorello, A., & Fraser, M. 2019, *NatAs*, **3**, 676
- Pastorello, A., Fraser, M., Valerin, G., et al. 2021b, *A&A*, **646**, A119
- Pastorello, A., Mason, E., Taubenberger, S., et al. 2019, *A&A*, **630**, A75
- Pastorello, A., Smartt, S. J., Mattila, S., et al. 2007, *Natur*, **447**, 829

- Pastorello, A., Valerin, G., Fraser, M., et al. 2021a, *A&A*, **647**, A93
- Pastorello, A., Zampieri, L., Turatto, M., et al. 2004, *MNRAS*, **347**, 74
- Patruno, A., Archibald, A. M., Hessels, J. W. T., et al. 2014, *ApJL*, **781**, L3
- Patterson, M. T., Bellm, E. C., Masci, F. J., et al. 2019, *PASP*, **131**, 018001
- Pellegrino, C., Howell, D. A., Terreran, G., et al. 2022, arXiv:2205.07894
- Penny, M. T., Gaudi, B. S., Kerins, E., et al. 2019, *ApJS*, **241**, 3
- Perley, D. A., Sollerman, J., Schulze, S., et al. 2022, *ApJ*, **927**, 180
- Perna, R., Lazzati, D., & Giacomazzo, B. 2016, *ApJ*, **821**, L18
- Petrov, P., Singer, L. P., Coughlin, M. W., et al. 2022, *ApJ*, **924**, 54
- Pfenniger, D., & Revaz, Y. 2005, *A&A*, **431**, 511
- Pfenniger, D. C. F., Combes, F., & Martinet, L. 1994, *A&A*, **285**, 79
- Phan-Bao, N., Crifo, F., Delfosse, X., et al. 2003, *A&A*, **401**, 959
- Piatti, A. E., & Carballo-Bello, J. A. 2020, *A&A*, **637**, L2
- Pichardo Marcano, M., Rivera Sandoval, L. E., Maccarone, T. J., Zhao, Y., & Heinke, C. O. 2021, *MNRAS*, **503**, L51
- Piran, T., Svirski, G., Krolik, J., Cheng, R. M., & Shiokawa, H. 2015, *ApJ*, **806**, 164
- Piro, A. L., & Kollmeier, J. A. 2018, *ApJ*, **855**, 103
- Press, W. H., Teukolsky, S. A., Vetterling, W. T., & Flannery, B. P. 1992, *Numerical Recipes in FORTRAN. The Art of Scientific Computing* (2nd ed.); Cambridge: Cambridge Univ. Press)
- Prieto, J. L., Kistler, M. D., Thompson, T. A., et al. 2008, *ApJL*, **681**, L9
- Prinzano, L., Magrini, L., Damiani, F., et al. 2018, arXiv:1812.03025
- Pruzhinskaya, M. V., Malanchev, K. L., Kornilov, M. V., et al. 2019, *MNRAS*, **489**, 3591
- Prša, A. 2018, *Modeling and Analysis of Eclipsing Binary Stars: The Theory and Design Principles of PHOEBE* (Bristol: Institute of Physics Publishing).
- Prša, A., Pepper, J., & Stassun, K. G. 2011, *AJ*, **142**, 52
- Pumo, M. L., Turatto, M., Botticella, M. T., et al. 2009, *ApJL*, **705**, L138
- Qu, H., & Sako, M. 2021, arXiv:2111.05539
- Qu, H., Sako, M., Möller, A., & Doux, C. 2021, *AJ*, **162**, 67
- Racusin, J. L. 2009, PhD thesis, Pennsylvania State University
- Racusin, J. L., Karpov, S. V., Sokolowski, M., et al. 2008, *Natur*, **455**, 183
- Radigan, J. 2014, *ApJ*, **797**, 120
- Ragosta, F., Marconi, M., Molinaro, R., et al. 2019, *MNRAS*, **490**, 4975
- Rahvar, S. 2015, *IJMPD*, **24**, 1530020
- Raiteri, C. M., Carnerero, M. I., Balmaverde, B., et al. 2018, arXiv:1812.03151
- Raiteri, C. M., Carnerero, M. I., Balmaverde, B., et al. 2021, *ApJS*, **258**, 3
- Raiteri, C. M., Carnerero, M. I., Balmaverde, B., et al. 2022, *ApJS*, **258**, 3
- Raiteri, C. M., Villata, M., Acosta-Pulido, J. A., et al. 2017, *Natur*, **552**, 374
- Raiteri, C. M., Villata, M., Carnerero, M. I., et al. 2019, *MNRAS*, **489**, 1837
- Raiteri, C. M., Villata, M., D'Ammando, F., et al. 2013, *MNRAS*, **436**, 1530
- Ramsay, G., Green, M. J., Marsh, T. R., et al. 2018, *A&A*, **620**, A141
- Rappaport, S., Joss, P. C., & Webbink, R. F. 1982, *ApJ*, **254**, 616
- Rebassa-Mansergas, A., Ren, J. J., Parsons, S. G., et al. 2016, *MNRAS*, **458**, 3808
- Rees, M. J. 1988, *Natur*, **333**, 523
- Reguitti, A., Pastorello, A., Pignata, G., et al. 2019, *MNRAS*, **482**, 2750
- Reid, I. N. 2003, *AJ*, **126**, 2449
- Reig, P. 2011, *Ap&SS*, **332**, 1
- Ren, S., He, K., Girshick, R., & Sun, J. 2015, *Advances in Neural Information Processing Systems* (New York: Curran Associates, Inc.), **91**
- Rest, A., Foley, R., Sinnott, B., et al. 2011, *ApJ*, **732**, 3
- Rest, A., Prieto, J., Walborn, N., et al. 2012, *Natur*, **482**, 375
- Rest, A., Sinnott, B., Welch, D., Prieto, J., & Bianco, F. 2013, *Proc. IAU*, **9**, 126
- Rest, A., Suntzeff, N. B., Olsen, K., et al. 2005, *Natur*, **438**, 1132
- Rest, A., Welch, D., Suntzeff, N., et al. 2008, *ApJL*, **681**, L81
- Revet, G., Chen, S. N., Bonito, R., et al. 2017, *SciA*, **3**, e1700982
- Richardson, N. D., & Mehner, A. 2018, *RNAAS*, **2**, 121
- Ricker, G. R., Winn, J. N., Vanderspek, R., et al. 2015, *JATIS*, **1**, 014003
- Riess, A. G., Yuan, W., Macri, L. M., et al. 2021, arXiv:2112.04510
- Righi, C., Tavecchio, F., & Guetta, D. 2017, *A&A*, **598**, A36
- Ripepi, V., Catanzaro, G., Molinaro, R., et al. 2021, *MNRAS*, **508**, 4047
- Robertson, B. E., Banerji, M., Cooper, M. C., et al. 2017, arXiv:1708.01617
- Robinson, T. D., & Marley, M. S. 2014, *ApJ*, **785**, 158
- Sajadian, S., & Poleski, R. 2019, *ApJ*, **871**, 205
- Sánchez-Sáez, P., Reyes, I., Valenzuela, C., et al. 2021, *AJ*, **161**, 141
- Sandrinelli, A., Falomo, R., & Treves, A. 2019, *MNRAS*, **485**, L89
- Schwamb, M. E., Hsieh, H., Bannister, M. T., et al. 2019, *RNAAS*, **3**, 51
- Schwamb, M. E., Jones, R. L., Chesley, S. R., et al. 2018, arXiv:1802.01783
- Setzer, C. N., Biswas, R., Peiris, H. V., et al. 2019, *MNRAS*, **485**, 4260
- Shafter, A. W. 2017, *ApJ*, **834**, 196
- Shostak, S., & Villard, R. 2004, in *IAU 213* (Cambridge: Cambridge Univ. Press), 409
- Simionescu, A., Werner, N., Urban, O., et al. 2015, *ApJL*, **811**, L25
- Simonetti, J. H., Cordes, J. M., & Heeschen, D. S. 1985, *ApJ*, **296**, 46
- Siwak, M., Ogloza, W., Moffat, A. F. J., et al. 2018, *MNRAS*, **478**, 758
- Smart, R. L., Marocco, F., Caballero, J. A., et al. 2017, *MNRAS*, **469**, 401
- Smartt, S. 2021, *BAAS*, **53**, 1
- Smartt, S., Eldridge, J., Crockett, R., & Maund, J. 2009, *MNRAS*, **395**, 1409
- Smartt, S. J., Chen, T.-W., Jerkstrand, A., et al. 2017, *Natur*, **551**, 75
- Smith, N. 2014, *ARA&A*, **52**, 487
- Smith, N. 2017, *RSPTA*, **375**, 20160268
- Smith, N., Andrews, J. E., Van Dyk, S. D., et al. 2016, *MNRAS*, **458**, 950
- Smith, N., & Frew, D. J. 2011, *MNRAS*, **415**, 2009
- Smith, N., Ganeshalingam, M., Chornock, R., et al. 2009, *ApJL*, **697**, L49
- Smith, N., Li, W., Silverman, J. M., Ganeshalingam, M., & Filippenko, A. V. 2011, *MNRAS*, **415**, 773
- Smith, N., Miller, A., Li, W., et al. 2010, *AJ*, **139**, 1451
- Soares-Santos, M., Holz, D. E., Annis, J., et al. 2017, *ApJL*, **848**, L16
- Solheim, J. E. 2010, *PASP*, **122**, 1133
- Soszyński, I., Udalski, A., Szymański, M. K., et al. 2009, *AcA*, **59**, 1
- Soszyński, I., Udalski, A., Szymański, M. K., et al. 2018, *AcA*, **68**, 89
- Soszyński, I., Udalski, A., Szymański, M. K., et al. 2019, *AcA*, **69**, 87
- Spergel, D., Gehrels, N., Baltay, C., et al. 2015, arXiv:1503.03757
- Spiro, S., Pastorello, A., Pumo, M. L., et al. 2014, *MNRAS*, **439**, 2873
- Stappers, B. W., Archibald, A. M., Hessels, J. W. T., et al. 2014, *ApJ*, **790**, 39
- Stassun, K. G., & Torres, G. 2016, *AJ*, **152**, 180
- Stassun, K. G., & Torres, G. 2018, *ApJ*, **862**, 61
- Stassun, K. G., & Torres, G. 2021, *ApJL*, **907**, L33
- Stauffer, J., Cody, A. M., Baglin, A., et al. 2014, *AJ*, **147**, 83
- Stefano, R. D. 2000, *ApJ*, **541**, 587
- Stefano, R. D. 2008, *ApJ*, **684**, 59
- Stickel, M., Padovani, P., Urry, C. M., Fried, J. W., & Kuehr, H. 1991, *ApJ*, **374**, 431
- Stoeckle, J. T., Morris, S. L., Gioia, I. M., et al. 1991, *ApJS*, **76**, 813
- Stone, N. C., Metzger, B. D., & Haiman, Z. 2017, *MNRAS*, **464**, 946
- Strader, J., Aydi, E., Britt, C., et al. 2018, arXiv:1811.12433
- Street, R. A., Adamson, A., Blakeslee, J. P., et al. 2020, *Proc. SPIE*, **11449**, 471
- Street, R. A., Bowman, M., Saunders, E. S., & Boroson, T. 2018a, *Proc. SPIE*, **10707**, 1070711
- Street, R. A., Fulton, B. J., Scholz, A., et al. 2015, *ApJ*, **812**, 161
- Street, R. A., Lund, M. B., Khakpash, S., et al. 2018b, arXiv:1812.03137
- Stroeer, A., & Vecchio, A. 2006, *CQGra*, **23**, S809
- Strotjohann, N. L., Ofek, E. O., Gal-Yam, A., et al. 2021, *ApJ*, **907**, 99
- Sullivan, P. W., Winn, J. N., Berta-Thompson, Z. K., et al. 2015, *ApJ*, **809**, 77
- Sundelius, B., Wahde, M., Lehto, H. J., & Valtonen, M. J. 1997, *ApJ*, **484**, 180
- Szklennár, T., Bódi, A., Tarczay-Nehéz, D., et al. 2020, *ApJL*, **897**, L12
- Tammann, G. A., & Sandage, A. 1968, *ApJ*, **151**, 825
- Tanvir, N. R., Fox, D. B., Levan, A. J., et al. 2009, *Natur*, **461**, 1254
- Tanvir, N. R., Laskar, T., Levan, A. J., et al. 2018, *ApJ*, **865**, 107
- Tanvir, N. R., Levan, A. J., González-Fernández, C., et al. 2017, *ApJL*, **848**, L27
- Tartaglia, L., Elias-Rosa, N., Pastorello, A., et al. 2016, *ApJ*, **823**, L23
- Tartaglia, L., Pastorello, A., Taubenberger, S., et al. 2015, *MNRAS*, **447**, 117
- Tarter, J. C. 2001, *Proc. SPIE*, **4273**, 93
- Terrell, D., & Wilson, R. E. 2005, *Ap&SS*, **296**, 221
- The Fermi-LAT collaboration 2019, arXiv:1902.10045
- Thomas, D., & Kahn, S. M. 2018, *ApJ*, **868**, 38
- Thomas, D., & Kahn, S. M. 2018, *ApJ*, **868**, 38
- Thomas, J. K., Charles, P. A., Buckley, D. A. H., et al. 2022, *MNRAS*, **509**, 1062
- Thompson, T. A., Prieto, J. L., Stanek, K. Z., et al. 2009, *ApJ*, **705**, 1364
- Tonry, J., Denneau, L., Heinze, A., et al. 2018, *PASP*, **130**, 064505
- Torres, G., Andersen, J., & Giménez, A. 2010, *A&ARv*, **18**, 67
- Townsend, L. K., Broos, P. S., Corcoran, M. F., et al. 2011, *ApJS*, **194**, 1
- Trabucchi, M., Wood, P. R., Montalbán, J., et al. 2019, *MNRAS*, **482**, 929

- Treasure, J. 2011, *Sound Business: How to Use Sound to Grow Profits and Brand Value* (Oxford: Management Books 2000 Ltd)
- Tremblin, P., Amundsen, D. S., Chabrier, G., et al. 2016, *ApJ*, 817, L19
- Tylenda, R., Hajduk, M., Kamiński, T., et al. 2011, *A&A*, 528, A114
- Udalski, A., Szymański, M. K., & Szymański, G. 2015, *AcA*, 65, 1
- Valenti, S., David, Sand, J., et al. 2017, *ApJL*, 848, L24
- Valenti, S., Pastorello, A., Cappellaro, E., et al. 2009, *Natur*, 459, 674
- Valtonen, M. J., Zola, S., Ciprini, S., et al. 2016, *ApJL*, 819, L37
- Van Dyk, S. D., Peng, C. Y., King, J. Y., et al. 2000, *PASP*, 112, 1532
- Van Paradijs, J., & Van der Klis, M. 2001, in *Low-mass X-ray Binaries*, ed. J. A. M. Bleeker, J. Geiss, & M. C. E. Huber (Dordrecht: Springer), 811
- van Velzen, S., & Farrar, G. R. 2014, *ApJ*, 792, 53
- van Velzen, S., Gezari, S., Hammerstein, E., et al. 2021, *ApJ*, 908
- van Velzen, S., Stone, N. C., Metzger, B. D., et al. 2019, *ApJ*, 878, 82
- van Velzen, S., et al. 2011, *ApJ*, 741, 73
- van Velzen, S., et al. 2019, *ApJ*, 872, 198
- VanderPlas, J. T. 2018, *ApJS*, 236, 16
- Ventura, P., Criscienzo, M. D., Schneider, R., et al. 2012, *MNRAS*, 424, 2345
- Ventura, P., Dell'Agli, F., Schneider, R., et al. 2014, *MNRAS*, 439, 977
- Venuti, L., Bouvier, J., Cody, A. M., et al. 2017, *A&A*, 599, A23
- Venuti, L., Bouvier, J., Flaccomio, E., et al. 2014, *A&A*, 570, A82
- Venuti, L., Bouvier, J., Irwin, J., et al. 2015, *A&A*, 581, A66
- Venuti, L., Cody, A. M., Rebull, L. M., et al. 2021, *AJ*, 162, 101
- Verde, L., Treu, T., & Riess, A. G. 2019, *NatAs*, 3, 891
- Villar, V. A., Guillochon, J., Berger, E., et al. 2017, *ApJL*, 851, L21
- Villarroel, B., Soodla, J., Comerón, S., et al. 2019, *AJ*, 159, 8
- Villata, M., Raiteri, C. M., Sillanpää, A., & Takalo, L. O. 1998, *MNRAS*, 293, L13
- Vink, J. S. 2012, *Ap&SS*, 384, 221
- Vos, J. M., Biller, B. A., Allers, K. N., et al. 2020, *AJ*, 160, 38
- Vreeswijk, P. M., Ledoux, C., Smette, A., et al. 2011, *A&A*, 532, C3
- Wagner, R. M., Vrba, F. J., Henden, A. A., et al. 2004, *PASP*, 116, 326
- Walker, B. N., & Kramer, G. 2005, *ACM Transactions on Applied Perception*, 2, 407
- Warner, B. 1995, *Cataclysmic Variable Stars*, Vol. 28 (Cambridge: Cambridge Univ. Press)
- Wevers, T., Pasham, D. R., van Velzen, S., et al. 2019, *MNRAS*, 488, 4816
- Whitney, B. A., Wood, K., Bjorkman, J. E., & Cohen, M. 2003, *ApJ*, 598, 1079
- Wiktorowicz, G., Middleton, M., Khan, N., et al. 2021, *MNRAS*, 507, 374
- Wilson, R. E., & Van Hamme, W. 2014, *ApJ*, 780, 151
- Wolter, A., Caccianiga, A., della Ceca, R., & Maccacaro, T. 1994, *ApJ*, 433, 29
- Wood, P. R. 2015, *MNRAS*, 448, 3829
- Wood, P. R., & Nicholls, C. P. 2009, *ApJ*, 707, 573
- Woosley, S. E. 1993, *ApJ*, 405, 273
- Wright, J. 2016, AGUFM, P11A
- Wright, J. T., Kanodia, S., & Lubar, E. 2018, *AJ*, 156, 260
- Wyzykowski, L., et al. 2017, *MNRAS*, 465, L114
- Yu, J., Huber, D., Bedding, T. R., et al. 2018, *ApJS*, 236, 42
- Zanella, A., Harrison, C. M., Lenzi, S., et al. 2022, arXiv:2206.13536